Aalborg Universitet

AALBORG UNIVERSITY
DENMARK

Control and Operation of Islanded Distribution System

Mahat, Pukar

Publication date:
2010

Document Version
Publisher's PDF, also known as Version of record

Link to publication from Aalborg University

Citation for published version (APA):
Mahat, P. (2010). *Control and Operation of Islanded Distribution System*. Department of Energy Technology, Aalborg University.

General rights
Copyright and moral rights for the publications made accessible in the public portal are retained by the authors and/or other copyright owners and it is a condition of accessing publications that users recognise and abide by the legal requirements associated with these rights.

- Users may download and print one copy of any publication from the public portal for the purpose of private study or research.
- You may not further distribute the material or use it for any profit-making activity or commercial gain
- You may freely distribute the URL identifying the publication in the public portal -

Take down policy
If you believe that this document breaches copyright please contact us at vbn@aub.aau.dk providing details, and we will remove access to the work immediately and investigate your claim.

Downloaded from vbn.aau.dk on: April 19, 2024

CONTROL AND OPERATION OF ISLANDED DISTRIBUTION SYSTEM

By

Pukar Mahat

Department of Energy Technology

A Dissertation Submitted to
the Faculty of Engineering, Science and Medicine, Aalborg University
in Partial Fulfillment for the Degree of
Doctor of Philosophy

September 2010

Aalborg, Denmark

Aalborg University
Department of Energy Technology
Pontoppidanstraede 101
9220 Aalborg East, Denmark

Copyright © Pukar Mahat, 2010
ISBN: 978-87-89179-93-3

Printed in Denmark by Aalborg University

To my parents

Acknowledgement

I am very thankful for the financial support provided by the Danish Public Service Obligation (PSO) program under the project 2006-1-6316, "Operation and Control of Modern Distribution Systems"

I would like to express my sincere gratitude and appreciation to my supervisors Professor Zhe Chen and Associate Professor Birgitte Bak-Jensen for their suggestions, patience and encouragement throughout the period of this work. Their invaluable support, understanding and expertise have been very important in completing this work.

Heartfelt sincere thanks are due to Stefan Frendrup Sörensen, Niels Andersen and Anders Foosnæs from the project steering committee for their invaluable discussions and help with data during the course of this work.

I would also like to extend my sincere thanks to Professor Robert H. Lasseter, Associate Professor Claus Leth Bak, and the faculty and staff of Department of Energy Technology. I would like to express my gratitude to Charles McEniry for his help on my papers. Many thanks go to my friends, especially Ranjan, Peiyuan and Jay.

Last but not least, I want to thank my parents and my family for their love and constant support.

Abstract

A yearly demand growth of less than 3%, concern about the environment, and various benefits of onsite generation have all resulted in a significant increase in penetration of dispersed and distributed generation (DG) in many distribution systems. This has also resulted in some power system operational challenges. But, on the other hand, it has also opened up some opportunities. One opportunity/challenge is an islanded operation of a distribution system with DG unit(s). Islanding is a situation in which a distribution system becomes electrically isolated from the remainder of the power system and yet continues to be energized by DG unit(s) connected to it. Currently, it is seen as a challenge and so far all DG units need to shut down when a distribution system is islanded. However, with the DG penetration expected to increase sharply, islanding is an opportunity to improve the reliability of power supply provided that various issues with islanding are properly addressed. Some of the issues with islanding are state (islanded or grid connected) detection, control of voltage and frequency, load control and protection.

In this dissertation, some of the major technical issues with islanding are addressed. A hybrid islanding detection technique, based on the average rate of voltage change and real power shift, is developed to overcome the problems with most of the existing islanding detection techniques. It uses a passive technique (average rate of voltage change) and an active technique (real power shift). However, the active technique is used only when the passive technique cannot clearly discriminate between islanded and grid connected conditions. DG units perform the best if they are operated with droop control and power factor control when they are operating parallel to the grid and if they are operated with isochronous control and voltage control when the distribution system is islanded. It is proposed that the DG units are controlled differently when the distribution system changes state from grid connected condition to islanded condition. However, isochronous controllers cannot be used with more than one generator connected to the same system. An isochronous controller with feedback has been developed in this research study. It performs relatively well in both islanded and grid connected conditions. Hence, if there is more than one DG unit in the distribution system, employing isochronous control in one DG unit and employing isochronous control with feedback in other DG units, during islanding, results in better frequency profile of the islanded distribution system. The DG control strategy needs to be changed again when the islanded distribution system is reconnected back to the transmission grid. Hence, grid reconnection detection algorithms have been proposed to detect when an islanded distribution system is reconnected back to the transmission grid. One of the grid reconnection detection algorithms is based on rate of change of speed over power. Another one is based on frequency deviation and real power shift. When a distribution system, with all its generators operating at maximum power, is islanded, the frequency will go down if the total load is more than the total

generation. An under-frequency load shedding procedure for islanded distribution systems with DG unit(s) based on frequency information, rate of change of frequency, customers' willingness to pay and loads' histories is proposed in this research. It sheds an optimal number of loads and stabilizes the frequency of the islanded distribution system. Short circuit power of a distribution system changes when it changes states. Short circuit power also changes when some of the generators in the distribution system are disconnected. This may result in elongation of fault clearing time and hence disconnection of equipments (including generators) in the distribution system or unnecessary operation of protective devices. An adaptive protection has been proposed in the research study to overcome the problem with change in short circuit power.

The algorithms, models and methodologies developed during the course of this research study have been tested in a distribution system with gas turbine and wind turbine generators. Simulation results show that they are able to correctly identify the states of distribution systems, maintain the voltage and frequency when the distribution system is islanded, maintain the power and power factor when the distribution system is connected to the grid, maintain the voltage and frequency after load and stochastic generation changes, shed an optimal number of loads to stabilize the frequency when the total demand is more than the generation in an islanded distribution system, and protect the distribution system against the short circuits even with the changing short circuit power.

The research study shows that running a distribution system in an islanded mode is a technically viable solution to improve the reliability of the power supply.

Table of Contents

Chapter 1

Introduction

The power industry started with distributed generation (DG). DG is a small generating plant serving on site customers. As an example, Edison's Pearl Steam Power Plant supplied 500 customers with electricity in downtown New York in 1882 [1]. However, due to the 'economy of scale' in large thermal generation coupled with a strong yearly demand growth that was stable at around 6-7% [2], the situation changed. Moreover, the cost of production (cost per kWh) of bulk quantities of electricity became much lower than the cost of producing small quantities of electricity. This lead to the demand of larger generating plants to satisfy the ever growing load demands. Furthermore, large transmission networks were built interconnecting generators and consumers and thus strengthened the security and reliability of supply. But the power industry faced new problems, at the turn of the 21st century, due to the environmental concern and oil crisis. This was coupled with less yearly demand growth of 1.6% to 3% [2]. This has lead to the renewed interest in distributed generation. The development and innovations in distributed generation technology is again changing the paradigm of power industry and it looks like this time it will be back to the distributed and dispersed generation.

1.1 Background and Motivation

The 'economy of scale' in the power industry has shrunk in the recent times and the utility's generation pattern is shifting from the 'economy of scale' to the 'economy of mass production' [2]. Recent studies have shown that the difference in the cost of electricity production between large and small scale generation has reduced to 30% in 2000 from 60% in 1960 [3]. This is mainly due to advancement in technologies like fuel cells, gas turbines, micro-hydro, wind turbines and photovoltaic in combination with new innovation in power electronics. Furthermore, the smaller size of DG requires less installation time and hence put the capital at less risk. Moreover, the electricity market deregulation, and the governments' and peoples' propensity towards green and renewable energy are forcing the power industry for yet another shift. Fig. 1. 1 shows the share of renewable power producing units in the total electricity generation in Europe and Denmark [4] in recent years. The share of electricity generated from renewable sources in the total gross electricity consumption in Europe has increased from 13.4% in 1998 to 16.7% in 2008. In Denmark, this share of renewable sources in total electricity consumption has increased significantly from 11.7% in 1998 to 28.7% in 2008. Apart from large scale hydro and offshore

wind parks, most renewable energy sources are DG. Hence, the increase in share of renewable power producing units can be perceived as an increase in penetration of distributed generation.

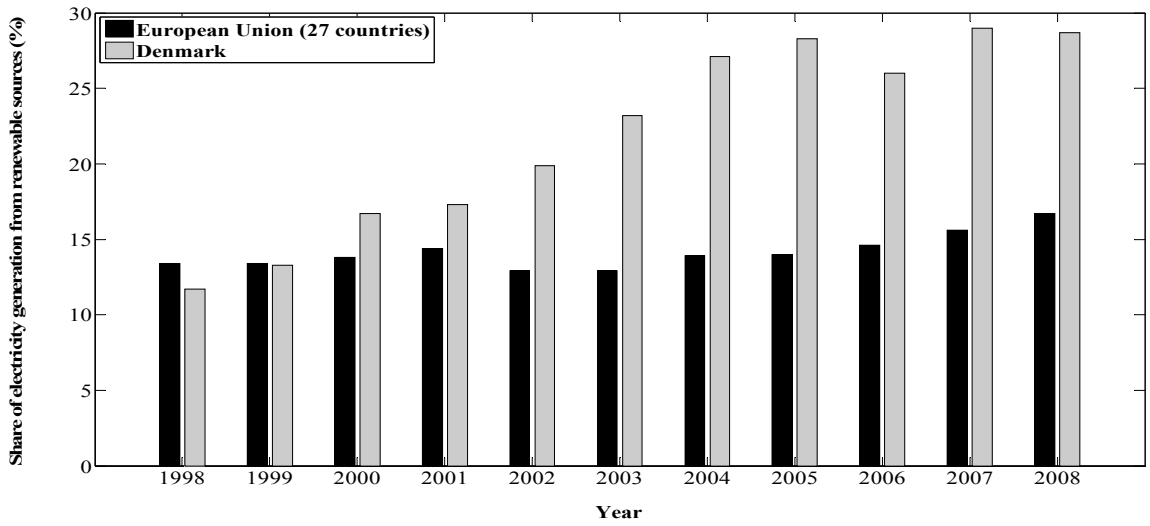

Fig. 1. 1. Share of renewable sources in total electricity generation

The popularity of DG is increasing. In fact, many distribution systems around the world already have a significant penetration of DG. This is clearly indicated by the increasing share of DG in electricity market. In the United States, for example, DG resources capacity increased from 9579 MW in 2004 to 22636 MW in 2008 [5]. In the UK, the installed capacity of DG has grown from 1.2 GW in 1993/4 to over 12 GW in 2008 [6]. In 2004, share of DG in the total generation capacity was 36% in Germany (45 GW out of 125 GW), 14.3% in Japan (39 GW out of 273 GW), 9.4% in Korea (6.1 GW out of 64.6 GW), 24.3% in Poland (8.4 GW out of 34.6 GW) and 31.3% in Russia (65.1 GW out of 208.2 GW) [7].

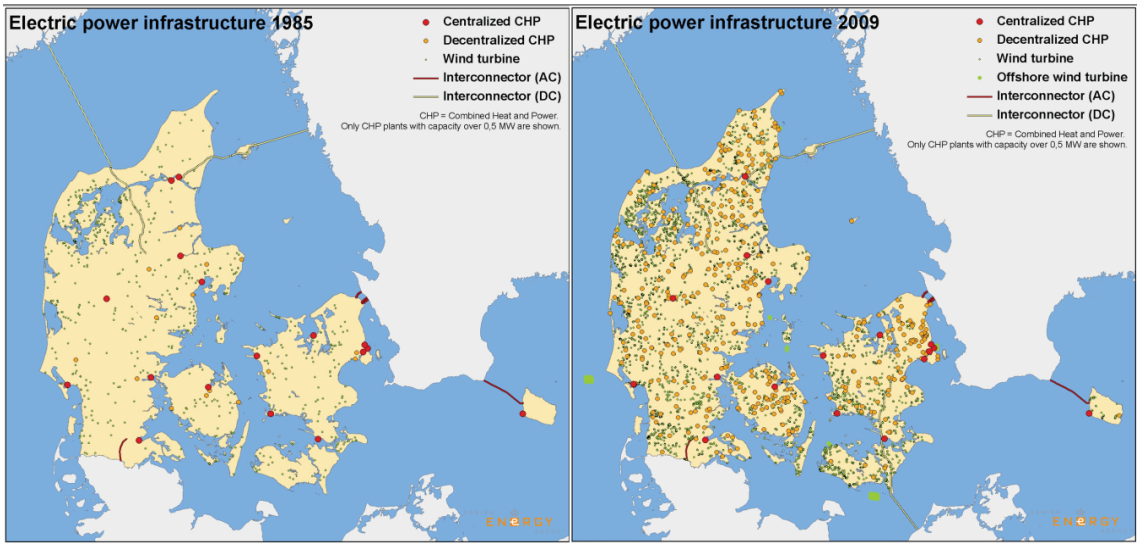

Fig. 1. 2. Overview of the Danish power infrastructure in 1985 and 2009 [8], [9]

Fig. 1. 2. shows the change in Danish power infrastructure from 1985 to 2009 [8], [9]. It shows that number of DG units has increased significantly in Denmark. This trend is likely to accelerate. In 2008, the installed capacity of small power plants and wind turbines was 1829 MW and 3166 MW, respectively in Denmark [10].

The European Union has set a target of 20% energy from renewable sources by 2020. It is expected that the share of electricity from renewable energy sources has to be more than 30% to achieve this target [11]. The electricity generation from the renewable source based DG is expected to rise to about 1,280 TWh/yr in 2030 from 490 TWh/yr in 2005 and the share of electricity generated to grow from about 15% to approximately 26% during the same timeframe [12]. A significant portion of these renewable source based generating units will be small generating units connected to distribution systems. However the increase in popularity of DG is not only due to environmental concerns but also due to various other benefits that it brings along with it.

DG has a relatively low capital cost compared to its central counterpart in response to an incremental change in the power demand. It can avoid transmission and distribution systems upgrade by locating power where it is most needed. According to the International Energy Agency (IEA), on-site production could result in cost savings in transmission and distribution of about 30% of the electricity costs [13]. DG can be used to supply some loads at peak periods when the electricity prices are high and may reduce the electricity cost of the customers. If strategically installed, DG can reduce losses in the distribution system as well as in the transmission system [14]. DG may level the load curve and reduce the loading of the branches [15]. The central generating companies can reduce load on their transmission equipment, provide local voltage support and increase economical benefits with DG [16]. Government may use them to introduce competition in the electricity supply market and thus create price reduction [16]. DG may reduce the wholesale power price by supplying power to the grid, which leads to reduction of demand required. The number of DG units in many distribution systems is increasing due to these various benefits. With a significant DG penetration, islanding operation of a distribution system with DG can be realized to supply power during network outage.

1.2 Problem Statement

Islanding is a situation in which a distribution system becomes electrically isolated from the remainder of the power system, due to a fault upstream or any other disturbance, and yet continues to be energized by the DG unit(s) connected to it. Apart from improved reliability, islanding operation increases the revenue of DG owner by additional sale. For the distribution network operators (DNOs), islanding operation can improve the overall security of power supply and they may also get additional revenue due to the improvement in the quality of supply indices

[17]. As for the customers, the main benefit of islanding is the reduction in the frequency and the duration of interruptions resulting from outages in the distribution and transmission systems. Despite all these advantages, currently almost all utilities require DG to shut down once a distribution system is islanded. IEEE 1547-2003 standard requires islanding to be detected and DG be disconnected at most within 2 seconds [18]. Similarly, IEC 61727 also require islanding detection and DG disconnection at most within 2 seconds [19]. The Danish grid code requires that island operation of power plants up to 25 MW is avoided [20]. Utilities have their reasons for avoiding islanding operation. Some of the reasons are as follows:-

- Line workers' safety can be threatened by DG sources feeding an islanded system.
- The islanded system may not be grounded resulting in high voltage in un-faulted phases when an earth fault occurs [21].
- The fault power contribution from DG may not be sufficient enough to allow satisfactory operation of protection system and hence may result in a sustained fault current [22].
- Many utilities use an instantaneous reclosing practice. When the distribution system and the transmission system are reconnected, it may result in out of phase reclosing. Large mechanical torques and currents are created, which can damage the generators and/or the prime movers [23].
- Most importantly, DG may not be able to maintain the voltage and frequency within desired limits in the distribution system when it is islanded [22].

With the significant penetration of DG in many distribution systems, the current practice of disconnecting DG, after islanding, will no longer be a practical or reliable solution in the future. It is also expected that there will be an increased competition among the energy suppliers to secure more customers by providing better power quality and reliability and island operation can improve the reliability of power supply. Also, the IEEE Std. 1547-2003 [18] states that the implementation of intentional islanding of DG is one of its tasks for future consideration. Furthermore, islanding can be economically beneficial [17], [24]. Thus, island operation of DG is a viable option provided that the issues with island operation are properly addressed. This research addresses some of the key issues with island operation.

1.3 Objectives

As mentioned in the previous section, islanding is an opportunity that comes with a lot of challenges. The overall objective of this research is to *solve some of the major technical issues with an islanded operation of a distribution system with distributed generation*. Specifically, the objectives of this research study are as follows:

1) To develop an effective state detection technique that can correctly identify when a distribution system is islanded (islanding detection) and when it is reconnected to the transmission grid (grid reconnection detection).

2) To develop control strategies for stable transition between different operation states and to ensure the voltage and frequency in an islanded distribution system is maintained within power quality limits and DG operate optimally when it is connected to the grid.

3) To develop a strategy to maintain the frequency in an islanded distribution system that has demand, which is higher than total generation capacity.

4) To solve problems with over current protection of a distribution system with changing fault power.

1.4 Scope and Limitations

The scopes and limitations of this research are as follows:

1) Only the major technical issues with an islanding operation of a distribution system are covered. Financial issues when implementing an islanded operation have not been covered in the research.

2) This study assumes that implementing communication is expensive for small distribution systems and hence local information has been used to develop the state detection techniques, control strategies and adaptive protection. It may be economical to implement communication in case of larger distribution systems.

3) The DG technologies have been limited to gas turbine generators (GTG), which are based on synchronous generators and fixed speed wind turbines (WTG), which are based on induction generators.

4) Variable speed wind turbines (doubly fed induction generator) has been considered only to illustrate the over current protection issues in an island operation.

5) In case of combined heat and power plants, which consists of gas turbines, heat generation is not considered. The electricity is considered as the main output of the plant.

6) Models have been developed in DIgSILENT Power Factory and many of the standard models available in DIgSILENT have been used.

1.5 Outline of the Thesis

The PhD dissertation contains seven chapters and three appendixes. It is organized as follows:

Chapter 1: Introduction

This chapter presents the evolution of the DG market. The increasing penetration of DG in many distribution systems, leading to the possibility of operating them in an island mode to increase the reliability of power supply, has been presented as the motivation of this research. The objectives, scopes and limitations of the study are also presented in this chapter.

Chapter 2: Islanding Detection

In this chapter, many of the currently available islanding detection techniques have been reviewed. Their short comings along with their advantages are also presented. The test distribution system, which is a part of a distribution system in Mid Himmerland, is presented. Moreover, a new hybrid islanding detection technique based on average rate of voltage change and real power shift is introduced. Simulation results to show the effectiveness of the proposed islanding detection technique is also presented in this chapter.

Chapter 3: Control and Operation of Distributed Generation

The chapter deals with the modelling of fixed speed wind turbine and gas turbine generators. Then, the problem with the existing speed governor control for GTG is presented. An isochronous controller with feedback is proposed to overcome the limitations of the isochronous controller and the droop controller. Similarly, the problem with voltage control for small generators is also presented. The chapter proposes that DG should operate in a power factor control and droop control mode when it is connected to the transmission system, and operate with an isochronous control or isochronous control with feedback and voltage control while it is islanded. The chapter also presents some simulation results that show that GTGs perform the best by changing the control strategies and they are able to control voltage and frequency of the islanded distribution system.

Chapter 4: Grid Reconnection and Detection

The chapter presents some criteria to connect an energised islanded distribution system back to the transmission grid. A grid reconnection detection technique, based on rate of change of speed over power for a small distribution system with a single DG unit that is capable of supplying loads all the time, is presented. Another grid reconnection detection technique for a larger distribution system with one or more DG units, based on average rate of frequency change and real power shift, is also presented. The chapter also presents some simulation results to show the effectiveness of the proposed grid reconnection detection techniques.

Chapter 5: Under-frequency Load Shedding

If a distribution system's total load demand exceeds the total generation, then some loads have to be shed when the distribution system is islanded and all the DG units are already producing maximum power. The chapter reviews some of the existing under-frequency load shedding techniques and presents their limitations. The chapter presents a new under-frequency load shedding technique based on loads' history and their willingness to pay to be supplied during islanding, the frequency, and the rate of change of frequency. It also presents some simulation results with highly frequency and voltage dependent loads and constant power loads to show the effectiveness of the proposed under-frequency load shedding technique.

Chapter 6: Over-Current Protection of Distribution System

When a distribution system changes states from a grid connected condition to an islanded condition or vice versa, there is a significant difference in the fault power. The chapter presents the problem with over-current protection of a distribution system with changing fault power. The chapter proposes the use of adaptive protection that chooses time over-current trip characteristics based on the distribution system state to protect it from over-current. Fault power also changes when some generators are lost while clearing a fault. The adaptive protection also takes that into account by identifying the faulty section. The chapter presents a faulty section detection technique based on the time over current characteristics.

Chapter 7: Conclusion

Some conclusions are drawn in this chapter. It also presents the contributions of this research project. The chapter ends with presenting some of the works that can be done in the future with reference to the work presented in this research.

Appendix A

It presents data for test systems, generators, excitation systems, speed governors and wind turbines' drive trains.

Appendix B

It presents wind turbine efficiency curve and some extra simulation results.

Appendix C

It presents the papers that have been produced during the course of this research project.

Chapter 2

Islanding Detection

As mentioned in the previous chapter, it is important to detect islanding and it should be done as soon as possible as it may cause injuries to line workers and result in out of phase reclosing. Current practice is that almost all utilities require DG units to be disconnected from the grid as soon as possible in case of islanding. IEEE 929-1988 standard [25] requires the disconnection of DG once it is islanded and IEEE 1547-2003 standard [18] stipulates maximum delay of 2 seconds for detection of an island and all DG units ceasing to energize the distribution system. The commonly used islanding detection techniques are presented in Section 2.1 and the proposed islanding detection technique is presented in Section 2.2. Section 2.3 describes the test distribution system in which the proposed islanding detection technique is tested and simulation results are presented in Section 2.4. Some conclusions are drawn in Section 2.5.

2.1 Islanding Detection Techniques

The main philosophy of most of the islanding detection techniques is to monitor some parameters and decide whether or not an islanding situation has occurred based on these parameters. Many techniques have been proposed for islanding detection in recent times and they can be broadly classified into remote and local techniques as shown in Fig. 2. 1. Local techniques can be further divided into passive and active techniques.

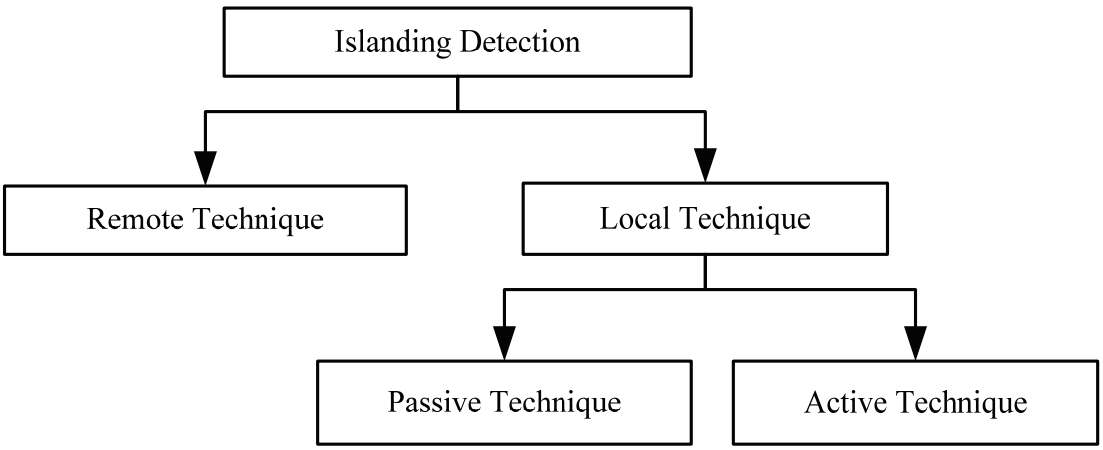

Fig. 2. 1. Islanding detection techniques

2.1.1. Remote Techniques

Remote islanding detection techniques are mainly based on communication between utilities and DG units as shown in Fig. 2. 2. The transmitter is at one side of the circuit breaker, which could island the distribution system, and the receivers are at the other side. The power lines are used as a communication channel. When the distribution system is connected to the grid, receivers receive signals from the transmitter. However, when the distribution system is islanded, the communication channel is broken and the receivers no longer receive signals and an island condition is detected. Power line signalling scheme [26] - [28] can be used to determine when the distribution system is islanded. Furthermore, Supervisory Control and Data Acquisition (SCADA) [29] may also be used to detect islanding. Even though, these techniques have better reliability than local techniques, they are complex and expensive to implement, particularly for small systems [30]. Furthermore, if there is any problem with the transmitter, it may lead to malfunction throughout the system. Therefore, local techniques are widely used to detect islanding.

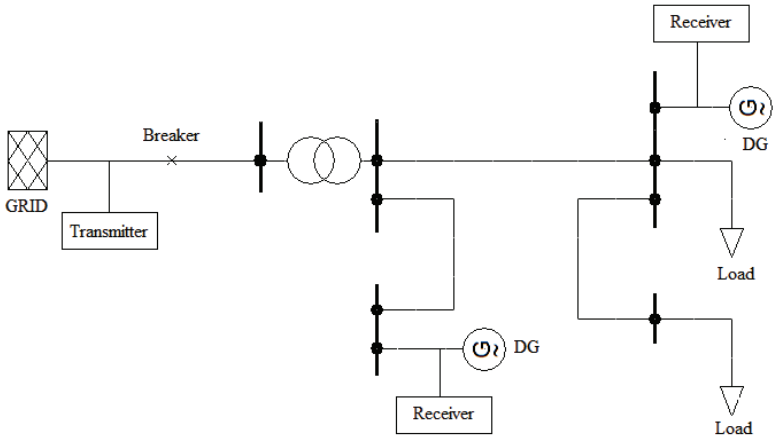

Fig. 2. 2. Remote islanding detection technique

2.1.2. Local Techniques

Local techniques are based on the measurement of some of the system parameters, like voltage, frequency, etc. As shown in Fig. 2. 1, it is further classified into passive and active techniques.

2.1.2.1. Passive Techniques

Passive techniques monitor the system parameters such as voltage, frequency, harmonic distortion, etc. These parameters vary greatly when the distribution system is islanded. Differentiation between islanded and non-islanded conditions is based upon the thresholds set for these parameters. Rate of change of output power of DG [26]-[29], [31], rate of change of

frequency [32], rate of change of frequency over power [33], voltage unbalance [34], [35], harmonic distortion [35],[37] and frequency monitoring with reconfiguration of frequency relay [38] are a few examples of passive islanding detection techniques. A detection technique that looks into a database created by extensive off-line calculations is presented in [39] to overcome some of the limitations of existing passive techniques. Wavelet based islanding detection techniques are presented in [40],[41]. Although passive methods are simple, their main problem is that it is difficult to detect islanding when the load and generation in an islanded distribution system closely match. Special care has to be taken while setting the thresholds for these parameters. If the threshold is set too low, then it could result in false islanding detection and if the threshold is set too high, islanding may not be detected. The limitation of passive detection techniques can be overcome by active techniques, which can detect islanding even under a perfect match of generation and demand in an islanded distribution system.

2.1.2.2. Active Techniques

Active methods directly interact with the power system operation by introducing perturbations. The main philosophy of active islanding detection techniques is that a small perturbation results in a significant change in system parameters when a distribution system is islanded, whereas the change is negligible when the distribution system is connected to the grid. Reactive power export error detection method [32], impedance measurement method [42], slip-mode frequency shift algorithm (SMS) [43], active frequency drift (AFD) [44], active frequency drift with positive feedback (AFDPF) [44], automatic phase-shift (APS) [45] and adaptive logic phase shift (ALPS) [46] are a few examples of active islanding detection techniques. The main problem with these techniques is that they introduce perturbations in the system. Furthermore, the perturbations are injected at predefined intervals even though it is unnecessary during most operating conditions. Also, if islanding occurs during an interval, then it has to wait for next perturbation to be applied before it can be detected, which further elongates the detection time. Applications of some of the active techniques are limited to the DG types and/or loads, i.e. reactive power export error detection method cannot be used when DG has to operate at unity power factor and methods based on phase shift are mostly useful for the inverter based DG. Also, AFD is very effective for purely resistive loads but it may fail for other loads [42]. Active methods based on impedance measurement introduce high frequency signals, AFD injects a distorted current waveform, and SMS, AFDPF, APS and ALPS shift the phase of output current. This often lowers the power quality. Therefore, there is a need to develop an efficient methodology to detect islanding of distribution systems with DG, without any adverse effect on the system.

2.2 Proposed Islanding Detection Technique

Most of the DG units around the world are required to operate at unity power factor. In [25], operation of the DG units close to unity power factor is recommended. Furthermore, it makes economical sense for small generators to produce only real power. Hence, it is likely that there will be a deficiency of reactive power once the distribution system is islanded. Capacitor banks may be the sole source of reactive power in the islanded distribution system with the DG units operating at unity power factor. But, the amount of reactive power that the capacitors produce is a function of voltage and once the voltage changes, as a result of islanding, then the reactive power generated by the capacitor bank will also change, which will further change the voltage. Thus, monitoring the voltage seems to be a sensible solution in detect islanding. However, as mentioned in the earlier section, passive methods have large non detectable zone (NDZ). The NDZ is the area representing all possible combinations of real and reactive power mismatches in an islanded distribution system for which islanding is not detected.

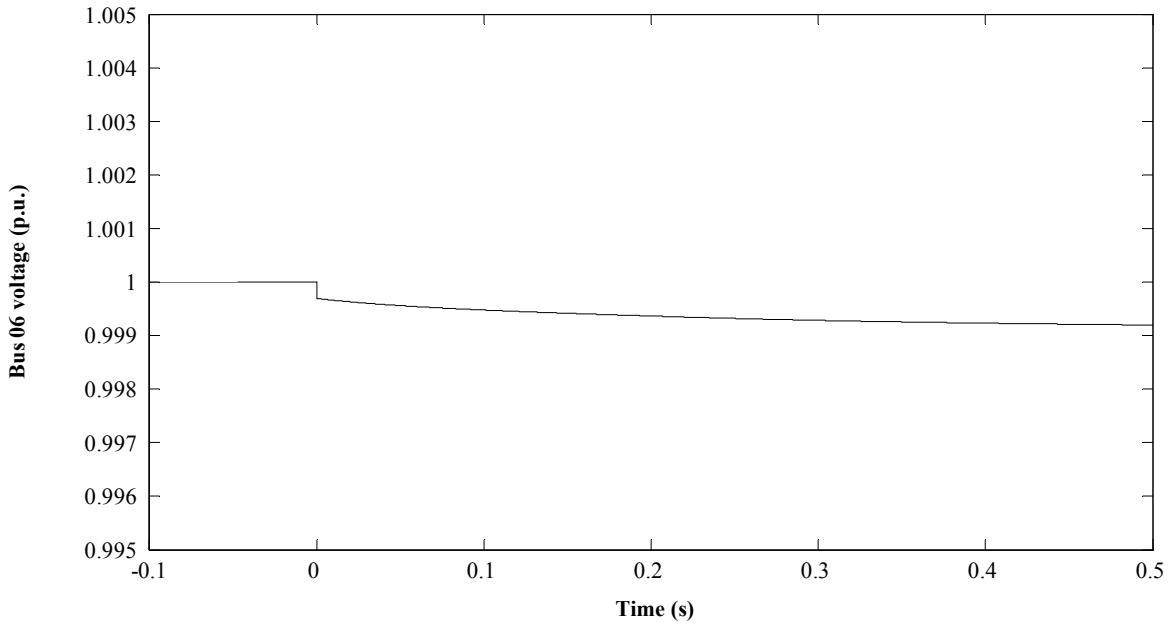

Fig. 2. 3. Voltage at Bus 06 during islanding

When a distribution system is islanded, the voltage continuously increases or decreases depending on power deficiency or surplus in the islanded distribution system. Hence, measuring the rate of voltage change gives a good indication of islanding of the distribution system. But, when the generation and demand in the distribution system closely matches, the rate of voltage change is very small. Fig. 2. 3 shows the voltage at Bus 06 when the test distribution system, presented in Fig. 2. 6, is islanded. The islanded distribution system has power deficiency of 10 kW and 10 kVAr and a total load of 9.15 MW and 2.47 MVAr. As it can be seen from Fig. 2. 3, the drop in the

voltage is very small and a drop of this size can be the result of any normal power system event. Furthermore, the rate of voltage change from *t=0.48s* to *t=0.5s*, according to Fig. 2. 3, is just 6 V/s. This value is very small to come to any conclusion. Hence, a hybrid islanding detection technique to detect islanding of a distribution system with DG is proposed in this study.

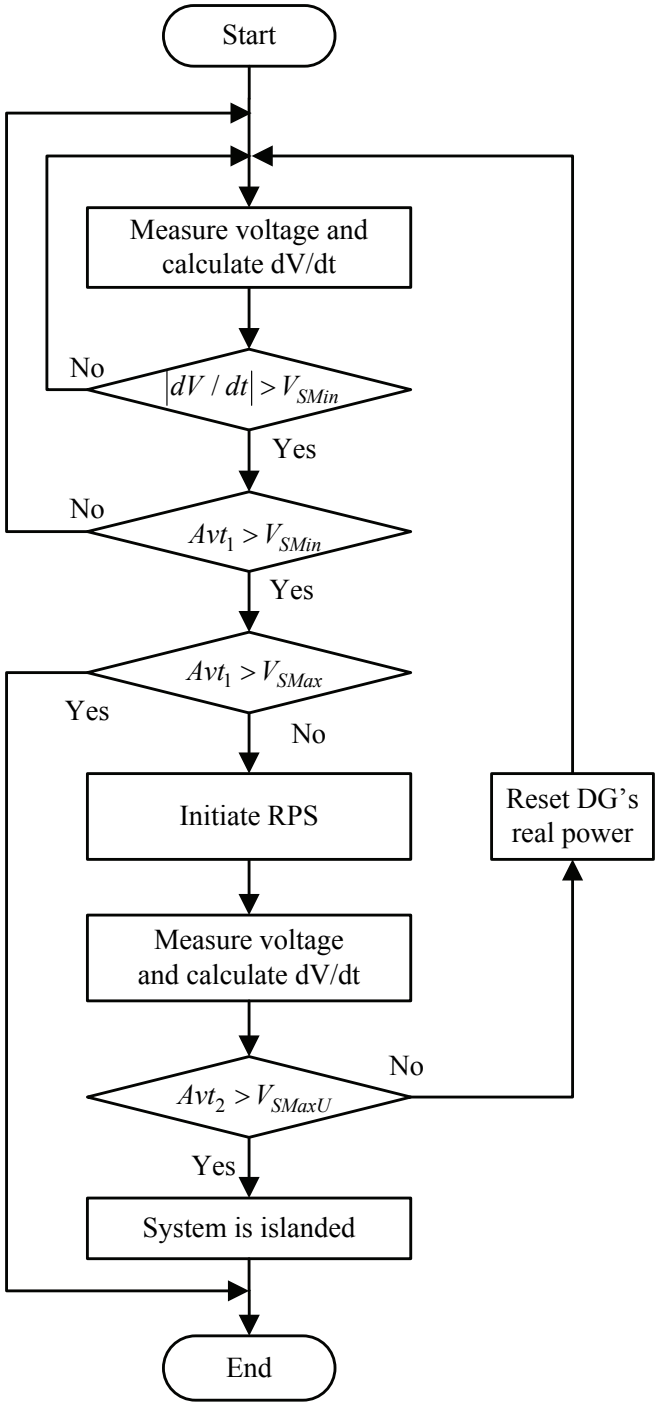

Fig. 2. 4. Flow chart of proposed islanding detection technique

The proposed islanding detection technique overcomes short comings of both active and passive techniques. It combines the average rate of voltage change (passive method) and real power shift (active method) to detect islanding. The flow chart of the proposed methodology is shown in Fig. 2. 4. The voltage is measured every voltage period at all the locations that need to detect if the distribution system is islanded or not. When $|dV/dt| > V_{SMin}$ (a minimum set point to suspect islanding) is detected, the magnitude of average rate of voltage change during 't_1' time interval (Avt_1) is used to check whether the system has been islanded or not. Avt_1 is given by equation (2.1).

$$Avt_1 = \left| \frac{1}{N_1} \sum_{i=1}^{N_1} \left(\frac{dV}{dt} \right)_i \right| \quad \textbf{(2.1)}$$

Where, N_1 is the number of dV/dt measurements in t_1 time interval. If Avt_1 is larger than V_{SMin}, islanding is suspected. Nevertheless, some events in the power system have only such a small influence in power system operation that they can be easily discarded as normal events. Also, if Avt_1 is larger than a maximum set point to detect islanding, V_{SMax}, as a result of a large mismatch of generation and demand, it is clear that the distribution system is islanded. However, if Avt_1 is between V_{SMin} and V_{SMax}, then the change in voltage can be the result of an islanding or any other normal event in the distribution system like load change, motor switching, etc. In such a situation real power shift (RPS) is used.

The RPS will increase or decrease the real power set point of DG with positive or negative $\sum_{i=1}^{N_1} \left(\frac{dV}{dt} \right)_i$, respectively. The change of the real power generation of DG also satisfies the condition of DG operating at unity power factor. Now, the magnitude of the average rate of voltage change for time interval 't_2' after the initiation of the RPS, (Avt_2), is used to differentiate islanding from any other event in the distribution system. If Avt_2 is larger than V_{SMaxU} (set point to detect islanding with the RPS), then it is from an islanding condition. Avt_2 is given by equation (2.2).

$$Avt_2 = \left| \frac{1}{N_2} \sum_{i=1}^{N_2} \left(\frac{dV}{dt} \right)_i \right| \quad \textbf{(2.2)}$$

Where, N_2 is the number of dV/dt measurements in t_2 time interval. dV/dt in the same direction as the RPS is only taken into account. If the RPS reduces the DG set point, then the voltage of the islanded distribution system decreases. But, if a rise in voltage is observed, it is because of any other event other than the RPS and hence ignored.

Many distribution systems use auto reclosing to clear temporary faults and hence it is essential to detect islanding before the auto-recloser operates to avoid out of phase reclosing. The Danish distribution system normally uses definite time over-current protection scheme and the clearing of fault is initiated at *50ms*. Furthermore, reclosers operate in a sequence of two "fast" and two "time delayed" trip operations before locking out. The typical recloser opening time used in the Danish distribution networks during the fast operation is *500ms*. Hence the islanding should be detected within *500ms*. If the fault is cleared during the RPS, the resulting dV/dt can be confusing for the detection method where the dV/dt produced by the islanding and the RPS should only be considered. Hence the fault should be cleared before or after the RPS. Assuming that relay and circuit breaker take less than *140ms* to clear a fault during an instantaneous pickup, t_1 and t_2 are chosen as *140ms* and *360ms*, respectively. If a utility practises other fault clearing and reclosing time, it should be insured that fault are not cleared during the RPS and islanding is detected before reclosers are closed by adjusting t_1 and t_2. If it is assumed that dV/dt is calculated once every voltage period, then N_1 and N_2 are 7 and 18, respectively. Avt_1 and Avt_2 are here forth called $Av7$ and $Av18$. $Av7$ is computed based upon the voltage measurement for the 7 voltage periods. Hence, in case of large mismatch ($Av7 > V_{SMax}$) islanding can be detected in almost *140ms*. In case of $V_{SMin} < Av7 < V_{SMax}$, the RPS is initiated and $Av18$ is computed based on the voltage measurement of the next 18 voltage periods. Hence, islanding can be detected in around 25 voltage periods even when the generation and load closely match.

The values for the RPS, V_{SMin}, V_{SMaxU} and V_{SMax} are also system specific and can be set accordingly. If high sensitivity is required, then V_{SMin} should be set smaller. It is recommended that V_{SMax} should be set a higher value such that it is equivalent to $Av7$ achieved by a voltage drop that results in islanding. V_{SMaxU} should be set corresponding to the RPS such that it is equal to $Av18$ achieved by an islanding and the RPS for a match of generation and demand.

2.3 Modelling of Test Distribution System

A 20 kV distribution network, owned by Himmerlands Elforsyning (HEF), in mid Himmerland, Denmark has been chosen for the study. The single line diagram of the distribution system is shown in Fig. 2. 5. There are 11 radial feeders, namely SØRP, STNO, STKV, STSY, JUEL, STK1, HJOR, FLØE, REBD, MAST and STCE. There is also a combined heat and power (CHP) plant with 3 gas turbine generators in feeder STKV. All GTGs have same specifications. The distribution system also has 3 fixed speed wind turbine generator at the end of feeder SØRP.

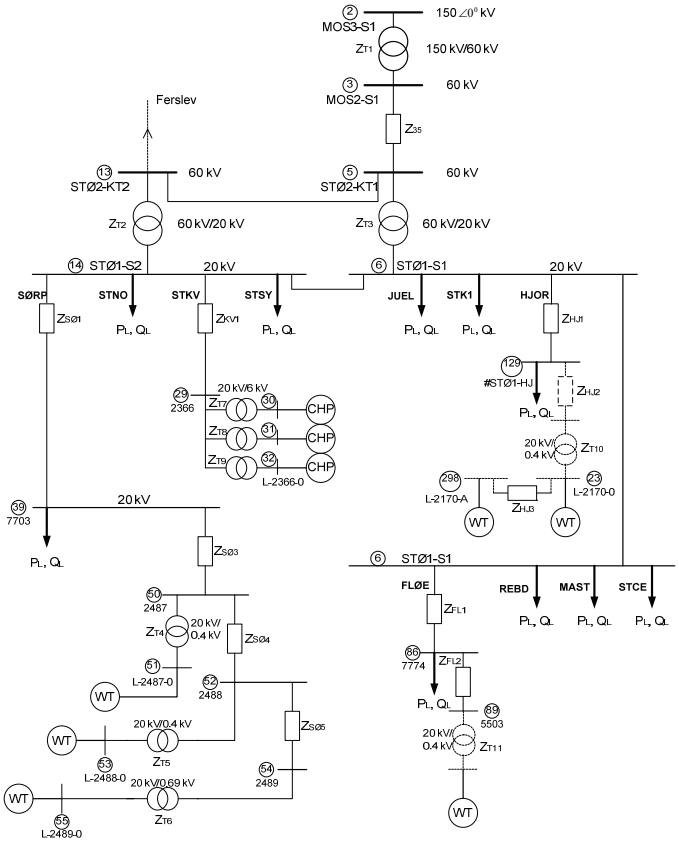

Fig. 2. 5. A local distribution network at Støvring in Nordjylland

SØRP, STKV, STNO, STSY, JUEL, FLØE, MAST and STCE are used to test the proposed methodology. Feeders STNO, STSY, JUEL, FLØE, MAST and STCE are modelled as an aggregated load connected at Bus 05 as they don't contain any distributed generation. SØRP is modelled as 8 line sections from Bus 05 to Bus 14. STKV is named as Z05-06 for naming convention. The distribution system is modelled as shown in Fig. 2. 6. The line data for the test system is given in Table AI. GTGs are synchronous generator based and their data is given in Table AII. They are connected to Bus 06 through transformers (GTGXmer). The fixed speed wind turbines are induction generator based and their data is given in Table AIII. They are connected to their respective buses through transformers (WTGXmr). The distribution system is connected to the transmission network at Bus 05 through a circuit breaker (CB) and a transformer (GridXmr). The transmission grid is represented by 'Tran Grid' in Fig. 2. 6. The data for the transformers are given in Table AIV and the transmission system data is presented in Table AV.

The whole test distribution system is modelled in DIgSILENT PowerFactory 13.2.334. Standard models of synchronous and induction generators, which are available in DIgSILENT, are used. The GAST model [47], which is one of the most commonly used dynamic models, is used to model the gas turbine generator set. For the purpose of this study, the wind turbines are modelled as a two-mass system [48] as it is adequate for the power system transient studies [49]. The WTGs

operate at unity power factor and so does the CHP. The data for the GTG governor system and the WTG system are given in Table AVI and Table AVII, respectively. The data for the base case load and generation is given in Table AVIII. A 2.5 MVAr capacitor bank is installed for simulation purpose to minimize the reactive power mismatch in the distribution system. Capacitor banks are also installed at Bus 12, Bus 13 and Bus 14 to cancel out the reactive power drawn by the WTGs.

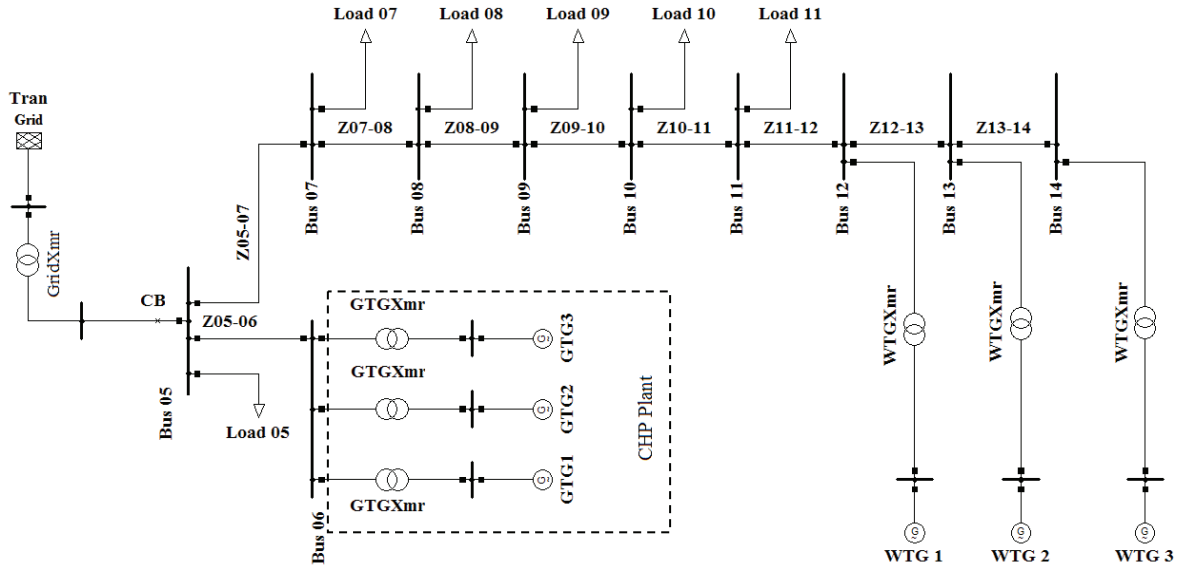

Fig. 2. 6. Model of the test distribution system

Loads are modelled as in (2.3).

$$\left.\begin{aligned} P &= P_0(1 + K_{f_p}\Delta f + K_{v_p}\Delta V) \\ Q &= Q_0(1 + K_{f_q}\Delta f + K_{v_q}\Delta V) \end{aligned}\right\} \textbf{(2.3)}$$

Where,

P_0 active power at base voltage and frequency;

P active power at new voltage and frequency;

Q_0 reactive power at base voltage and frequency;

Q reactive power at new voltage and frequency;

K_{f_p} coefficient of active load's dependency on frequency;

K_{f_q} coefficient of reactive load's dependency on frequency;

K_{v_p} coefficient of active load's dependency on voltage;

K_{v_q} coefficient of reactive load's dependency on voltage;

Δf deviation on frequency;

ΔV deviation on voltage.

Loads' dependency on frequency and voltage is very difficult to determine. Hence, for simplicity two different load models are simulated. One is with $K_{f_p} = K_{f_q} = K_{v_p} = K_{v_q} = 0$ (load Type1), and another is with $K_{f_p} = K_{f_q} = K_{v_p} = K_{v_q} = 1$ (load Type2) to show the effectiveness of the proposed methodology for a wider range of voltage and frequency dependencies. Load Type1 is a constant power load and load Type2 is a highly frequency and voltage dependent load. Hence, if the methodology works for both types of loads, then it should work for any type of loads in the power system. A look-up table with $Av7$ for different power mismatch is given in Table 2. 1. The total generation in the system is 9.93 MW and 2.5 MVAr and loads are modelled as Type2. The table may be referred to set the values of V_{SMin}, based on the required sensitivity

Table 2. 1. Lookup table for choosing $Av7$

Power Deficiency	$Av7$ (V/s)
1 kW + 1 kVAr	2.3
5 kW + 5 kVAr	40
10 kW + 10 kVAr	78.6
50 kW + 50 kVAr	387.5

2.4 Simulation Results and Discussions

Various events (islanding, load change, capacitor switching, induction motor starting, short circuit, etc.) have been simulated to show the effectiveness of the proposed methodology. Islanding is simulated by opening CB at *time (t) = 0 seconds (s)*. Other events are also simulated at *t=0s* unless otherwise stated. The value for V_{SMin} is set at 40 V/s. According to the Table 2. 1, this can detect islanding of a distribution system with a power mismatch of 5 kW and 5 kVAr or more. It is assumed that the distribution system is islanded for a voltage change of more than 5%. For a 20 kV distribution system, a change in voltage by 5% gives $Av7$ of 7142 V/s. Therefore, V_{SMax} is set at 7200 V/s. The GTGs are chosen to control the RPS as they are the only power sources with power control capability in the test distribution system. The RPS changes the GTGs' power set point by 5%. The RPS is initiated after t_1 time has passed, if necessary. If initiated, the RPS gradually increases or decreases GTG's power with positive or negative $\sum_{i=1}^{N_1}\left(\frac{dV}{dt}\right)_i$ at the GTG bus, respectively. Voltage measurement during t_2 is used to calculate $Av18$ and the RPS is deactivated after t_2 time has passed. V_{SMaxU} is set at 100 V/s as the RPS of 0.05 p.u. gives $Av18$ of more than 100 V/s for a match of the total generation and demand for load Type2. Four different scenarios,

with four different loading conditions, are considered to test the proposed islanding detection technique.

2.4.1. Scenario 1

In scenario 1, the load at Bus 05 is adjusted to 9.1 MW and 2.6 MVAr. This results in power deficiency of 1.5 MW and 1.5 MVAr in the distribution system when it is islanded. Fig. 2. 7 shows the Bus 06 voltage during the islanding. The magnitude of average rate of voltage change for the first seven voltage cycles, $Av7$, is 10975 V/s and 7792 V/s, for load types Type1 and Type2, respectively, which are larger than V_{SMax} (set at 7200 V/s). Hence, islanding is detected without the RPS as $Av7 > V_{SMax}$.

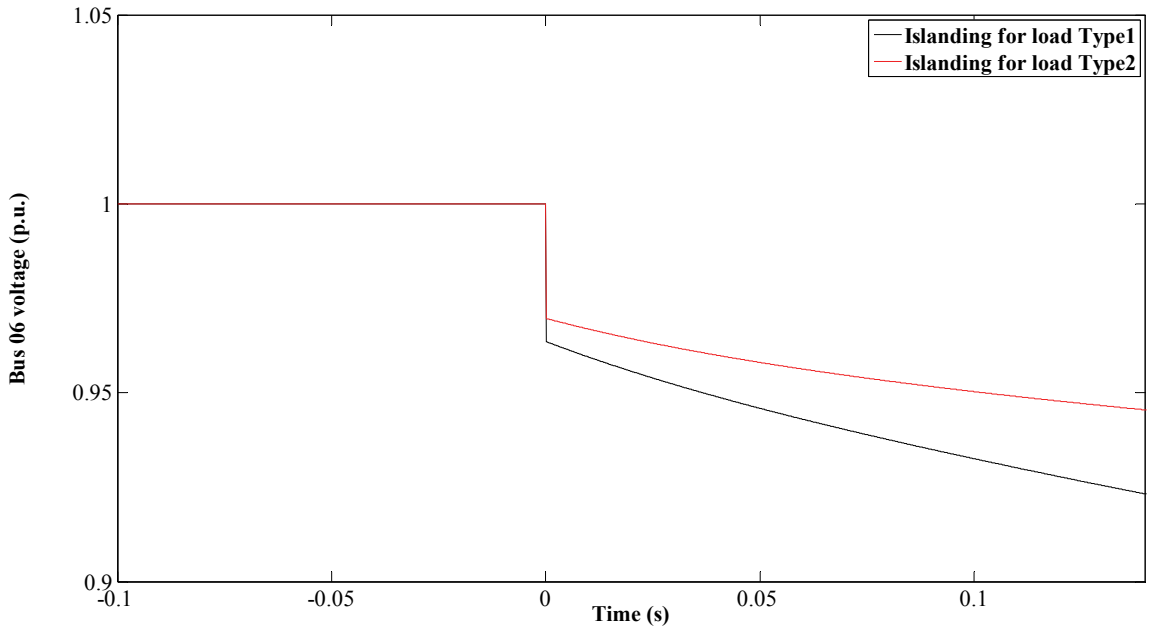

Fig. 2. 7. Bus 06 voltage for islanding in scenario 1

2.4.2. Scenario 2

In scenario 2, the load at Bus 05 is adjusted to 7.604 MW and 1.114 MVAr resulting in real and reactive power deficiency of 0.01 MW and 0.01 MVAr in the distribution system, respectively. Islanding is simulated by opening CB. The deficiency in power in the islanded distribution system results in drop in voltage. Fig. 2. 8 shows the voltage at Bus 06. $Av7$, for this case, is 108 V/s, and 78.9 V/s, respectively for load types Type1 and Type2. Since $Av7$ is larger than V_{SMin} but smaller than V_{SMax}, the RPS is initiated at *t =0.14s.* As a result, $Av18$ for islanding are 205 V/s and 118.5 V/s for load types Type1 and Type 2, respectively. Islanding is detected correctly as the values for $Av18$ for both load types are larger than V_{SMaxU}.

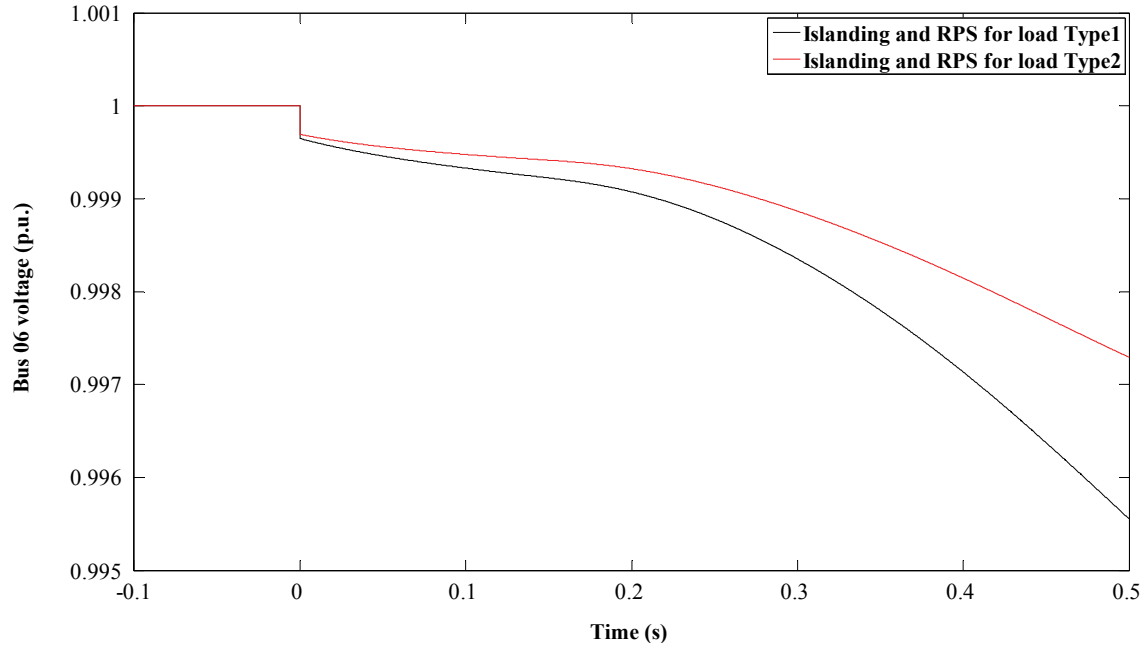

Fig. 2. 8. Bus 06 voltage for islanding and RPS in scenario 2

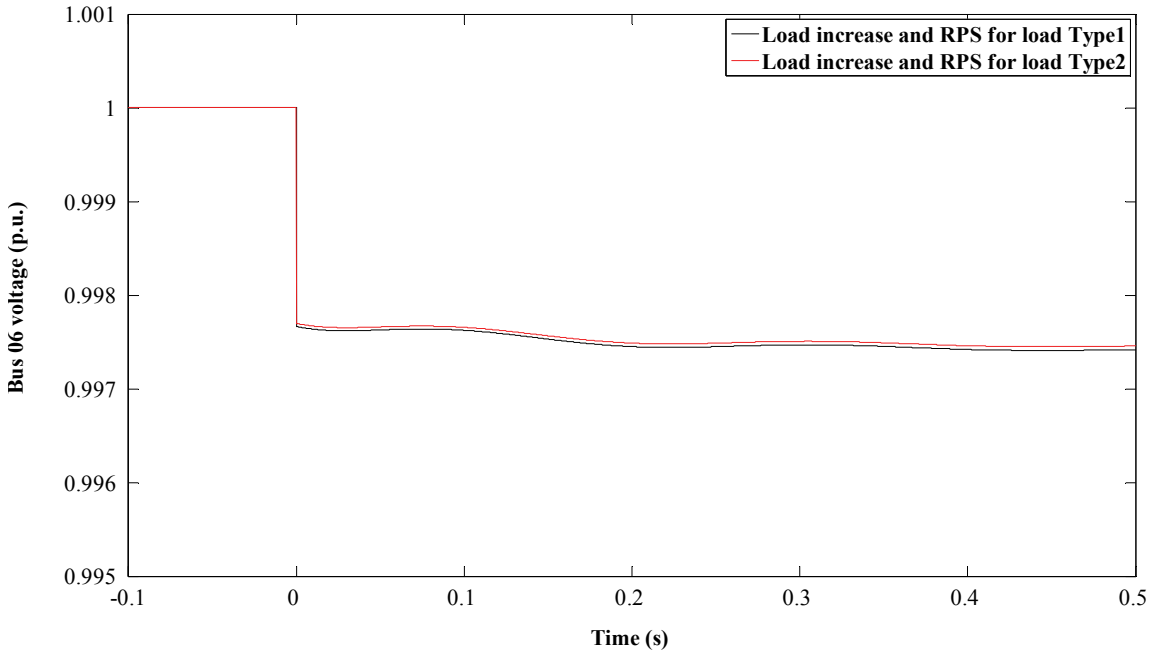

Fig. 2. 9. Bus 06 voltage for Load05 increasing and RPS in scenario 2

Some events in power system like, load increase, switching off of capacitors, faults, starting of motors, switching off of DG units also result in decrease in voltage. These events are also simulated to show the effectiveness of the proposed methodology. Fig. 2. 9 shows the change in voltage at Bus 06 for Load05 increasing and the RPS. In case of Load05 increasing by 1 MW and 1 MVAr, $Av7$ for load types Type1 and Type2 are 350 V/s and 345 V/s, respectively, which are larger than V_{SMin} but smaller than V_{SMax}. Thus, the RPS is initiated. $Av18$ for both load types

is around 7.2 V/s, which is smaller than V_{SMaxU}. Hence, the algorithm ignores the event as any other event other than islanding.

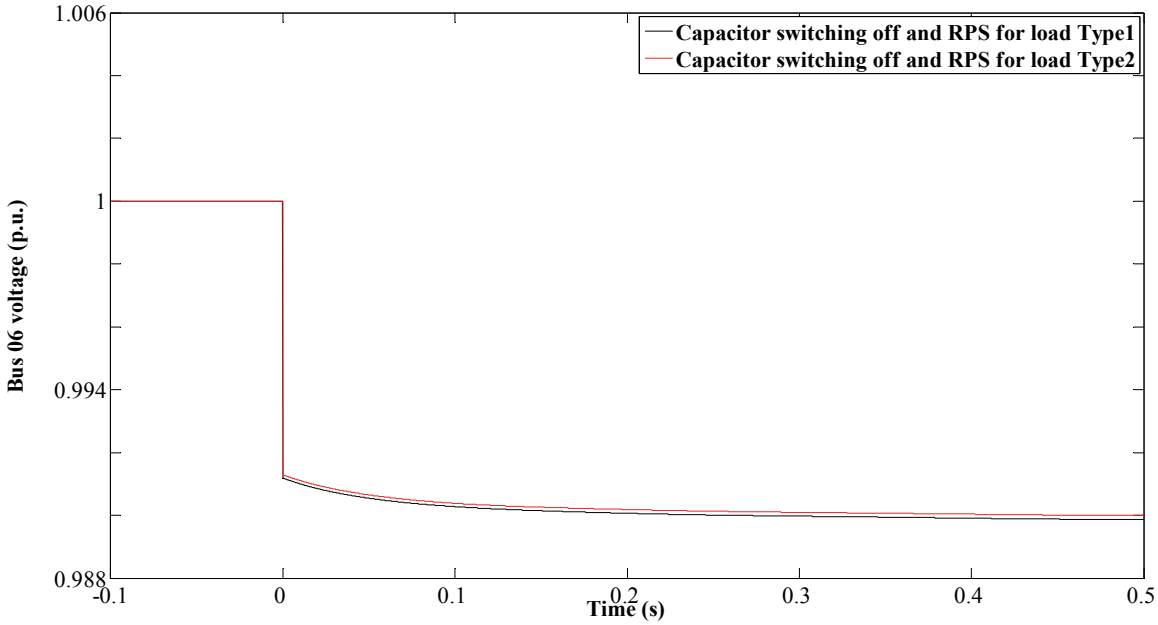

Fig. 2. 10. Bus 06 voltage for capacitor switching off and RPS in scenario 2

Fig. 2. 10 shows the voltage at Bus 06 when the capacitor at Bus 09 switches off at *t=0s* and the RPS is initiated at *t=0.14s*. $Av7$ measured for capacitor switching off event, is 1405 V/s and 1390 V/s for load types Type1 and Type2, respectively. The RPS, initiated as a result of $V_{SMax} > Av7 > V_{SMin}$, results in $Av18$ of 16.83V/s and 15.83 V/s for load types Type1 and Type2, respectively. $Av18$ is smaller than V_{SMaxU} for both load types. Hence, as should be the case, no islanding is detected.

Fig. 2. 11 shows the voltage at Bus 06 when an induction motor load of 0.5 MW is started at Bus 08 at *t=0s* and the RPS is initiated at *t=0.14s*. In case of the induction motor starting at Bus 08 event, $Av7$ is 2586 V/s and 2528 V/s for load types Type1 and Type2, respectively. Again, the values for $Av7$ is larger than V_{SMin} but smaller than V_{SMax}. The RPS is, then, initiated and it results in $Av18$ of 31.1 V/s and 29.2 V/s for load types Type1 and Type2, respectively. They are smaller than V_{SMaxU}. Hence, the algorithm correctly identifies the induction motor starting event as not islanding.

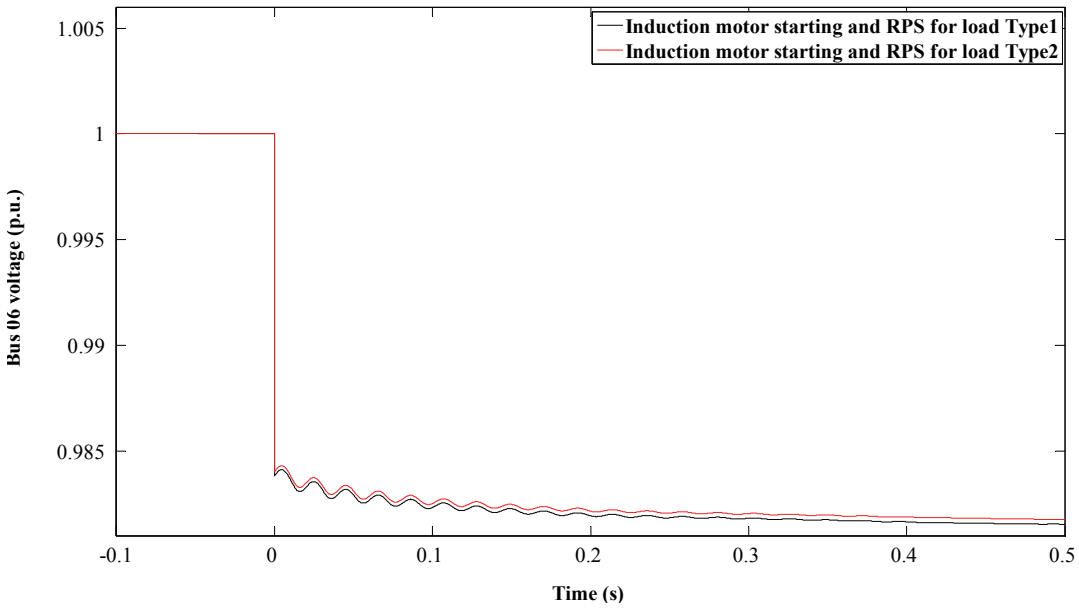

Fig. 2. 11. Bus 06 voltage for induction motor starting and RPS in scenario 2

For the next example, a 3 phase short circuit at Bus 12 is simulated at *t=0s,* the fault is cleared by opening the breaker at the beginning of the line Z11-12 at *t=0.12s.* Fig. 2. 12 shows the voltage at Bus 06 for the short circuit event and the RPS. $Av7$ is 2021 V/s and 1993 V/s for load types Type1 and Type2, respectively. The RPS is initiated as a result of this. $Av18$ of 20.6 V/s and 17.3 V/s are achieved for load types Type1 and Type2, respectively. $Av18s$ are smaller than V_{SMaxU} for all load types. Hence, islanding is not detected.

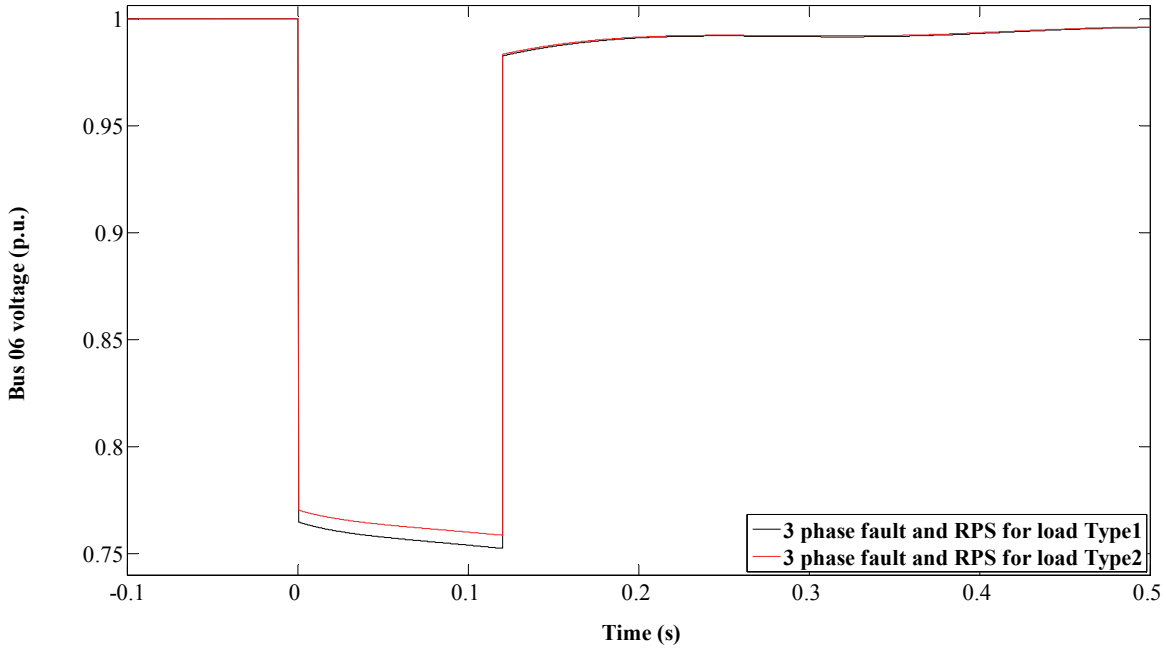

Fig. 2. 12. Bus 06 voltage for three phase fault and RPS in scenario 2

Distribution systems in Denmark and many other countries in Europe use compensated grounding technique that permits sustained operation with fault. As the earth faults don't produce a significant fault current, clearing the fault takes longer time. As an example a single phase to ground fault is simulated at Bus 12 at *t=0s*. The line to line voltage of the faulted phase at Bus 06 for the short circuit event and the RPS is presented in Fig. 2. 13.

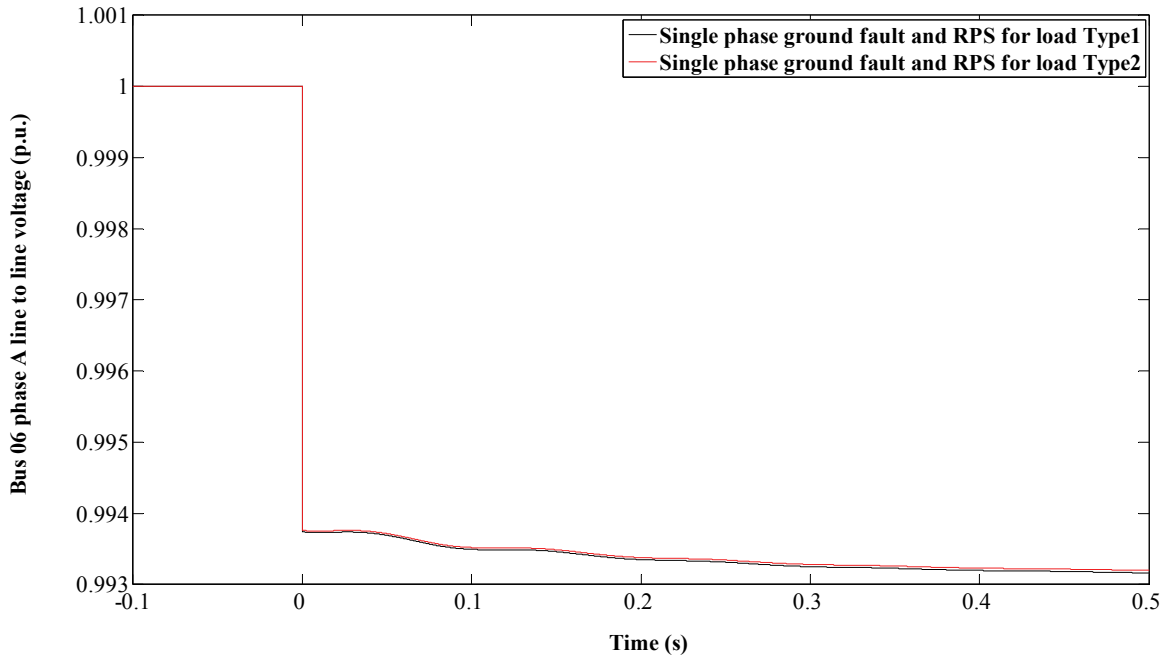

Fig. 2. 13. Bus 06 phase A line to line voltage for a single phase to ground fault and RPS in scenario 2

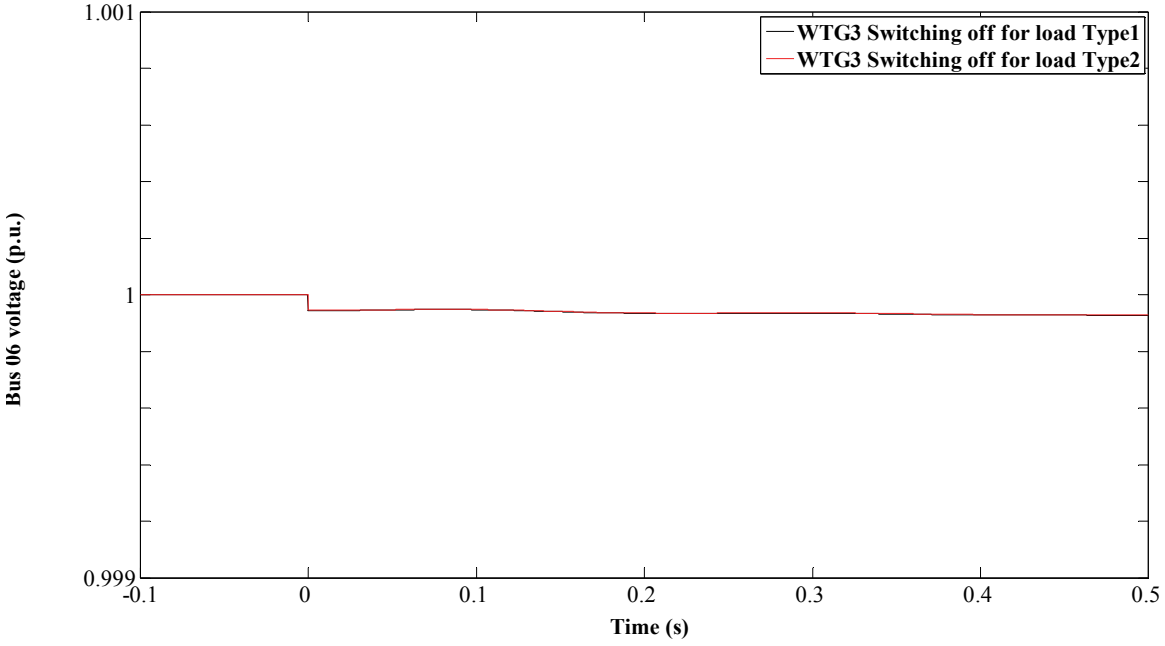

Fig. 2. 14. Bus 06 voltage for WTG3 switching off in scenario 2

In case of a single phase to ground fault, $Av7$ are measured to be 931 V/s and 927 V/s for load types Type1 and Type2, respectively. The RPS is initiated as a result of that. The resulting $Av18$ is around 17 V/s for both load types which are smaller than V_{SMaxU}. Again, the methodology clearly differentiated non islanding event.

An event with WTG3 switching off is now simulated at *t=0s*. The Bus 06 voltage for the event is shown in Fig. 2. 14. $Av7$ for WTG3 switching off event is around 8.2 V/s for both load types. It is interesting to note that $Av7$ for this event is even smaller than V_{SMin}. Therefore, the RPS is not initiated ignoring the event as any other event other than islanding.

2.4.3. Scenario 3

In scenario 3, the load at Bus 05 is adjusted to 7.804 MW and 1.314 MVAr resulting in a power surplus of 0.01 MW and 0.01 MVAr in the distribution system. The surplus of power in the distribution system results in an increase in the voltage in the buses when the distribution system is islanded.

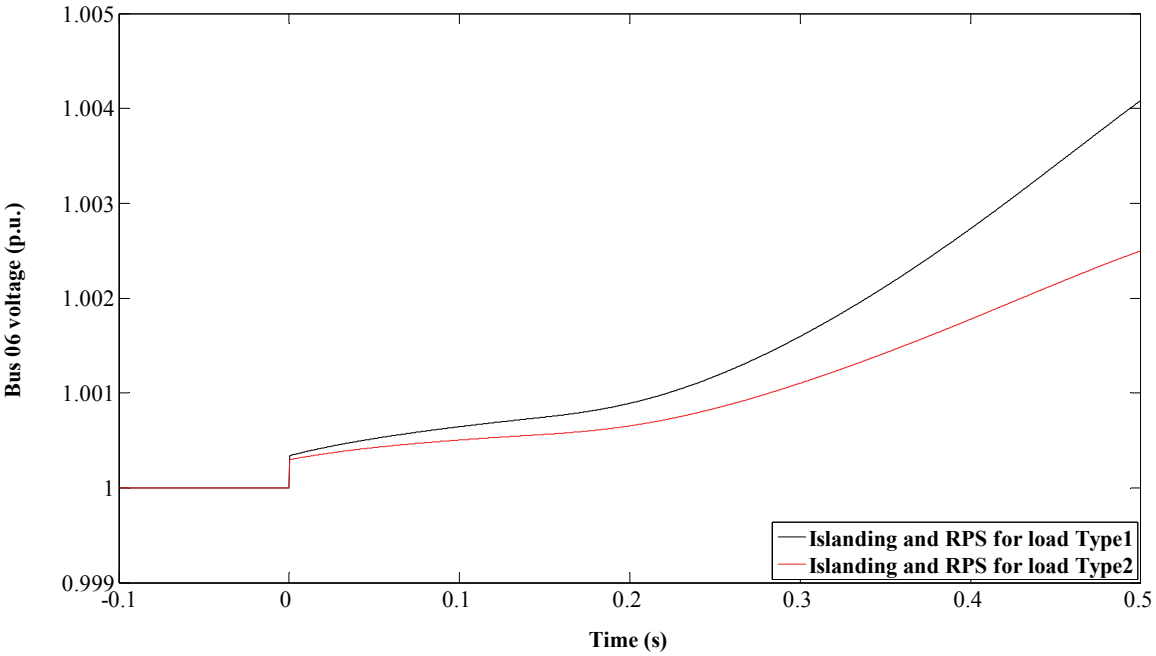

Fig. 2. 15. Bus 06 voltage for islanding and RPS in scenario 3

Fig. 2. 15 shows the voltage at Bus 06 for the islanding event at *t=0s* and the RPS initiation at *t=0.14s*. $Av7$ is 103.7 V/s and 78.9 V/s, respectively for load types Type1 and Type2. Since $V_{SMin} < Av7 < V_{SMax}$, the RPS is initiated. As a result, $Av18$ for islanding are 186.5 V/s and 108.1 V/s for load Type1 and Type2, respectively. Islanding is correctly detected as $Av18 > V_{SMaxU}$. Events in power system like capacitor switching on or load decease also results in increase in

voltage. Therefore, these events are also simulated to see the effectiveness of the proposed islanding detection technique in differentiating these events from islanding.

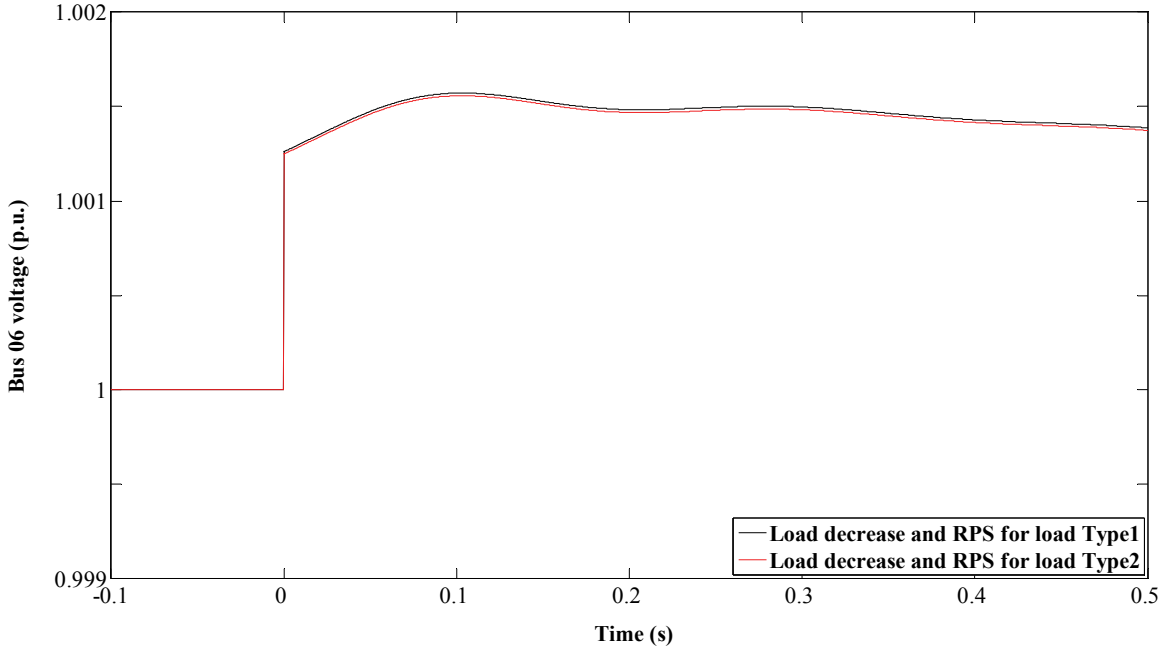

Fig. 2. 16. Bus 06 voltage for load decreasing and RPS in scenario 3

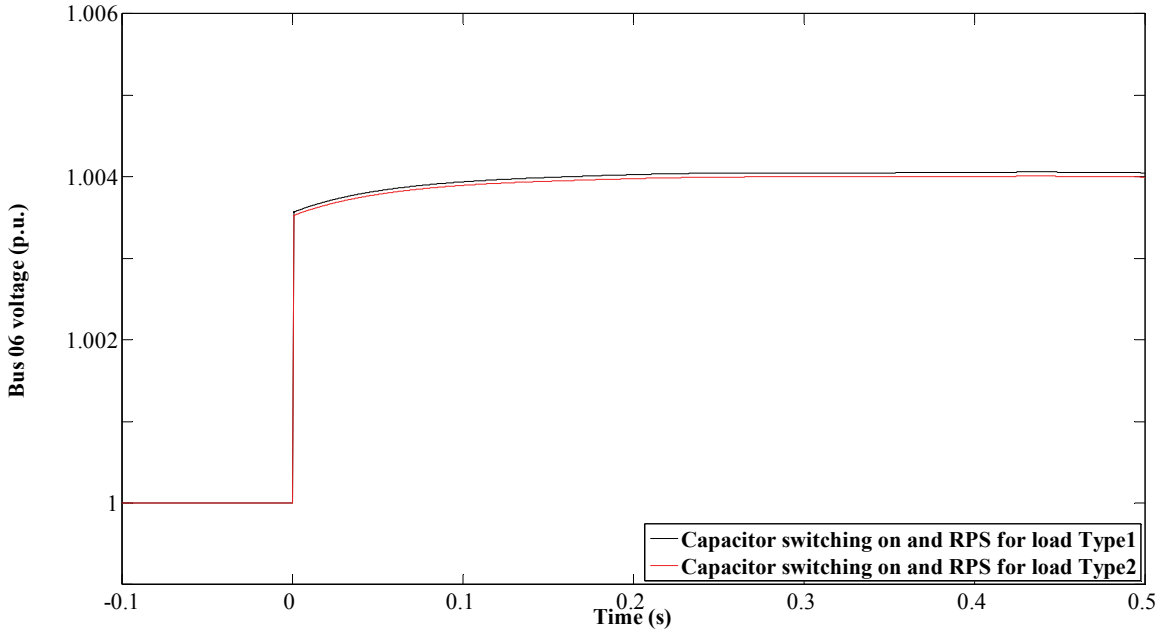

Fig. 2. 17. Bus 06 voltage for capacitor switching on and RPS in scenario 3

Fig. 2. 16 shows the change in Bus 06 voltage for Load05 decreasing by 1 MW and 0.5 MVAr at *t=0s* and the RPS initiation at *t=0.14s*. $Av7$ for the load decreasing event are 220 V/s and 218 V/s for load types Type1 and Type2, respectively. Similarly, $Av18$ for the event, after the

RPS is initiated, is 1 V/s for both load type. This means that islanding is, correctly, not detected as $Av18 < V_{SMaxU}$.

Next, a 1.0 MVAr capacitor switching on at Bus 10 at *t=0s* is simulated. Bus 06 voltage for the event and the RPS initiation at *t=0.14s* is shown Fig. 2. 17. $Av7$, for capacitor switching on event, are 569 V/s and 562.7 V/s for load types Type1 and Type2, respectively. Again, the values for $Av7$ is larger than V_{SMin} but smaller than V_{SMax} and the RPS is initiated. $Av18$ for load types Type1 and Type2 are respectively 3.6 V/s and 3.2 V/s, which are smaller than V_{SMaxU}. Hence, the algorithm correctly ignores the event as non islanding event.

2.4.4. Scenario 4

In scenario 4, the load at Bus 05 is adjusted so that the distribution system has deficiency of 0.01 MW and 0.01 MVAr before the events occur. An islanding is simulated by opening the breaker *at t =0s*.

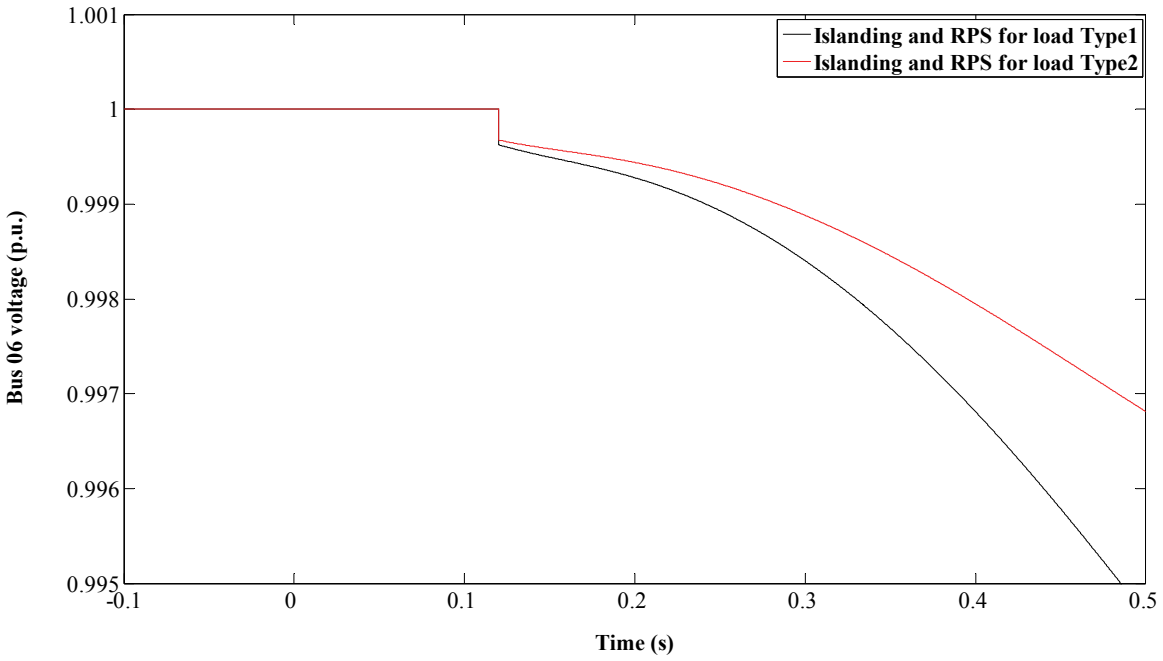

Fig. 2. 18. Bus 06 voltage for islanding and RPS in scenario 4

Fig. 2. 18 shows the Bus 06 voltage for the islanding and the RPS initiation at *t=0.14s*. $Av7$ of 99.8 V/s and 78.7 V/s are achieved for the islanding case, for load types Type1 and Type2, respectively. Therefore, RPS is initiated and $Av18$ of 270.7 V/s and 155.4 V/s are achieved for load types Type1 and Type2, respectively, meaning that island is detected.

An event of WTG3 connecting to the distribution system also results in drop of voltage and hence it is simulated to see the effectiveness of the proposed methodology. Fig. 2. 19 shows the Bus 06 voltage for a wind turbine generator at Bus 14 (WTG3) switching on at *t=0s* and the RPS

initiation at *t=0.14s*. $Av7$ for WTG3 switching on event are 1251 V/s and 1236 V/s for load types Type1 and Type2, respectively. $Av7$ s are larger than V_{SMin} but smaller than V_{SMax}. Thus, the RPS is initiated. Now, $Av18$ for load types Type1 and Type2 are both around 22 V/s, which is smaller than V_{SMaxU}. Hence, correctly, islanding is not detected.

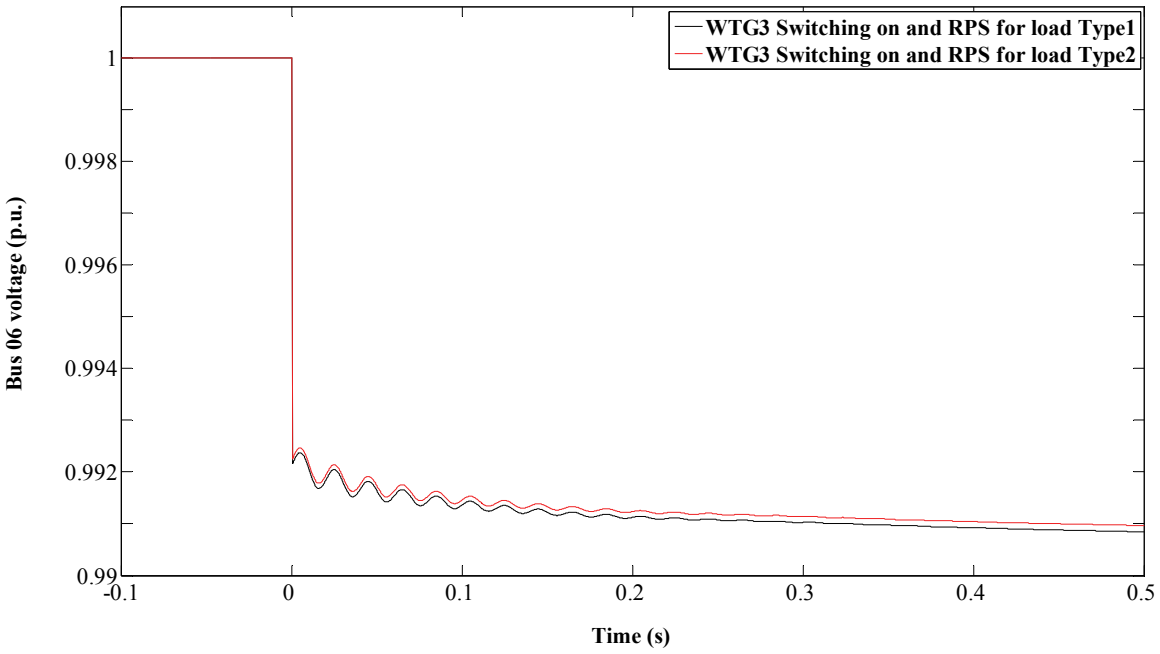

Fig. 2. 19. Bus 06 voltage for WTG3 switching on and RPS in scenario 4

Many events in the power system produce voltage change that can have the average rate of voltage change, which can easily exceed the average rate of voltage change achieved by islanding. Also some of the events produce very small change in voltage. If the RPS is applied for those voltage changes, then it may have to be applied frequently. By setting V_{SMin} to detect the islanding for power mismatch of 5 kW and 5 kVAr and more, initiation of the RPS for small events are avoided. However, islanding with a smaller power mismatch is also missed. Therefore, setting a V_{SMin} is system specific and depends on choice of sensitivity. If a close match between demand and generation is expected, then V_{SMin} should be kept small. This may result in the frequent RPS initiation. On the other hand, frequency of the RPS initiation can be reduced by setting higher V_{SMin} at the expense of sensitivity.

The simulation results show that when there is a large mismatch in generation and demand, islanding can easily be detected by observing the rate of voltage change. As expected, it is difficult to detect islanding when load and generation in the islanded distribution system closely match by simply observing the rate of voltage change. The simulation results also show that the RPS initiated after the suspicion of islanding results in higher rate of voltage change when the distribution system

is actually islanded compared to other events in the distribution system when it is still connected to grid. In other words, the RPS doesn't change the bus voltages much when the distribution system is connected to the transmission grid. However, the RPS initiated after the suspicion of islanding changes the bus voltages significantly when the distribution system is islanded. Hence, the RPS can have absolute discrimination between islanding and other events even when the load and generation of islanded distribution system closely match. Table 2. 2 summarizes all the results.

Table 2. 2

Summary of results for islanding and different events

Events	*Av*7 (V/s)		*Av*18 (V/s)	
	Load		Load	
	Type1	Type2	Type1	Type2
Scenario 1				
Islanding	10975	7792	-	-
Scenario 2				
Islanding	108	78.9	205	118.5
Load increase	350	345	7.6	7.2
Capacitor switch off	1405	1390	16.83	15.83
Induction Motor starting	2586	2528	31.1	29.2
3 phase short circuit	2021	1993	20.6	17.3
1 phase to ground fault	931	927	17.56	17.11
WTG switching off	8.28	8.21	-	
Scenario 3				
Islanding	103.7	78.9	186.5	108.1
Load decrease	220	218	1	1
Capacitor switch on	569.1	562.7	3.61	3.27
Scenario 4				
Islanding	99.75	78.71	270.6	155.39
WTG switching on	1251	1236	22.1	22.06

2.5 Conclusions

The recently developed islanding detection algorithms can be mainly divided into passive and active techniques. The passive techniques have larger non detection zone. On the other hand, active techniques have small or no non detection zones but they introduce perturbations at regular interval. This may degrade the power quality. Moreover, the perturbations are unnecessary at times. A hybrid technique has been proposed to detect islanding of a distribution system with DG units operating at unity power factor. It combines the real power shift and the average rate of voltage

change to detect islanding under various loading conditions. The proposed technique uses the RPS only when the passive technique (average rate of voltage change) cannot have a clear discrimination for the suspected islanding condition. This eliminates the necessity of injecting disturbance from time to time to detect islanding unlike other active techniques. The RPS only changes the real power of DG, which satisfies the condition of DG operating at unity power factor. Simulation results show that the proposed technique is able to discriminate islanding from various other events in the distribution system. Furthermore, islanding can be detected even when the load and the generation closely match. Although the method may fail to detect islanding for a perfect match of demand and generation in the islanded distribution system, any subsequent change in load or generation in the islanded distribution system leads to change in voltage and the islanding being detected.

Chapter 3

Control and Operation of Distributed Generation

When islanding is detected, the owner of the distributed generation has two choices; either to shut down or continue to operate DG and supply the loads in the islanded distribution system. Although most countries requires DG to be shutdown when it is islanded because of various issues mentioned in Chapter 1, it can operate in island mode to increase the reliability of the power supply provided that all the issues with islanding is properly addressed. Europe has been able to integrate a large number of wind turbines and small district combined heat and power plants (DCHP) into the power system [50] and these are also the two technologies that have been widely used in Denmark [51]. Gas turbines have become increasingly popular due to their lower greenhouse emission as well as the higher efficiency, especially when connected in a combined cycle setup [52]. The large wind farms connected at transmission level have variable speed WTGs but old small wind turbines connected at the distribution level are largely fixed-pitch and fixed-speed turbines. Hence the scope of this chapter is limited to only the gas turbines and the fixed-speed and fixed-pitch wind turbines DG technologies. However, issues with voltage and frequency discussed in this chapter are valid for all the DG technologies. Moreover, the controller and the control strategies developed in this chapter may be used in other DG technologies.

Distribution systems can take advantage of this significant DG penetration and operate in island mode. However, there are various issues to be resolved before islanding operation can be realized. One of the main issues with the islanding operation are control of frequency and voltage in the islanded distribution system. Section 3.1 deals with the modelling of fixed-speed and fixed-pitch wind turbines. Section 3.2 deals with the modelling of gas turbine generators. Section 3.3 and Section 3.4 deal with load-frequency control and voltage-VAr control, respectively. Control and operation of DG for island operation is presented in Section 3.5. Some simulation results are presented in Section 3.6 and some conclusions are drawn in Section 3.7.

3.1 Wind Turbine Model

A WTG model consists of an aerodynamic model, a mechanical model and a generator model. The mechanical model for the drive train can be modelled as a two-mass model or a single-mass model. In the two-mass model, one mass accounts for hub and blades and the other accounts for the rotor of the generator. In the single-mass model, all the rotating parts of the windmill are lumped in a single mass. Various wind turbine models have been proposed in different literatures

[48], [53]-[56]. A simplified block diagram of a fixed-pitch fixed-speed wind turbine system is shown in Fig. 3. 1. For the purpose of this study, wind turbines are modelled as a two-mass system as it is adequate for power system transient studies [49].

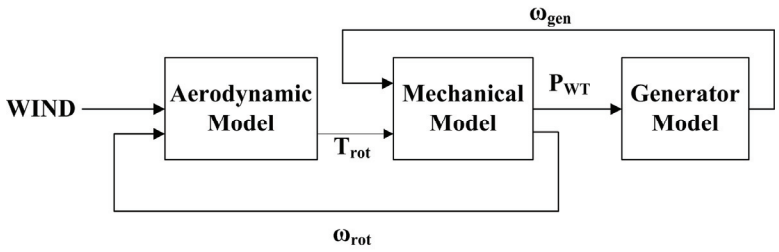

Fig. 3. 1. Simplified wind turbine generator model

In the aerodynamic model block, the aero dynamic torque (T_{rot}) developed by wind is given by equation 3.1 [57].

$$T_{rot} = \frac{1}{\omega_{rot}} C_p \left(\frac{\rho \pi R^2 v^3}{2} \right) \tag{3.1}$$

Where, ρ is the air density, R is the turbine rotor radius, v is the wind velocity, ω_{rot} is the rotor speed and C_p is the power coefficient, which is a function of the tip speed ratio (λ) for the fixed-pitch turbines. λ is given by equation 3.2 [57].

$$\lambda = \frac{R\omega_{rot}}{v} \tag{3.2}$$

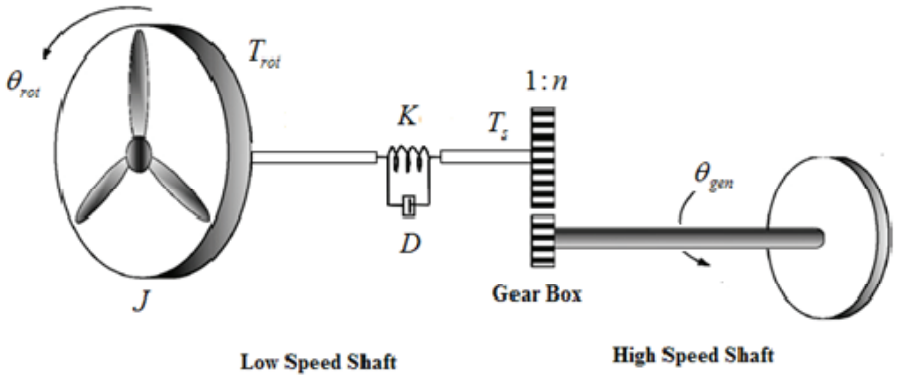

Fig. 3. 2. Two mass model of a of wind turbine drive train

The mechanical block for the drive train is shown in Fig. 3. 2 [48], [53]. In case of a two-mass model, the low speed shaft is modelled by a stiffness *K* and a damping coefficient *D*. The high-speed shaft is assumed stiff. Also, an ideal gear-box with a ratio *(1:n)* is included. The angular difference between the two ends of the flexible shaft (θ) is given as in equation 3.3 and the rotor speed is given as in equation 3.4 [53].

$$\frac{d\theta}{dt} = \omega_{rot} - \frac{\omega_{gen}}{n} \tag{3.3}$$

$$\frac{d\omega_{rot}}{dt} = \frac{\left(T_{rot} - T_s\right)}{J} \tag{3.4}$$

where, ω_{gen} is the generator speed and J is the inertia of the rotor. The mechanical torque on the low speed shaft (T_S) is given by equation 3.5 and the power from the wind turbine to generator (P_{WT}) is given by equation 3.6 [53], [58]. Here, K is the drive train stiffness and D is the drive train damping constant.

$$T_s = K\theta + D\left(\omega_{rot} - \frac{\omega_{gen}}{n}\right) \tag{3.5}$$

$$P_{WT} = \frac{\omega_{gen}}{n} T_S \tag{3.6}$$

3.2 Modelling of Gas Turbine

A gas turbine usually consists of a compressor and a turbine operating under the Brayton cycle [59]. Fig. 3. 3 shows the simple layout of the gas turbine operating in a simple cycle without any heat recovery. The Brayton cycle consists of four completely irreversible processes namely; isentropic compression, isobaric heat addition, isentropic expansion, and isobaric heat rejection as shown in Fig. 3. 4.

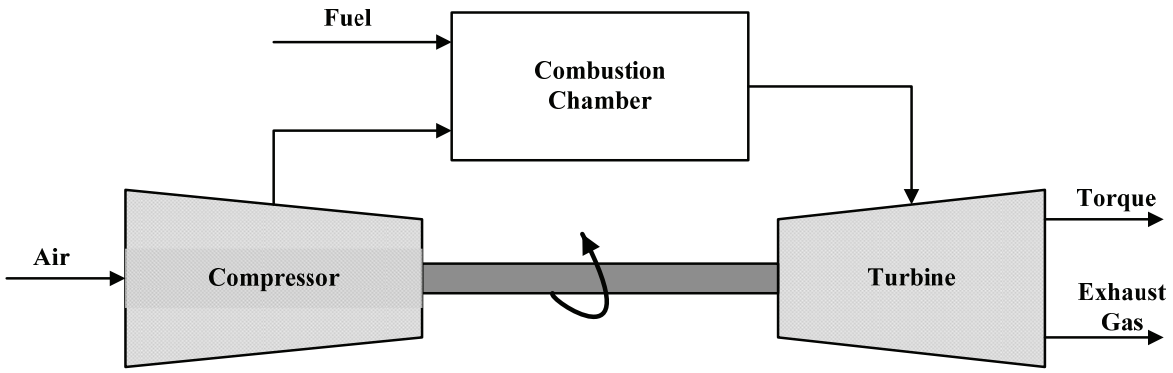

Fig. 3. 3. Open cycle gas turbine

Various gas turbine models have been proposed for stability analysis. Rowen proposed a simplified mathematical model for heavy duty gas turbines in [60]. He extended the model by including inlet guide vanes in [61]. But the control loops for the speed and acceleration remained

essentially the same. IEEE also presented a model of gas turbine in [62]. Another model for gas turbine is GAST model [47]. CIGRE presented yet another gas turbine model in [63]. These models and other models are reviewed in details in [64]. The GAST model is the most commonly used dynamic model for power system studied [65] and hence also used for the purpose of this study.

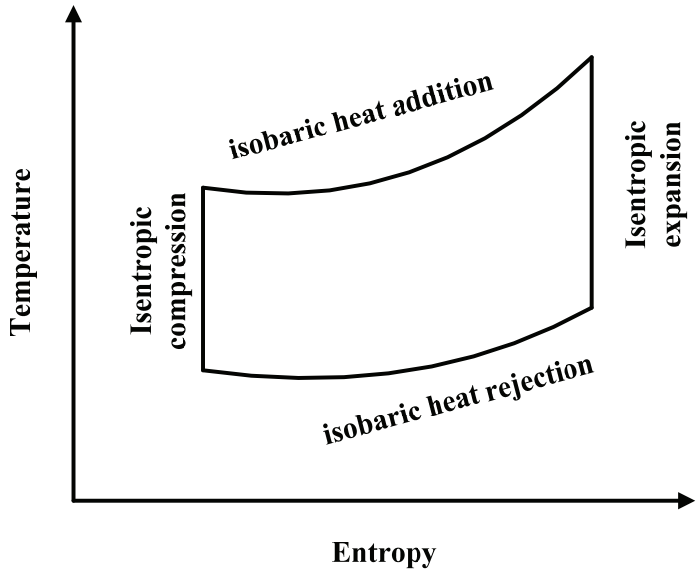

Fig. 3. 4. Temperature versus entropy diagram of the Brayton cycle

The GAST model for the gas turbine generator is shown in Fig. 3. 5. In Fig. 3. 5, T_1 is the controller time constant, T_2 is the fuel system time constant, T_3 is the load limiter time constant, A_T is the ambient temperature load limit, K_T is the temperature control loop gain, V_{Min} and V_{Max} are the fuel controller's minimum and maximum output, respectively, and D_{Turb} is the frictional losses factor.

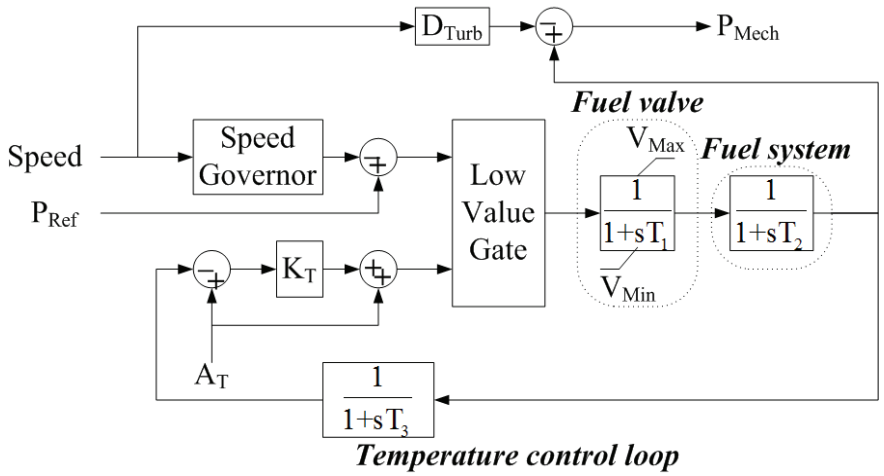

Fig. 3. 5. GAST model for gas turbines

The speed governor compares the generator's speed with the reference speed and outputs and an error signal which goes into the low value gate. The low value gate also gets input from the temperature control loop. It selects the lowest input. When the load on the turbine increases, the output power of the gas turbine also increases. If this increase is higher than the maximum rated power at ambient temperature, the temperature control loop is activated. In other words, its output will take control of the response of the turbine as its output will be lower than that of the speed governor. However, if the output power is less than the ambient temperature load limit, the speed governor output will take control of the turbine response. Since the power produced by the fixed speed wind turbines is a function of the wind speed only, their output power cannot be controlled. The only way to control the power and hence the frequency in the test distribution system, when it is islanded, is by controlling the power of the gas turbines by choosing a suitable speed governor control.

3.3 Load-Frequency Control and Modelling of Speed Governor

The conventional speed governor control is the droop control, which is a proportional (P) control. A droop, usually refereed in percentage, is a straight line function with a slope that is given by the ratio of change in frequency and the generator loading in percentage. Fig. 3. 6 shows a 6% droop curve. It changes the reference speed whenever there is a load change in the system and finds the new operating point based on its droop characteristics.

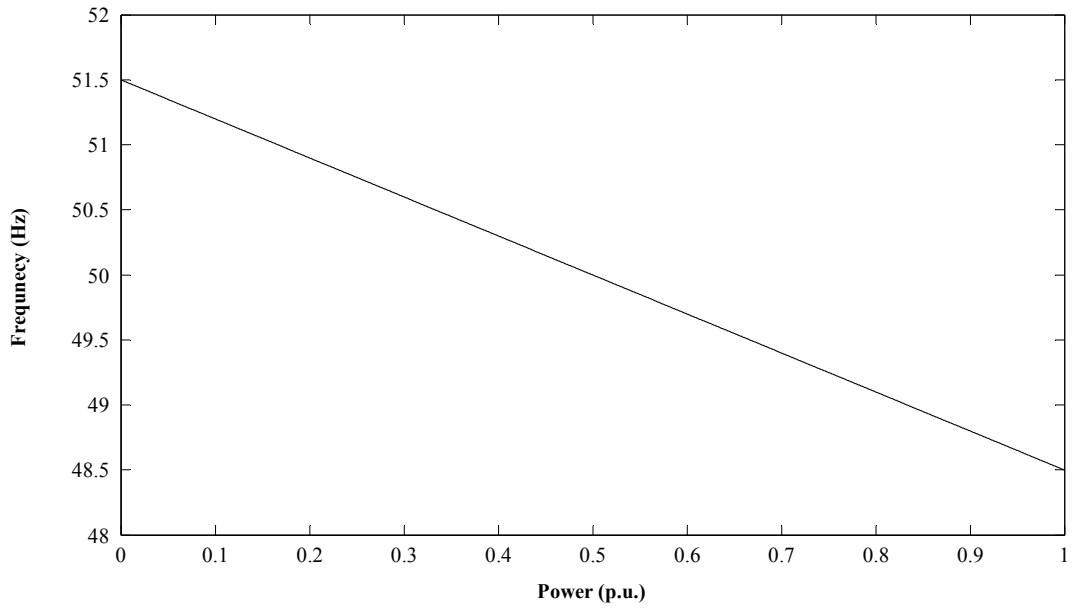

Fig. 3. 6. A 6% droop curve

The GAST model with the speed droop controller is shown in Fig. 3. 7, where R represents speed droop. As a case study, the test distribution system, presented in Fig. 2. 6, is islanded at *t=0s*. In this case, the GTGs have 5% droop and their output power is 1 MW each.

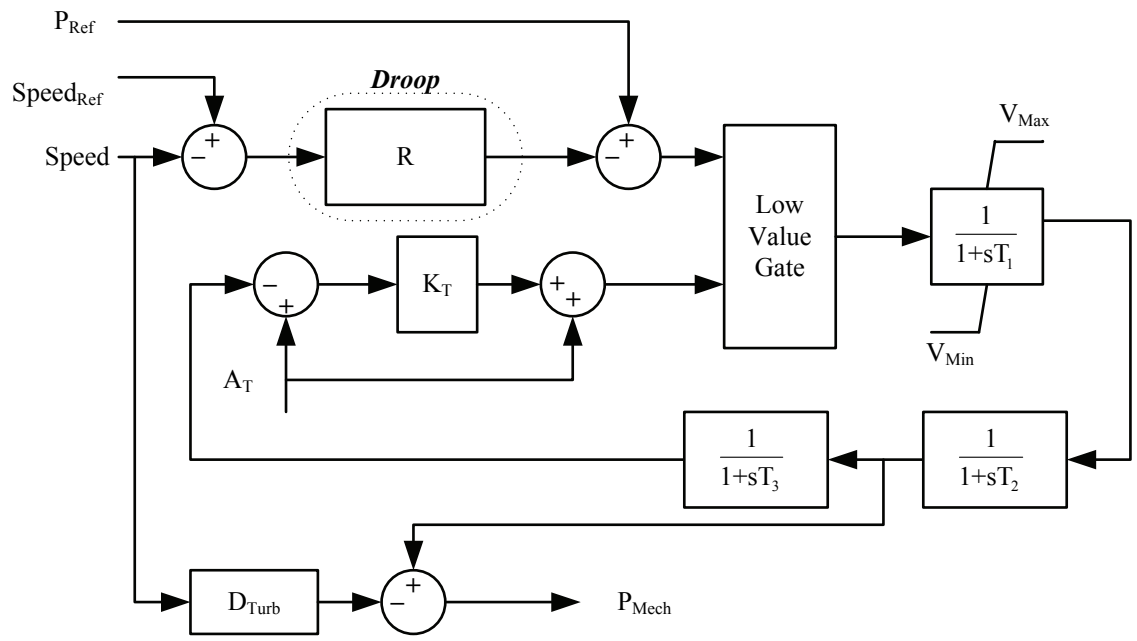

Fig. 3. 7. GAST model for gas turbines with droop control

When islanded, the distribution system has a real power deficiency of around 5 MW and generators have reserve of 6 MW. Fig. 3. 8 shows the frequency of the islanded distribution system. The frequency settles well below 49 Hz and this may be unacceptable in many power utilities. The alternative to the droop control is an isochronous control.

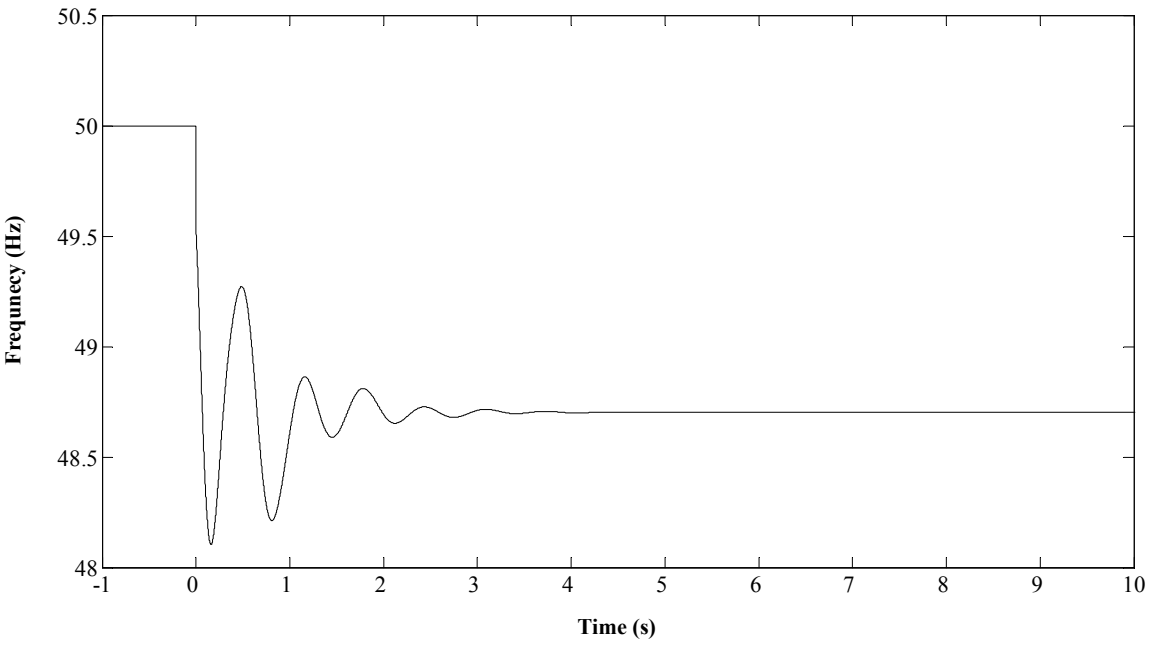

Fig. 3. 8. Frequency of the islanded distribution system with speed droop control

An isochronous controller is basically a Proportional Integrator (PI) controller which has the ability to return to original speed after a change in load. The GAST turbine model with an

isochronous controller is shown in Fig. 3. 9. K_i and T_i are the isochronous controller's gain and time constant, respectively.

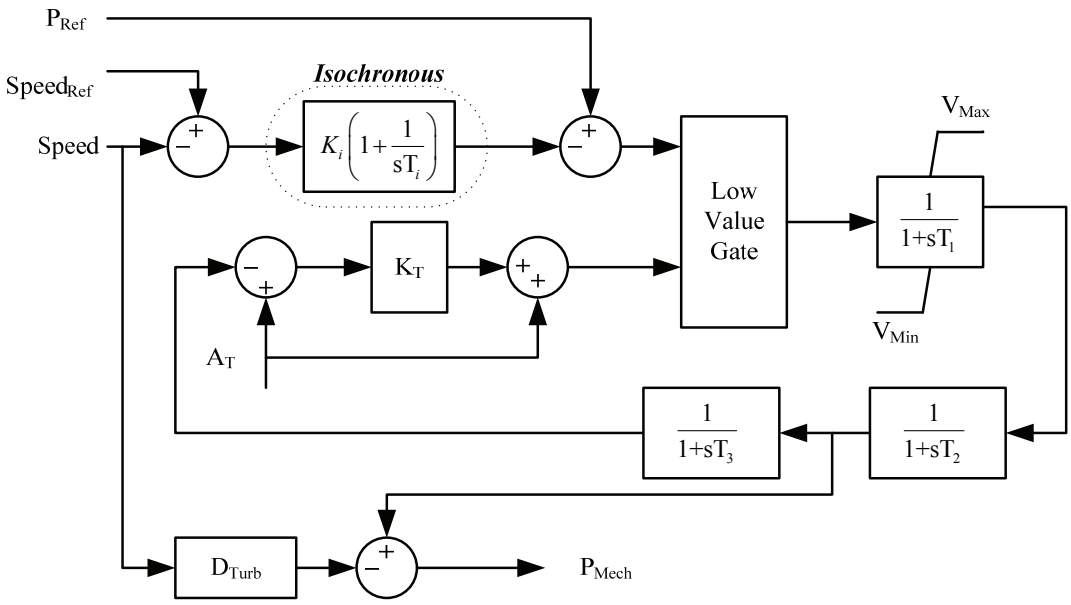

Fig. 3. 9. GAST model for gas turbines with isochronous controller

In another test case, the distribution system, presented in Fig. 2. 6, is again islanded at *t=0s*. The GTGs output power is again 1 MW each. Moreover, for simulation purpose, each GTG have isochronous controller with K_i=40 and T_i =*1s* and controller time constant as 0.1.

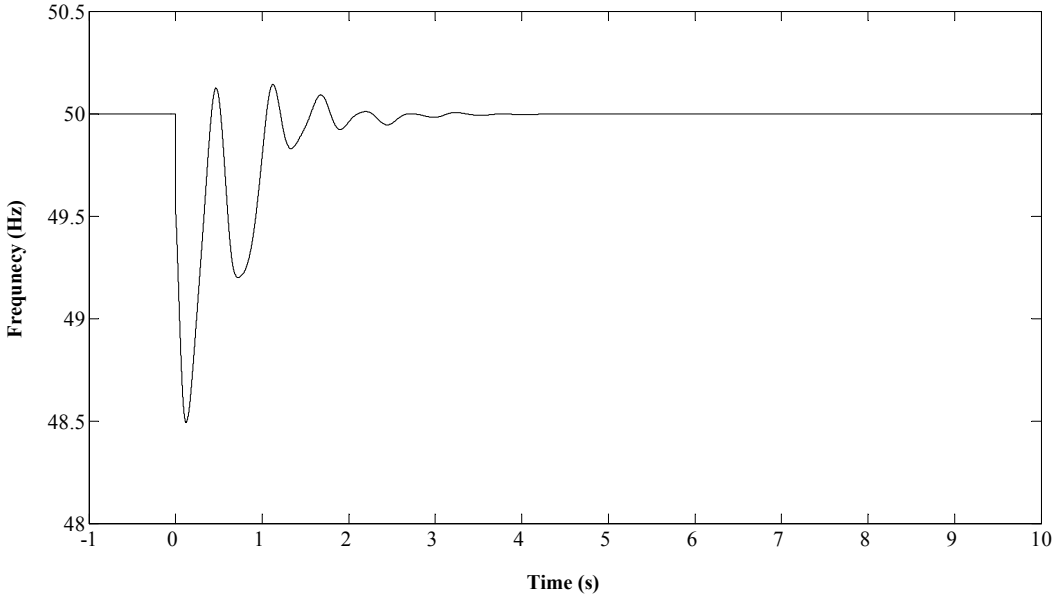

Fig. 3. 10. Frequency of the islanded distribution system with isochronous controller

The frequency of the islanded distribution system with isochronous controller is shown in Fig. 3. 10. As shown in Fig. 3. 10, the isochronous controller brings the frequency back to 50 Hz when the distribution system is islanded. To see the performance of isochronous controller when the distribution system is connected to the grid, a test case is simulated by changing grid frequency slightly while the GTG, with isochronous controller, is still connected to the grid. Fig. 3. 11 shows the change in grid frequency and the GTG turbine power. As shown in Fig. 3. 11, the isochronous controller lowers the GTG turbine power as a consequence of the increase in grid frequency, to bring the speed back to reference speed. But, since the grid is too strong compared to the small DG units, they cannot bring the frequency back to the reference. Eventually, the turbine power becomes zero. It makes no economical sense to reduce the power generation to zero to maintain system frequency to nominal when the reduction in power production is hardly having any impact in system frequency.

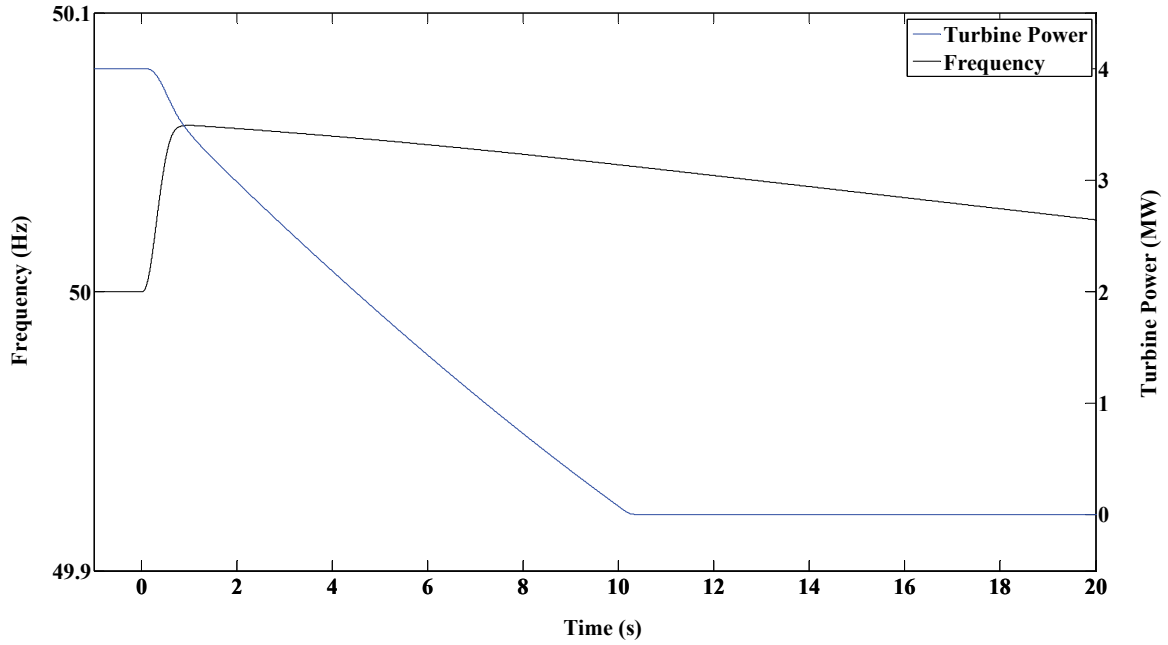

Fig. 3. 11. Performance of isochronous controller during grid frequency change

On the other hand, the droop control changes the speed reference and finds the new operation point, as shown in Fig. 3. 12, when the grid frequency deviates. Therefore, for a small DG, having a droop control helps when the distribution system is connected to the transmission grid as output power does not change much with changing grid frequency. On the other hand, the isochronous controller brings frequency back to reference when the distribution system is islanded. But, keeping the same control strategy all the time may result in output power and/or frequency, which are undesirable when the distribution system changes states. The most desirable is to have least fluctuation in power when the small generators are connected to grid. Though at the same time, maintaining frequency within an acceptable limit for islanding operation is also a priority.

This led to the development of isochronous controller with feedback, which is presented in Fig. 3. 13. K_{FB} is the feedback gain.

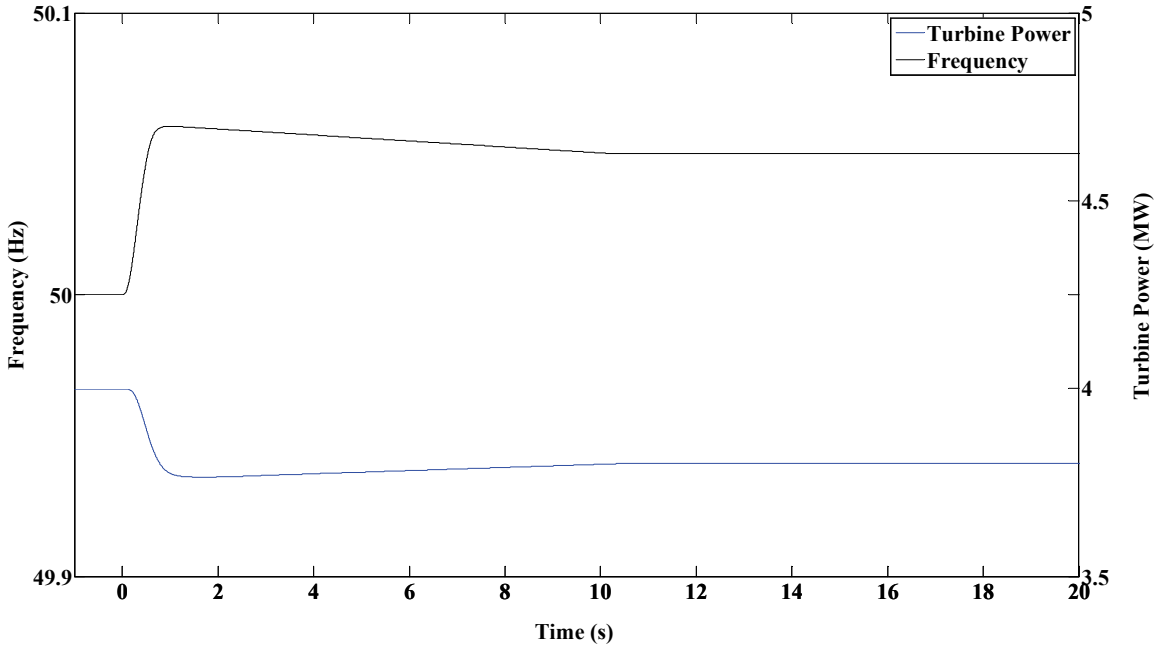

Fig. 3. 12. Performance of droop controller during grid frequency change

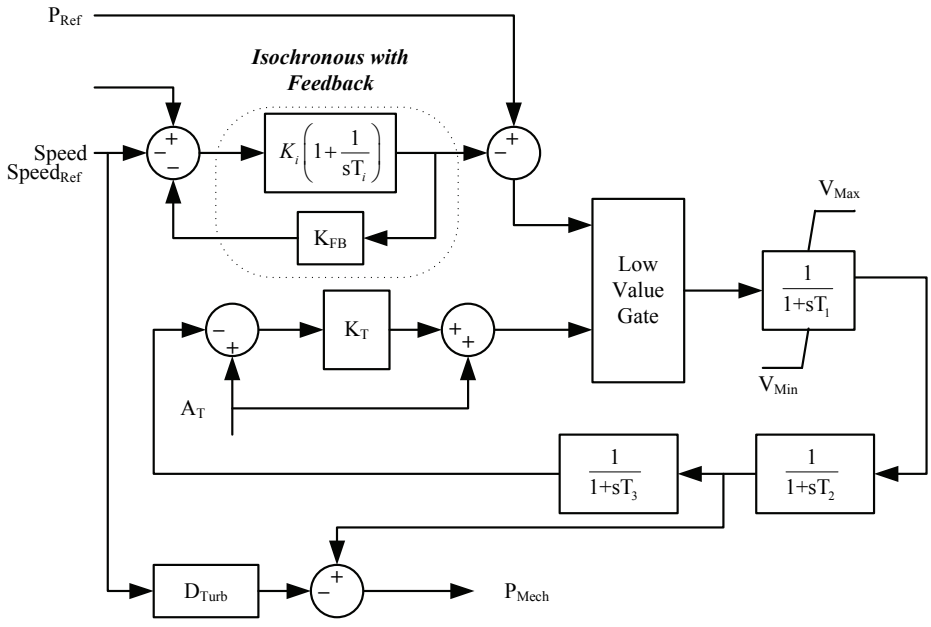

Fig. 3. 13. GAST model for gas turbines with isochronous controller with feedback

A scenario using the distribution system, presented in Fig. 2. 6 is simulated where the grid frequency is increasing as shown in Fig. 3. 12. The distribution system is connected to the grid and the GTGs employ the isochronous controller with feedback. Fig. 3. 14 shows the turbine power

with the isochronous controller with feedback compared to the output power using the droop controller and the isochronous controller. The isochronous controller with feedback finds the new operating point similar to the speed droop controller and does not reduce power to zero when grid frequency increases.

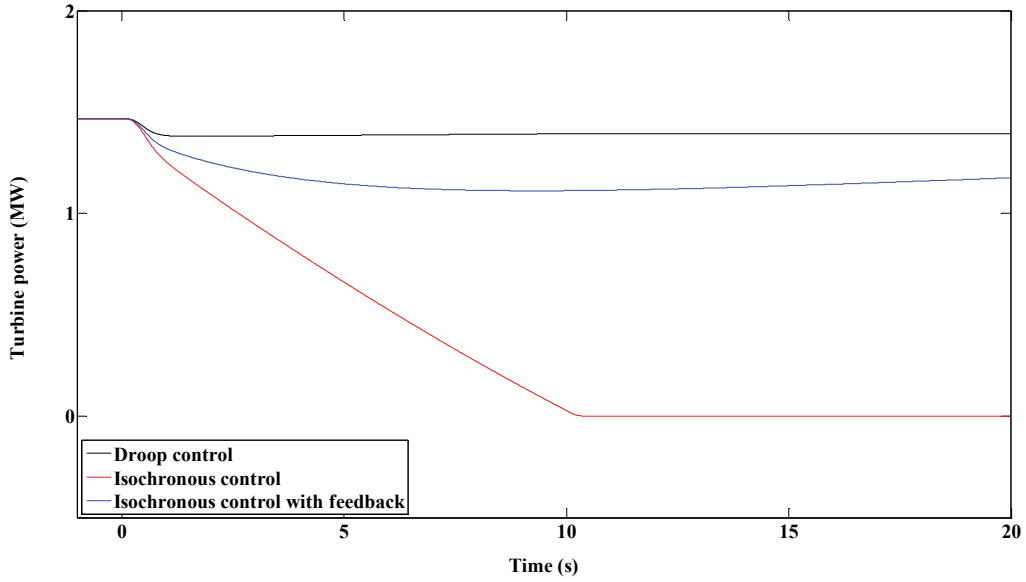

Fig. 3. 14. Performance of controllers during grid frequency change

Fig. 3. 15 shows the frequency of the distribution system, with these three different controllers, when it is islanded. Although the isochronous controller with feedback does not bring the frequency back to nominal value, the final frequency error is significantly less compared to the one with the speed droop controller.

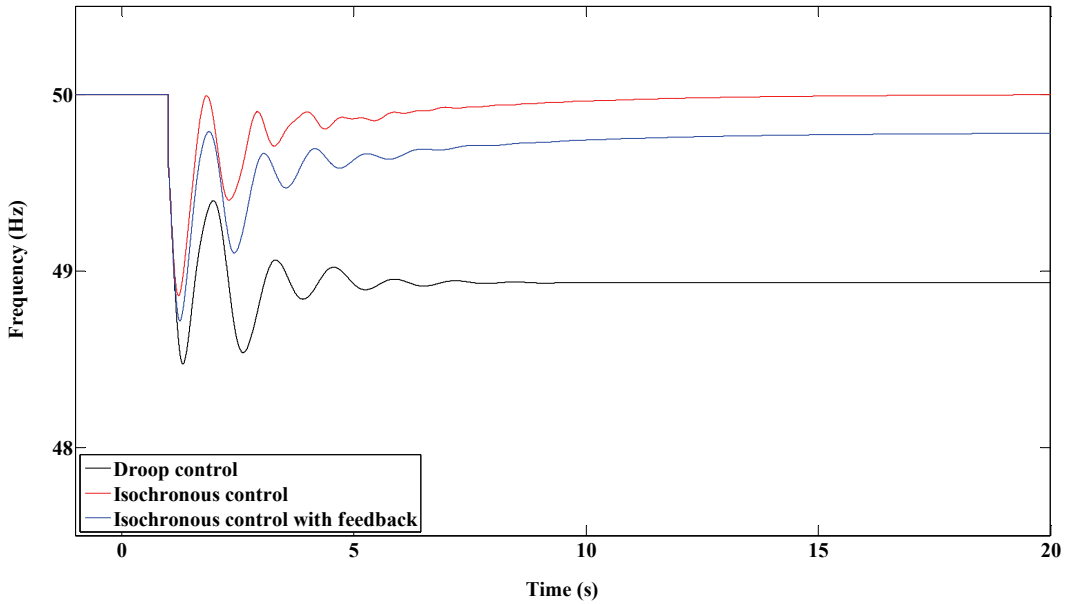

Fig. 3. 15. Performance of controllers during islanding

It can be seen from Fig. 3. 14 and Fig. 3. 15 that the isochronous controller with feedback performs relatively well in both islanded and grid connected conditions. The output power is not driven to limits when the power system frequency fluctuates and it keeps the frequency within acceptable limits when the distribution system is islanded.

3.4 Voltage-VAr Control and Modelling of Excitation System

When a generator is connected to utility, the two oblivious choices of control for the excitation system are the terminal voltage control and reactive power control (VAr control) or power factor (PF) control. When the excitation system is designed for VAr or PF control, generator tends to follow the voltage variation of the grid rather than try to regulate the voltage. Some utilities may require the small generators to operate at unity power factor and there is economic incentive to do that as well. In addition, the impact of change in reactive power of these small generators in the system voltage is minimal when they are connected to stiff grid. When the grid voltage change, the small generators try to maintain voltage at the set point when they are designed to control terminal voltage. This may cause over or under excitation.

A simple test system with a 4.9 MVA DG connected to a strong grid is presented in Fig. 3. 16. The transmission grid is modelled by twenty 255 MVA synchronous generators operating in parallel. The generators data and their excitation systems data are presented in Table AIX and Table AX, respectively.

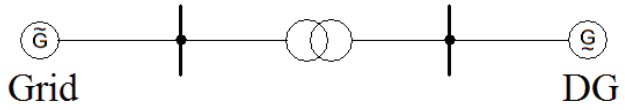

Fig. 3. 16. A simple test system

Fig. 3. 17 and Fig. 3. 18 show the reactive power from the DG when there is an increase and decrease in terminal voltage, respectively. The increase in terminal voltage leads to under excitation of the generator and may result in loss of synchronism [66]. On the other hand, low terminal voltage may cause overloading and excessive heating of the generators. According to [67], small generators' operation at VAr/power factor control mode is justifiable. However, when the distribution system is islanded, the voltage might go beyond the power quality limits. In such a case, small generators have to maintain the distribution system voltage by operating in voltage control mode.

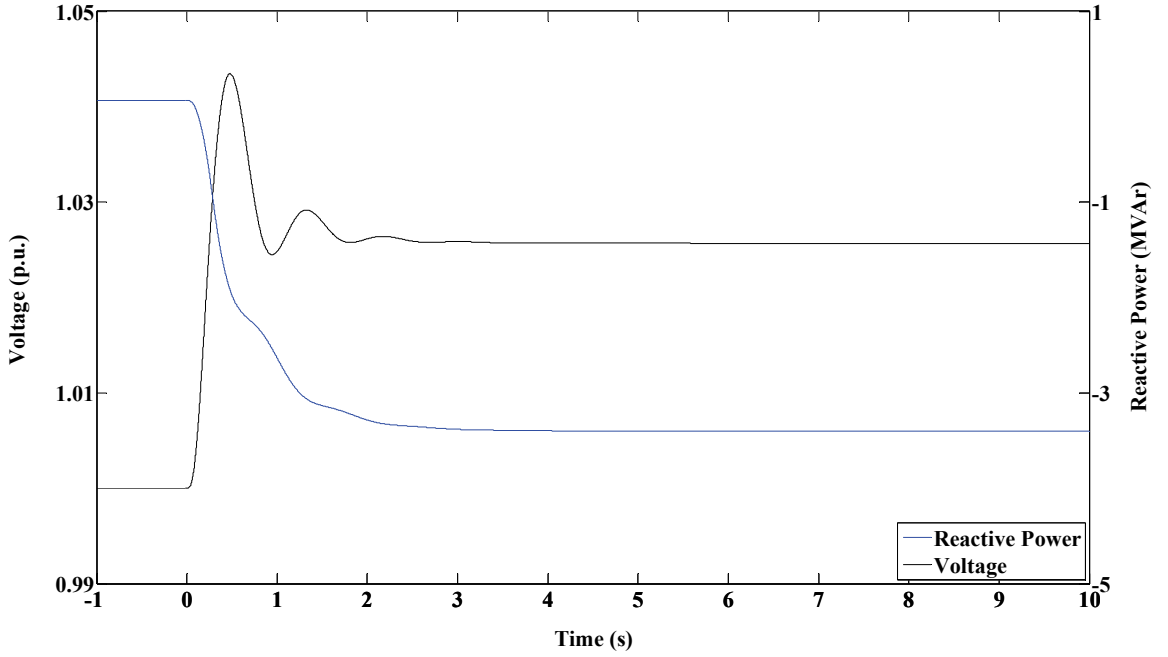

Fig. 3. 17. Reactive power of DG for voltage rise at terminal

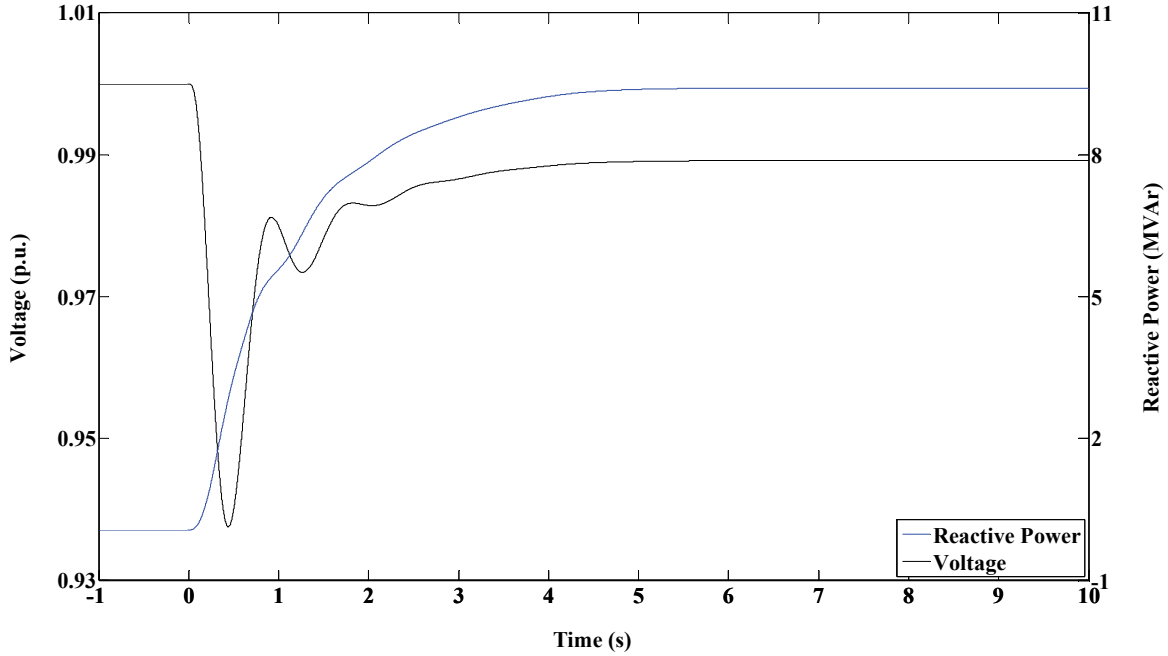

Fig. 3. 18. Reactive power of DG for voltage drop at terminal

The IEEE Type AC5A excitation system, which is a simplified model for brushless excitation systems, is used to represent small excitation systems and has been widely implemented by the industries [68]. Hence, for the purpose of this study, this model has been used. The IEEE Type AC5A excitation system is presented in Fig. 3. 19. The time constant (Ta) and the gain (Ka) are associated with the voltage regulator. The output of the voltage regulator is used to control the exciter.

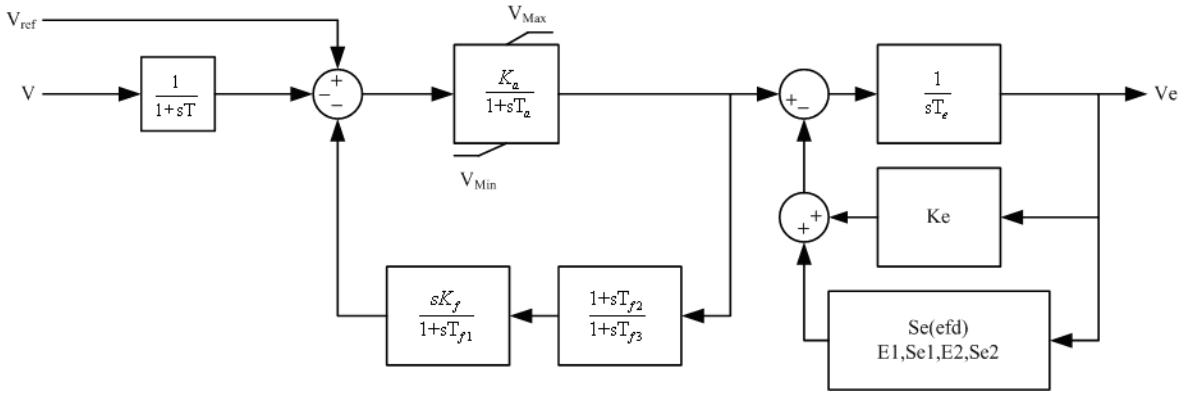

Fig. 3. 19. IEEE Type AC5A excitation system

3.5 Control and Operation of Distributed Generator for Island Operation

A control strategy for an inverter based DG is proposed in [69]. The inverter acts as current controlled voltage source inverter while the system is connected to grid and as a voltage controlled voltage source inverter while it is islanded. A control strategy where DG operates in a PQ control scheme while it is connected to grid and a voltage and frequency control scheme while it is islanded is presented in [70]. A technique to control an inverter based DG using local information and employing speed droop control is presented in [30]. Another control strategy for inverter based DG employing speed droop is presented in [70]. The theme of these control techniques is to control the real and reactive power, while the distribution system is connected to grid, and control the voltage and frequency when the system is islanded. A speed droop characteristic is used to control diesel generators for micro-grid operation in [71]. In [72], a speed droop characteristic is used to control hydro generators for island operation. Another frequency control based on droop characteristics for combined cycle gas turbine is presented in [73]. Control of GTG for island operation is presented in [74] where the GTG keeps its power fixed when the distribution system is connected to grid and controls frequency when the distribution system is islanded. However it does not explain how the frequency is controlled. As mentioned earlier, the speed droop controller changes its reference speed with change in frequency and finds a new operating point for the generators. However, the frequency may settle outside the power quality limit when the distribution system is islanded. On the other hand, an isochronous controller can bring the frequency back to nominal value when the distribution system is islanded. Unfortunately, when connected to grid, its operating point is driven to either lower or upper limits even with a slight deviation in frequency. Isochronous controller with feedback might be used to control distributed generation's power. But, its performance is not as good as the droop controller when the distribution system is connected to transmission grid and as the isochronous controller when the distribution system is islanded. There are many islanding detection techniques proposed in recent times. Hence, they can be used to choose the optimal control strategy when the distribution system changes state (from grid

connected mode to island mode) i.e. to use droop control when the distribution system is connected to grid and isochronous control when it is islanded. However, isochronous controller cannot be used with more than one generator connected to the same system since all the generators else would need to have the same speed set point; otherwise each generator will try to bring the frequency to its reference setting [75]. Therefore, the frequency of an islanded distribution system should be controlled by operating one DG in isochronous mode and other DG units, if any, in isochronous control with feedback control mode as the isochronous controller with feedback performs better than the droop controller when a distribution system is islanded. Moreover, the control of excitation system should be changed from power factor control to voltage control when a distribution system is islanded.

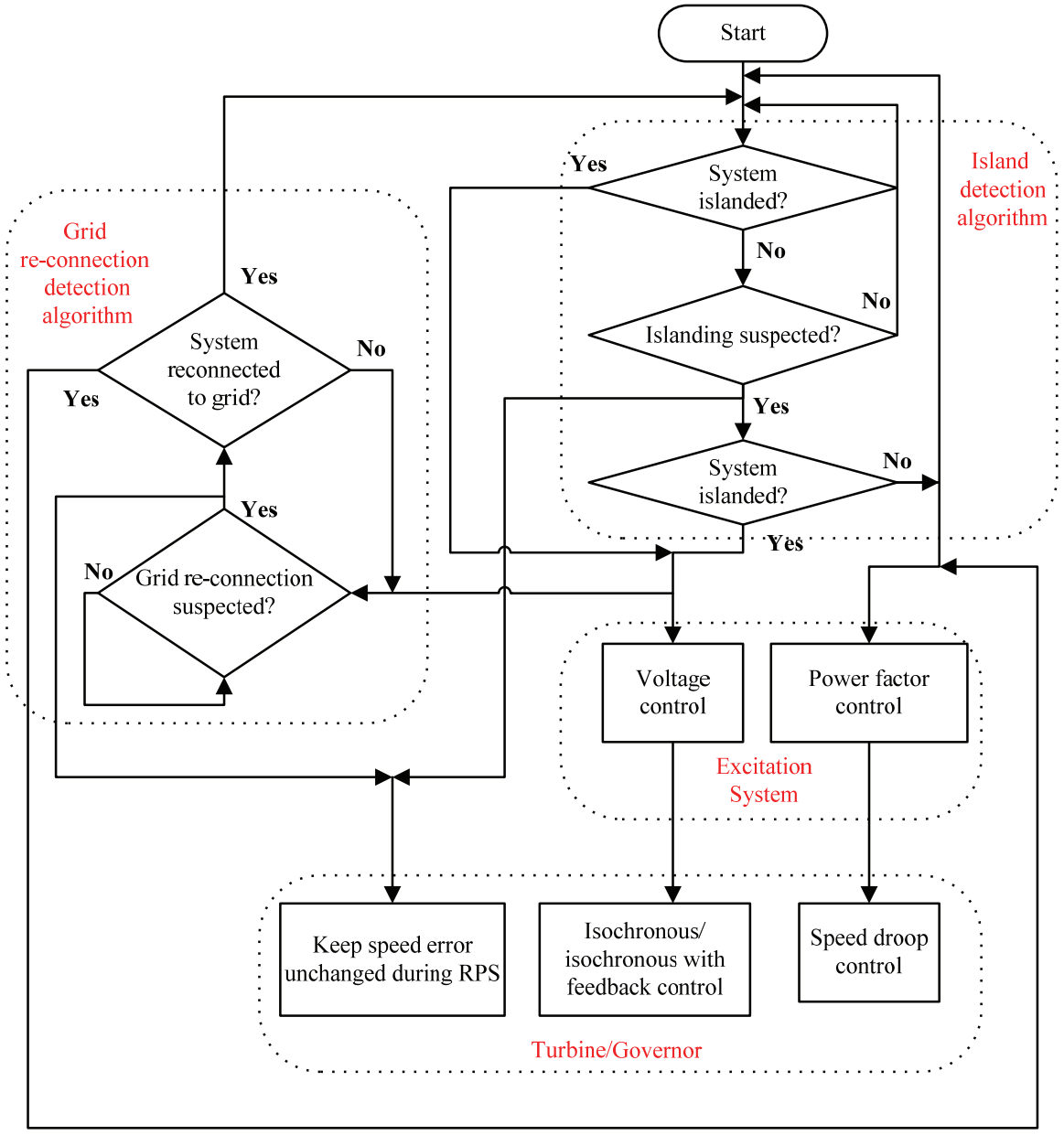

Fig. 3. 20. Flow chart of DG control

The flow chart of the DG control for island operation is presented in Fig. 3. 20. The methodology checks when the distribution system is islanded. Any suitable islanding detection technique, that is currently available, can be used for islanding detection. However, islanding detection technique presented in Chapter 2 has been used here. It should be noted that, during the RPS, the speed error is kept constant. If the speed error is not kept constant, then it will counteract the RPS. As a result, the desired change in power, to correctly detect islanding, may not be achieved. The DG units are operated in constant power factor mode with a speed droop governor when they are connected to grid. But, when the islanding detection technique determines that the distribution system has been islanded, DG units change control strategy to operate in voltage control mode. The DG unit with the largest capacity operates in isochronous mode while the others operate with isochronous controllers with feedback. By changing the control strategies, both voltage and frequency can be kept within the limit. However, this is limited to DG units, which can control its power. DG like fixed-speed fixed pitch wind turbines cannot control its power. Hence, the only way to control frequency in the islanded distribution system, like the one shown in Fig. 2. 6, is by controlling the GTGs. When the distribution system is reconnected to the grid, it is necessary to detect that and change the DG control strategy back to speed droop control and power factor control. Grid reconnection detection is presented in details in Chapter 4.

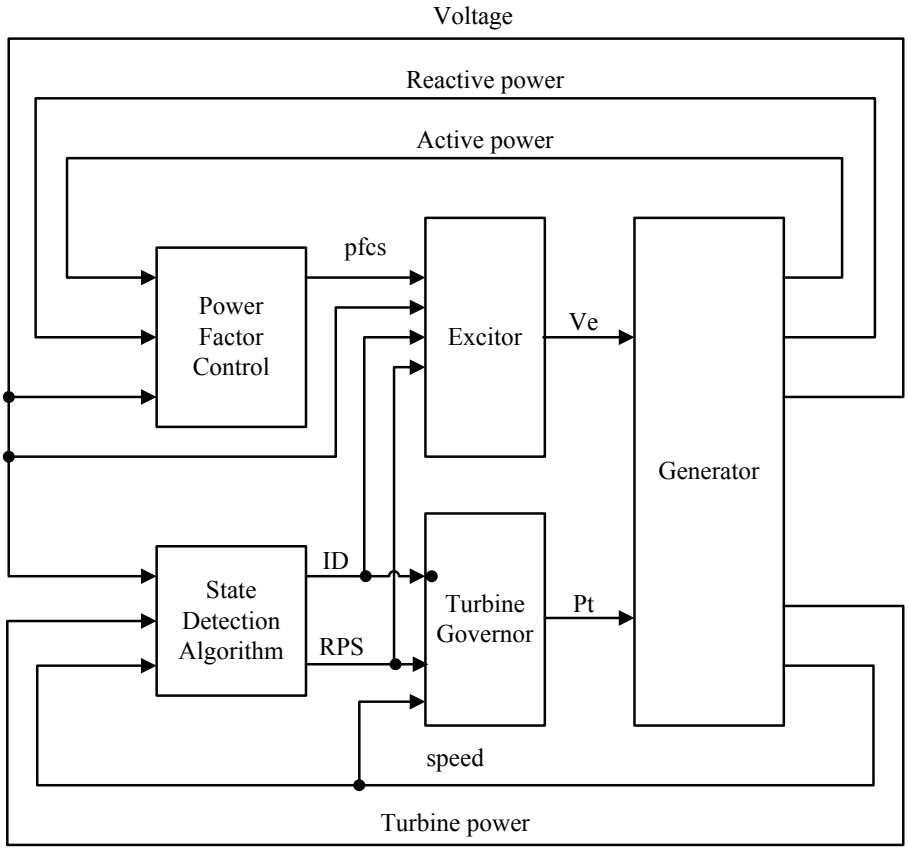

Fig. 3. 21. GTG control block diagram

The block diagram of the GTG control is shown in Fig. 3. 21. It consists of a power factor controller and a state detection algorithm in addition to the generator, turbine-governor and exciter. Both exciter and governor get additional input signals from the state detection algorithm whereas the power factor controller gives signals only to the exciter. 'ID' is the islanding detection signal. It is '1' when the distribution system is islanded and '0' when it is connected to grid. The 'pfcs' refers to the power factor control signal from the power factor controller. 'Pt' and 'Ve' are the turbine power and the excitation voltage, respectively.

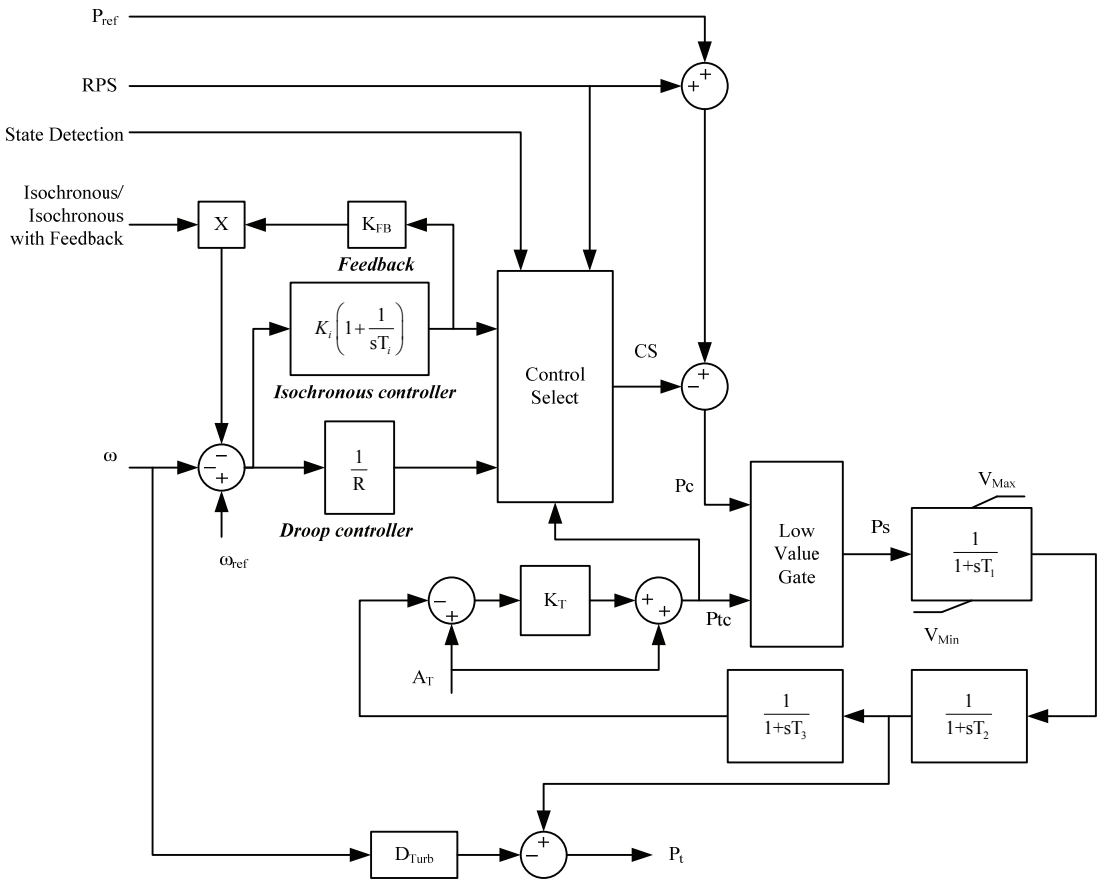

Fig. 3. 22. Modified GAST model for GTG

The modified GAST model with droop, isochronous, and isochronous with feedback controllers is presented in Fig. 3. 22. The 'Isochronous/Isochronous with Feedback' signal deactivates the feedback when isochronous control is chosen whereas; it actives the feedback when isochronous control with feedback is chosen. 'Control Select' chooses the error signal from the droop controller or the isochronous controller based upon the output of the state detection algorithm. However, it keeps the speed error constant during the RPS as mentioned earlier. Also, it keeps the speed error constant when the temperature control loop is activated. Otherwise, the speed error keeps on increasing as a result of total amount of load being more than total generation.

Hence, when the total amount of load becomes less than generation due to some load shedding or load decrease, reduction in speed error takes longer time. As a result, frequency takes longer time to reach the reference. Hence, by keeping the speed error constant, when the temperature control loop is active, frequency can be brought within the limit faster when the total amount of load is less than generation. This is explained in details in the next section.

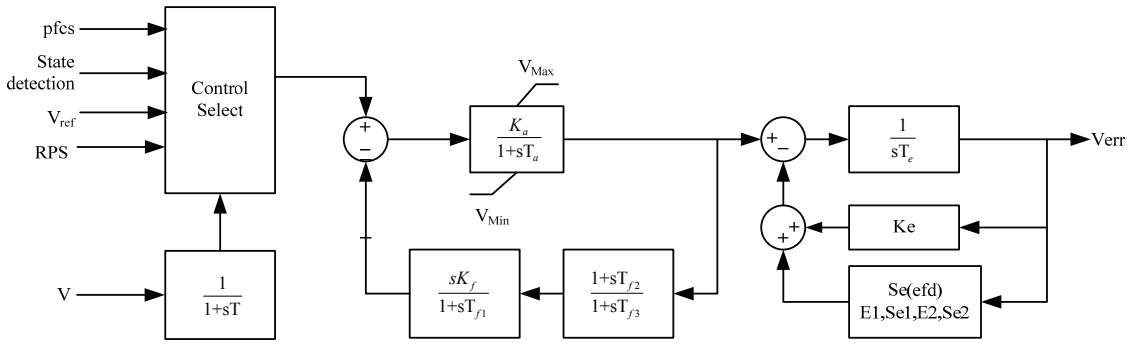

Fig. 3. 23. Modified IEEE type AC5A excitation system

The modified IEEE Type AC5A excitation system is shown in Fig. 3. 23. The 'pfcs' signal is deactivated by the 'Control Select' when the distribution system is islanded. The excitation system, then, follows the voltage set point and regulates the distribution system voltage. During the RPS when the distribution system is still connected to grid, 'Control Select' gives no output signal and, hence, there will be no change in excitation voltage. Any change in voltage will, thus, be due to the RPS only. The power factor controller is shown in Fig. 3. 24. K_{pf} and T_{pf} are the gain and the time constant of the power factor controller, respectively.

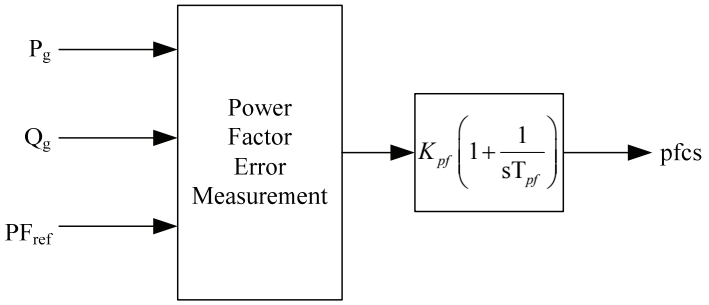

Fig. 3. 24. Power factor control system

3.6 Simulation Results and Discussions

The test distribution system, presented in Fig. 2. 6, is used to test the DG control strategy. The demand and the generation have been changed and it is presented in Table AXI. The output power of each GTG is 2.7 MW. There is an excess of 432 kW of real power and a deficiency of 2.758 MVAr of reactive power when the distribution system is islanded. Loads are modelled as in

equation (2.3) and the values of K_{f_p}, K_{v_p}, K_{f_q} and K_{v_q} are chosen as 0.5 for simplicity as loads' dependency on voltage and frequency is difficult to determine. The speed governor data of the GTGs are presented in Table AXII and the excitation system data is presented in Table AX. The data for the power factor controller is presented in Table AXIII. The wind turbine aerodynamic efficiency curve is presented in Fig. B. 1.

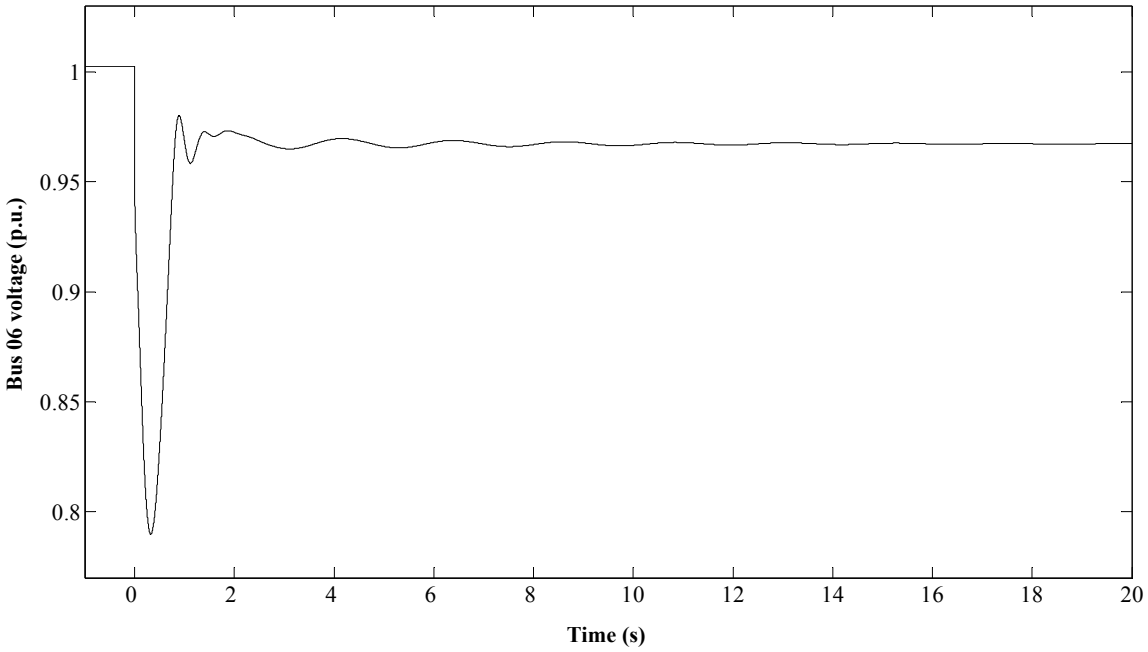

Fig. 3. 25. Bus 06's voltage

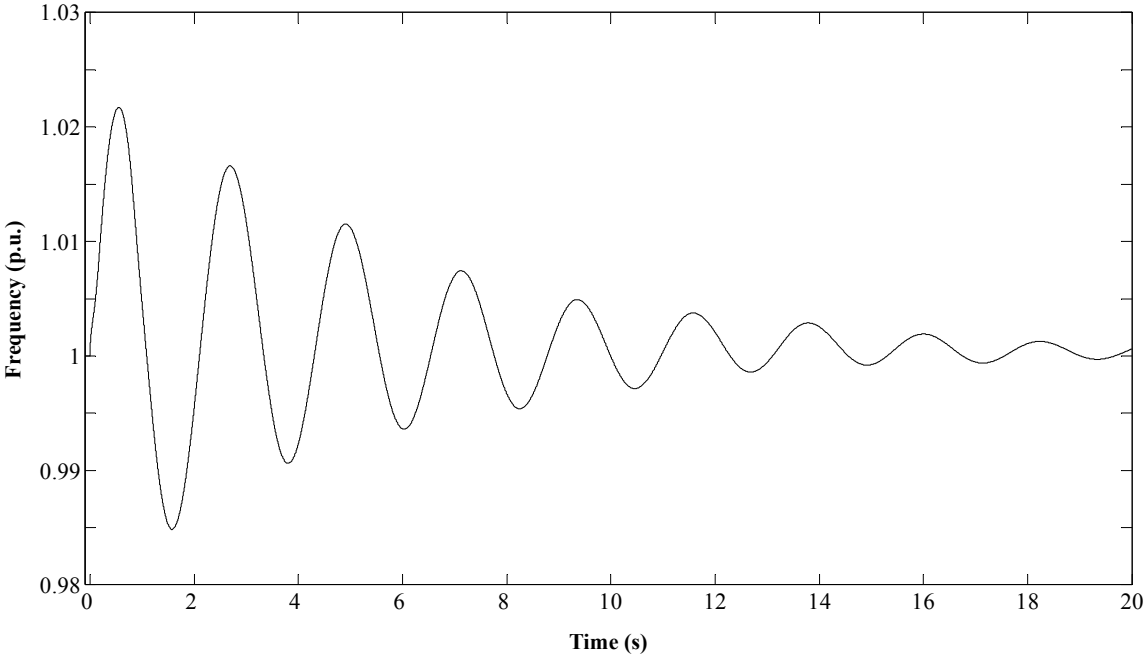

Fig. 3. 26. Islanded distribution system's frequency

Islanding is simulated at *t=0s*. Fig. 3. 25 shows the voltage at Bus 06. Since $Av7$ is 21.6 kV/s, islanding is detected at *t =0.14s*. Fig. 3. 26 shows the frequency of the islanded distribution system. The GTG1 switch its control strategy from droop/power factor control to isochronous/voltage control. Similarly, GTG2 and GTG3 switch their control strategy to isochronous control with feedback and voltage control. Fig. 3. 25 and Fig. 3. 26 show that the DG controllers bring the voltage within reasonable limits and also bring the frequency back to 1 p.u. by changing the control strategy.

Now, the GTGs' output are set at 2 MW to show the effect of changing the control strategy of GTG2 and GTG3 to isochronous with feedback rather than keeping in droop control when the distribution system is islanded. Fig. 3. 27 shows the distribution system frequency with the droop controller and the isochronous controller with feedback in GTG2 and GTG3. The frequency is brought back closer to nominal value with the isochronous controller with feedback than with the droop controller.

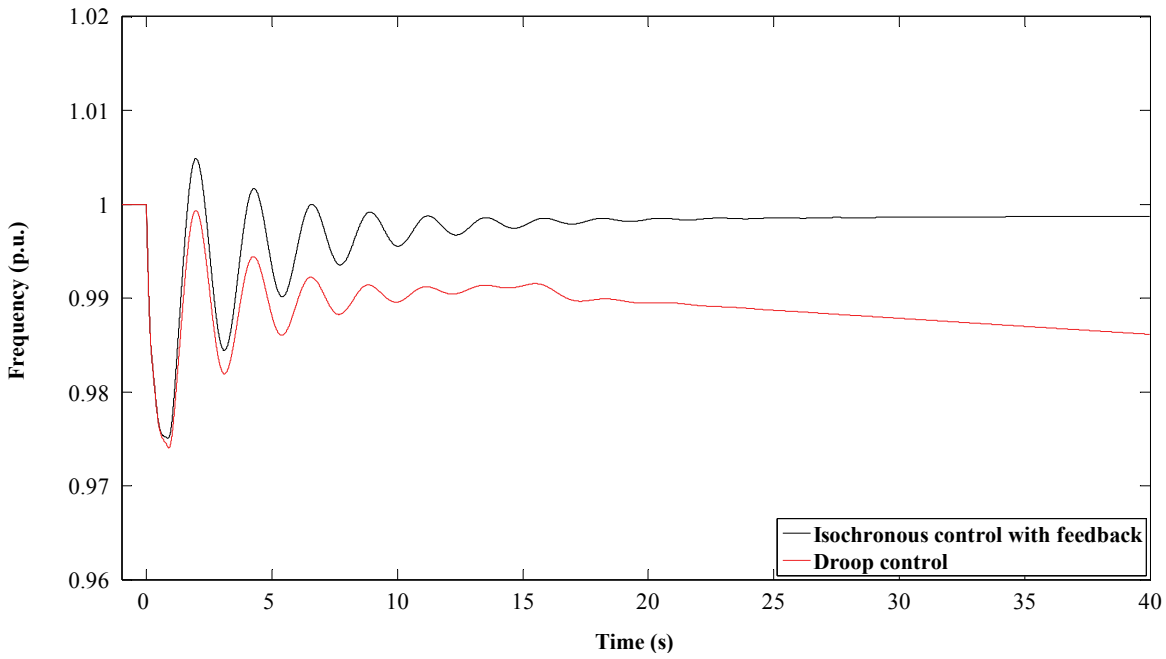

Fig. 3. 27. Distribution system frequency for islanding with isochronous controller with feedback and droop controller

Now to show the impact of limiting the speed error when the temperature loop is activated, a case is simulated with change in load and generation. Load05 is increased by 1.4 MW and a 2.5 MVAr capacitor is added at Bus 09 and output of GTG1, GTG2 and GTG3 are adjusted to 2.5 MW, 3 MW and 3 MW, respectively. The distribution system is islanded at *t=0s* and the load at Bus 05 is reduced by 1.4 MW at *t=100s*. When the distribution system is islanded, the temperature control loops of GTGs are activated as the total amount of load on the GTGs is higher than their maximum rated power at the ambient temperature. However, the speed error keeps on increasing,

with the demand exceeding the generation, until the load at Bus 05 decreases at *t=100s* making the total demand less than the total generation. Fig. 3. 28 shows the speed error (Pc) and the output of the temperature control loop (Ptc), the two inputs of the low value gate of GTG1, and the output signal (Ps) of the low value gate of GTG1.

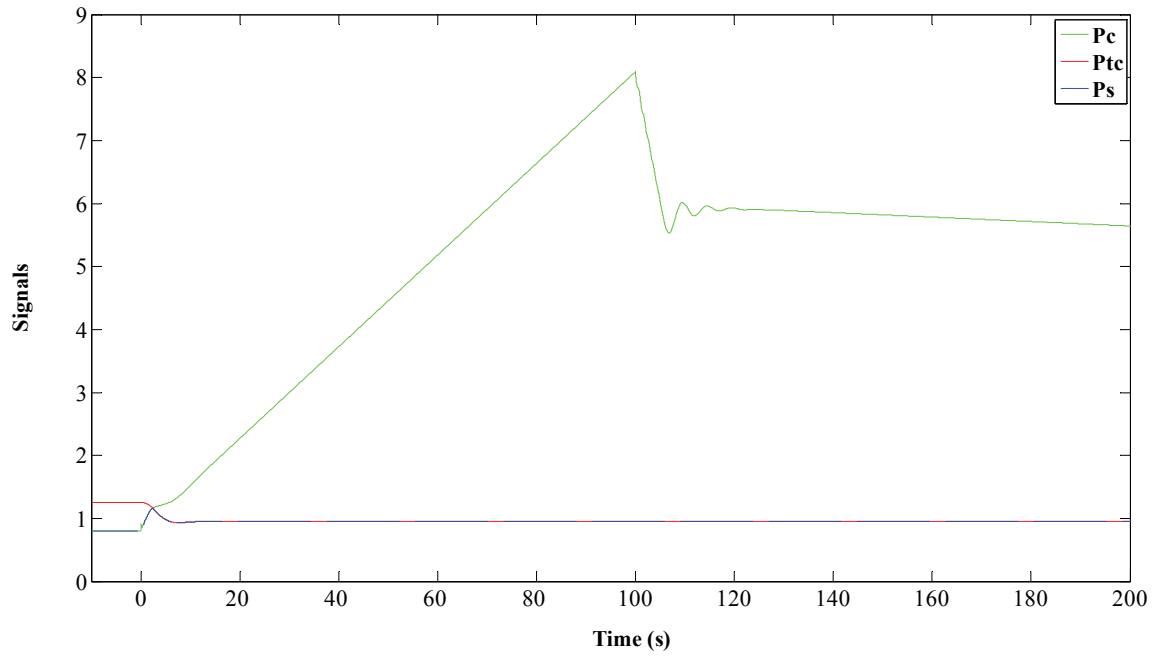

Fig. 3. 28. Controller's signals without limit

It can be seen from the Fig. 3. 28 that the temperature control loop governs the output of GTG1 when the distribution system is islanded as the total amount of load in the distribution system is higher than the rated power of GTGs at the ambient temperature. The GTGs continue to produce the rated power and the speed error keeps on increasing. When the load at Bus 05 decreases at *t=100s,* the total demand in the distribution system becomes less the total generating capacity. Ideally, the GTGs should reduce its power and maintain the frequency at nominal value. However, the GTGs continue to produce the rated power as the speed error is large and its takes some time before the speed error becomes less than the output of the temperature control loop. Fig. 3. 29 shows the three signals of the low value gate of GTG1 when the speed error is limited. It can be seen from Fig. 3. 29 that when the load at Bus 05 decreases *t=100s,* the speed error becomes less than the output of the temperature control loop and starts controlling the power of GTG.

Fig. 3. 30 shows the distribution system frequency when the speed error is limited and when it is not. Without limit, the GTG1 continue to produce maximum power even after the load decrease and a large frequency over shoot results. But, when the limit is used, the turbine reduces the power faster and brings the frequency to 1 p.u. faster. Also, the frequency overshoot, after load decrease, is reduced by the use of limit.

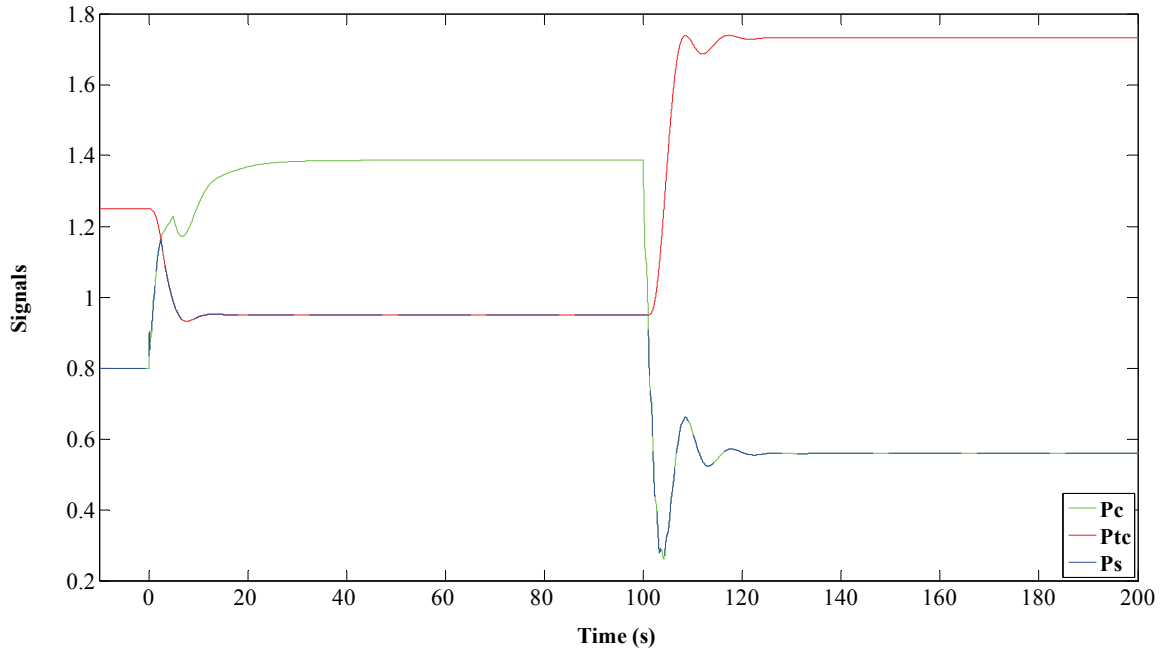

Fig. 3. 29. Controller's signals with limit

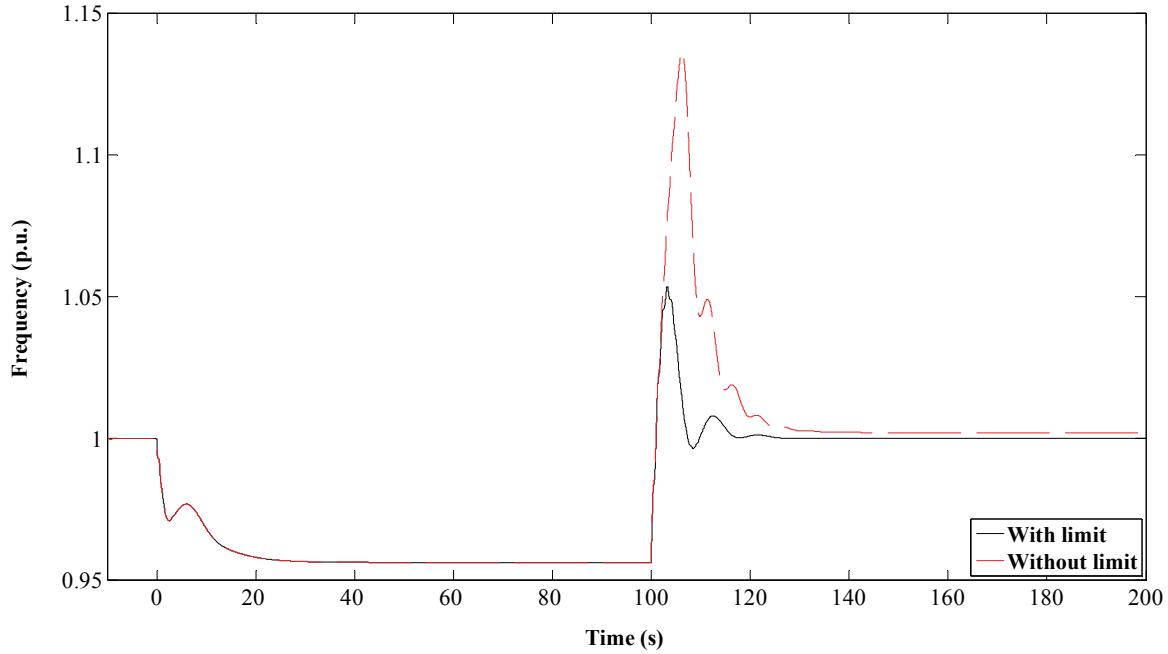

Fig. 3. 30. Distribution system frequency with and without limit

Next a change in grid voltage by 0.5% is simulated. The power factor of GTG1 is presented in Fig. 3. 31 compared to the reference power factor. The power factor controller brings the power factor to unity after the disturbance.

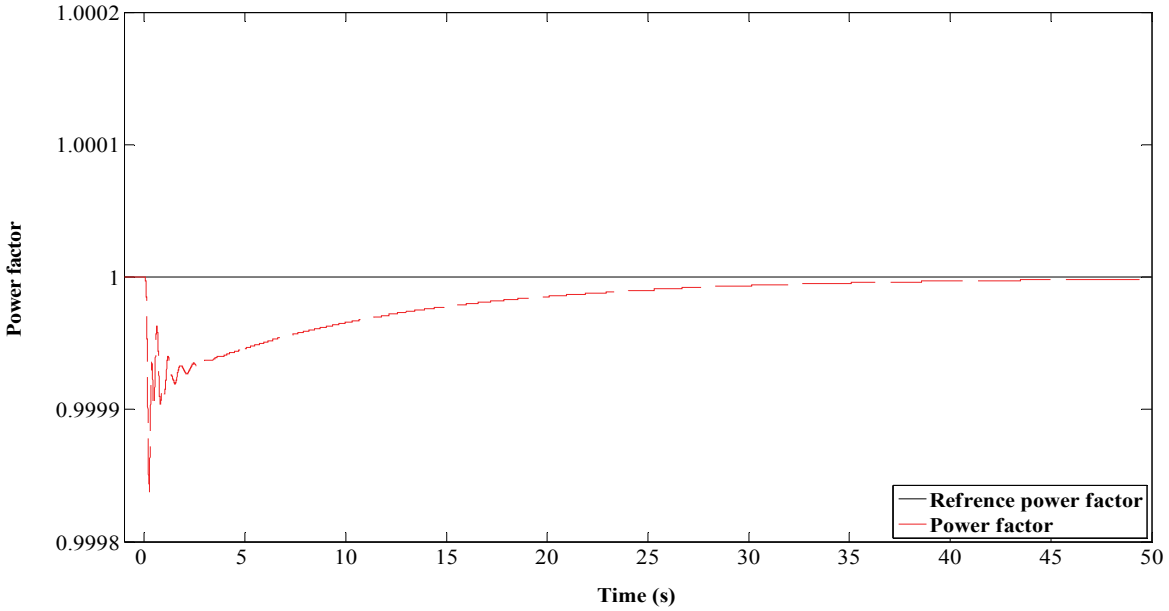

Fig. 3. 31. GTG1 power factor

A case with a small power mismatch is also simulated. For simulation purpose, a 2.5 MVAr capacitor bank is installed at Bus 09 and the initial power set points of the GTGs are set at 2.5 MW. Load05 is adjusted to 6.75 MW and 1.28 MVAr resulting in power mismatch of 20 kW and 20 kVAr in the islanded distribution system. Islanding is simulated at *t=0s*.

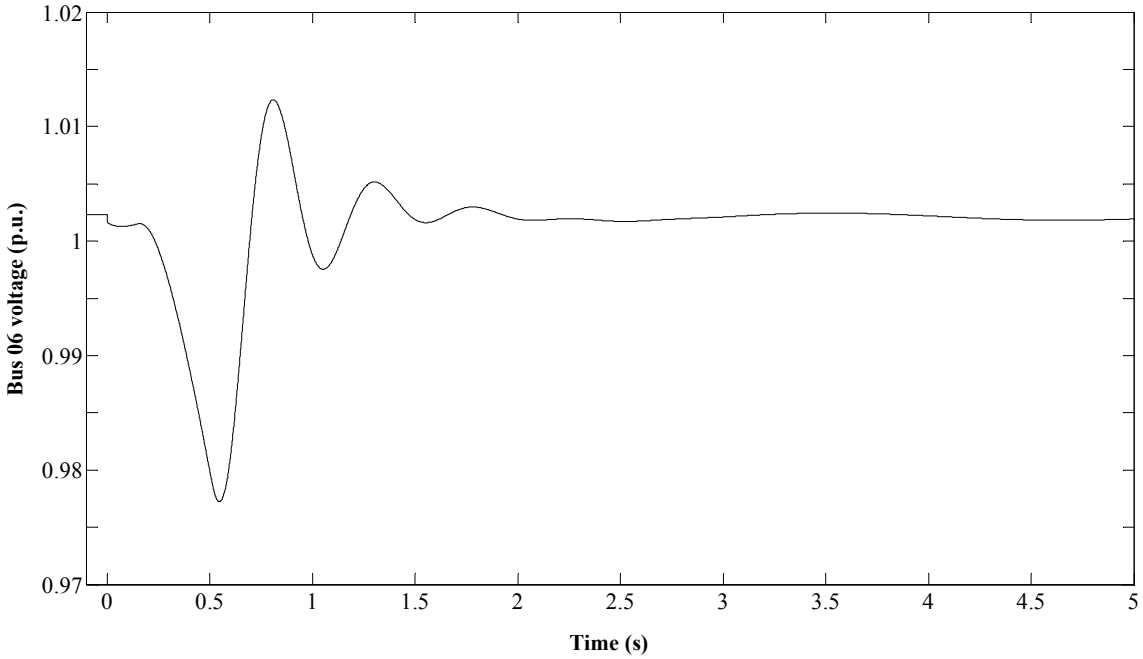

Fig. 3. 32. Bus 06 voltage

The voltage at Bus 06 is presented in Fig. 3. 32. $Av7$ for this case is 123.7 V/s and hence the RPS is initiated. $Av18$, after the initiation of the RPS, is 1202.02 V/s. Therefore, islanding is detected correctly. The control is switched from droop control to isochronous control in GTG1 and

from droop control to isochronous control with feedback in GTG2 and GTG3. Also, the GTGs switch from power factor control mode to voltage control mode. Fig. 3. 33 shows the frequency of the distribution system.

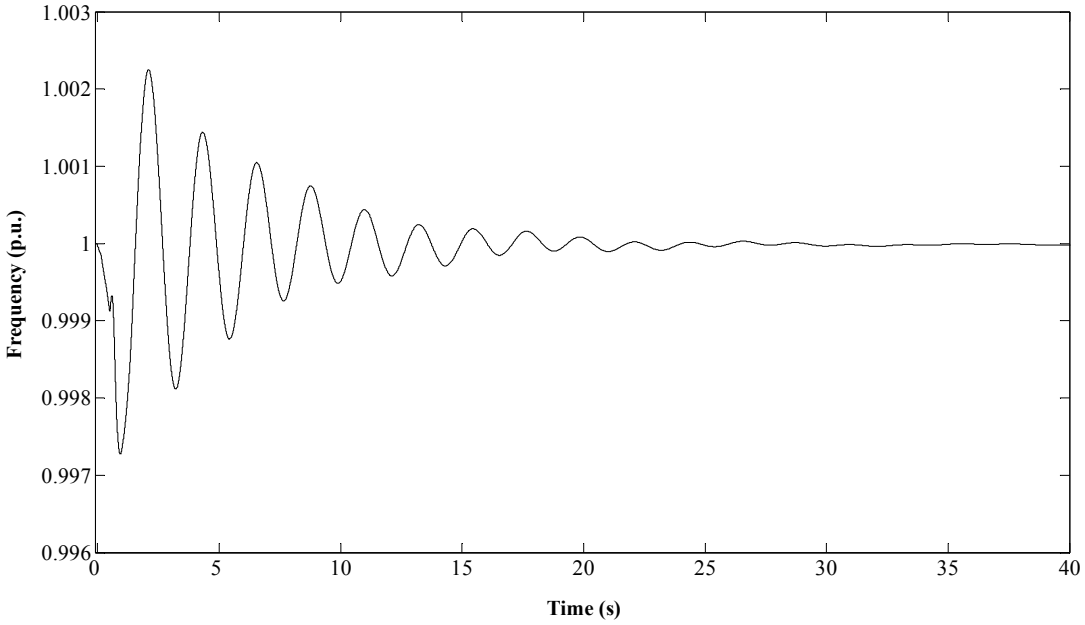

Fig. 3. 33. Frequency of the distribution system

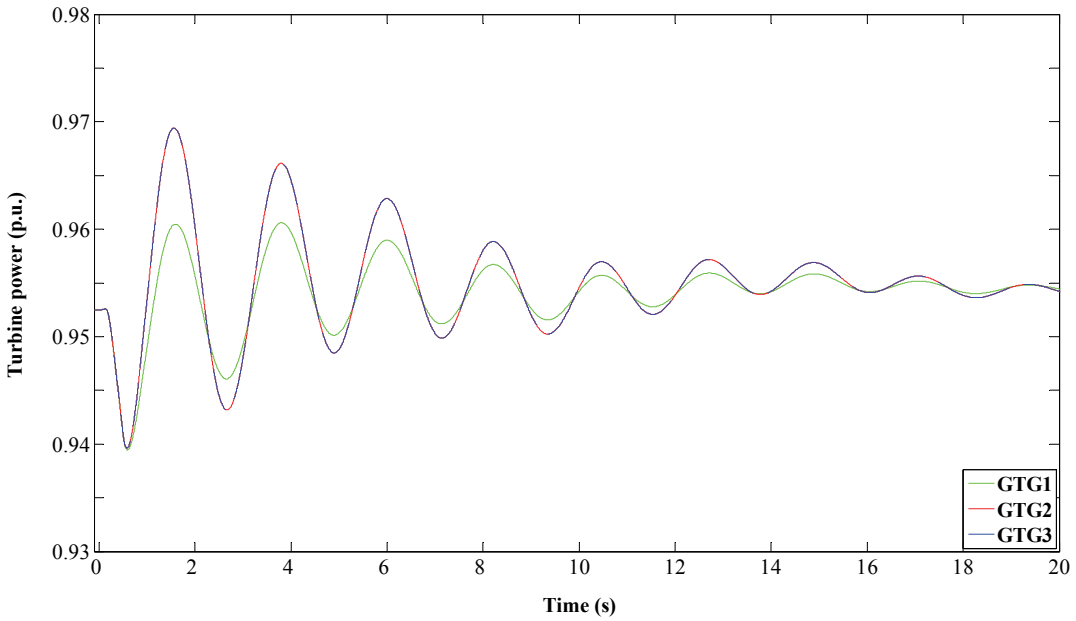

Fig. 3. 34. GTGs Turbine power

Fig. 3. 32 and Fig. 3. 33 show the DG control strategy is able to maintain the frequency and voltage of the islanded distribution system within acceptable ranges. Fig. 3. 34 shows the turbine power of the GTGs. The GTGs increase their power when the distribution system is islanded to bring the frequency back to the reference.

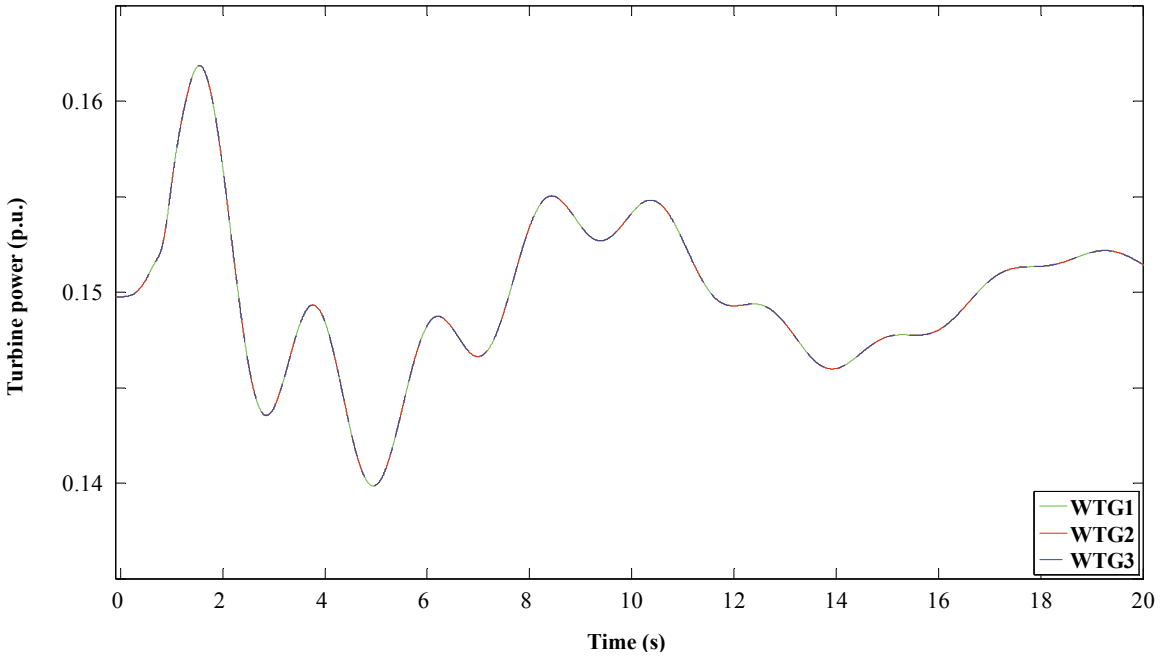

Fig. 3. 35. WTG Turbine power

Fig. 3. 35 shows the turbine power of the WTGs. Change in the WTGs' rotor torque and the low speed shaft torque is presented in Fig. B. 2. Change in the WTGs' rotor and generator speed is presented in Fig. B. 3. Fig. B. 4 and Fig. B. 5 show the change in tip speed ratio and the power coefficient of the WTGs', respectively.

With the change in rotor speed, the tip speed ratio changes and hence the aerodynamic efficiency of the WTG also changes (according to the aerodynamic efficiency curve and equation 3.2). Moreover, with the change in the generator and rotor speeds, the power output of the wind turbine also changes (according to equations 3.5 and 3.6).

Fig. 3. 36 shows the output of the 'Control Select', the droop controller and the isochronous controller, and the RPS for GTG1. It clearly shows that the 'Control Select' selects isochronous control when islanding is detected and droop control at other time. However, it keeps the speed error constant when the RPS is initiated. Similarly the output of the 'Control Select', the droop controller and the isochronous controller, and the RPS for GTG2 and GTG3 is presented in Fig. B. 6. Again it shows that 'Control Select' selects isochronous control with feedback when islanding is detected and droop control other time.

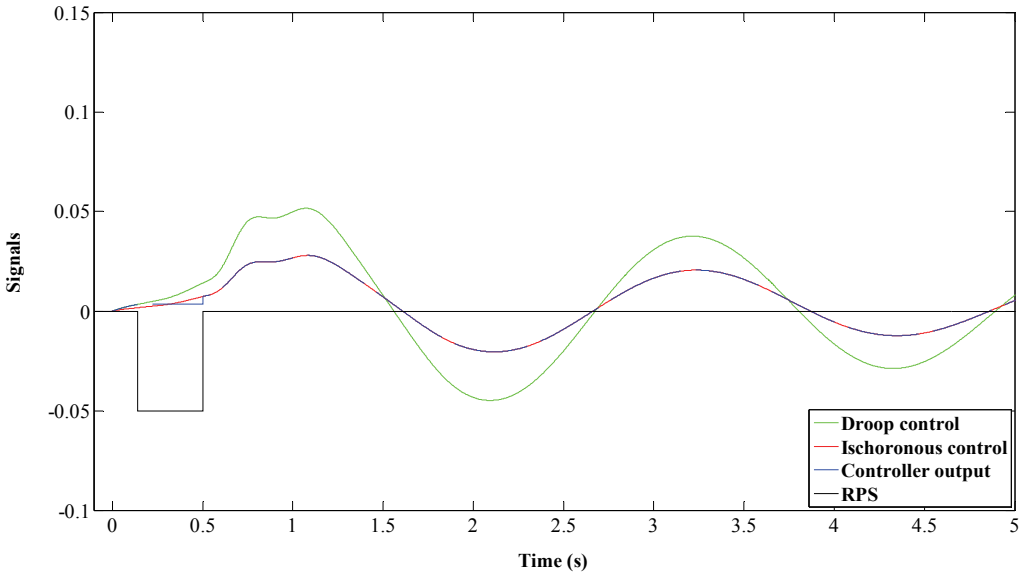

Fig. 3. 36. Signals of GTG1 turbine controller

3.7 Conclusions

The speed droop controller is very effective to control power when the generator is connected to the grid. But, depending on power imbalance in the islanded distribution system, the final settling frequency can be outside the power quality limit. On the other hand, the isochronous controller can bring the frequency back to nominal value when the distribution system is islanded. However, when connected to the grid, its operating point is driven to either lower or upper limit even with the slightest of deviations in the frequency. The isochronous controller with feedback can find a new operating point when the frequency of the strong grid, to which it is connected, deviates. It also keeps the frequency within an acceptable limit when the distribution system is islanded. The isochronous controller with feedback is the better choice when the same control strategy is to be used for load frequency control when the distribution system changes states. Furthermore, when a small synchronous generator based DG is connected to the grid in voltage control mode, it may cause either over or under excitation of the generator that may result in overload or loss of generator synchronism. However, when the distribution system is islanded they have to maintain the voltage. An islanding detection technique, as the one presented in Chapter 2, can effectively determine when the power system is islanded. This information can be used to choose the optimal control strategy based on the state of the distribution system. Hence, when the distribution system is connected to the grid, the DG units operate at a constant power factor with speed droop control. When islanded, one of the DG units will be operated in isochronous mode, while the rest will be operated with isochronous controllers with feedback. By changing the control strategy, frequency and voltage is maintained when the distribution system is islanded. Also new operating points for the DG units are found when there is a disturbance in the grid when the distribution system is still connected to it.

Chapter 4

Grid Reconnection and Detection

An islanded distribution system itself is a small power system. With the proper voltage and frequency control, it can operate without the support of the main grid. Issues with the voltage and the frequency are presented in Chapter 3 and some solutions are also presented. Even though the reliability of the electricity supply is improved by allowing island operation, the reliability of the overall system in an island operation is less compared to grid-connected operation [76]. Hence, it is desirable to reconnect the distribution system back to the transmission system when the transmission system is back to normal operating conditions. As mentioned in Chapter 3, keeping the same control for the turbine and the excitation system, when the distribution system changes state from grid connected to island and vice versa, is not an optimal solution. Thus, it is necessary to detect the states of the distribution system and chose the optimal control strategy. The shift from grid connected mode to island mode can be easily detected through an islanding detection technique. Many islanding detection techniques have been developed in recent years. Chapter 2 deals with the islanding detection issues. However, little work has been done regarding grid reconnection detection. This can be achieved with communication devices. But, implementing such a communication system is considerably complex and requires high cost [30] and may not be economical for small distribution systems. Thus, there is a need to develop a grid reconnection detection algorithm using local information. Section 4.1 deals with the issue of connecting an energised distribution system back to the transmission grid. Two grid reconnection detection techniques are presented in Section 4.2. Some conclusions are drawn in Section 4.3.

4.1 Grid Reconnection

Reconnecting a distribution system to the transmission grid is similar to synchronizing a DG to a distribution system or a central power station to a transmission system. The difference between the voltages, frequencies and phases of the distribution system and transmission system should be within certain limits before they can be reconnected. By controlling the DG's governor the frequency and phase can be controlled. Similarly, by controlling the excitation system, the voltage can be controlled and the distribution system and transmission system can be synchronized. This is possible if the synchronizing switch is close to the DG unit. But the synchronizing switch can be far away from DG and there may be multiple DG units in the islanded distribution system. Hence, DG can be made to change the voltage and frequency with the use of communication only. As mentioned earlier, communication can be expensive for small distribution systems. Since the

DG units are able to control the voltage and frequency of the islanded distribution system, the distribution system can wait for the voltage, frequency and phase differences to be within the limits before it is connected back to grid. A grid reconnection algorithm is proposed in this section to be implemented in the substations where the distribution system is connected to the transmission grid. It is based on [18] and it monitors the voltage, frequency and phases of the distribution system and the transmission system and connects them when the following criteria are met:

- the difference in frequencies is less than 0.1 Hz and the grid frequency is within 50±0.1 Hz;
- the difference in voltages is less than 5%; and
- the two systems are in phase.

4.2 Grid Reconnection Detection

Similar to the need to detect islanding, there is a need to detect grid reconnection as output power of the DG units are driven to their limits, with the isochronous control, with the slightest of changes in the grid frequency. Also under or over excitation may result if DG is left to control the terminal voltage when the distribution system is connected to the grid. Hence, the DG control strategy has to be changed back to droop control and power factor control when the distribution system is reconnected to grid by correctly identifying grid reconnection. Two grid reconnection detection algorithms are presented in this section. The first one is a passive technique for a distribution system with a single DG units and the second one is an active technique for a distribution system with one or more DG unit(s).

4.2.1. Passive Grid Reconnection Detection Technique

A simple passive method to detect grid reconnection is presented here. It assumes that the total load in the distribution system is always within the capacity of the generation when it is islanded. Also, it is assumed that there is only one DG in the islanded distribution system and the isochronous control is used when the DG is operating in the island mode. It is also assumed that only the DG needs to know the state of the distribution system. Other components of the distribution system may also need to know the state of the distribution system as discussed in the later chapters. The proposed methodology is explained with a GTG.

Two systems will be in phase from time to time when they operate at different frequencies. Hence, when the distribution system is reconnected to the grid, the grid determines the frequency of the whole system and the GTG changes its turbine power with the slightest of differences in frequencies to bring the frequency back to its own reference, with the isochronous control. As the transmission grid is stronger than the GTG, change in the GTG speed as a result of change in turbine power is minimal. Hence grid reconnection can be detected if speed and power of the GTGs

are monitored. The flowchart of the proposed grid reconnection detection technique is presented in Fig. 4. 1.

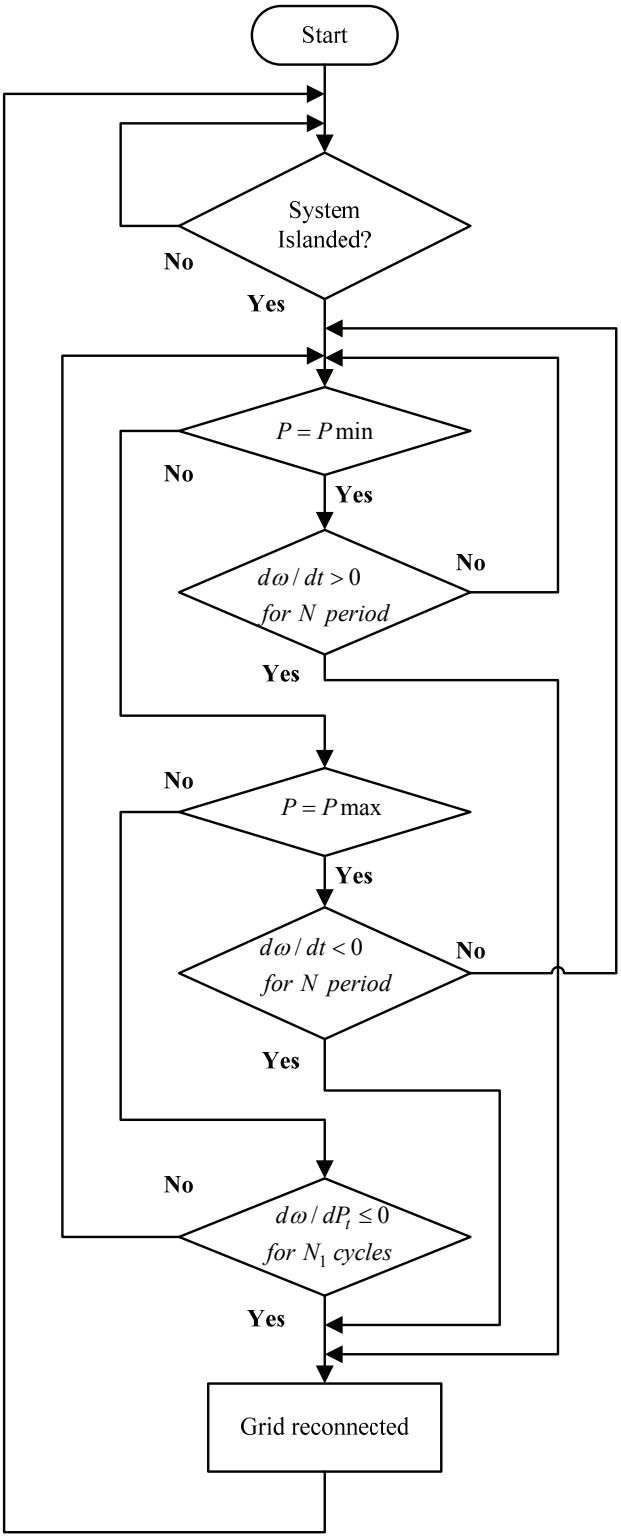

Fig. 4. 1. A passive grid reconnection detection technique

The GTG speed and its turbine power are measured every voltage period. Grid reconnection is detected when the GTG turbine power (P_t) is minimum (P_{min}) or GTG is at no load condition and speed (ω) is increasing, as there are no other power sources in the islanded distribution system. Grid reconnection is also detected when the GTG turbine power is maximum (P_{max}) or GTG is at full load condition and speed is decreasing as it is assumed that the local loads are always within the capacity of the GTG. Furthermore, grid reconnection is also detected when the rate of change of speed over power ($d\omega/dP_t$) of the GTG is less or equal to zero for N_1 voltage periods as change in power is not having the desired impact on speed. Observing $d\omega/dP_t$ or $d\omega/dt$ for a certain time reduces chances of false grid reconnection detection during transient conditions.

4.2.2. Modelling of the Test System to Test the Passive Grid Reconnection Detection Technique

A small distribution system with a GTG and two loads is used to test the proposed methodology. The test distribution system is shown in Fig. 4. 2.

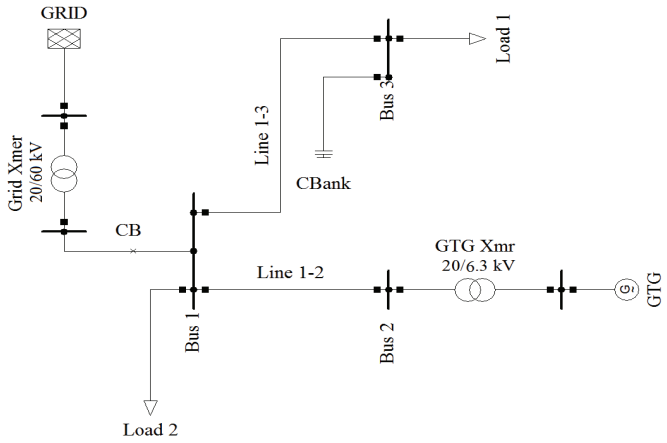

Fig. 4. 2. A simple test distribution system to test passive grid reconnection detection algorithm

The distribution system is connected to the transmission network (GRID) at Bus 1 via a circuit breaker (CB) and a transformer (Grid Xmer). The generator data are given in Table AII and the line data are given in Table AXIV. In the test case, Load 1 and Load 2 are 1 MW and 0.2 MVAr, and 1.51 MW and 0.5 MVAr, respectively. Test case production from the GTG is 2.59 MW. A 900 kVAr capacitor bank (CBank), with six 150 kVAr capacitors, is installed for the simulation purpose to make power deficiency in the distribution system as low as 0.01 MW and 0.01 MVAr. In a real system, loads are always voltage and frequency dependent. As mentioned earlier, it is very difficult to determine voltage and frequency dependency of the loads. Hence, for simplicity, load is modelled as in equation (2.3) and values of K_{f_p}, K_{v_p}, K_{f_q} and K_{v_q} are chosen

as 0.5. It is assumed that total load in the system is always within the capacity of the generator. Also the real and reactive power demands of the loads at the nominal voltage and frequency are assumed to remain constant during the period of the simulation.

4.2.3. Simulation Results and Discussions for Passive Grid Reconnection Detection Technique

The standard model for a synchronous generator available in DIgSILENT is used for the study. The parameters for the turbine governor controller is same as that of GTG1 in Table AXII and the parameter for the exciter is the same as that of DG in Table AX. Similarly, parameters for the power factor controller are given in Table AXIII. According to the islanding detection technique described in Chapter 2, the minimum set point to suspect islanding (V_{SMin}), the set point to detect islanding without the RPS (V_{SMax}) and the set point to detect islanding with the RPS (V_{SMaxU}) are set as 40 V/s, 7200 V/s and 100 V/s, respectively. The RPS is set at 5%. The distribution system is islanded at *t=0s* by opening the CB. The GTG is controlled at unity power factor while it is connected to grid. Similarly, N and N1(in Fig. 4. 1) are both set at 25 as extensive simulations have shown that it is more than enough for the test system.

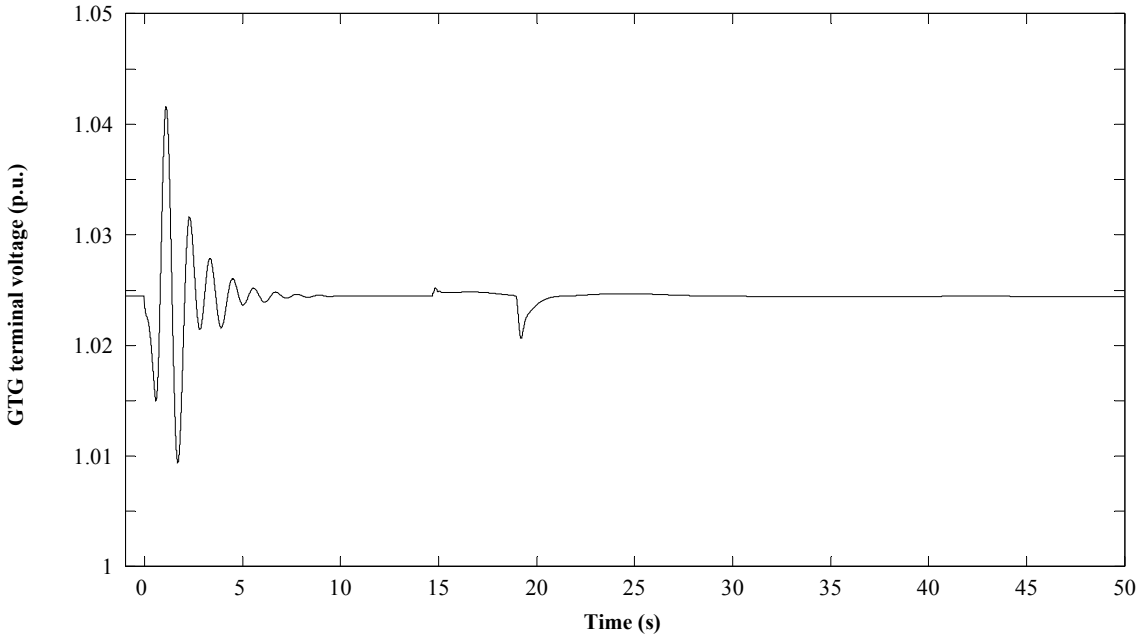

Fig. 4. 3. GTG terminal voltage for islanding and RPS

Fig. 4. 3 shows the GTG terminal voltage for islanding at *t=0s* and the RPS initiation at *t=0.14s*. When the distribution system is islanded, the GTG terminal voltage goes down initially due to the power deficiency in the distribution system. The magnitude of average rate of voltage change for 7 periods ($Av7$) is 293.3 V/s, which is higher than V_{SMin} but not higher than V_{SMax}.

Hence, the RPS is initiated at $t = 0.14s$. Now, the magnitude of average rate of voltage change for 18 periods ($Av18$), after initiation of the RPS, is 385.1 V/s, which is higher than V_{SMaxU} . Hence islanding is correctly identified at $t=0.5s$.

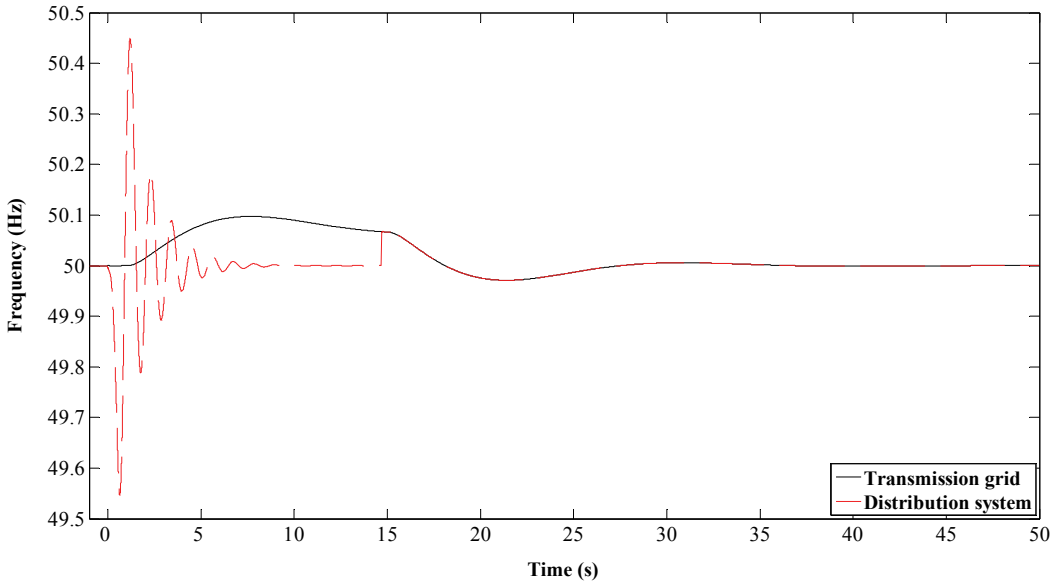

Fig. 4. 4. Transmission and distribution system frequencies

In a power system, grid frequency fluctuates from the nominal value and so does the islanded distribution system's frequency. Thus, from time to time, the distribution system becomes in phase with transmission system as the two systems do not operate at same frequency all the time. To simulate this, the grid frequency is changed as shown in Fig. 4. 4. It also shows the distribution system frequency.

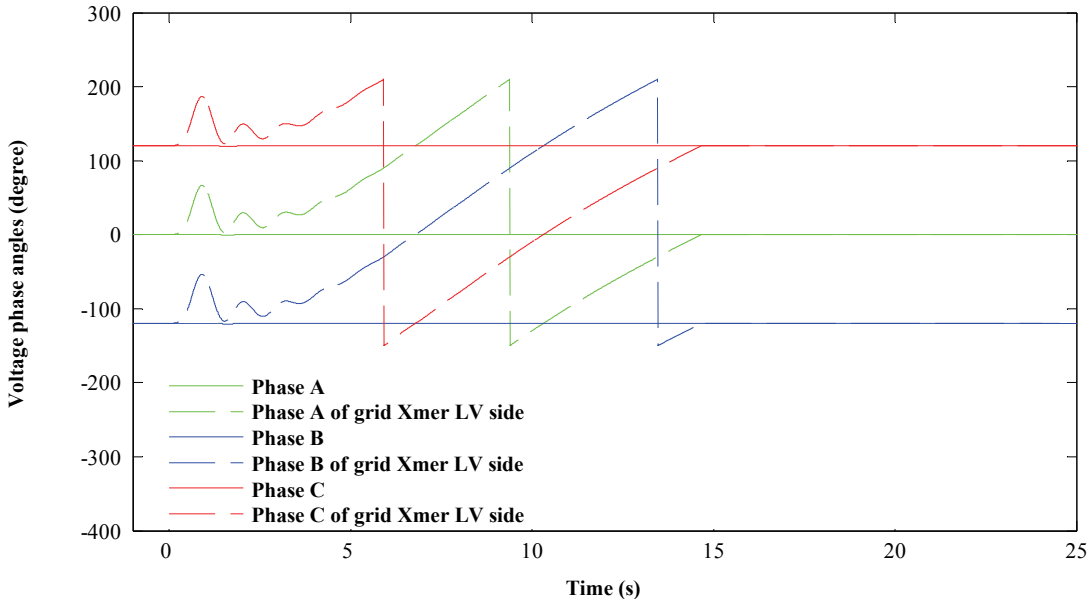

Fig. 4. 5. Bus 1 and grid transformer LV side voltage phase angles

Fig. 4. 5 shows the angles of voltage phases at either sides of the CB when the distribution system is islanded and the grid frequency changes as shown in Fig. 4. 4. At *t=14.68s,* differences in the voltage, frequency and phase between the islanded distribution system and the transmission grid are within the limits specified in Section 4.1 and hence the distribution system is reconnected back to the transmission system.

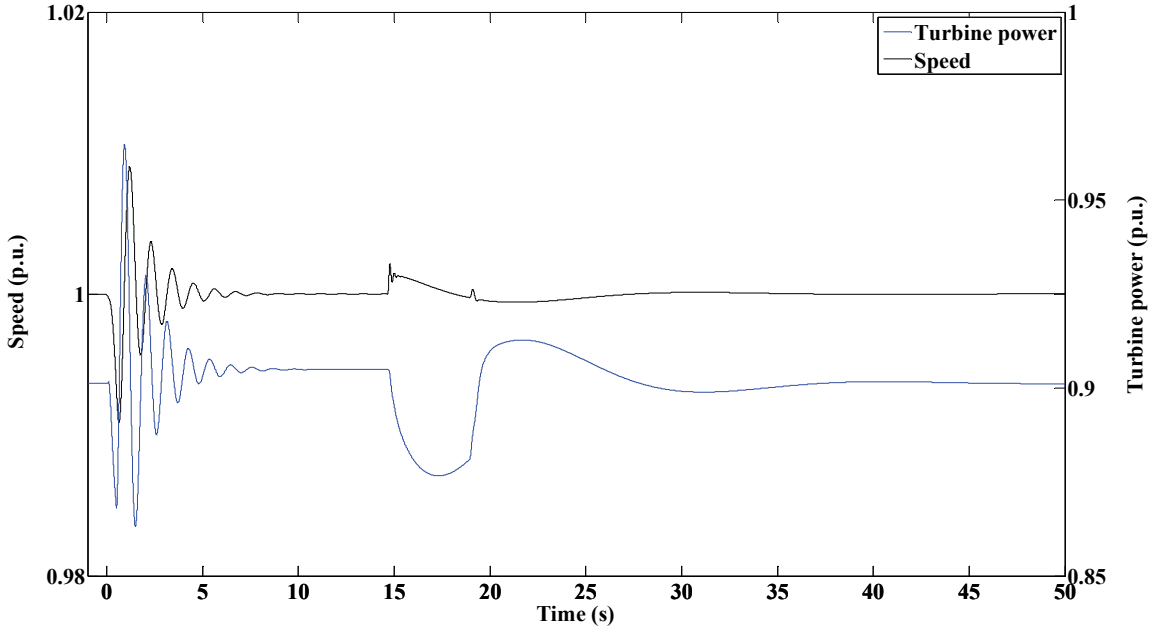

Fig. 4. 6. GTG speed and power for islanding and grid reconnection

Fig. 4. 6 shows the changes in the GTG turbine power and its speed. When the distribution system is reconnected to the grid, the grid frequency is not 50 Hz. The GTG changes its power to bring the speed back to reference. Since the grid is too strong compared to the GTG, change in the GTG power has hardly any impact in system frequency decline. At *t=18.94s,* $d\omega/dP_t$ becomes zero or less for the twenty fifth period and grid reconnection is detected by the grid reconnection detection algorithm. The reference power factor and power factor of the GTG is presented in Fig. B. 7. Similarly, the power set point of the GTG and the turbine power is presented in Fig. B. 8 and the output of the control select is presented in Fig. B. 9. Fig. B. 7 shows that the excitation control of the GTG does not try to correct the power factor of the GTG when the distribution system is islanded. However, when the grid reconnection detection algorithm detects that the distribution system is reconnected to the grid, it no longer tries to maintain the voltage but now maintains the power factor of the GTG at the reference value. Similarly, Fig. B. 8 shows that the GTG's governor does not regulate the power at a set value. Instead it maintains the frequency when the distribution system is islanded. But, it maintains the power to a set value when the distribution system is reconnected to the grid. Fig. B. 9 shows the GTG control strategy switching from droop control to

isochronous control and back to droop control when the distribution system is islanded and reconnected back to the transmission grid, respectively.

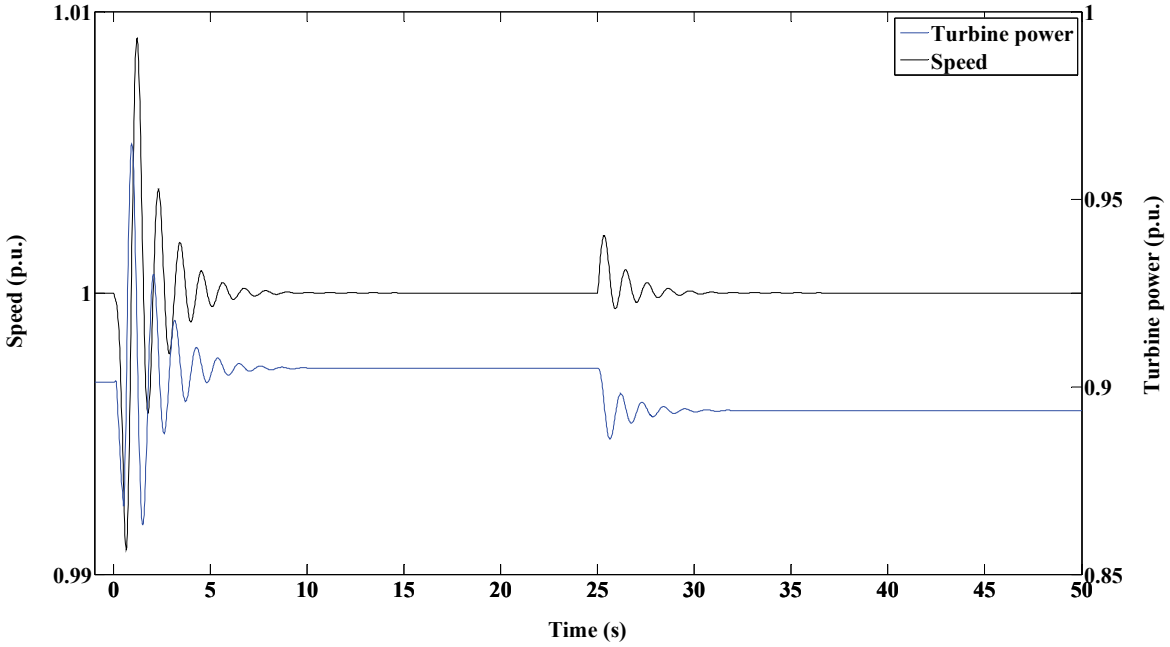

Fig. 4. 7. GTG speed and power for islanding and load decrease

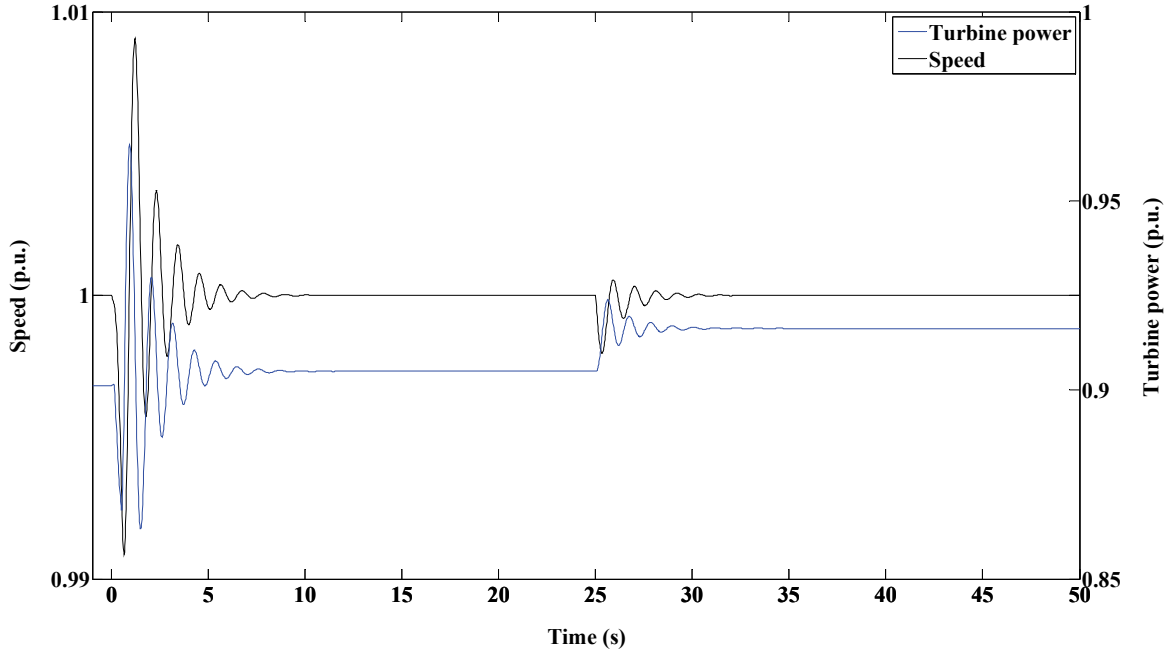

Fig. 4. 8. GTG speed and power for islanding and load increase

Fig. 4. 7 shows the power and the speed of the GTG for a new simulation where Load 1 is decreased by 3%. Similarly, Fig. 4. 8 shows the power and the speed of the GTG for another simulation where Load 1 is increased by 3%. The total amount of load after the load increase is within the capacity of the GTG. Thus, the speed is brought back to reference valueafter the events.

The islanding of the distribution system is simulated at *t=0s*. Both load changing events are simulated at *t=25s*. The GTG reacts to the load changing events. $d\omega / dP_t$ is not zero or less for twenty five consecutive periods for the load changing events at any time.

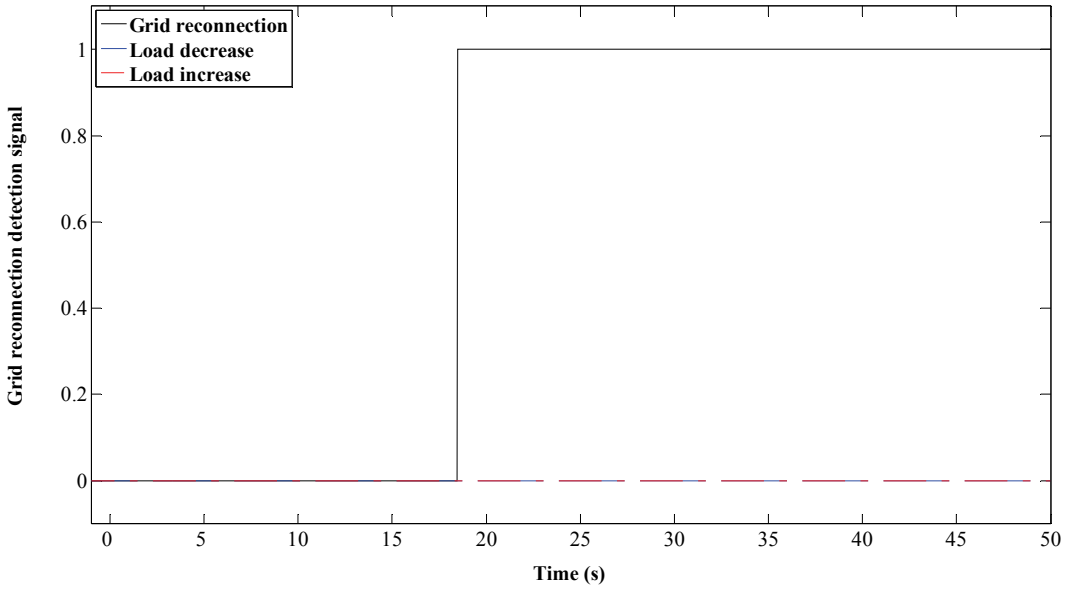

Fig. 4. 9. Grid reconnection detection signal for islanding and load changes

Fig. 4. 9 shows the output of the grid reconnection detection algorithm for grid reconnection, load decrease and load increase events. It can be seen from the figure that the grid reconnection detection algorithm correctly identifies the grid reconnection event from the load changing events.

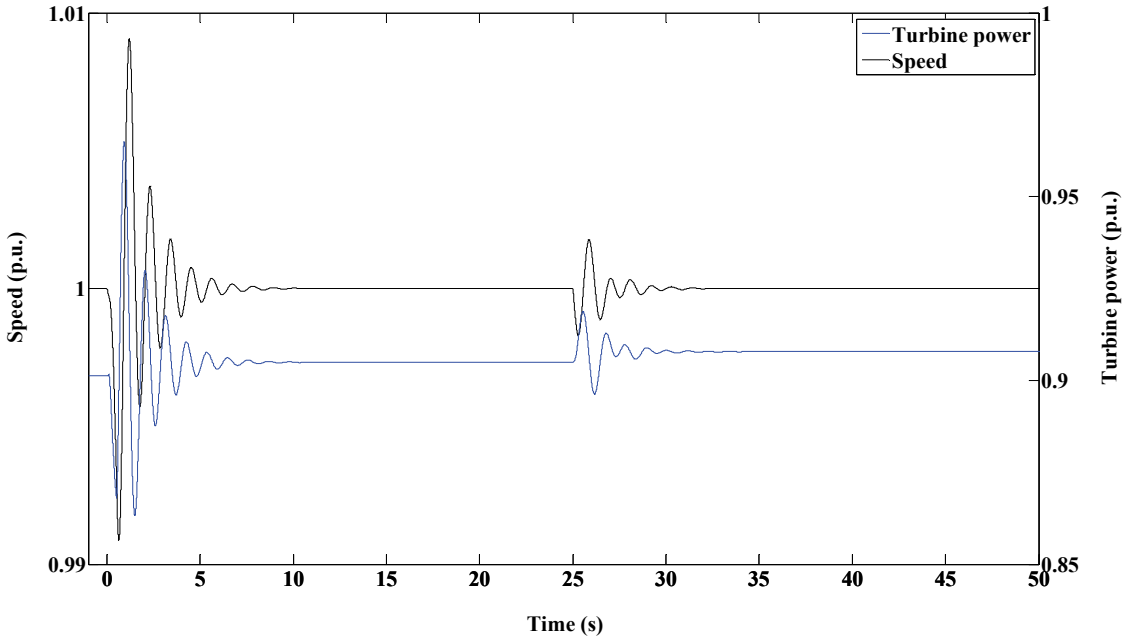

Fig. 4. 10. GTG speed and power for islanding and a 0.15 MVAr capacitor switching on at Bus 3

A 0.15 MVAr capacitor switching on at Bus 3 at *t=25s* is also simulated and Fig. 4. 10 shows the speed and output power of the GTG for islanding, at *t=0s,* and the capacitor switching on event. A 0.15 MVAr capacitor at Bus 3 switching off at *t=25s* event is also simulated. Fig. 4. 11 shows the GTG power and speed when the distribution system is islanded and when a capacitor switches off. Fig. 4. 12 shows the GTG power and speed when the distribution system is islanded, at *t=0s,* and a 110 kW induction machine switches on at *t=25s.*

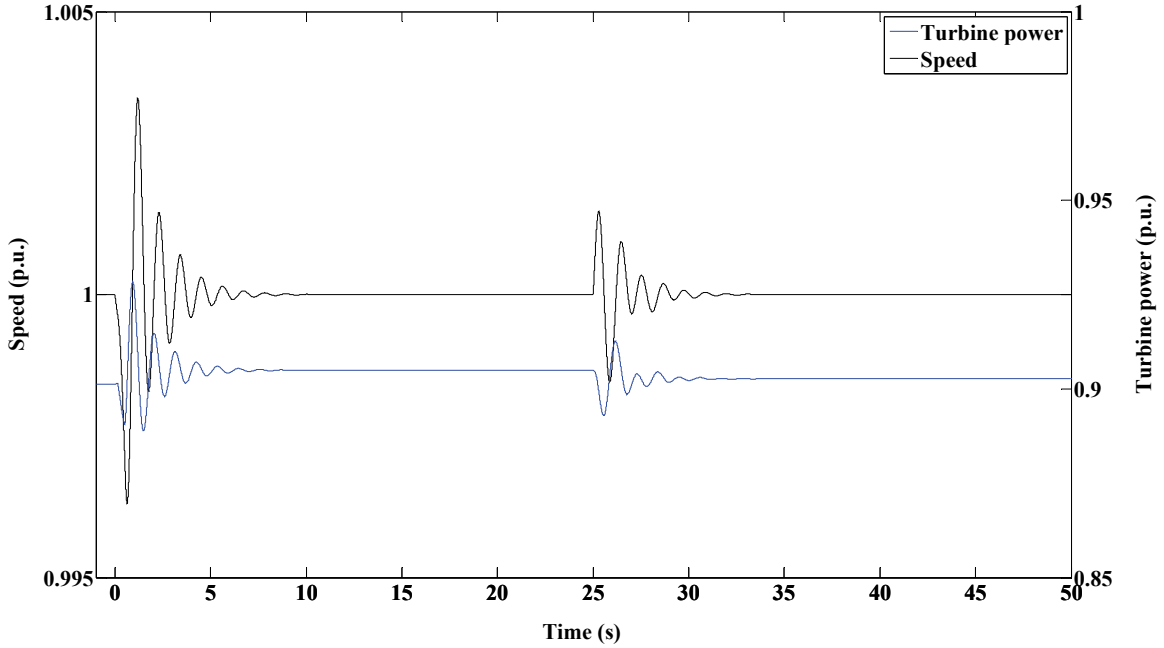

Fig. 4. 11. GTG speed and power for islanding and a 0.15 MVAr capacitor at Bus 3 switching off

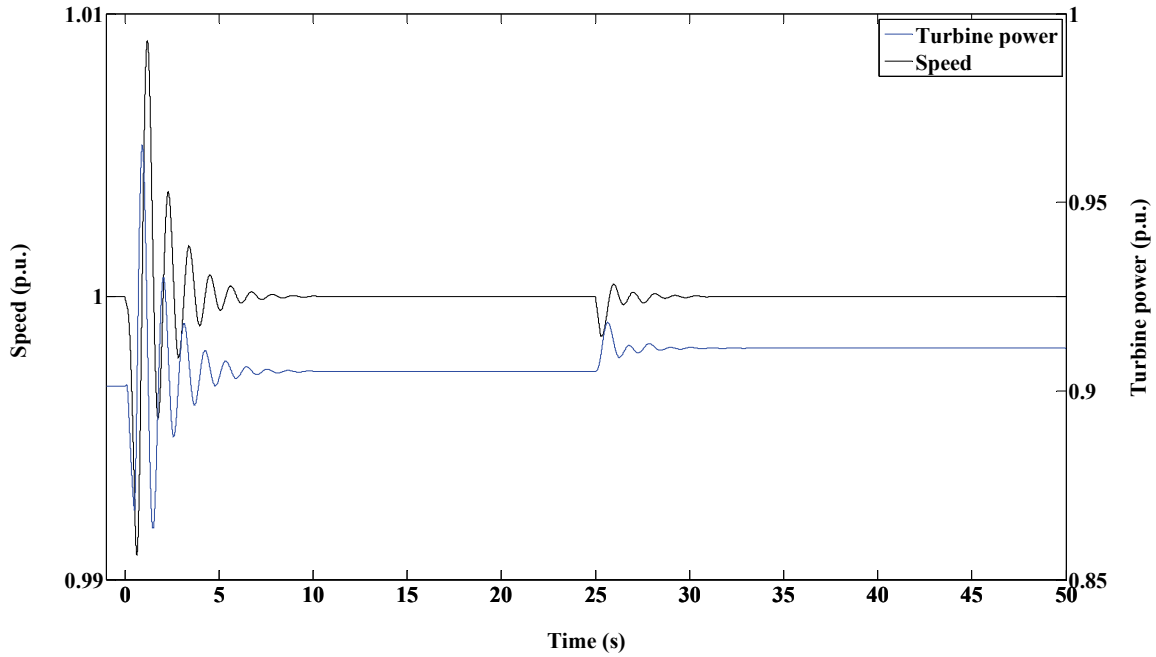

Fig. 4. 12. GTG speed and power for islanding and a 110 kW induction motor starting at Bus 2

Fig. 4. 13 shows the output of the grid reconnection detection algorithm for the capacitor switching events and the induction motor starting event. It shows that the grid reconnection algorithm correctly identifies these events as non grid reconnection events as $d\omega / dP_t$ is never zero or less for twenty five consecutive periods after these events.

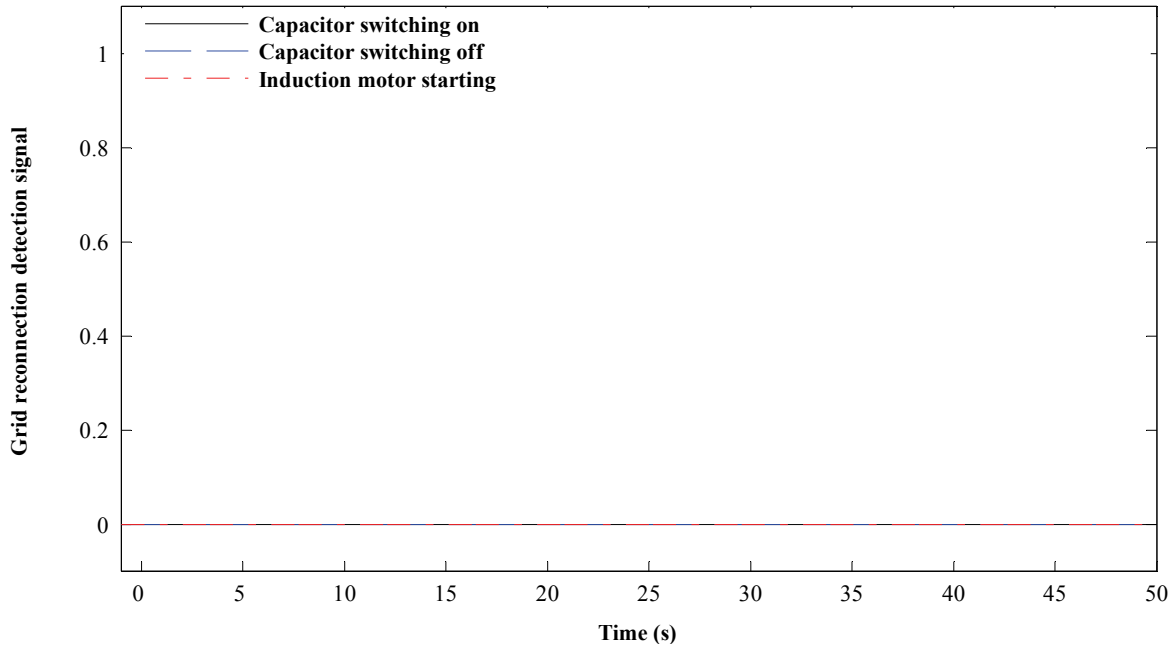

Fig. 4. 13. Grid reconnection detection signal for capacitor switching and induction motor starting

Fig. 4. 9 and Fig. 4. 13 show that the proposed grid reconnection detection can correctly detect the grid reconnection event from other normal events in a simple islanded distribution system. Although the grid reconnection detection presented in this section is simple, its application is limited to simple distribution systems with only one generator. There can be more than one DG in the distribution system and loads may not always be within the capacity of the generators. In such a case, the change in output power of DG may not be able to change the speed in same direction. As an example, frequency may continue to go down when the total amount of load is more than the total generation capacity, even if the generators increase their power. Furthermore, other elements (for instance protection relays) in the distribution system might also need to know the status of the distribution system as discussed in later chapters. Hence, grid reconnection detection should be done by monitoring parameters that are not specific to some elements (like output power or speed of the generator) but those parameters that can be measured at any place (like voltage and frequency).

4.2.4. Active Grid Reconnection Detection Technique

As mentioned earlier, the islanded distribution system and grid does not always operate at the nominal frequency. But, from time to time they are in phase if they are operating at different frequencies. Thus, there will be jump in frequency when the distribution system is reconnected to grid after the fulfilment of the grid reconnection criteria. Hence, the grid reconnection can be identified by monitoring the distribution system frequency.

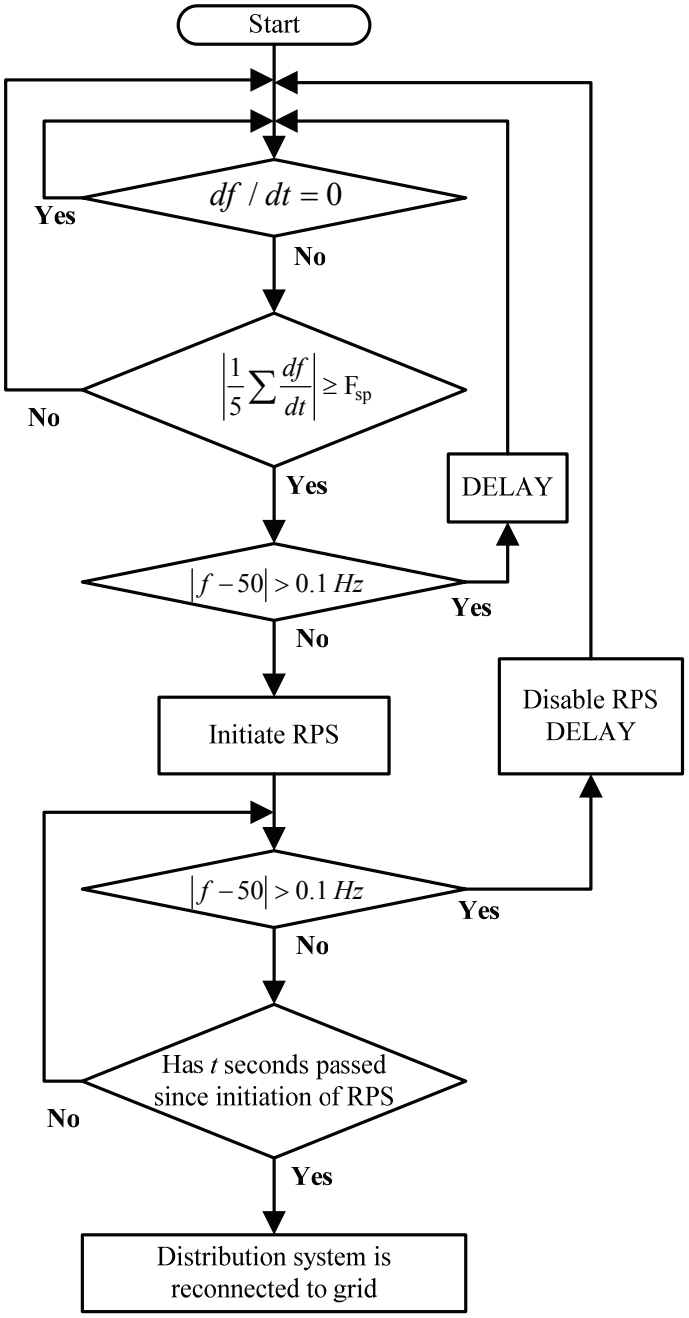

Fig. 4. 14. Active grid reconnection detection flowchart

The flowchart for the active grid reconnection detection algorithm is shown in Fig. 4. 14. Frequency is measured every voltage period and grid reconnection is suspected when there is a change in frequency. If the frequency goes outside the range of 50±0.1 Hz, it is obvious that the distribution system is still islanded as frequency is maintained within the range of 49.9-50.1 Hz in the Union for the Co-ordination of Transmission of Electricity (UCTE) system [77] under normal operating condition. Moreover, the distribution system is reconnected back to the transmission grid only when the transmission system frequency is within the range of 50±0.1 Hz. However, if the islanded distribution system frequency changes but stays within the range of 50±0.1 Hz, it can be the result of grid reconnection or any other events in the distribution system. To differentiate the events in the distribution system from grid reconnection, real power shift (RPS) is initiated as in the case of the islanding detection procedure. The RPS increases or decreases the power set point of the generators with increasing or decreasing frequency, respectively. As mentioned earlier, the speed error is kept constant during the RPS as the desired change in power, to correctly detect grid reconnection, may not be achieved if the speed error is not kept constant. If the distribution system is still islanded, the RPS pushes the frequency outside the range of 50±0.1 Hz. However, if the distribution system is reconnected to the grid, the frequency remains within the range of 50±0.1 Hz. If the frequency stays within the range of 50±0.1 Hz for 't' seconds after the initiation of the RPS, grid reconnection is detected and the RPS is disabled. But all the events in power systems result in some change in frequency. Hence, it is not a good idea to disturb the distribution system, which is already fragile, from time to time. Thus, magnitude of average rate of change of frequency over five periods ($Af5$) is calculated when frequency changes. The RPS is only initiated if $Af5$ is greater than a set point to suspect grid reconnection (F_{sp}) and the frequency, at the same time, is within the range of 50±0.1 Hz. F_{sp} is set according to the sensitivity required. If grid reconnection is to be detected even for a very small difference in the distribution system and the grid frequencies, F_{sp} should be set at low value. A small delay is added to account for transients due to the RPS. Some power system may not be strong enough to hold the frequency within 50±0.1 Hz and some may use different frequency (like 60 Hz in some countries). In that case, the range for the frequency should be chosen accordingly.

4.2.5. Modelling of the Test System to Test Active Grid Reconnection Detection Technique

The test distribution system presented in Fig. 2. 6 is used to test the grid reconnection detection methodology. The load and the generation data is presented in Table AXI. The output power of each GTG is 2.7 MW and each WTG is 80 kW. There is an excess of 432 kW of real power and deficiency of 2.758 MVAr of reactive power when the distribution system is islanded. Loads are modelled according to equation (2.3) and values of K_{f_p}, K_{v_p}, K_{f_q} and K_{v_q} are chosen

as 0.5. The speed governor data of the GTGs are presented in Table AXII and the excitation system data is presented in Table AX. The data for the power factor controller is presented in Table AXIII. The wind turbine aerodynamic efficiency curve is presented in Fig. B. 1. 't' is chosen as 2 seconds as the RPS drives the frequency outside the limits well within this time frame even when the frequency is at 50 Hz.

4.2.6. Simulation Results and Discussion for Active Grid Reconnection Detection Technique

Islanding is simulated by opening the circuit breaker (CB), in Fig. 2. 6, at *time (t)=0s*. Again, the minimum set point to suspect islanding (V_{SMin}), the set point to detect islanding without the RPS (V_{SMax}) and the set point to detect islanding with the RPS (V_{SMaxU}) are set as 40 V/s, 7200 V/s and 100 V/s, respectively. The RPS is chosen as 5 % and F_{sp} is chosen as 0.1 Hz/s since a difference of 0.01 Hz between the grid and the islanded distribution system frequencies will result in $Af5$ equal to 0.1 Hz/s. The delay gives the transients, due to the RPS and large events, enough time to die out. In this study, delay is chosen as 10s as the transient, due to RPS, die out within this time.

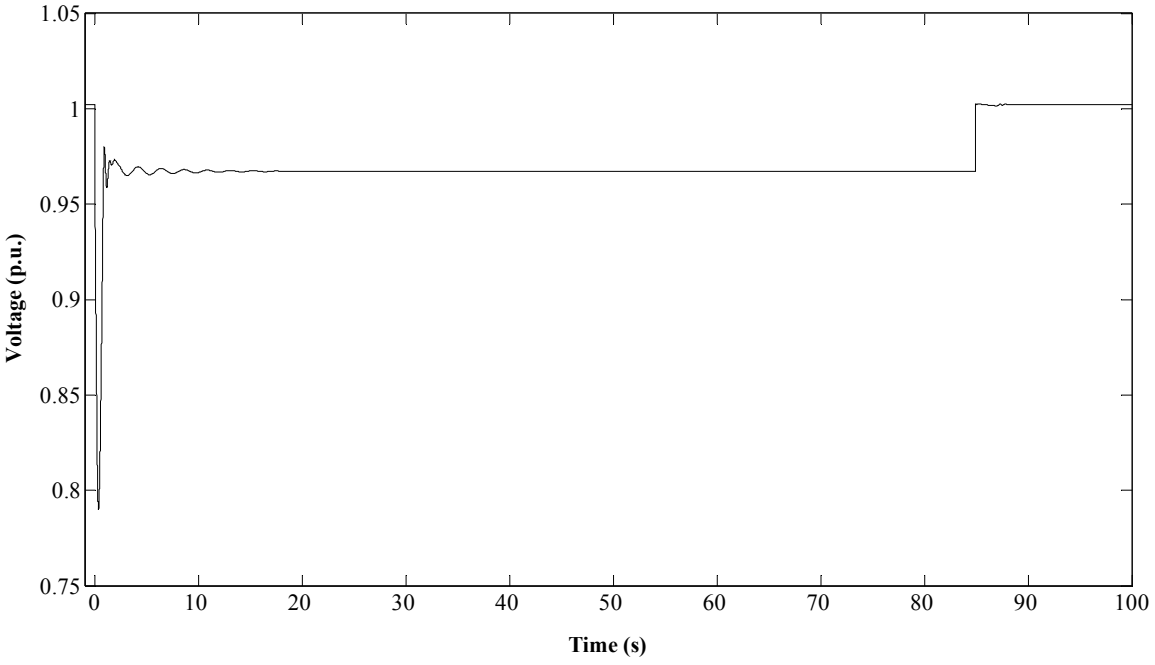

Fig. 4. 15. Bus 06 voltage for islanding and grid reconnection

Fig. 4. 15 shows the voltage at Bus 06 for islanding, and grid reconnection and RPS for the test distribution system described in Section 4.2.5. Islanding is detected at *t=0.14s* as $Av7 = 21.6\ kV/s$ which is higher than V_{SMax}. The GTG1 changes its control strategy from droop and power factor control to isochronous and voltage control whereas, GTG2 and GTG3 change

their control strategy from droop and power factor control to isochronous with feedback and voltage control.

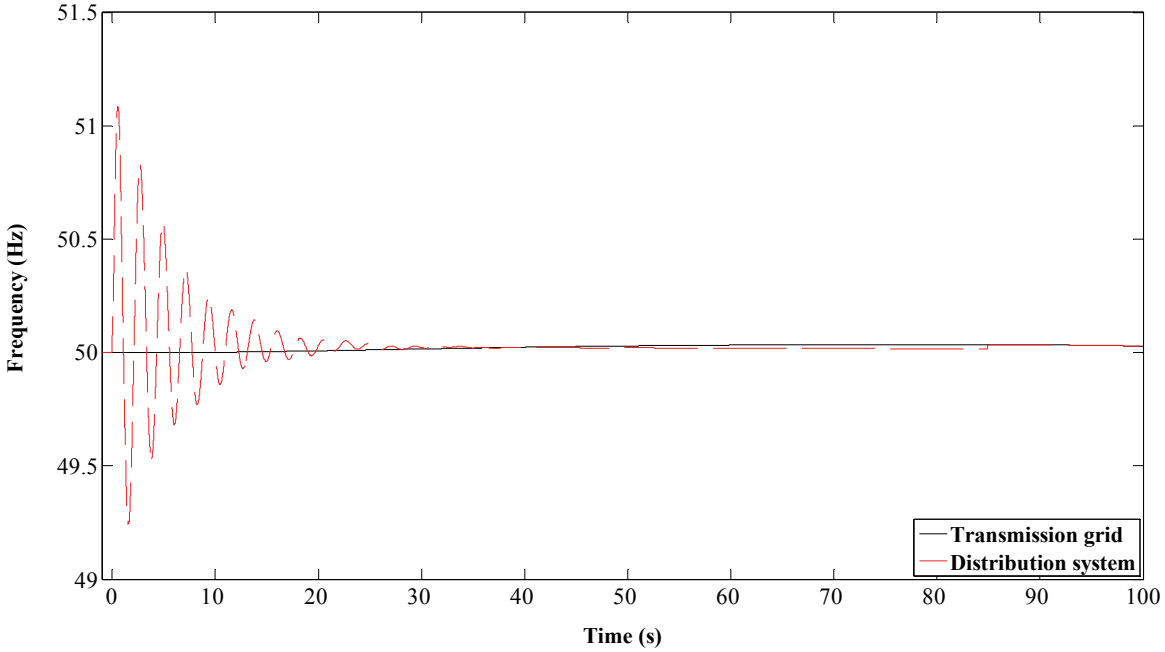

Fig. 4. 16. Grid and distribution system frequency during islanding and grid reconnection events

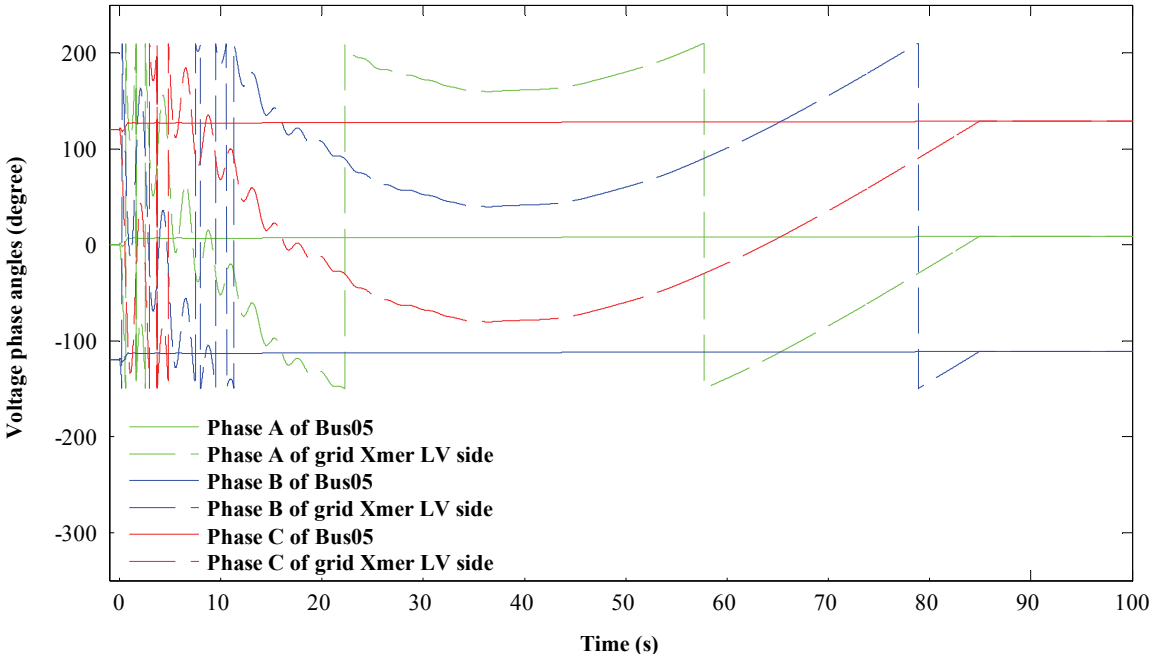

Fig. 4. 17. Bus 05 and grid transformer LV side voltage phase angles for islanding and grid reconnection.

The grid frequency and the islanded distribution system's frequency deviate from 50 Hz from time to time. To simulate this, grid frequency is changed as shown in Fig. 4. 16. The distribution system frequency is also shown in Fig. 4. 16. At *t=84.92s,* all the criteria for grid

resynchronization are met and the two systems are reconnected. Fig. 4. 17 shows the angles of voltage phases at either sides of CB when the distribution system is islanded from the transmission at *t=0s* and reconnected back at *t=84.92s.*

After the distribution system is reconnected to the grid, $Af5$ is 0.192 Hz/s at *t =85.02s,* which is greater than F_{sp} and the frequency is within the range of 49.9-50.1 Hz. Thus, the RPS is activated. Even after the RPS, the system frequency remains within the range of 49.9-50.1 Hz for 2 seconds and hence grid reconnection is detected at *t=87.02s.* The RPS is deactivated and the controls of GTGs are shifted back to power factor control and droop control mode. The reference power factor and power factor of the GTG1 are presented in Fig. B. 10. The GTG1 follows the reference power factor when the distribution system is connected to the grid. However, it maintains the voltage while the distribution system is islanded. Similarly, the power set point of the GTG1 and the turbine power are presented in Fig. B. 11. Again the GTG1 produces power according to the power set point when the distribution system is connected to the grid and the frequency is 50 Hz. But, it does not follow the power set point while the distribution system is islanded. Instead it maintains the frequency of the islanded distribution system. The output of the control select of the GTG1 is presented in Fig. B. 12. It clearly shows the GTG1 operates in a droop control mode when the distribution system is connected to grid and operates in an isochronous mode when the distribution is islanded. The speed error is kept constant when the RPS is initiated.

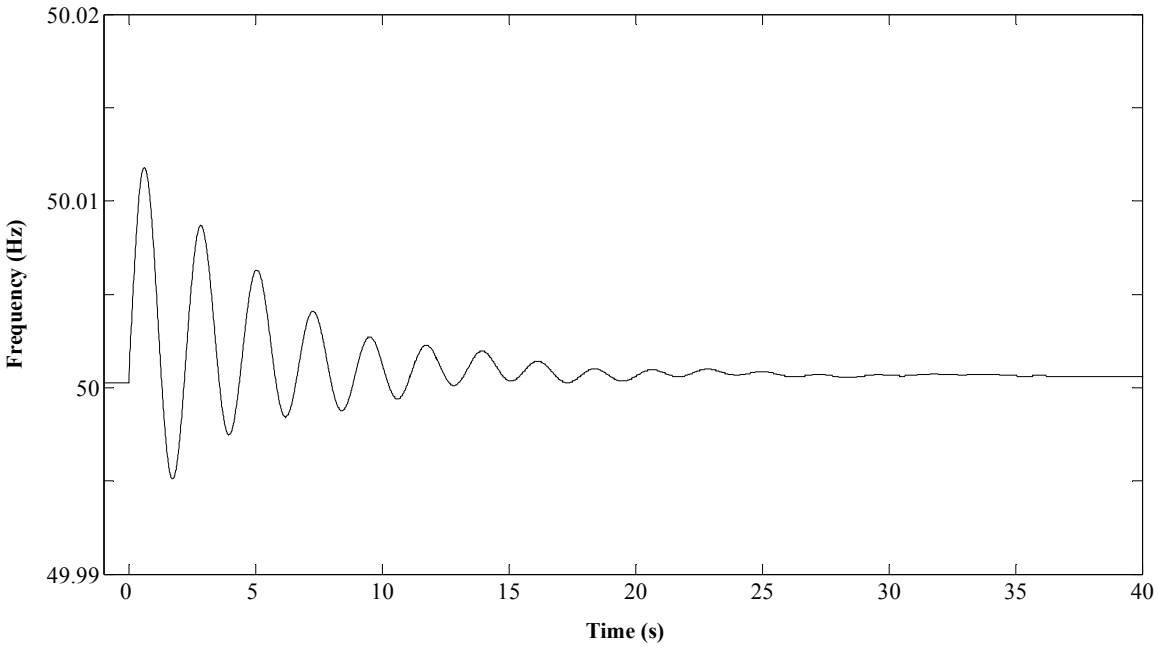

Fig. 4. 18. Distribution system frequency for Load05 decreasing by 10 kW and 4 kVAr during island condition

To show the effectiveness of the grid reconnection detection algorithm, various normal events in the power system have been simulated. Fig. 4. 18 shows the change in frequency when Load05 decrease by 10 kW and 4 kVAr at *t=0s*. The load decrease is less than 0.2 % of Load05. $Af5$ is always less than F_{sp}. As a result the RPS is not initiated and the event is neglected as a non grid reconnection event.

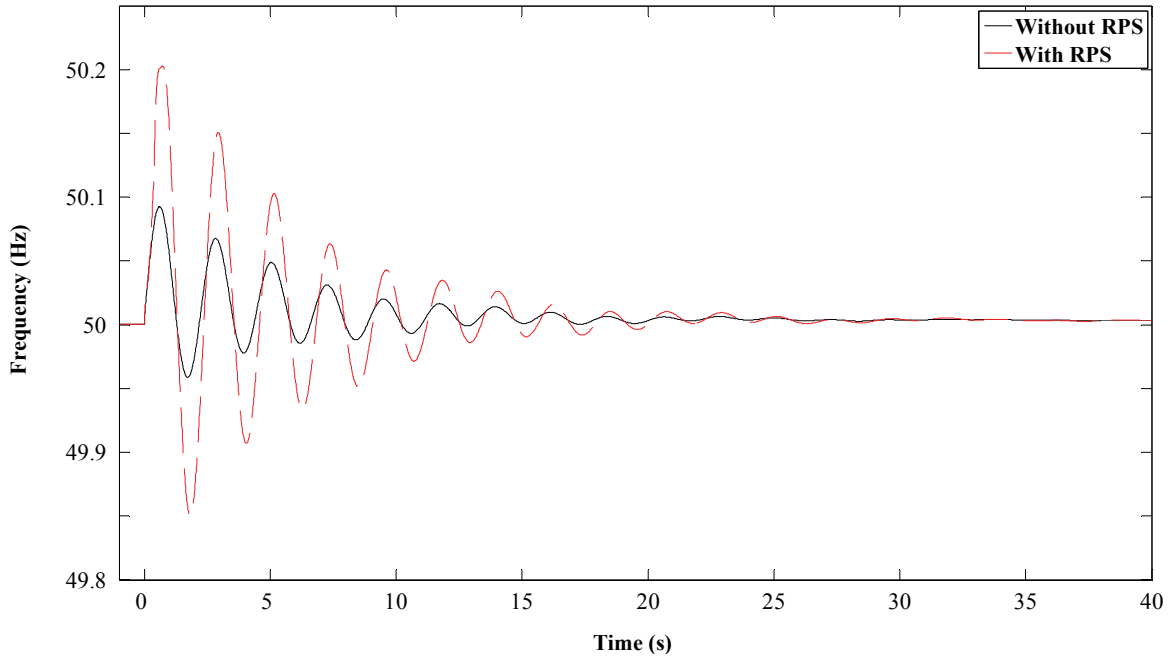

Fig. 4. 19. Distribution system frequency for Load05 decreasing by 80 kW and 20 kVAr during island condition

Fig. 4. 19 shows the change in frequency when Load05 decrease by 80 kW and 20 kVAr at *t=0s*. The load decrease is around 1.3 % of Load05. $Af5$ is 0.265 Hz/s, which is higher than F_{sp} and hence the RPS is initiated. The RPS push the frequency above 50.1 Hz and the grid reconnection detection algorithm detects that the distribution system is still islanded. Fig. 4. 19 also shows the distribution system frequency for the load decrease event without the RPS. The frequency is not pushed beyond 50.1 Hz without RPS. This highlights the necessity of using the RPS.

Fig. 4. 20 shows the change in frequency when Load05 increases by 80 kW and 20 kVAr at *t=0s*. The RPS is initiated as $Af5$ is 0.265 Hz/s and frequency reaches 49.9 Hz at *t=0.42s*. It is detected the distribution system is still islanded and the RPS is disabled. Fig. 4. 20 also shows the frequency of the distribution system for the load increase event without the RPS. Again the frequency stays within 50±0.1 Hz without the RPS.

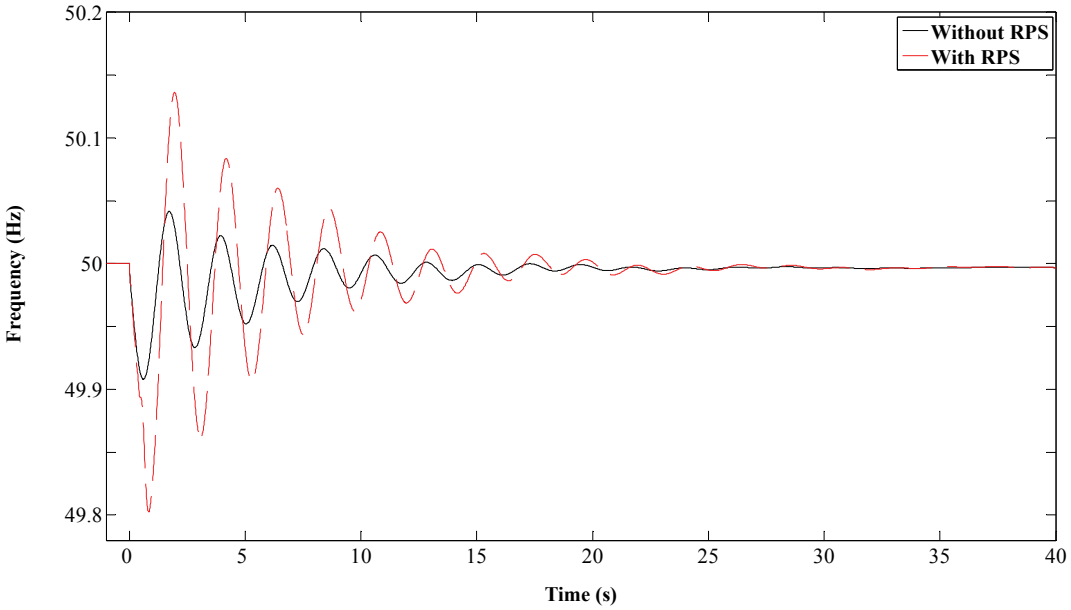

Fig. 4. 20. Distribution system frequency for Load05 increasing by 80 kW and 20 kVAr during island condition

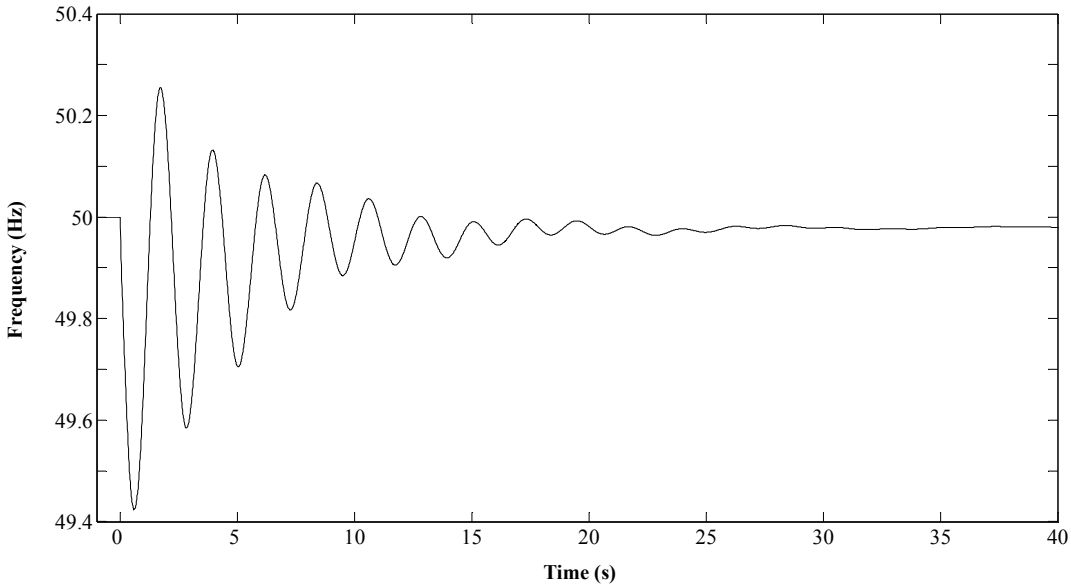

Fig. 4. 21. Distribution system frequency for Load05 increasing by 0.5 MW and 0.05 MVAr during island condition

Fig. 4. 21 shows the distribution system frequency when the load increases by 0.5 MW and 0.05 MVAr at *t=0s.* The load increase is around 8% of Load05. The frequency goes below 49.9 Hz within *t=0.1s.* Hence, it is clear that the distribution system is not yet connected to the grid. Frequency oscillates as a result of the load increase event. The delay helps the frequency to settle down and avoid unnecessary use of the RPS. After *t=10s,* the oscillating frequency does not result in $\Delta f 5$ greater than F_{sp}.

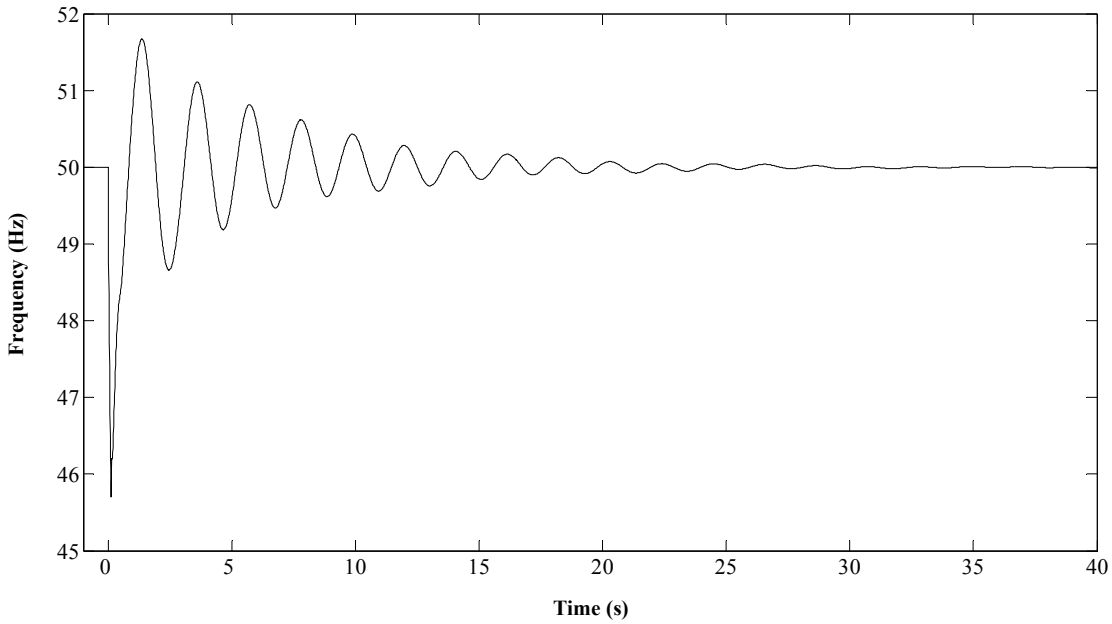

Fig. 4. 22. Distribution system frequency for a three phase fault at Bus 14 during island condition

A three phase fault, with a fault resistance of 10 Ω, at Bus 14 is also simulated at *t=0s.* The fault is cleared by opening the breaker at the beginning of the line Z13-14 at *t=0.12s.* Fig. 4. 22 shows the distribution system frequency for the event. Again, the frequency goes below 49.9 Hz and the grid reconnection detection algorithm ignores the event. At *t=10.1s,* the frequency is above 50.1 Hz and again the grid reconnection detection algorithm ignores the event even though $Af5$ is greater than F_{sp}. After *t=19.3s,* $Af5$ is no longer greater than F_{sp}.

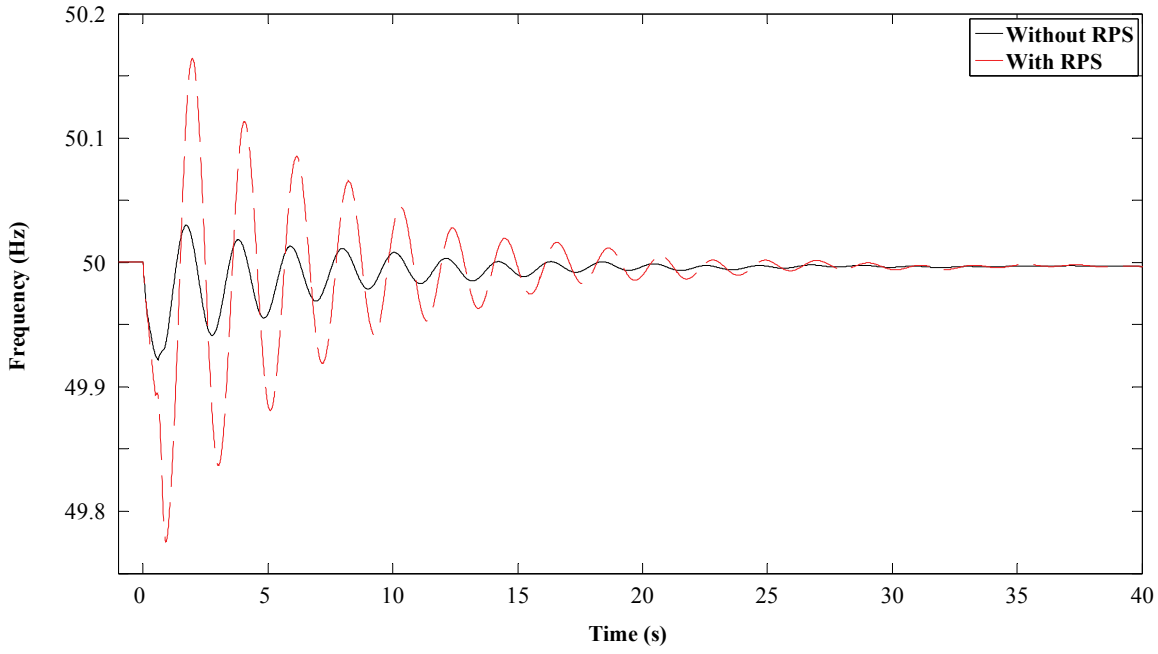

Fig. 4. 23. Distribution system frequency for a single phase to ground fault at Bus 14 during island condition

Fig. 4. 23 shows the distribution system frequency when a single phase to ground fault, with zero fault impedance, occur at Bus 14 at *t= 0s.* The fault is cleared at *t=0.57s* by opening the breaker at the beginning of the line Z13-14 . $Af5$ is 0.286 Hz/s at *t=0.1s* and RPS is initiated as the frequency is within the range of 49.9-50.1 Hz. As a result, the frequency is pushed beyond 49.9 Hz and the algorithm correctly identifies the fault as not a grid reconnection event. Fig. 4. 23 also shows the frequency of the islanded distribution system for a single phase to ground fault event only. Again, the frequency does not go outside 50±0.1 Hz without the RPS.

Fig. 4. 24 shows the distribution system frequency when the wind speed decreases by 0.5 m/s at *t=0s.* Now, $Af5$ is always less than F_{sp} and hence no RPS is initiated and the algorithm identifies the event as non grid reconnection event. The GTGs with their controller increase their power to cover the decrease in WTGs' power and stabilize the frequency around 50 Hz.

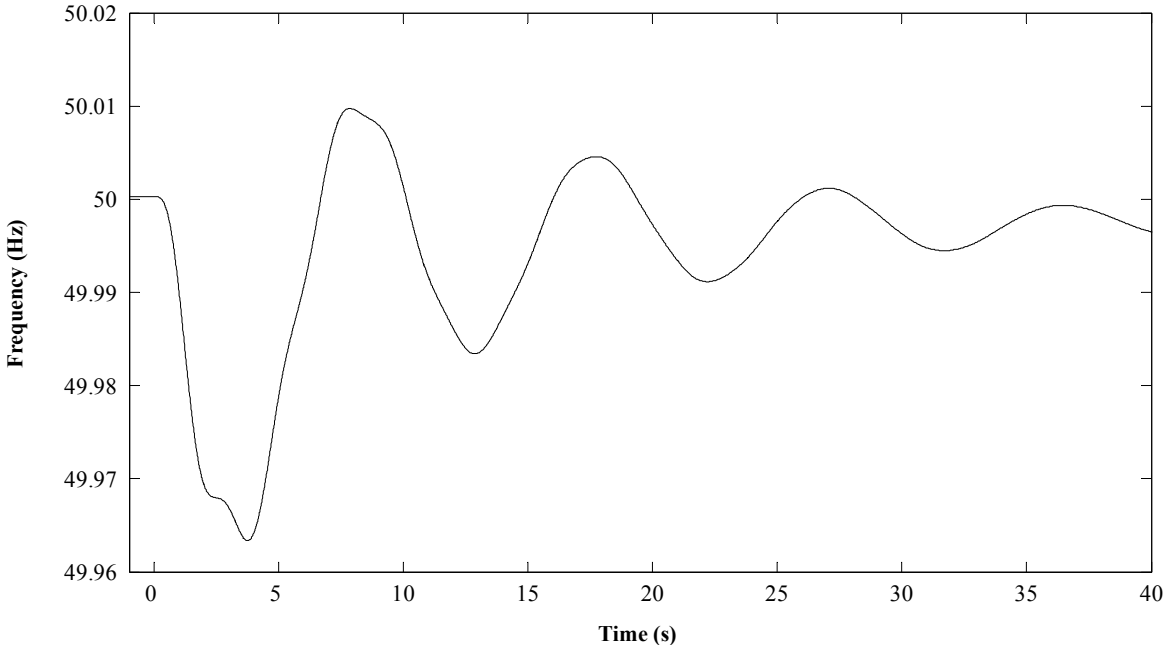

Fig. 4. 24. Distribution system frequency for wind speed decrease by 0.5 m/s during island condition

Fig. 4. 25 shows the distribution system frequency when the wind speed is increased by 1 m/s at *t=0s.* The resulting frequency change produces $Af5$ of 0.102 Hz/s at *t=1.2s,* which is greater than F_{sp}. Furthermore, the frequency is within the range of 49.9-50.1 Hz and hence the RSP is initiated. RPS pushes the frequency above 50.1 Hz. Thus, it is determined that the distribution system is still islanded and the RPS is disabled. The frequency plot, without the RPS, shows that the frequency would have gone above 50.1 Hz anyways. However, the RPS is initiated as $Af5$ is more than F_{sp} and the frequency is with the range of 49.9-50.1 Hz. The initiation of the RPS could have been avoided by choosing a higher value for F_{sp}, but it would have resulted in the need for a higher frequency jump during grid reconnection for it to be detected.

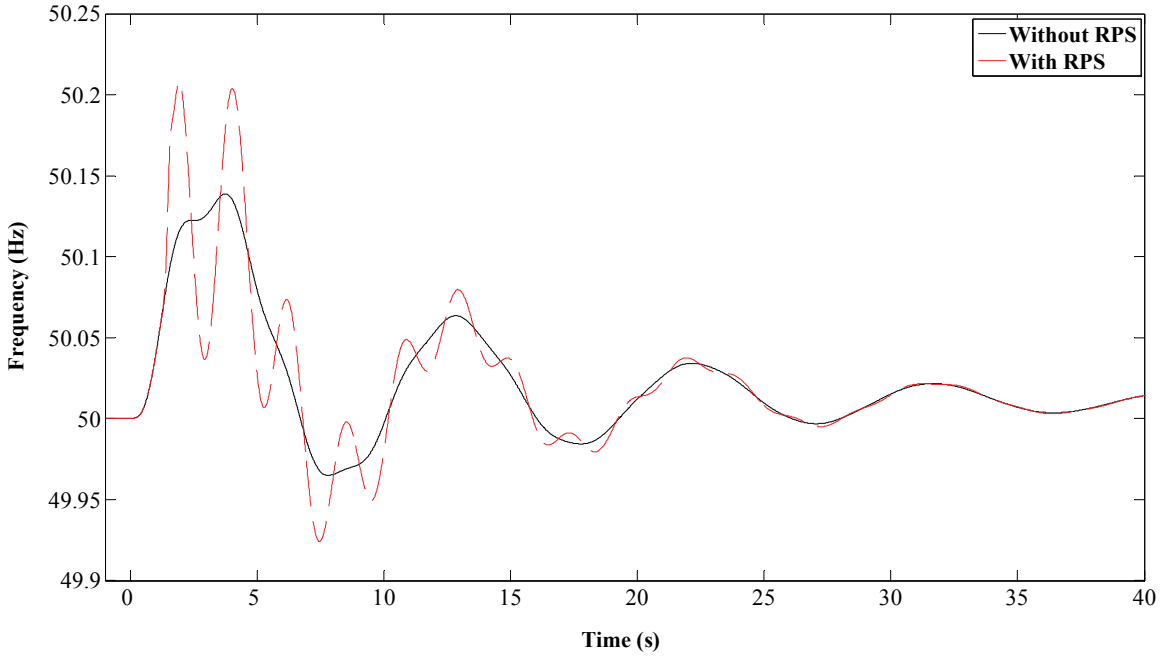

Fig. 4. 25. Distribution system frequency for wind speed increase by 1 m/s during island condition

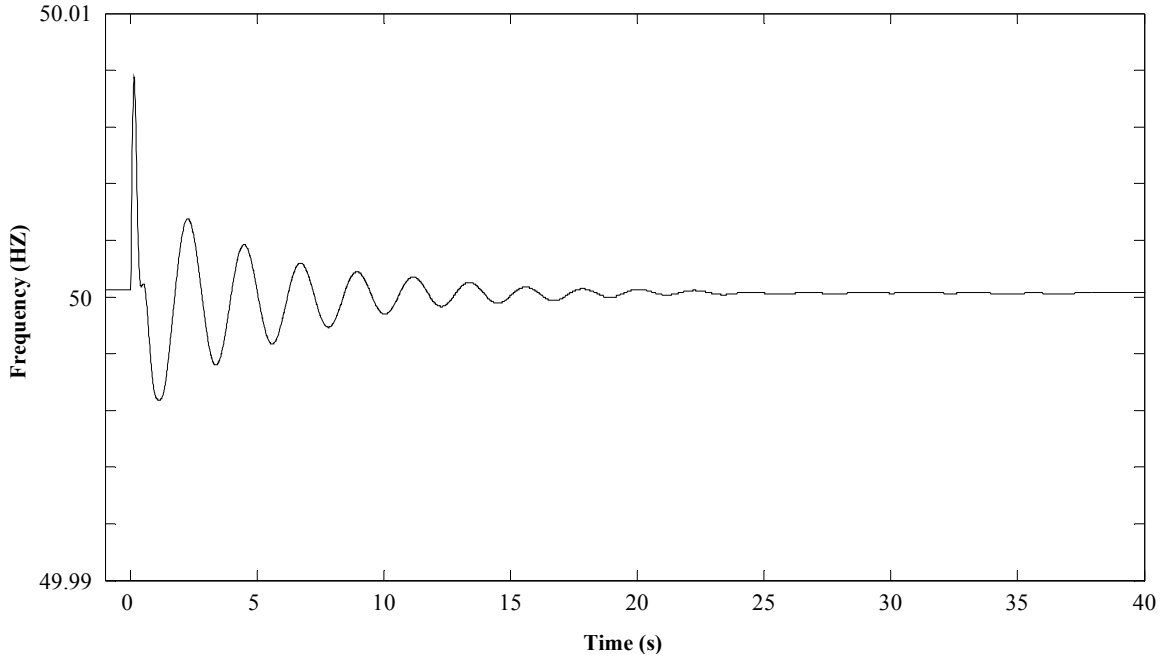

Fig. 4. 26. Distribution system frequency for a 0.2 MVAr capacitor switching off at Bus 12 during island condition

Fig. 4. 26 shows the distribution system frequency for a 0.2 MVAr capacitor switching off at Bus 12 during island condition. The capacitor switching off results in a slight reduction in voltage. Hence, the loads' real power demands are also reduced as they are voltage dependent and the distribution system frequency increases slightly. However, the average rate of frequency change

is not high enough to initiate the RPS. The event is ignored as any other event other than grid reconnection.

Fig. 4. 27 shows the distribution system frequency for a 45 kW induction motor switching on at Bus 12, *at t= 0s,* during island condition and the RPS initiation at *t=0.1s.* The RPS is initiated as $Af5$ is 0.262 Hz/s, which is larger than F_{sp}. The RPS pushes the frequency below 49.9 Hz to conform that the distribution system is still islanded. Fig. 4. 27 also shows the islanded distribution system's frequency for motor staring event without RPS. The frequency stays within 49.9-50.1 Hz. If the RPS was not been initiated, the algorithm would have identified the event as a grid connection event. This again highlights the necessity of the RPS.

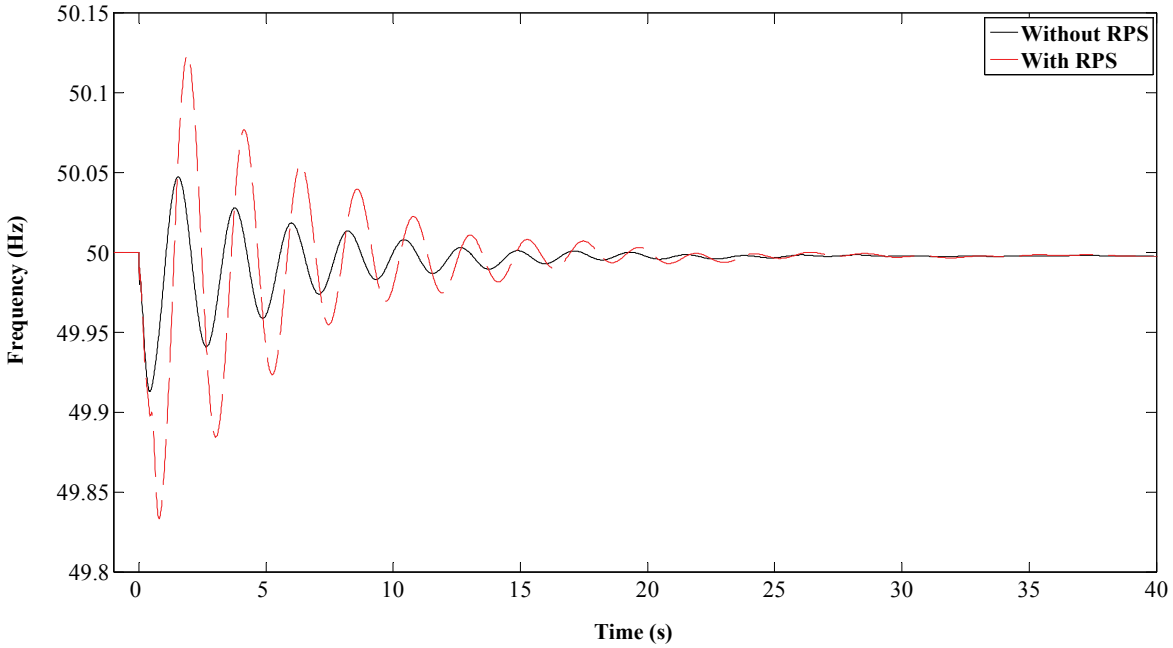

Fig. 4. 27. Distribution system frequency for a 45 kW induction motor switching on at Bus 12 during island condition

All the results are summarized in Table 4. 1. Some small events like a small load changes and a small wind speed changes occur very often. If a perturbation is applied for these events, then it has to be applied too frequently. Furthermore, events like a small capacitor switching, which are not that frequent, also results in very small frequency change and hence can be ignored. Again events like a large load change and a three phase faults results in large frequency deviations and hence can be ignored as non grid reconnection events as the distribution system is reconnected back to the transmission grid only when the transmission grid frequency is within 49.9 Hz to 50.1 Hz. Hence, the methodology successfully neglects the small events and it also neglects the large events. The methodology can correctly differentiate grid reconnection event from other normal events.

Table 4. 1

Summary of results for different events

Events	Time when $\Delta f_5 > F_{SP}$ (s)	Δf_5 (Hz/s)	RPS initiated	Time when $\lvert F-50\rvert > 0.1$ Hz (s)
Grid Reconnection	85.02	0.192	Yes	-
10 kW and 4 kVAr load decrease	-	-	No	-
80 kW and 20 kVAr load decrease	0.1	0.265	Yes	0.36
80 kW and 20 kVAr load increase	0.1	0.265	Yes	0.42
0.5 MW and 0.05 MVAr load increase	0.1	1.68	No	0.06
Three phase fault	0.1	37.78	No	0.02
Single phase to ground fault	0.1	0.286	Yes	0.46
Wind velocity decrease by 0.5 m/s	-	-	No	-
Wind velocity increase by 1 m/s	1.2	0.102	Yes	1.42
200 kVAr capacitor switching off	-	-	No	-
45 kW induction motor starting on	0.1	0.262	Yes	0.42

Various events are simulated while the distribution system is islanded. Results (Fig. 4. 18 to Fig. 4. 27) show that the controllers are able to maintain frequency close to the reference while the distribution system is islanded.

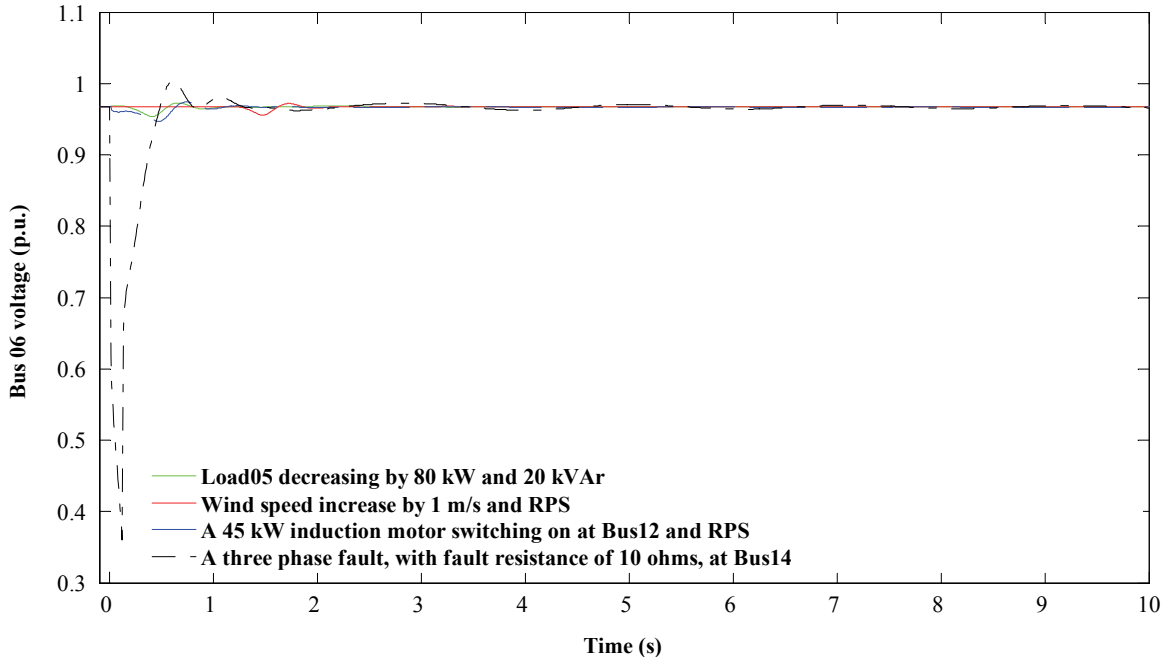

Fig. 4. 28. Voltage at Bus 06 during islanded and various events

Fig. 4. 28 shows the voltage at Bus 06 during selected events while the distribution system is islanded. The figure shows that the voltage of the islanded distribution system is also maintained during those events.

Delay helps the frequency to settle down after a large event and the RPS. But, in case of a large event, the frequency may take longer time to settle down and the RPS may be initiated after the delay which is unnecessary. In case of the three phase fault, $Af5$ is greater than F_{sp} even after the delay of 10s. But, the RPS is not initiated as the frequency is above 50.1 Hz. However, it is quite possible that the frequency could have been within the range with a fault at another location or with a different fault resistance. Again, increasing the delay will help to overcome this problem but then the grid reconnection can go unnoticed. Furthermore, F_{sp} is chosen as 0.1 Hz/s assuming that the difference in the frequencies of the distribution and transmission systems will be at least 0.01 Hz when they are reconnected. But, there is also the possibility that the difference in frequencies may be even smaller than 0.01 Hz when the two systems reconnect and grid reconnection can go undetected. Reducing the value of F_{sp} can overcome this problem but then the RPS will be initiated too frequently while the distribution system is islanded. However, disturbing a system, which is already fragile, frequently is also not a good idea. Hence, choosing F_{sp} and delay time is system specific. If high sensitivity is desired, lower values of F_{sp} and delay time should be chosen. On other hand if infrequent disturbance is desired, higher values of F_{sp} and longer delay time should be chosen. But, how small the value of F_{sp} is chosen; the possibility of the distribution and transmission systems reconnecting with $Af5$ smaller than F_{sp} cannot be neglected. One of the possible solutions is putting minimum frequency difference requirement to reconnect the two systems similar to the requirement on maximum frequency difference. This may elongate the islanding time. Another possible solution is initiating the RPS when $Af5$ smaller than F_{sp} for a long time; half an hour for an example. Furthermore, the frequency of the islanded distribution system can be maintained at some frequency other than 50 Hz (49.95 for an example) and that will insure that the two systems operate at different frequency and they become in phase form time to time.

4.3 Conclusion

When the GTG is connected to the grid, it operates at a constant power factor with speed droop controller. One of the GTG operates in isochronous mode, when islanded, while the rest operate with isochronous controllers with feedback and all the GTGs control voltage. Hence, it is necessary to detect islanding and grid reconnection to choose the optimal control strategy based on the state of distribution system. Two grid reconnection detection algorithms are presented. The first reconnection detection algorithm is simple but it is applicable to only small distribution systems

with a single DG unit that has enough capacity to supply local loads. It is based on rate of change of speed over power. The second grid reconnection technique is based on the frequency, rate of frequency change and RPS. The grid reconnection can be detected at every location and is applicable to a distribution system with one or more DG units.

Chapter 5

Under-frequency Load Shedding

When a distributed system with DG units is islanded, most often frequency will change. The frequency will either go up if there is excess generation or down if there is excess load. If the frequency goes up, it can be controlled by reducing the output power of the generators. Similarly, when the frequency goes down, it can be brought back by increasing the output power. Photovoltaic generators uses maximum power point tracking, variable speed wind turbines optimize power co-efficient (Cp) to produce maximum power, DCHPs are operated at maximum power. Thus, if all the generators are operating at maximum power and the frequency goes down, the only way to bring the frequency back to normal is to shed some loads.

The problem of optimal load shedding has been extensively investigated. A static load shedding strategy has been proposed in [78], which keeps on shedding a fixed amount of load with decreasing frequency. A fast acting load shedding is proposed for implementation in the System Control Centre in [79]. Supervisory Control and Data Acquisition (SCADA) based load shedding strategy has been proposed in [80]. Another load shedding scheme based upon SCADA for an isolated system is presented in [81]. And still another load shedding strategy based on the on-line measurement of the loads and load-frequency characteristics is presented in [82]. Loads with smaller frequency dependency are shed first and those with larger frequency dependency are shed later. The problem with these methods is that real time information of loads is not always available and implementing online load measurement is expensive for small distribution systems. Furthermore, system's load-frequency dependency is often hard to determine especially with constantly changing loads. There is also an adaptive load shedding strategy, which changes the relay settings according to the frequency decay curve [83] as well as a load shedding method based on the frequency information and integration of df/dt to find the amount of load to be shed [84]. Other adaptive load shedding strategies based on df/dt are presented in [85]-[89]. But the need of real time load and generation data still persists. Furthermore, system inertia which is needed to calculate the amount of load to be shed is difficult to determine when the system has significant penetration of generations, which are stochastic in nature such as wind turbines generators. The load shedding problem for the islanded distributed system should be treated differently from the large power system because of differences in characteristics. Islanded distribution systems often have small generators and hence small inertia. Thus, the frequency tends to decay more rapidly. Fig. 5. 1 shows the distribution system frequency when the test distribution system, presented in

Fig. 2. 6, is islanded while all the DG units are operating at maximum power and the distribution system has a 1.84 MW power deficiency. Loads are assumed as constant power loads. Islanding is simulated at *t=0s.* The distribution system collapses within 0.24 seconds of islanding. Hence, it is critical to shed loads quickly to stabilize the frequency.

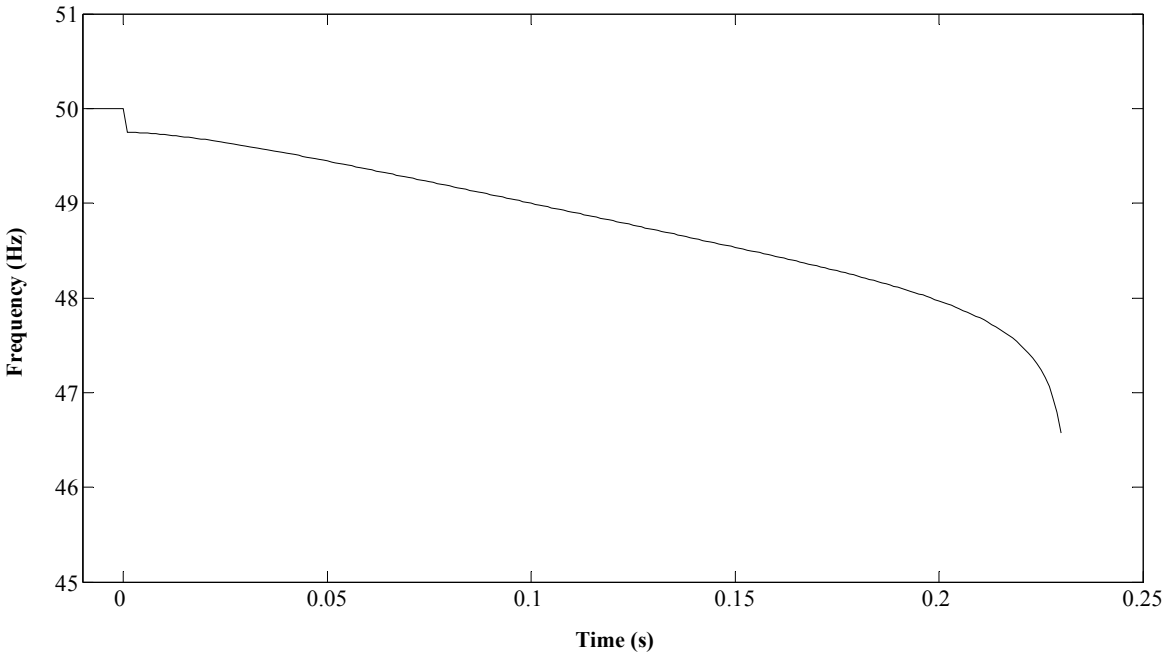

Fig. 5. 1. Frequency of the test distribution system, presented in Fig. 2. 6, after islanding

Load shedding in the distribution system may not be governed by technical reasons alone but also by economical reasons. With the concept of custom power, customers will pay more for better power quality and reliability. A study in Sweden shows that willingness to pay (WTP) is significantly higher for unplanned outages [90]. Distribution system operators are obligated to supply loads that are paying more without any regards to demand size. Furthermore, without real time load and generation data, the amount of load to be shed is unknown. When the frequency goes down in a distribution system, it should be brought back near to the reference by shedding a number of loads. Hence, the optimal load shedding strategy for an islanded distribution system should shed an optimal number of loads. The dynamic or adaptive load shedding technique sheds loads when the rate of change of frequency (RoCoF) is less than certain preset value. Based upon this philosophy, islanding is simulated in the test distribution system at *t=0s* and loads are shed when for RoCoF is less than -10 Hz/s for the first time and shed even when in RoCoF is less than zero only other times. Since the loads' real time demand is unknown, loads are shed one at a time. Load 09 and Load 10 are shed at *t=0.09s* and *t=0.18s* after islanding. Both loads have real power demand of 119 kW. The frequency of the test distribution system is presented in Fig. 5. 2. The third load is to be shed at *t=0.27s* but the test distribution system collapse before that time. The reason is that not enough loads are shed from the start. Hence, the first step of load shedding is critical in not

letting the frequency reach a low level from where it might be difficult to recover the system. The main objective of load shedding is to maintain the stability of the system by shedding loads but at the same time it should not shed more loads than required. An under-frequency load shedding for islanded distribution systems with DG units based on frequency information, rate of change of frequency, customers' WTP and loads' histories is presented here. Loads' histories can be easily obtained from data logs at load points. WTP can be determined by asking customers how much they are willing to pay for being supplied during islanding. This can be done at the same time when customers chose the electricity tariff scheme. Ranking of load (NL) for load shedding is based on WTP.

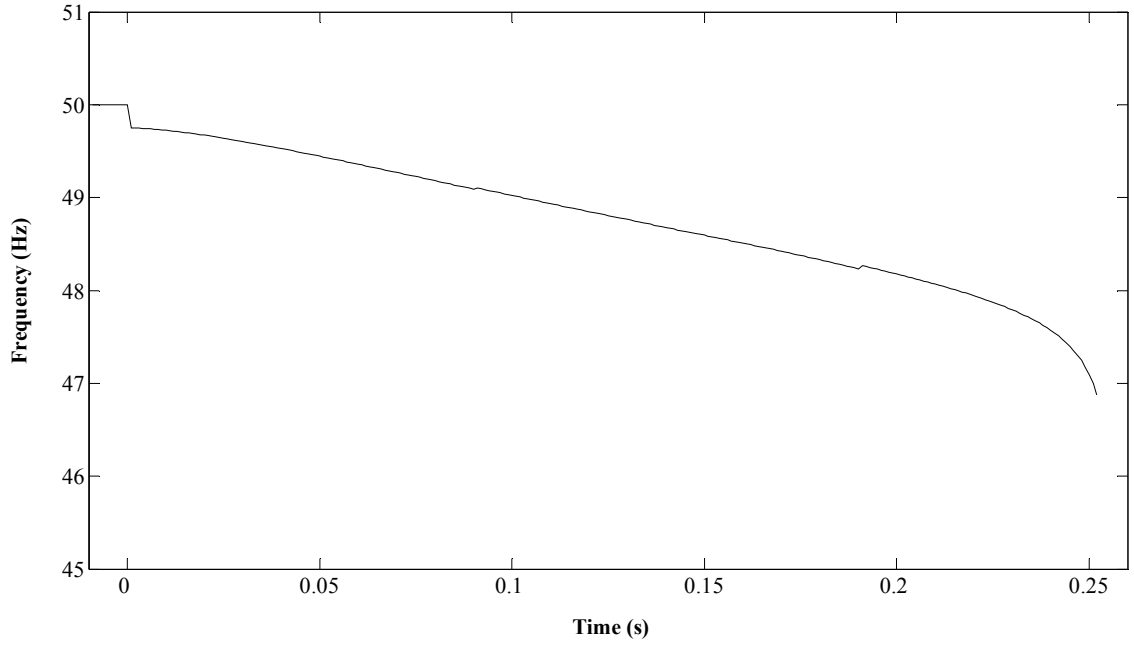

Fig. 5. 2. Frequency after islanding and traditional load shedding of the test distribution system presented in Fig. 2. 6

The proposed methodology is presented in Section 5.1. The test distribution system in which the proposed methodology has been tested is presented in Section 5.2. Simulation results are presented in Section 5.3 with some discussion and Section 5.4 draws some conclusions.

5.1 Proposed Methodology

The load shedding scheme is to be implemented at every load points. Loads are ranked based on their willingness to pay. A *look-up table*, like Table 5. 1, is created and loads are shed according to it. It is created using the loads history and loads' willingness to pay.

5.1.1. Procedure to Creation of Look-up Table

A look-up table is created, using the past information on loads and their willingness to pay, in the following way:

Step 1: Rank all the loads with the load that is willing to pay the least ranked first and the load that is willing to pay the most ranked last.

Step 2: Consider guaranteed generations only. Generation from sources like wind, solar, etc may not be available all the time. In the case of the test distribution system, guaranteed generation is 9 MW from GTGs.

Step 3: Consider loads as constant PQ loads since dependency on frequency and voltage is difficult to determine.

Step 4: Find the peak real power demand of individual loads for a previous period (P_{ppi}) from data available. As an example, for the month of October 2006, the peak real power demand of previous period for Load JUEL (P_{ppJUEL}) is 0.919 MW (its peak real power demand for the month of September 2006)

Step 5: Find the rate of change of frequency corresponding to a load ($RoCoFL_i$) by simulating an islanding with a system having a real power deficiency equivalent to (P_{ppi}). For example, Load JUEL's peak real power demand for the previous period is 0.919 MW. Islanding is simulated by adjusting the loads in the island such that it has real power deficiency of 0.919 MW. The RoCoF measured (-27.43 Hz/s) is the $RoCoFL_i$ associated with Load JUEL.

Step 6: Repeat Step 5 for all the loads.

Step 7: Calculate $\sum_{i=1}^{NL} RoCoFL_i$ and create a look-up table like Table 5. 1. NL is the ranking of the individual load. Hence, if a load is ranked 2 (NL=2), $\sum_{i=1}^{NL} RoCoFL_i$ is sum of $RoCoFL_i$ of loads ranked 1 and 2. This gives a rough idea of how many loads should be shed to bring the frequency back to normal when the distribution system is islanded.

The best scenario will be to shed the exact number of loads in the first step. However, the real time information on loads and stochastic generations are not always available. Moreover, when the loads have some dependency on frequency, frequency can be stabilized above the power quality

limit even by shedding less amount of load than required. Therefore, underestimating the number of loads to be shed in the first step and shedding other loads, if necessary, helps in shedding optimal number of loads. By considering the peak demand of loads, guaranteed generations and constant PQ loads, the RoCoF calculated will be lower compared to an actual case where all the loads might not be at peak or might have certain dependency on voltage and frequency or there might be some non-guaranteed generations. As an example, if we consider the WTGs in the test distribution system, then the power deficiency of 0.919 MW during islanding results in the RoCoF of -21.83 Hz/s which is higher than -27.43 Hz/s (RoCoF with WTGs). This gives an impression that frequency can be brought back by shedding less than 0.919 MW but it may not be the case. Similarly, the RoCoF for islanding will be higher when loads have some dependency on voltage and frequency compared to the case when they are independent of voltage and frequency. This also gives the impression that the frequency can be stabilized by shedding less loads and this may not be true as well. Finally, the load (Load JUEL for an example) might have the demand which is less than its P_{ppi}. Due to the estimations made during the creation of look-up table, the frequency may not be stabilized after the first step of load shedding and further loads may need to be shed.

5.1.2. Under-frequency Load Shedding Scheme

The flowchart of under-frequency load shedding scheme is shown in Fig. 5. 3. Frequency is measured every half voltage cycle and RoCoF is calculated. If the RoCoF is negative, it might be necessary to shed some loads. If the RoCoF is higher than $RoCoFL_{LL}$ (maximum RoCoF to start load shedding without waiting for frequency to go below certain value), then the methodology waits for the frequency to go below f_{LL} (lower limit of power quality), as a decay in frequency can be result of some normal events and the frequency might stabilize itself after sometime. $RoCoFL_{LL}$ should be set according to the normal frequency range. If the RoCoF calculated is lower than $RoCoFL_{LL}$, some loads should be shed quickly as the frequency tends to decay rapidly in a small system. Since the first step of load shedding is critical, the number of loads to be shed in first step of load shedding (N) is determined from the look-up table. If the RoCoF calculated is between corresponding $\sum_{i=1}^{NL} RoCoFL_i$ of two loads in the look-up table, NL corresponding to load which has the smallest $\sum_{i=1}^{NL} RoCoFL_i$ among those two loads is chosen as N. For example, if the RoCoF calculated is -30 Hz/s and loads ranked 3 and 4 have $\sum_{i=1}^{NL} RoCoFL_i$ of -28 Hz/s and -35 Hz/s, respectively, then N is chosen as 4. Then, the load shedding of N loads are initiated. Ideally, the frequency should now come back to normal operating range with the load shedding but sometimes some other loads may need to be shed to bring the frequency back. This is because of the

assumptions made while forming the look-up table as explained in the previous section. After the load shedding is initiated, the load shedding scheme waits some time before it measures the frequency again. This delay (Delay in Fig. 5. 3) accounts for the calculations and the circuit breaker operation time. In other words, loads whose ranking are higher than N waits for loads ranked N and lower to be shed. After the delay time has passed, the load shedding schemes waits for the frequency to go down below f_{LL} and for RoCoF to be negative for 'T' times before further loads are shed. The distribution system does not have the luxury of spinning reserve and secondary control like the transmission system. Thus, the only way to bring the frequency above the lower power quality limit is to shed some more loads when the DG units are already operating at their maximum capacity. Waiting for the RoCoF to be negative for some time makes sure the frequency is not coming back to nominal and it takes some time for the frequency oscillation to die out. Choosing a longer 'T' may result in the frequency reaching a lower value, especially when loads are highly frequency and voltage dependent, as less loads are shed in first step of load shedding. However, if a smaller 'T' is chosen, there is always a possibility of shedding loads during transients. Choosing 'T' is system specific and depends on the preference between an optimal load shedding and a better frequency profile. When enough loads are shed, the frequency goes up and settles around 50 Hz. It is quite possible that the frequency may overshoot after the last step of load shedding as a result of the total generation now becoming more than the total demand in the islanded distribution system. In such a case the frequency will oscillate and take some time to settle. Furthermore, the frequency may go below f_{LL} during the oscillation. Hence, it is desirable to let the frequency settle down and not shed load, even with the fulfilment of load shedding criteria, during oscillation. The oscillation is even more in an islanded distribution system with small inertia and slower generators. Hence the methodology waits for some time (Delay2 in Fig. 5. 3) if the frequency goes above f_{UL} (upper limit of normal range of frequency). The frequency over shoot may also occur during load decrease. After the distribution system is connected to the grid and it is detected by the grid reconnection detection algorithm, the shed loads are reconnected. Furthermore, it may happen that the decline in frequency is due to some severe events other than islanding. The islanding detection algorithm, in such situation, detects that the distribution system is still connected to the grid and hence the shed loads are reconnected. Islanding detection takes some time. The time lost in detecting islanding, in some cases, may become the difference between a sustained island operation and a distribution system collapse. Hence, it seems reasonable to prepare the distribution system for island operation by shedding loads when frequency drops. With the islanding and grid reconnection detection algorithms, the state of the distribution system is always known and loads can be reconnected whenever the distribution system is not islanded.

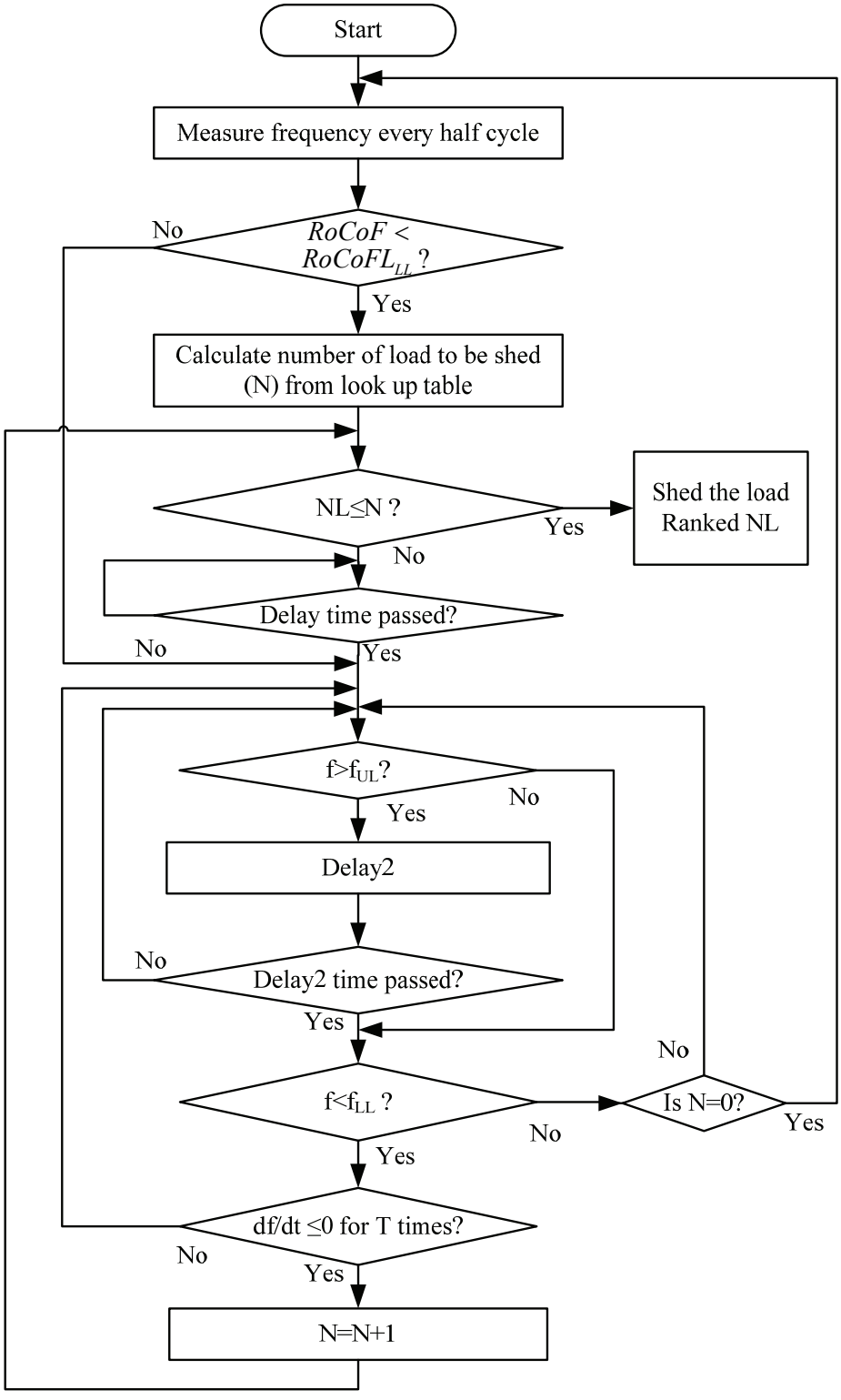

Fig. 5. 3. Proposed methodology for under-frequency load shedding

5.2 Modelling of the Test System

The test distribution system, presented in Fig. 2. 6 is used to test the proposed load shedding scheme. However, Load 05 is modelled in details, in this case, and test system with this change is shown in Fig. 5. 4. Load JUEL, Load MAST, Load STNO, Load FLØE, Load STCE, and Load STSY makes up previous Load 05.

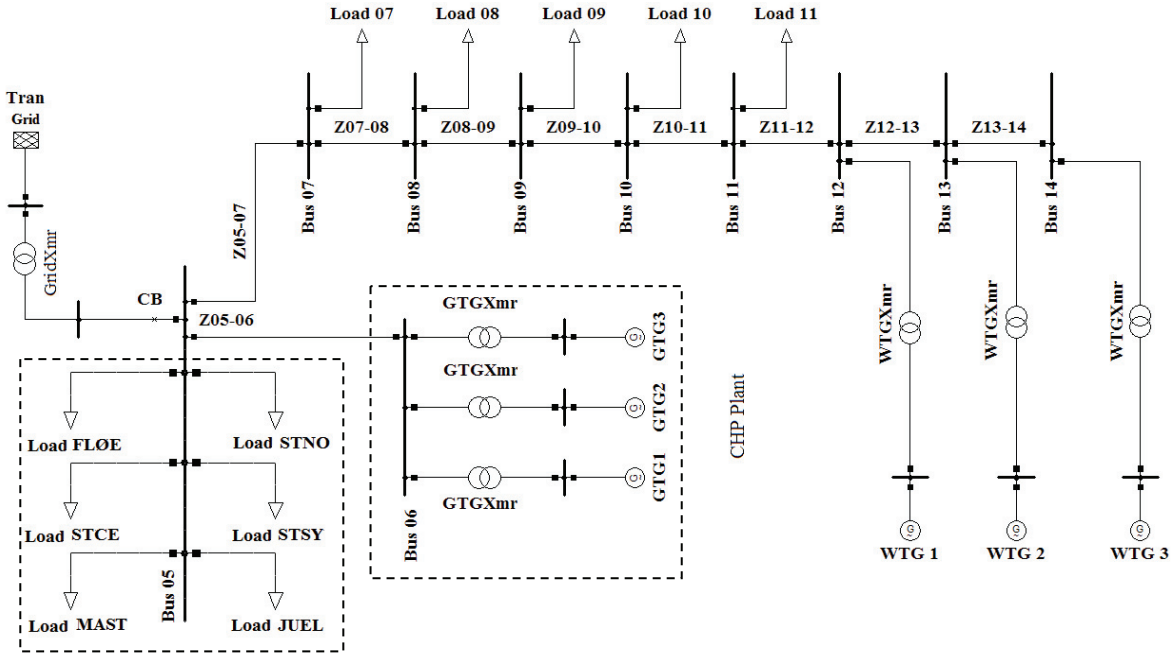

Fig. 5. 4. Test distribution system with detailed loads at Bus 05

Data for peak demand of the individual loads for September 2006 and October 2006 are given in Table AXV. The speed governor data of the GTGs are presented in Table AXII and the excitation system data is presented in Table AX. The data for the power factor controller is presented in Table AXIII. The wind turbine aerodynamic efficiency curve is presented in Fig. B. 1.

5.3 Simulation Results and Discussions

Two scenarios have been simulated; one with frequency and voltage dependent loads and another with constant power loads. The delay time is chosen as 80 milliseconds, as equipments currently available in market can shed a load within this time frame. Various cases, under these two scenarios, have been simulated to show the effectiveness of the proposed methodology. All these events are simulated at *t=0s.* As mentioned in previous chapter, under normal operating condition, the frequency is within 49.9-50.1 Hz in the UCTE system. Abnormal operating condition can be assumed if frequency goes below 49.9 Hz. Hence, $RoCoFL_{LL}$ is set at -10 Hz/s as a frequency drop of 0.1 Hz in 0.01s gives the RoCoF of -10 Hz/s. F_{LL} is set at 0.98 p.u. (49 Hz) and F_{UL} is set at 50.5 Hz. 'T' is chosen as 5 as simulation results shows that the proposed methodology can shed an

optimal number of loads without letting the frequency to go down to a very low value if 'T' is chosen as 5. When the frequency goes higher than 50 Hz, the speed controller reacts and frequency may go below 49 Hz and rise again. Various simulations results have shown that the time taken for the frequency to fall below 50.5 Hz and rise above 49 Hz is well within 5s. Hence, Delay2 is chosen as 5 seconds.

5.3.1. Scenario 1

The individual load's peak demand in September 2006 is used to create the look-up table and the proposed methodology is tested during the distribution system's peak demand of October 2006, which is presented in Table AXVI. The output power of the GTGs is 3 MW each and WTGs are producing 80 kW each. The test system has the real power deficiency of 1.84 MW, in this case. Loads are modelled as constant power loads. Three cases with different WTP are simulated. Islanding is simulated at *t=0s* and islanding is detected at *t=0.14s* in all cases. The control strategy of GTG1 is changed from droop control to isochronous control and the control strategy of GTG2 and GTG3 is changed from droop to isochronous control with feedback. All the GTGs regulate voltage after islanding is detected. When the distribution system is islanded, the frequency goes to 49.72 Hz at *t=0.01s* resulting in a RoCoF of -28 Hz/s.

Case 1

Table 5. 1

Look-up table for case 1

Load Rank (NL)	Load	P_{ppi} (MW)	WTP	$RoCoFL_i$ (Hz/s)	$\sum_{i=1}^{NL} RoCoFL_i$ (Hz/s)
1	Load 09	0.127	0.81	-11.46	-11.46
2	Load 10	0.127	0.83	-11.46	-22.92
3	Load 11	0.127	0.86	-11.46	-34.38
4	Load 07	0.509	0.87	-18.98	-53.35
5	Load 08	0.801	0.89	-24.95	-78.30
6	Load JUEL	0.919	0.91	-27.43	-105.74
7	Load MAST	1.588	0.92	-42.39	-148.13
8	Load STNO	1.878	0.93	-49.48	-197.61
9	Load FLØE	2.036	0.95	-53.54	-251.14
10	Load STCE	2.489	0.96	-66.15	-317.29
11	Load STSY	2.992	1	-82.55	-399.83

In this case, smaller loads are willing to pay less so they are shed first. The ranking of loads and their willingness to pay is listed in Table 5. 1. RoCoF resulting from islanding (-28 Hz/s) is

between $\sum_{i=1}^{NL} RoCoFL_i$ of loads ranked 2 and 3. Hence, number of loads to be shed (N) according to the methodology is 3. Thus, the load shedding is initiated at *t=0.01s* and loads ranked 1, 2 and 3 are shed at *t=0.09s*. Loads ranked 4 and above wait till *t=0.09s* before measuring frequency and calculating RoCoF again. At *t=0.14s,* RoCoF becomes negative for 5 continuous half cycles with the frequency below 0.98 p.u. and thus N becomes 4. Load ranked 4 is shed at *t=0.22s.* Load ranked 5 is shed at *t= 0.35s* and load ranked 6 is shed at *t=0.48s* with the fulfilment of both load shedding criteria. Fig. 5. 5 shows the test distribution system's frequency during islanding and load shedding for Case 1.

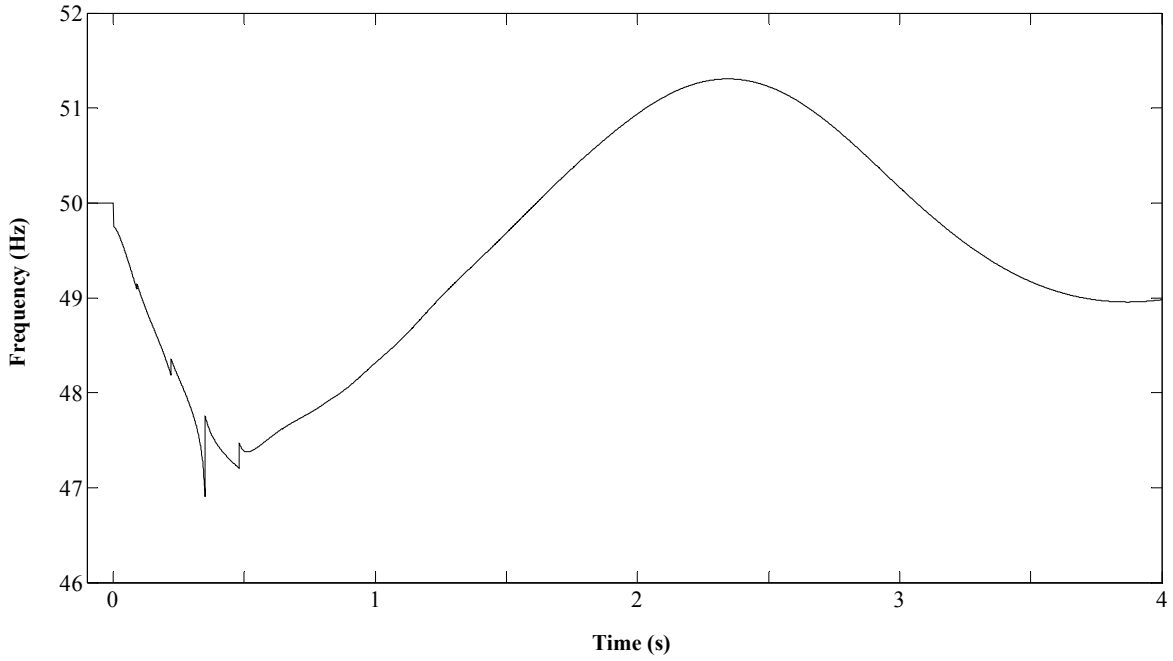

Fig. 5. 5. Test distribution system's frequency during islanding and load shedding (loads up to NL=6 in Table 5.1. are shed) for Case 1

Ideally, the frequency should have been close to the nominal value after the first step of load shedding. However, other loads are also shed as the wind turbines are not considered while creating the lookup table. Furthermore, the demand of each loads ranked from 1 to 3 at the time of load shedding is 119 kW whereas their peak demand for the previous period is 127 kW each. The total real power demand of load ranked 1-5 is almost equal to the total real power deficiency of the islanded distribution system. Hence, shedding of load ranked 6 results in overshooting of the frequency. Frequency goes higher than 50.5 Hz and 'Delay2' is initiated even though the load shedding criteria is not fulfilled during the 'Delay2'. However, frequency may go below 0.98 p.u. depending upon the amount of load shed at the last step. Fig. 5. 6 shows the frequency of the distribution system when only loads ranked 1-5 are shed with shedding time remaining the same. It can be seen that frequency is not coming above 0.98 p.u.. Fig. 5. 5 and Fig. 5. 6 show that proposed

methodology is able to bring the frequency back within the normal operating range by shedding an optimal number of loads.

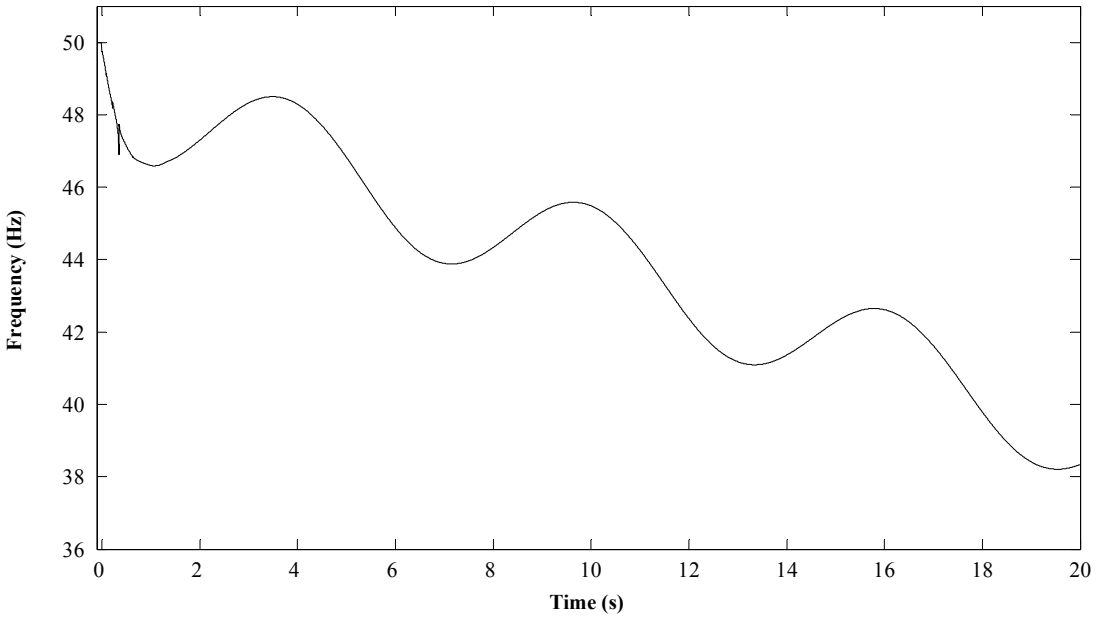

Fig. 5. 6. Test distribution system's frequency during islanding and non optimal load shedding (only shedding loads up to NL=5 in Table 5.1) for Case 1

Case 2

Table 5. 2

Look-up table for case 2

Load Rank (NL)	Load	P_{ppi} (MW)	WTP	$RoCoFL_i$ (Hz/s)	$\sum_{i=1}^{NL} RoCoFL_i$ (Hz/s)
1	Load STSY	2.992	0.79	-82.55	-82.55
2	Load 10	0.127	0.84	-11.46	-94.00
3	Load 11	0.127	0.85	-11.46	-105.47
4	Load MAST	1.588	0.86	-42.39	-147.86
5	Load 09	0.127	0.89	-11.46	-159.31
6	Load JUEL	0.919	0.9	-27.43	-186.74
7	Load STCE	2.489	0.91	-66.15	-252.89
8	Load FLØE	2.036	0.95	-53.54	-306.43
9	Load 07	0.509	0.98	-18.98	-325.40
10	Load STNO	1.878	0.99	-49.48	-374.88
11	Load 08	0.801	1	-24.95	-399.83

The ranking of loads and their willingness to pay is listed in Table 5. 2. In this scenario, Load STSY is willing to pay the least. The real power demand of STSY at the time of islanding, 1.697 MW, is slightly less than the real power deficiency of the distribution system. Furthermore, Load 10 and Load 11, which are the two smallest loads, are ranked 2 and 3.

Similar to case 1, first load shedding is initiated at *t=0.01s* and Load STSY is shed at *t=0.09s* as RoCoF resulting from island is less than -10 Hz/s and Load STSY has $\sum_{i=1}^{NL} RoCoFL_i$ of -82.545 Hz/s. Hence N is just 1. Although Load STSY had the highest real power demand in the month of September 2006, it is only the fourth largest load when islanding is simulated (during the system peak of October 2006). As a result, shedding Load STSY only does not bring the frequency within the power quality limits and hence the frequency continues to decay. Therefore, the second load shedding is initiated at *t=0.39s* when the RoCoF become negative for 5 times while the frequency being less than 0.98 p.u. Hence, Load 10 is shed at *t=0.47s*. The third load shedding is initiated at *t=0.53s* when the RoCoF become negative for 5 times while the frequency being less than 0.98 p.u and Load 11 is shed at *t=0.61s*. No more loads are shed and the frequency is brought within the limit. Fig. 5. 7 shows the frequency of test distribution system for Case 2.

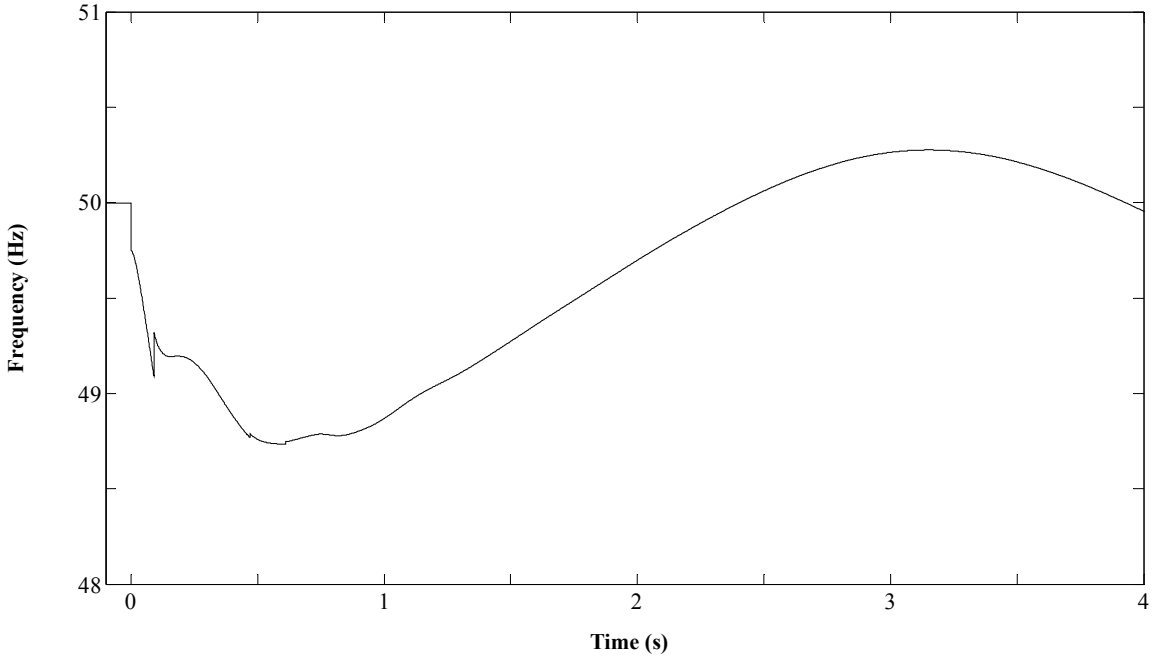

Fig. 5. 7. Test distribution system's frequency during islanding and load shedding (loads up to NL=3 in Table 5.2. are shed) for Case 2

Fig. 5. 8 shows the frequency of the distribution system when only loads ranked 1 and 2 are shed with shedding times remaining the same. Again, it can be seen that frequency is not coming within the normal operating range when only two loads are shed.

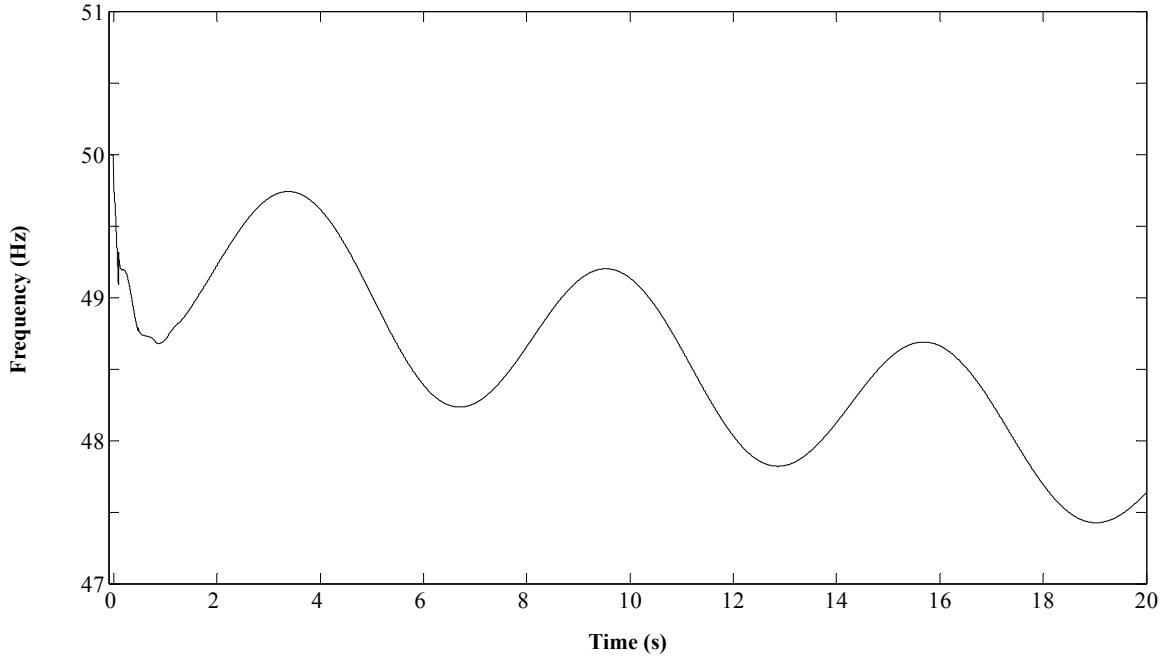

Fig. 5. 8. Test distribution system's frequency during islanding and non optimal load shedding (only shedding loads up to NL=2 in Table 5.2) for Case 2

Case 3

In this case, WTP of the loads are randomized. The ranking of loads and their willingness to pay is listed in Table 5. 3.

Table 5. 3

Look-up table for case 3

Load Rank (NL)	Load	P_{ppi} (MW)	WTP	$RoCoFL_i$ (Hz/s)	$\sum_{i=1}^{NL} RoCoFL_i$ (Hz/s)
1	Load JUEL	0.919	0.79	-27.43	-27.43
2	Load FLØE	2.036	0.84	-53.54	-80.97
3	Load 11	0.127	0.85	-11.46	-92.42
4	Load 08	0.801	0.86	-24.95	-117.38
5	Load 07	0.509	0.89	-18.98	-136.35
6	Load STNO	1.878	0.9	-49.48	-185.83
7	Load STSY	2.992	0.91	-82.55	-268.38
8	Load STCE	2.489	0.95	-66.15	-334.53
9	Load 09	0.127	0.98	-11.46	-345.99
10	Load 10	0.127	0.99	-11.46	-357.45
11	Load MAST	1.588	1	-42.39	-399.83

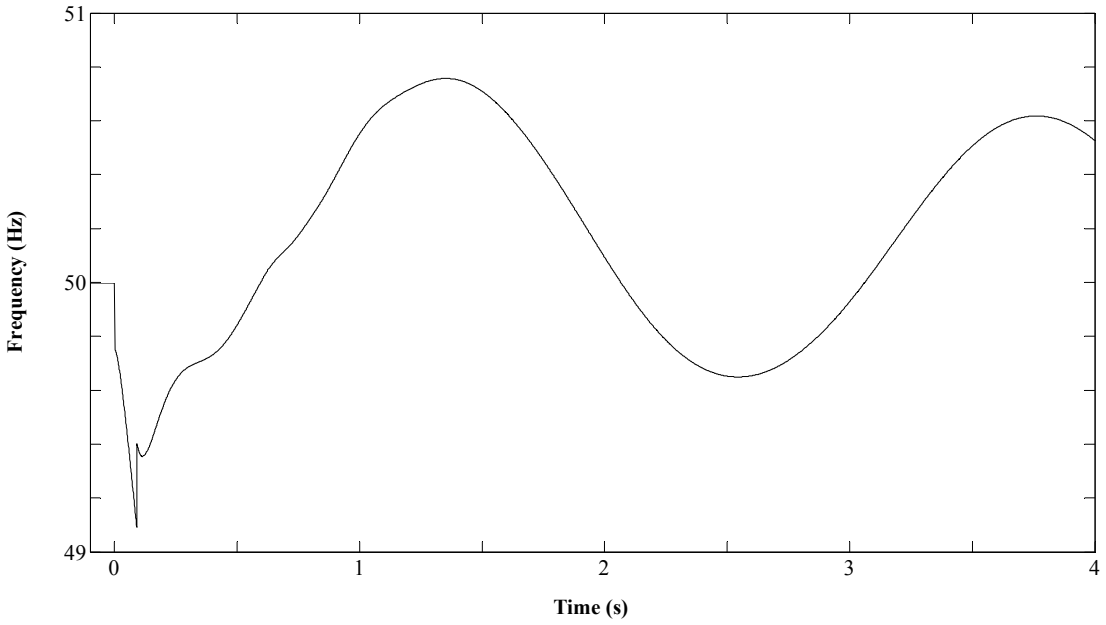

Fig. 5. 9. Test distribution system's frequency during islanding and load shedding (loads up to NL=2 in Table 5.3 are shed) for Case 3

It can be seen from the look-up table that the $\sum_{i=1}^{NL} RoCoFL_i$ for the first load is –27.43 Hz/s, which is larger than the RoCoF calculated when the distribution system is islanded (-28 Hz/s). But RoCoF, due to islanding, is also larger than $\sum_{i=1}^{NL} RoCoFL_i$ of load ranked 2 (-80.97 Hz/s). Hence, N is 2.

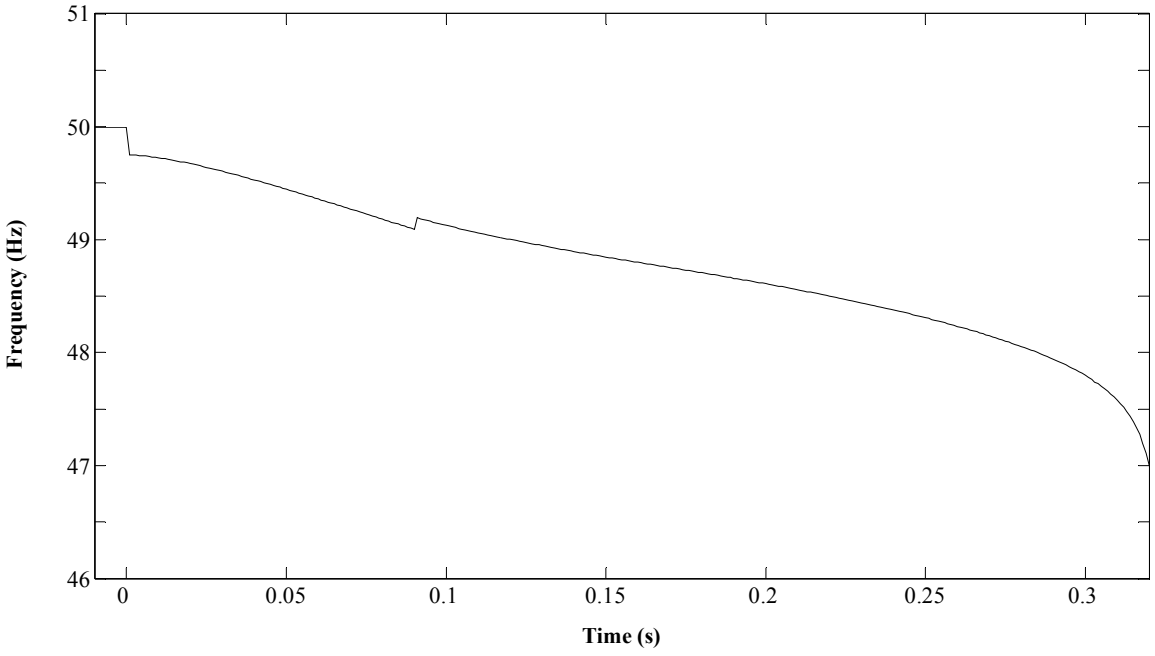

Fig. 5. 10. Test distribution system's frequency during islanding and non optimal load shedding (only shedding first load in Table 5.3) for Case 3

The loads ranked 1 and 2 are shed at *t=0.09s*. The frequency continues to rise and no more loads are shed. Fig. 5. 9 shows the frequency of the test distribution system for Case 3. Again the frequency rises above 50.5 Hz after final step of load shedding and Delay2 is active. However, the frequency does not go below 49 Hz and, hence, no more loads would have been shed even if Delay2 had not been activated. Fig. 5. 10 shows the frequency of the distribution system when only the load ranked 1 is shed with shedding time remaining the same. The distribution system collapses after *t=0.32s*.

A total of 2.315 MW and 0.918 MVAr of loads is shed in Case 1. Similarly, a total of 1.935 MW and 0.434 MVAr, and a total of 2.337MW and 0.661 MVAr of loads are shed in Case 2 and Case 3, respectively. 20 seconds simulations of the three cases is presented in Fig. 5. 11. A large amount of load is shed in the last step of load shedding in Case 1 and the in first step of load shedding in Case 3. It results in frequency overshoot. The frequency oscillates and settles to a steady state value after some time. The mismatch between the generation and demand, and the turbine and governor characteristics defines the oscillation of the system frequency. Furthermore, change in loading of the distribution system changes the damping of the system [91]-[93] and it also determines the oscillation of the frequency.

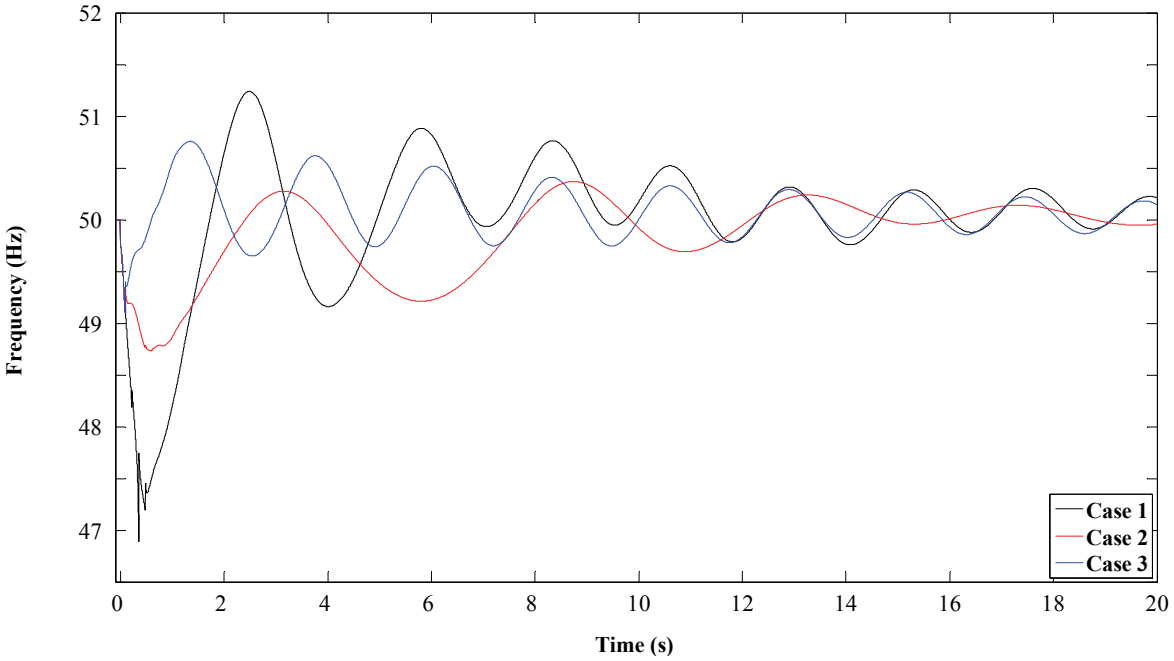

Fig. 5. 11. Distribution system's frequency during islanding and load shedding for scenario 1

In term of frequency dip, Case 1 is the worst case. The frequency goes to the lowest value as the least amount of load is shed in the first step of load shedding. On the other hand, Case 3 is the best case in term of the frequency dip as a large amount of load is shed in the first step. However, it is the worst case in term of the total amount on load shed. Case 2 is the best case in

term of the total amount of load shed. Furthermore, in Case 2, Load STSY (load ranked 1) has $\sum_{i=1}^{NL} RoCoFL_i$ of -82.545 Hz/s, which is much less compared to the RoCoF due to islanding. Hence, ideally the frequency should be brought back to limit by shedding load ranked 1. However, its real power demand at the time of islanding is less compared to its peak demand for the past period. Hence few more loads are shed. Moreover, if 'T' was chosen as 6, then the test system would have collapsed at *t=0.36s*.

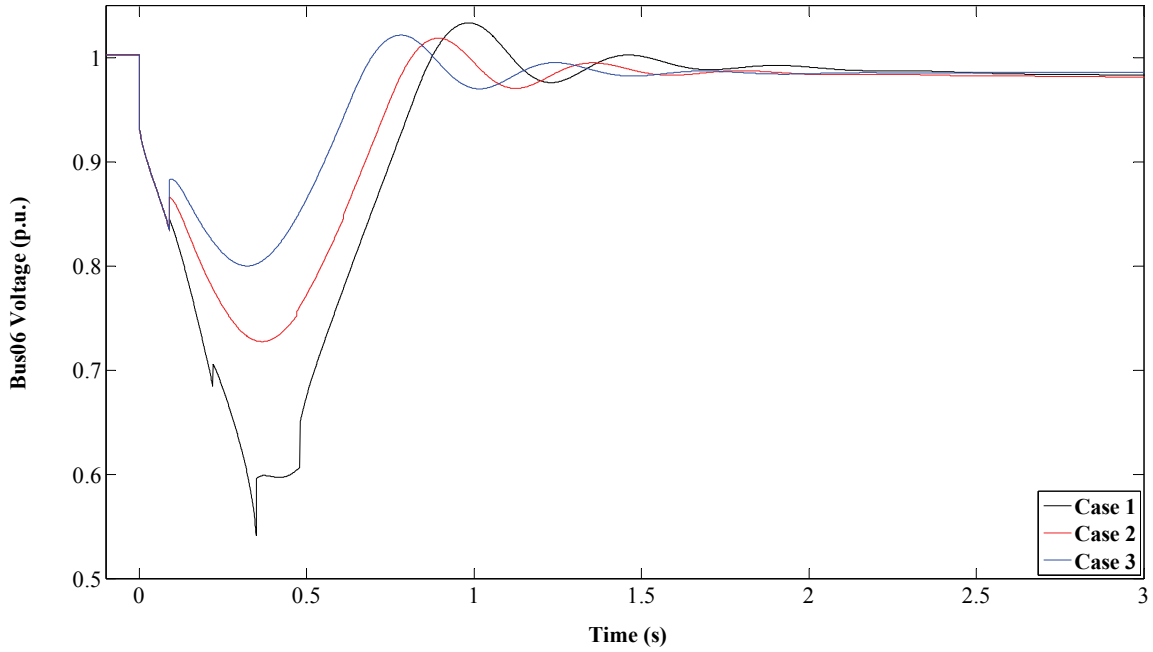

Fig. 5. 12. Bus 06 voltage during islanding and load shedding in scenario 1

Fig. 5. 12 shows the voltage at Bus 06 during the islanding and load shedding event for the three cases. The controllers with the help of load shedding are also able to bring the voltage back within the acceptable limit. As expected, the voltage dip is maximum for Case 1 in which a small amount of load is shed in the first step. On the other hand, the dip is the least for Case 3, which shed the largest amount of load in the first step of load shedding.

Fig. 5. 13 shows the output power of GTG1. In Case 3, because of the largest amount of load shedding, speed error becomes positive faster and GTG1 reduces its turbine power quicker. However, in Case 2, the frequency takes longer time than in other cases to exceed the nominal frequency, as the least amount of load are shed, and hence GTG1 lowers it turbine power later than in other two cases.

With the change in the frequency, the power output from the WTGs also changes. This further affects the power mismatch in the islanded distribution system. Fig. 5. 14 shows the output power of the WTGs.

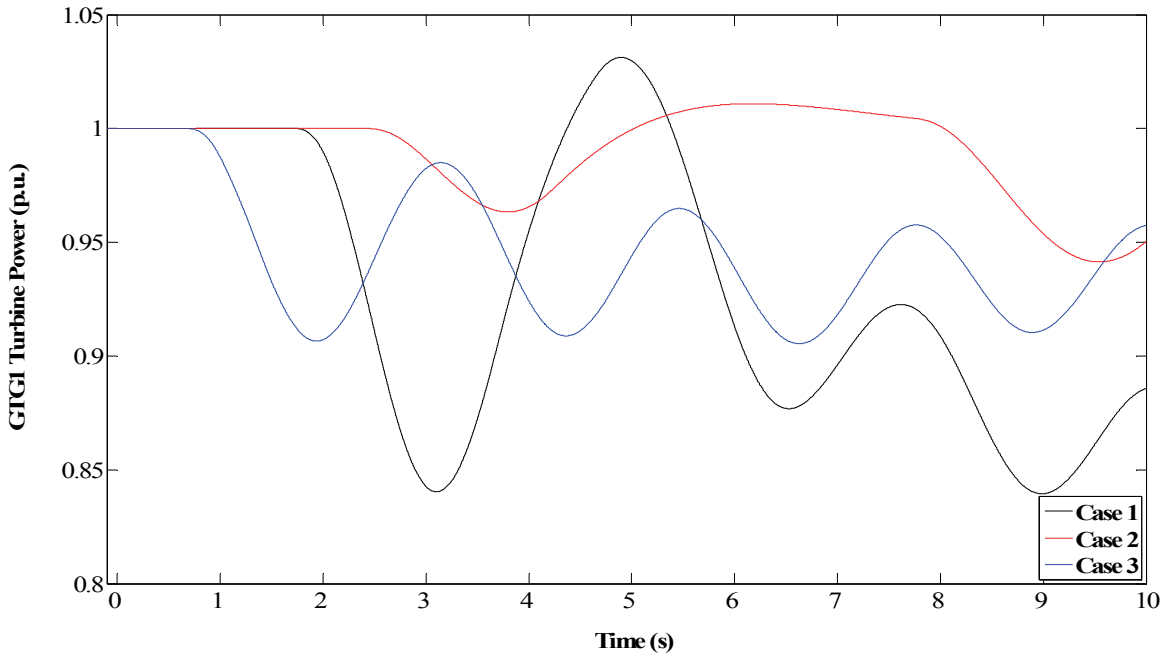

Fig. 5. 13. GTG1 turbine power during islanding and load shedding in scenario 1

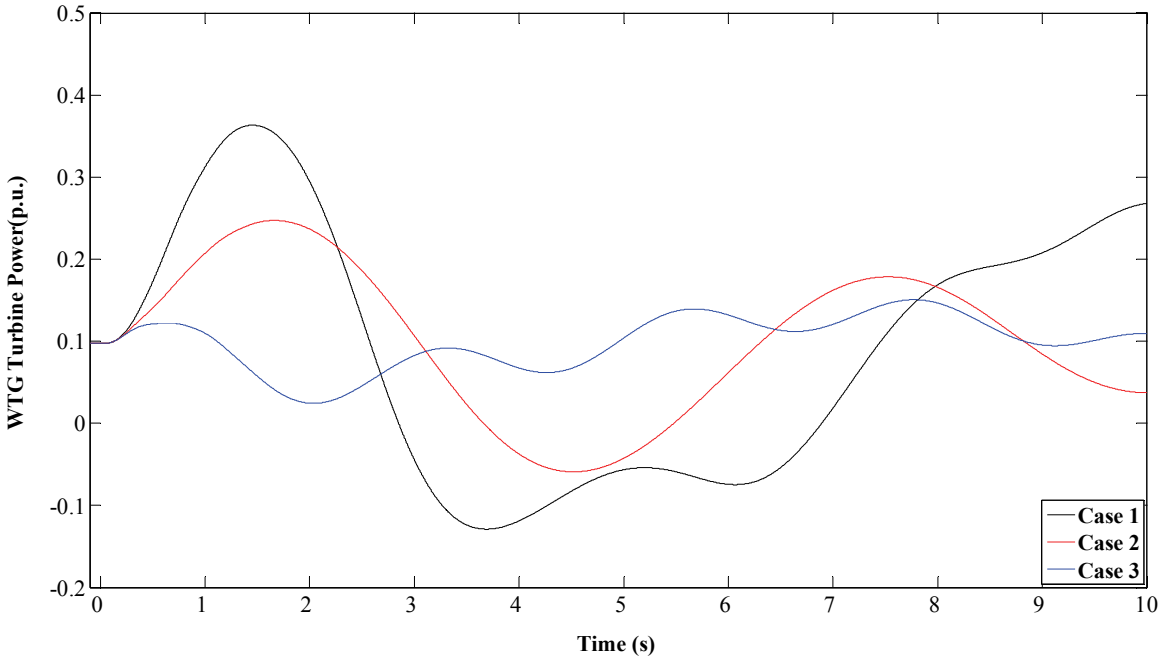

Fig. 5. 14. WTG turbine power during islanding and load shedding in scenario 1

5.3.2. Scenario 2

To demonstrate that the scope of the proposed load shedding scheme is not limited to just one specific case, another scenario is simulated with different sets of load data. Individual load's peak demand of October 2006 is used to create the look-up table and the proposed methodology is tested during the peak demand of November 2006. The load data is presented in Table AXV and

Table AXVI. Note that Table AXV shows the peak demand of individual loads for the month of October 2006 whereas Table AXVI shows the demand of the individual load during the test system's peak demand for the month of October 2006. The output power of the GTGs is 3 MW each and the WTG is 80 kW each. The test system has a real power deficiency of 2.49 MW. As mentioned earlier, the loads' voltage and frequency dependency is hard to quantify. Loads are considered as constant PQ loads in Scenario 1. To test the effectiveness of the proposed methodology in the cases when the loads have some dependency on voltage and frequency, loads are modelled, according to equation (2.3), by choosing the values of K_{f_p}, K_{v_p}, K_{f_q} and K_{v_q} as 0.5. When the frequency and voltage reduce after islanding, the real and reactive power demands of the loads also reduce. This reduces the imbalance between the demand and generation in the islanded distribution system. Furthermore, when the loads are voltage and frequency dependent, the magnitude of RoCoF, after islanding, is less compared to the situation when loads are independent of voltage and frequency. Again, three cases are simulated to show the efficacy of the proposed under-frequency load shedding methodology when voltage and frequency dependent loads are willing to pay differently. Islanding is simulated at *t=0s* and islanding is detected at *t=0.14s* in all cases. When the distribution system is islanded, frequency goes to 49.74 Hz at *t=0.01s* resulting in RoCoF of -26 Hz/s.

Case 4

Similar to Case 1, smaller loads are willing to pay less, and hence are shed earlier, and larger loads are willing to pay more. The ranking of loads and their willingness to pay is listed in Table 5. 4. It can be seen from the look-up table that the number of loads to be shed at the first step is 3 as the RoCoF resulting from islanding is between $\sum_{i=1}^{NL} RoCoFL_i$ of loads ranked 2 and 3. Thus, N=3.

Loads ranked 1, 2 and 3 are shed at *t=0.09s*. Now, the frequency should have rose above the power quality limit after the first step of load shedding. But, more loads need to be shed due to the assumption made while creating the look-up table. At *t=0.14s* RoCoF becomes negative for 5 continuous half cycles with the frequency below 0.98 p.u.. Therefore, the load ranked 4 is shed at *t=0.22s*. Similarly, loads ranked 5, 6 and 7 are shed at *t=0.36s, t=0.50s* and *t=0.82s,* respectively after the fulfilment of the load shedding criteria. After the last load shedding, the frequency goes above 50.5 Hz and 'Delay2' is activated. Fig. 5. 15 shows the test distribution system's frequency during islanding and load shedding.

Table 5. 4

Look-up table for case 4

Load Rank (NL)	Load	P_{ppi} (MW)	WTP	$RoCoFL_i$ (Hz/s)	$\sum_{i=1}^{NL} RoCoFL_i$ (Hz/s)
1	Load 09	0.126	0.81	-11.44	-11.44
2	Load 10	0.126	0.83	-11.44	-22.88
3	Load 11	0.126	0.86	-11.44	-34.32
4	Load 07	0.503	0.87	-18.85	-53.17
5	Load 08	0.792	0.89	-24.76	-77.93
6	Load JUEL	0.882	0.91	-26.65	-104.58
7	Load STCE	1.759	0.92	-46.52	-151.10
8	Load FLØE	1.883	0.93	-49.60	-200.71
9	Load STNO	2.143	0.95	-56.38	-257.08
10	Load STSY	2.907	0.96	-79.54	-336.63
11	Load MAST	3.173	1	-89.33	-425.96

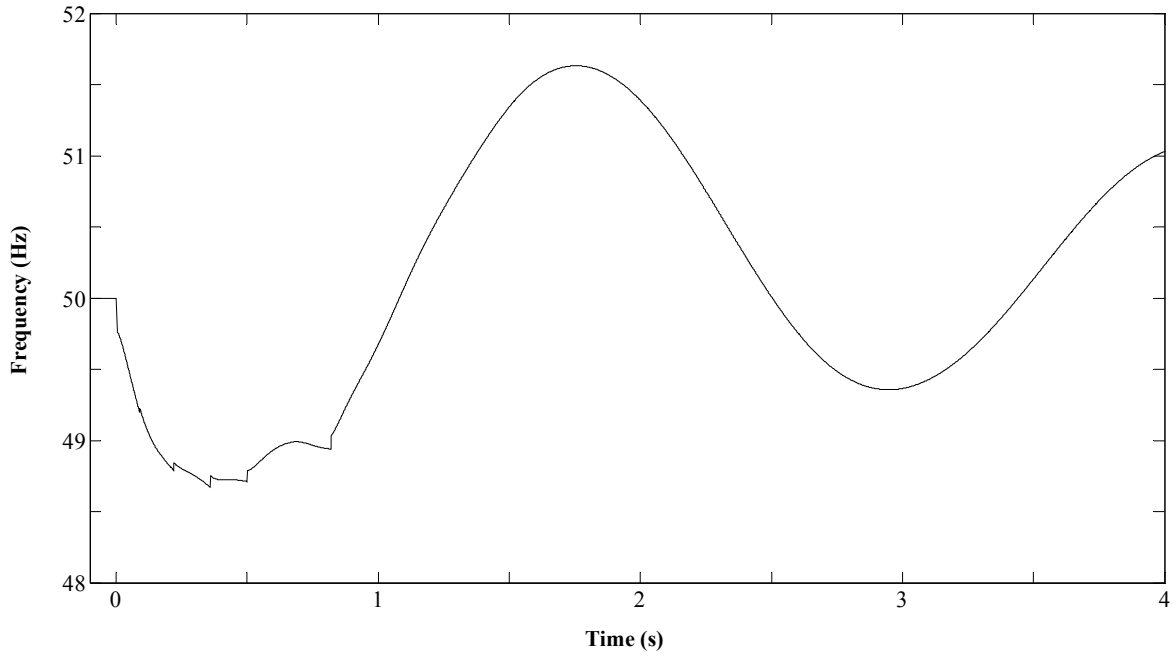

Fig. 5. 15. Test distribution system's frequency during islanding and load shedding (loads up to NL=7 in Table 5.4 are shed) for Case 4

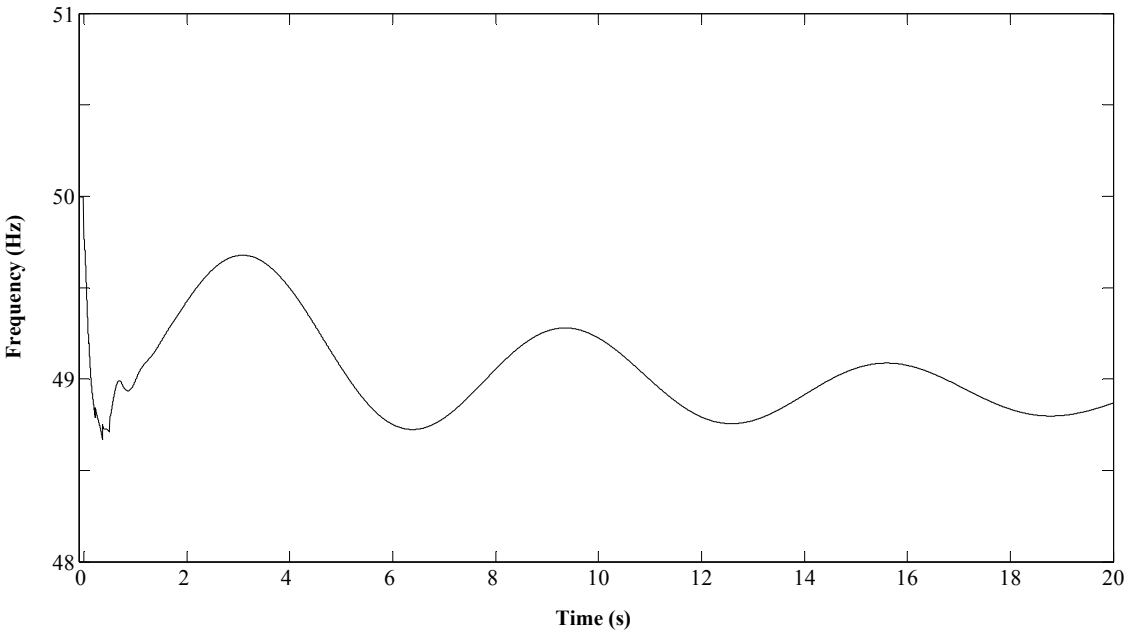

Fig. 5. 16. Test distribution system's frequency during islanding and non optimal load shedding (only shedding loads up to NL=6 in Table 5.4) for Case 4

Fig. 5. 16 shows the frequency of the distribution system when only loads ranked 1-6 are shed with shedding times remaining the same. It can be seen from the figure that the frequency is not coming above the normal operating range when only 6 loads are shed. This shows that the proposed methodology is able to shed an optimal number of loads, which is 7 in this case.

Case 5

Table 5. 5

Look-up table for case 5

Load Rank (NL)	Load	P_{ppi} (MW)	WTP	$RoCoFL_i$ (Hz/s)	$\sum_{i=1}^{NL} RoCoFL_i$ (Hz/s)
1	Load MAST	3.173	0.79	-89.33	-89.33
2	Load 09	0.126	0.84	-11.44	-100.77
3	Load 10	0.126	0.85	-11.44	-112.21
4	Load 11	0.126	0.86	-11.44	-123.65
5	Load STCE	1.759	0.89	-46.52	-170.17
6	Load JUEL	0.882	0.9	-26.65	-196.82
7	Load STNO	2.143	0.91	-56.38	-253.19
8	Load 07	0.503	0.95	-18.85	-272.05
9	Load STSY	2.907	0.98	-79.54	-351.59
10	Load 08	0.792	0.99	-24.76	-376.35
11	Load FLØE	1.883	1	-49.60	-425.96

In this scenario, Load MAST is willing to pay the least. Similar to Case 2, the total real power demand of the load ranked first is slightly less than the total real power deficiency in the distribution system at the time of islanding. The next three highest ranked loads are the smallest loads of the test distribution system at the time of islanding. The ranking of loads and their willingness to pay is listed in Table 5. 5.

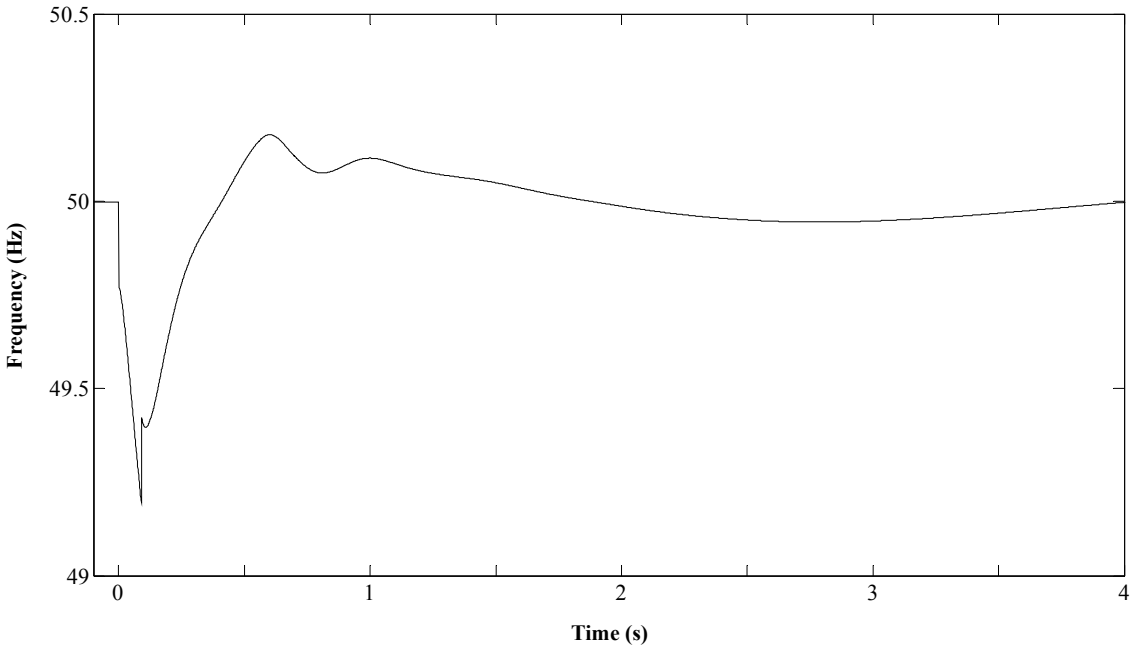

Fig. 5. 17. Test distribution system's frequency during islanding and load shedding (the load ranked first in Table 5.5 is shed) for Case 5

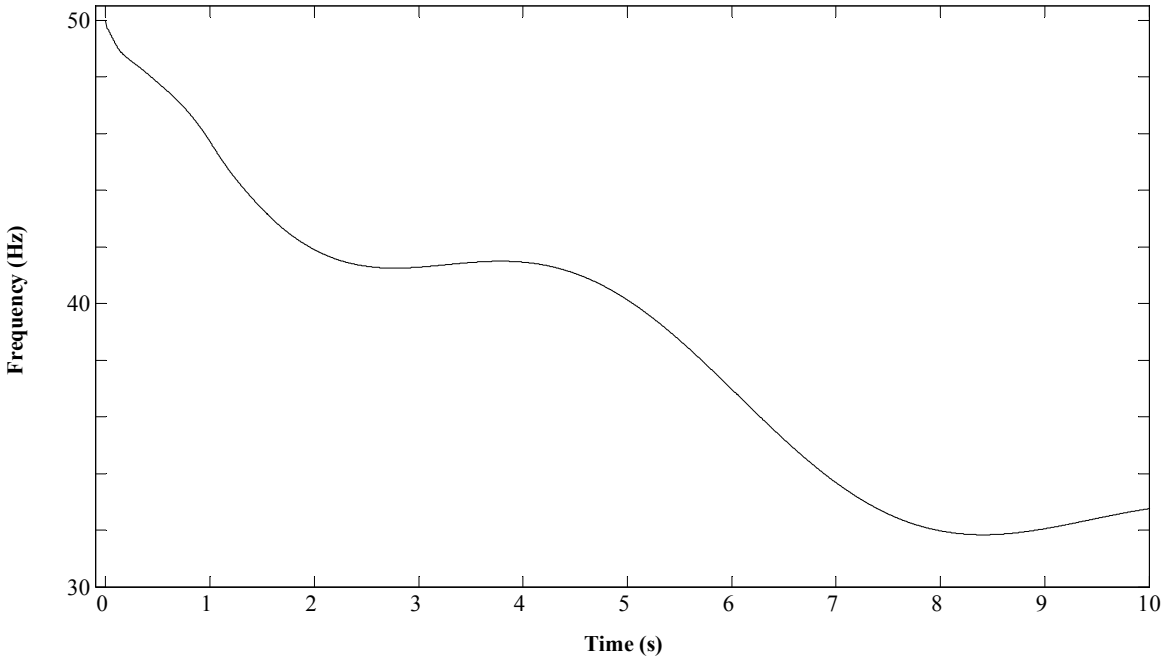

Fig. 5. 18. Test distribution system's frequency during islanding and no load shedding for Case 5

The RoCoF due to islanding is -26 Hz/s, which is smaller than -10 Hz/s but larger than $\sum_{i=1}^{NL} RoCoFL_i$ of load ranked 1 (-89.33 Hz/s). Hence the number of load to be shed is 1. The load ranked 1 is shed at *t=0.09s.* The frequency rises and settles around 50 Hz and hence no more loads are shed. Fig. 5. 17 show the test distribution system frequency for islanding and load shedding.

The real power demand of the Load MAST at the time of load shedding is 2.442 MW (Table AXVI). The frequency is brought within the limit by shedding lesser amount of load than the total deficiency of the islanded distribution system (2.49 MW). This is because of reduction is demand of the loads with reduced voltage and frequency. Hence, at some value of voltage and frequency, the demand and generation becomes equal and the islanded distribution system becomes stable. On the other hand, in Case 2, the total amount of shed loads must be at least equal to the total power deficiency of the islanded distribution system as loads' demand are independent of voltage and frequency. Hence, the frequency decreases continuously if not enough amount of load is shed as shown in Fig. 5. 8. Fig. 5. 18 shows the test distribution system without any load shedding after islanding. As expected, the frequency continuously decreases.

Case 6

Similar to Case 3, the WTP of the loads have been randomized. The ranking of loads and their willingness to pay is listed in Table 5. 6.

Table 5. 6

Look-up table for case 6

Load Rank (NL)	Load	P_{ppi} (MW)	WTP	$RoCoFL_i$ (Hz/s)	$\sum_{i=1}^{NL} RoCoFL_i$ (Hz/s)
1	Load JUEL	0.882	0.79	-26.65	-26.65
2	Load STNO	2.143	0.84	-56.38	-83.02
3	Load 11	0.126	0.85	-11.44	-94.46
4	Load STSY	2.907	0.86	-79.54	-174.01
5	Load 09	0.126	0.89	-11.44	-185.45
6	Load 07	0.503	0.9	-18.85	-204.30
7	Load 10	0.126	0.91	-11.44	-215.74
8	Load STCE	1.759	0.95	-46.52	-262.26
9	Load 08	0.792	0.98	-24.76	-287.02
10	Load MAST	3.173	0.99	-89.33	-376.35
11	Load FLØE	1.883	1	-49.60	-425.96

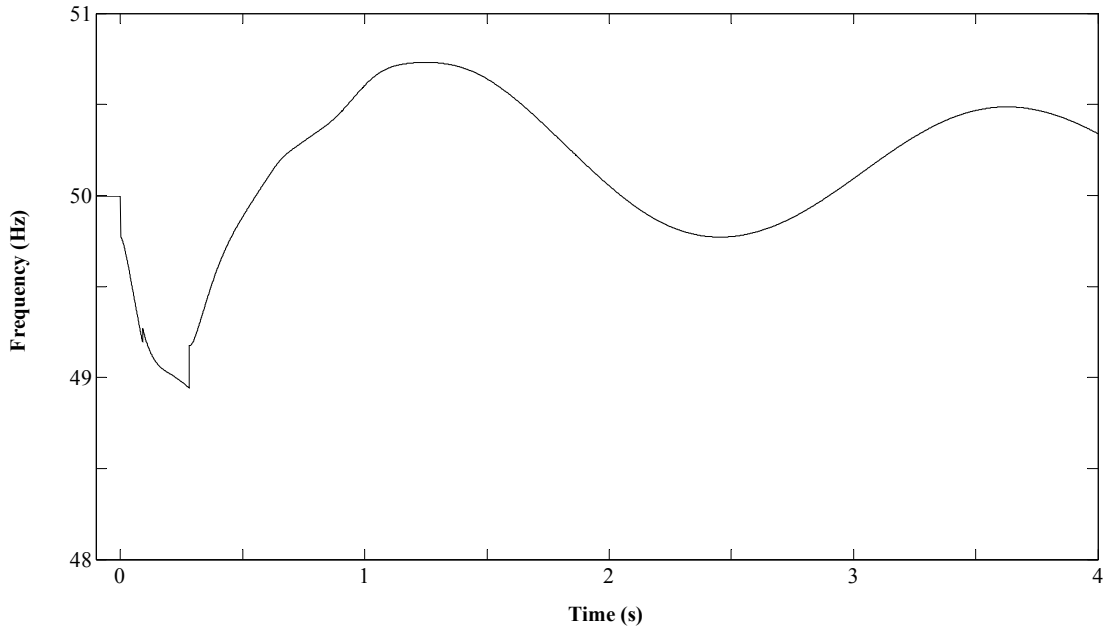

Fig. 5. 19. Test distribution system's frequency during islanding and load shedding (loads up to NL=2 in Table 5.6 are shed) for Case 6

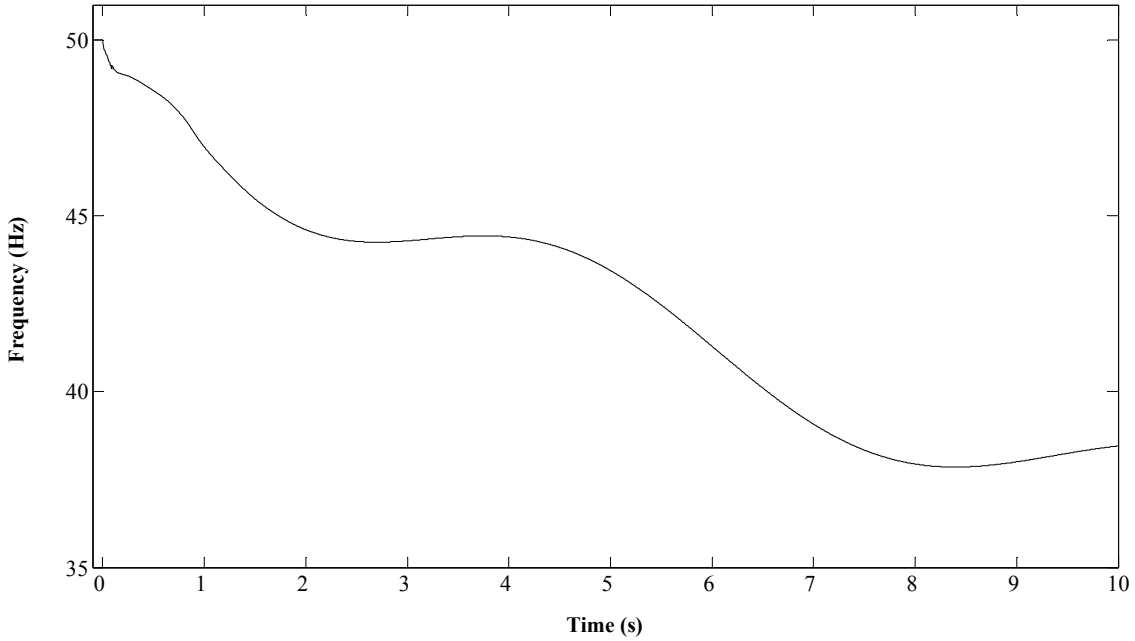

Fig. 5. 20. Test distribution system's frequency during islanding and non optimal load shedding (only shedding first load in Table 5.6) for Case 6

It can be seen from the look-up table that the $\sum_{i=1}^{NL} RoCoFL_i$ for the first load is –26.65 Hz/s, which is smaller than the RoCoF calculated when the distribution system is island. Since the RoCoF due to islanding is smaller than -10 Hz/s, N is 1 and the load ranked 1 is shed at *t=0.09s*. The load shedding criteria is again fulfilled at *t=0.27s* and hence load ranked 2 is shed at *t=0.35s*.

No more loads are shed and frequency comes above 50 Hz. Although Delay2 is activated as a result of frequency going above 50.5 Hz, load shedding criteria is not fulfilled during the delay time and hence loads would not have been shed even without Delay2. Fig. 5. 19 shows the frequency of test distribution system for Case 6.

Fig. 5. 20 shows the frequency of the distribution system when only load ranked 1 is shed with the shedding time remaining the same. With only one load shed, the frequency doesn't come back above 0.98 p.u.

A total of 3.53 MW and 0.97 MVAr of loads is shed in Case 4. Similarly, in Case 5 and Case 6, a total of 2.44 MW and 0.789 MVAr of loads, and a total of 3.25 MW and 0.936 MVAr of loads are shed, respectively. Hence Case 4 is the worst case in term of total amount of load shed. The least amount of load is shed in Case 5 among all the cases in Scenario 2. In term of frequency dip, Case 4 is also the worst case as the amount of load shed in the first step of load shedding is the least. As expected, Case 5 is the best case in term of frequency dip as the most amount of load is shed in the first step of load shedding.

20 seconds simulation of the three cases is presented in Fig. 5. 21. When the total amount of load shed becomes more than the total real power deficiency in the islanded distribution system, the frequency rises above 50 Hz and the GTGs start to reduce power to bring the frequency back to 50 Hz. As mentioned earlier, the oscillation of the frequency is defined by the governor and turbine characteristics, and change in damping due to change in the loading of the distribution system.

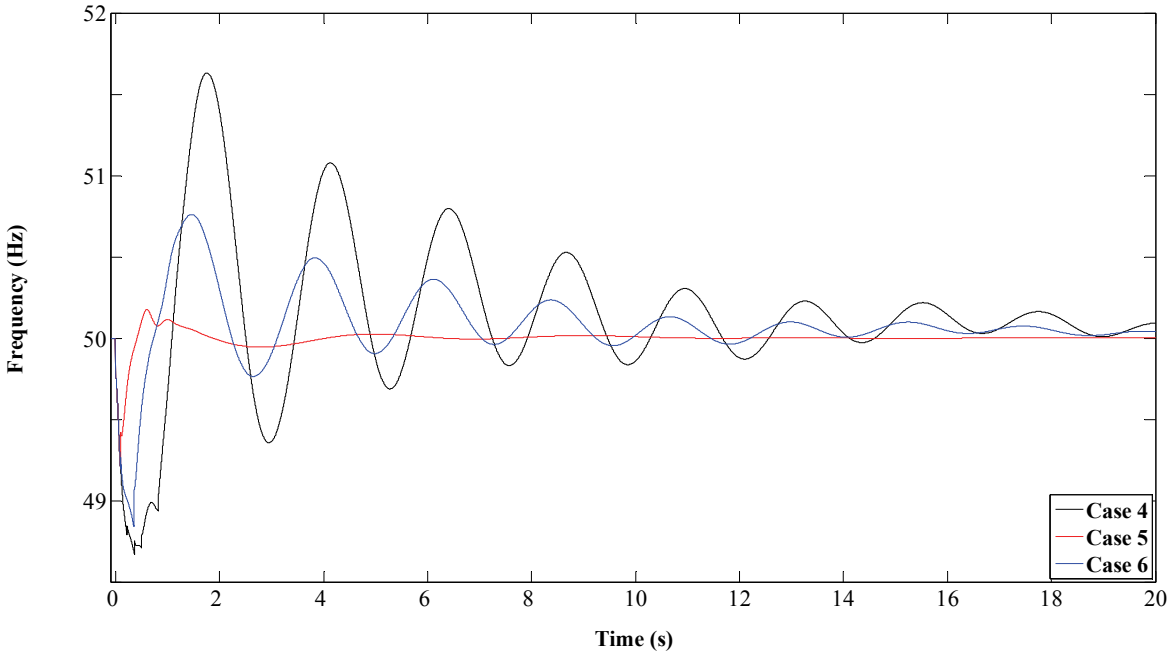

Fig. 5. 21. Distribution system's frequency during islanding and load shedding for scenario 2

With loads' voltage and frequency dependence, their power demand reduces with decrease in voltage and frequency. This results in reduction in mismatch between generation and demand. Hence the frequency dip is also less when the loads have certain voltage and frequency dependency compared to the case when they are constant power loads as it can seen from Fig. 5. 11 and Fig. 5. 21. In fact, in Case 5, the frequency is brought within the normal operating range by shedding less amount of load than the total mismatch of the system.

Fig. 5. 22 shows the voltage at Bus 06 of the distribution system for cases 4-6. Again, it shows that by changing the control strategy from power factor control to voltage control, with load shedding, the GTGs are able to maintain the voltage of the islanded distribution system. The loads' voltage and frequency dependency reduces the power demand of the load, when the voltage and frequency decrease, after islanding. This reduces the power mismatch in the island. Hence, the voltage profile is better when loads have some voltage and frequency dependence compared to cases when loads are constant power loads as it can be seen from Fig. 5. 12 and Fig. 5. 22.

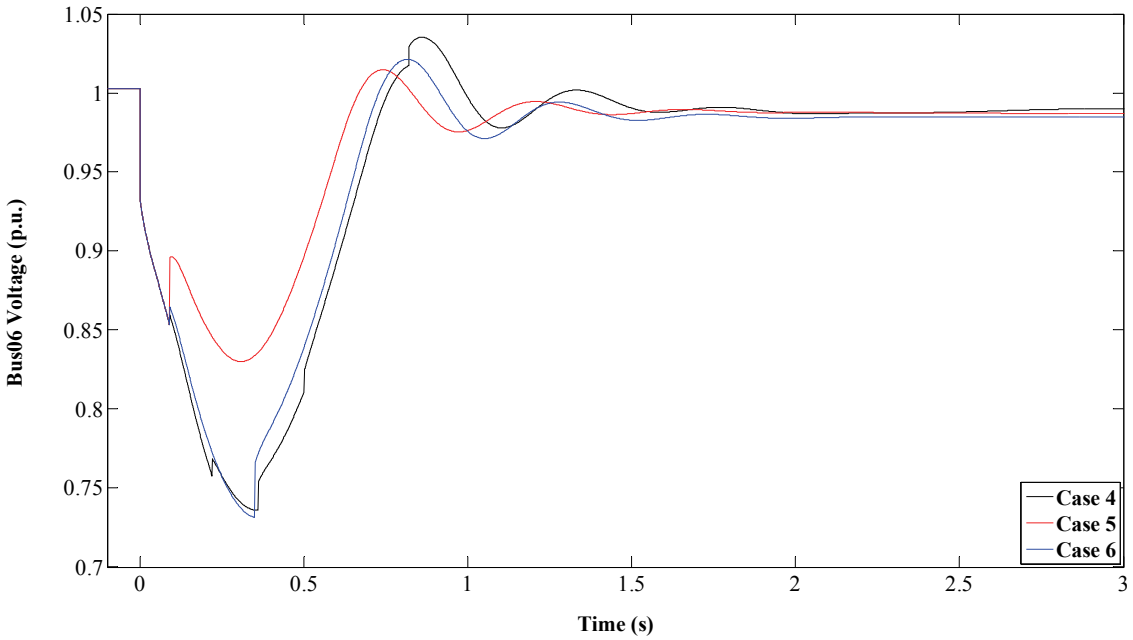

Fig. 5. 22. Bus 06 voltage during islanding load shedding scenario 2

Fig. 5. 23 shows the output power of GTG1. The frequency goes above 50 Hz the earliest in case of Case 5 and, hence, GTG1 also starts reducing the power the earliest in Case 5. The final steady state output power of GTG1 is the closest to 1 p.u. in Case 5 as the total amount of load shed is minimum compared to Case 4 and Case 6. Similarly, Fig. 5. 24 shows the output power of the WTGs. In Case 5, frequency does not oscillate much after load shedding and as a result the WTGs' output power also does not fluctuates much.

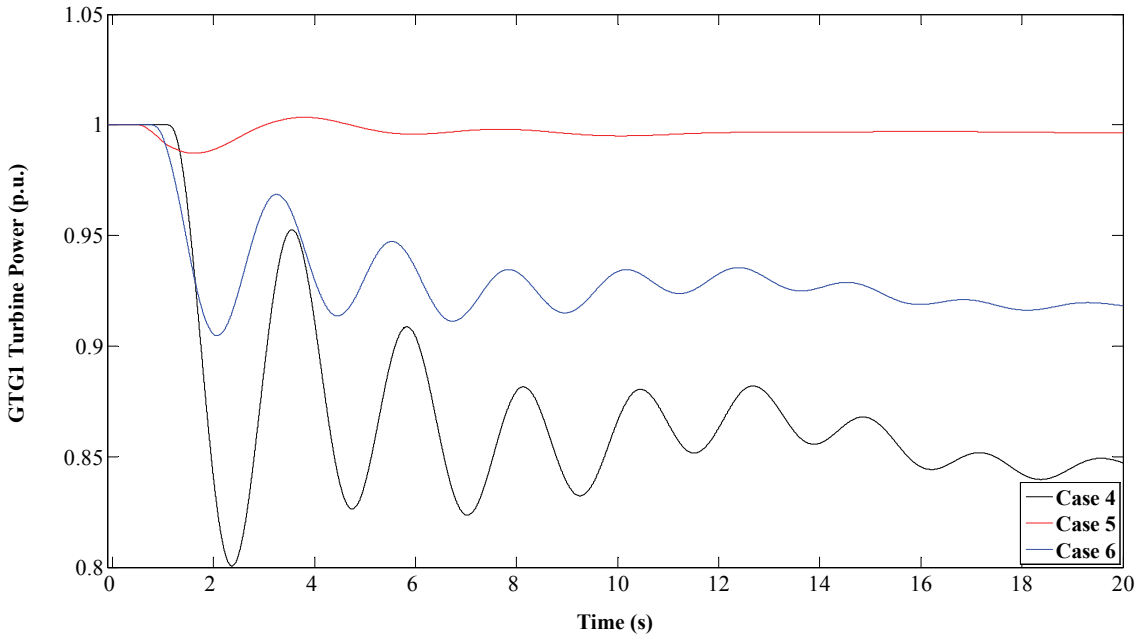

Fig. 5. 23. GTG1 turbine power during islanding load shedding scenario 2

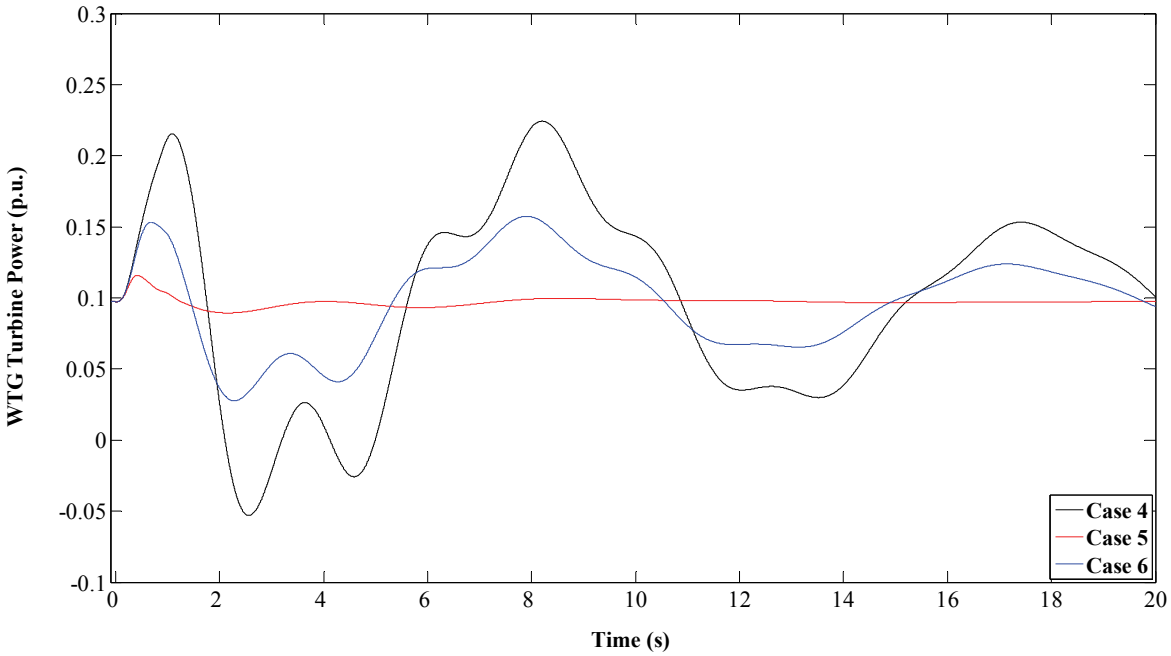

Fig. 5. 24. WTG turbine power during islanding load shedding scenario 2

Scenario 1 showed that the proposed load shedding scheme sheds an optimal number of loads when loads are constant PQ loads. Scenario 2 showed that the proposed load shedding scheme can shed an optimal number of loads even when loads are highly voltage and frequency dependent. These two scenarios demonstrate the effectiveness of the proposed methodology for a wide range of voltage and frequency dependency. Furthermore, these two scenarios also use two different set of data. Six different cases under these two scenarios show the proposed load shedding technique is able to shed an optimal number of loads, when an islanded distribution system does

not have enough generation to supply all the loads, even with the changing demand, WTP, and characteristics of the loads.

Table 5. 7 summarizes the results. Voltage is measured every half voltage cycle. The normal operating range for the voltage, for a 20 kV distribution system in Denmark, is 0.95-1.05 p.u.. Similarly, normal operating range for frequency is 49.9-50.1 Hz in the UCTE system, as mentioned before. Table 5. 7 also presents minimum time taken before the voltage and frequency comes back to normal operating range for the first time after islanding. Table 5. 7 shows that in Scenario 2, when the loads are voltage and frequency dependent, the worst voltage and frequency dip is less compared to the worst voltage and frequency dip in Scenario 1, when the loads are constant PQ loads, even when power deficiency is more in case of Scenario 2 compared to scenario 1.

Table 5. 7

Summary of the result

Cases	Number of load shed	Amount of load shed		Lowest frequency (HZ)	Lowest voltage at Bus 06 (p.u.)	Time when frequency comes above 49.9 Hz (s)	Time when voltage at Bus 06 comes above 0.95 p.u. (s)
		Active (MW)	Reactive (MVAr)				
1	6	2.315	0.918	46.90	0.541	1.58	0.8
2	2	1.935	0.434	48.73	0.728	2.27	0.74
3	2	2.337	0.661	49.09	0.8	0.54	0.62
4	7	3.53	0.97	48.67	0.736	1.06	0.69
5	1	2.44	0.79	49.2	0.83	0.33	0.59
6	2	3.25	0.94	48.84	0.731	0.65	0.66

Fig. 5. 25 shows the voltage and frequency range for which the WTG connected at a voltage level below 100 kV should produce power [94] and Table 5. 8 shows the frequency range for which a thermal power plant of 1.5 MW or higher should operate in Denmark [20].

Considering the technical requirement for the thermal power plants and wind turbines, the frequency goes below 47 Hz, the lowest operating range of WTG, momentarily only in Case 1. A load is shed when frequency goes below 47 Hz and then the frequency goes above 47 Hz immediately. The frequency is within the operating range of GTG all the time. However, the operating range may vary with different countries. Furthermore, in an interconnected system, like the UTCE, frequency going below 47 Hz can be interpreted as a very severe disturbance. But, as can be seen from Case 1, a deficiency of less than 2 MW might result in the frequency going down below 47 Hz when a small distribution system is islanded. As mentioned earlier, when the loads are

constant PQ loads, the frequency continuously decays until enough amount of load is shed. On the other hand, when the loads are voltage and frequency dependent, the distribution system finds the new stable frequency and voltage based on the power mismatch in the distribution system and loads' voltage and frequency dependency. However the steady state frequency may be below the generators operating range. Hence, if the generators are disconnected, it results in further mismatch and eventually leads to collapse of the whole distribution system. Hence, it is sensible to start shedding loads when the frequency decays. The loads can be connected after the islanded distribution system is reconnected back to the transmission grid. Also, the frequency and voltage fluctuate more often in distribution system, when it is islanded. Hence, the frequency and voltage criteria should be relaxed for island operation. Generators should be able to handle larger RoCoV and RoCoF.

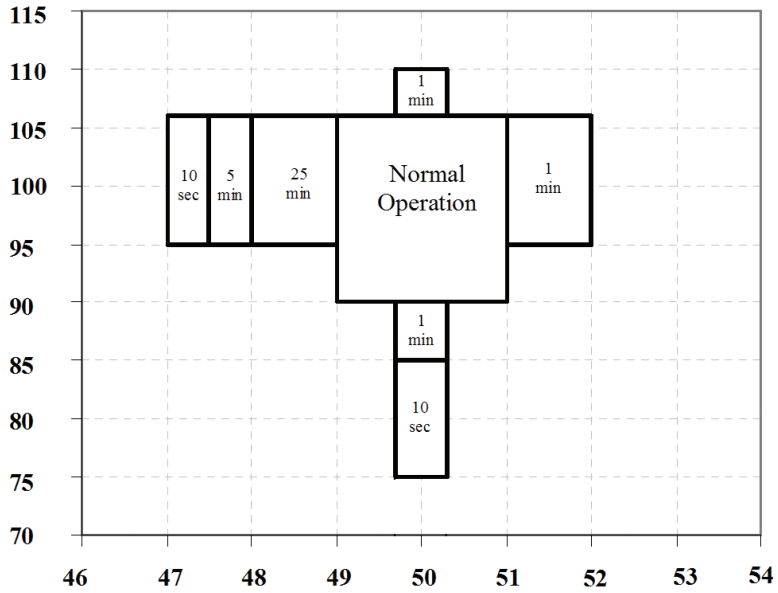

Fig. 5. 25. Voltage and frequency requirement for normal operation for WTG

Table 5. 8

Frequency range and operating time thermal power station units of 1.5 MW and higher

Frequency range (Hz)	Operating time
f< 47	≥ 300 ms
47 ≤ f ≤ 47.5	> 10 sec
47.5 < f ≤ 49	> 30 min
49 < f ≤ 50.5	Normal
50.5 < f ≤ 51	> 30 min
51 < f ≤ 53	> 3 min
f > 53	≥ 300 ms

WTP is chosen as the load prioritization criteria in this project but other criteria can also be chosen like sensitivity. Hospitals, airports or semiconductor industry can be characterized as more sensitive loads than residential load. Also, a distribution company may rank loads to maximize its revenue. It may shed a smaller load which is willing to pay more rather than a large load. However, it needs to know the real time load demand. The load ranking criteria may vary but the proposed load shedding scheme can be implemented to shed an optimal number of loads regardless of the load prioritization criteria. The load shedding scheme helps to stabilize the frequency of islanded distribution system which does not have any reserve margin. This proposed load shedding scheme cannot be directly implemented in distribution systems where DG may not operate at maximum power all the time.

Scenario 1 is simulated again without load SNTO and the GTGs' output power is set at 2.5 MW each (Scenario 3). The real power deficiency in the distribution system is 1.39 MW, which is less than the reserve margin (1.5 MW) of the distribution system. Another case, with the GTGs' output power set at 2 MW each, is also simulated. Now the reserve of the system is 3 MW. The frequency of the test distribution system is presented in Fig. 5. 26. An observation that can be made from Fig. 5. 26 is that the frequencies reach the lowest value around the same time (0.65s) after islanding. This seems to suggest that for a distribution system with some reserve, the problem of load shedding can be solved by adjusting 'T' in the proposed methodology and shedding load only when frequency goes below F_{LL}.

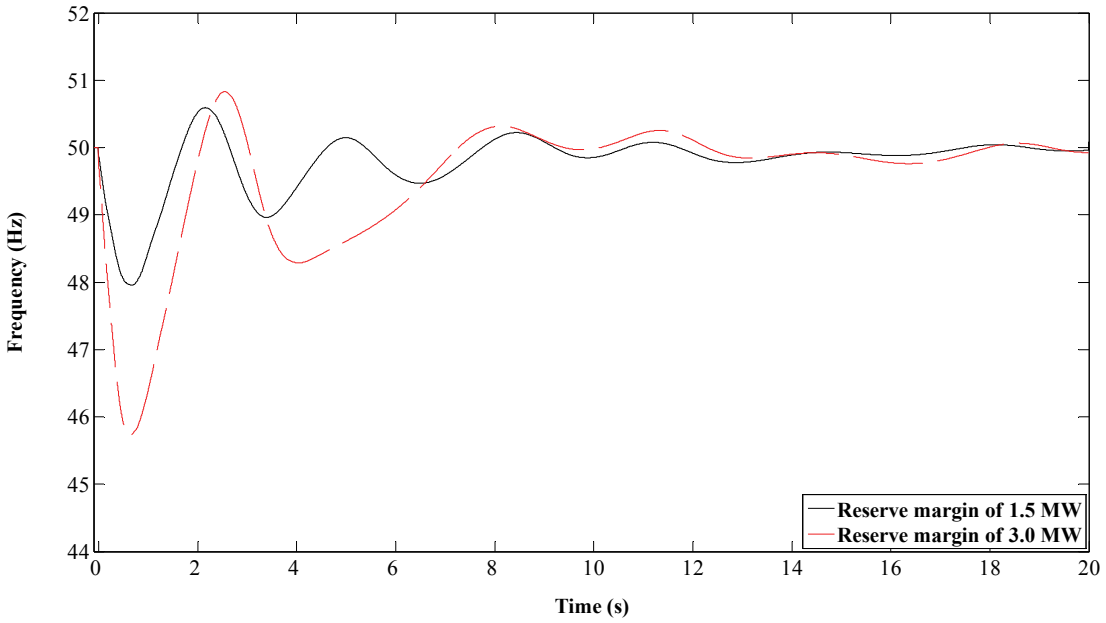

Fig. 5. 26. Frequency of the test distribution system for islanding when DG has some reserve

Now the scenario 3 is simulated again. But, the demand of the distribution system is increased by 1 MW and the GTGs' output power is set at 2.5 MW each. The distribution system

has the power deficiency of 2.386 MW and a reserve of 1.5 MW. The frequency of the distribution system is presented in Fig. 5. 27. The distribution system collapses *t=0.42s* after islanding. Based on Fig. 5. 26, if the distribution system waits for more than *t=0.65s* before it starts shedding loads, then the distribution system will have no chance to survive when the power deficiency is more than the reserve as shown by Fig. 5. 27. When the real time information on demand and generation is not available, whether to wait for the frequency to rise or start shedding the load when frequency falls is a real dilemma. It is the choice to be made by the distribution system operator. Waiting for frequency to rise, after generators start increasing power, results in optimal load shedding but it may result in system collapse when the deficiency in the islanded distribution system is more than the reserve margin. On the other hand, shedding the load when the frequency falls, without waiting for generators to take care of this frequency drop, insures the distribution system will not collapse but shedding of some of the loads may be unnecessary. Moreover, when the frequency goes below certain value, the generator protection may trip the generator and ultimately the distribution system may collapse. In such a case loads should be shed to protect the distribution system from collapsing irrespective of the reserve margin. It is recommended that the reserve margin of the distribution system, if desired, is kept small such that when the distribution system islands with power deficiency less than the reserve margin, frequency does not go below 49 Hz.

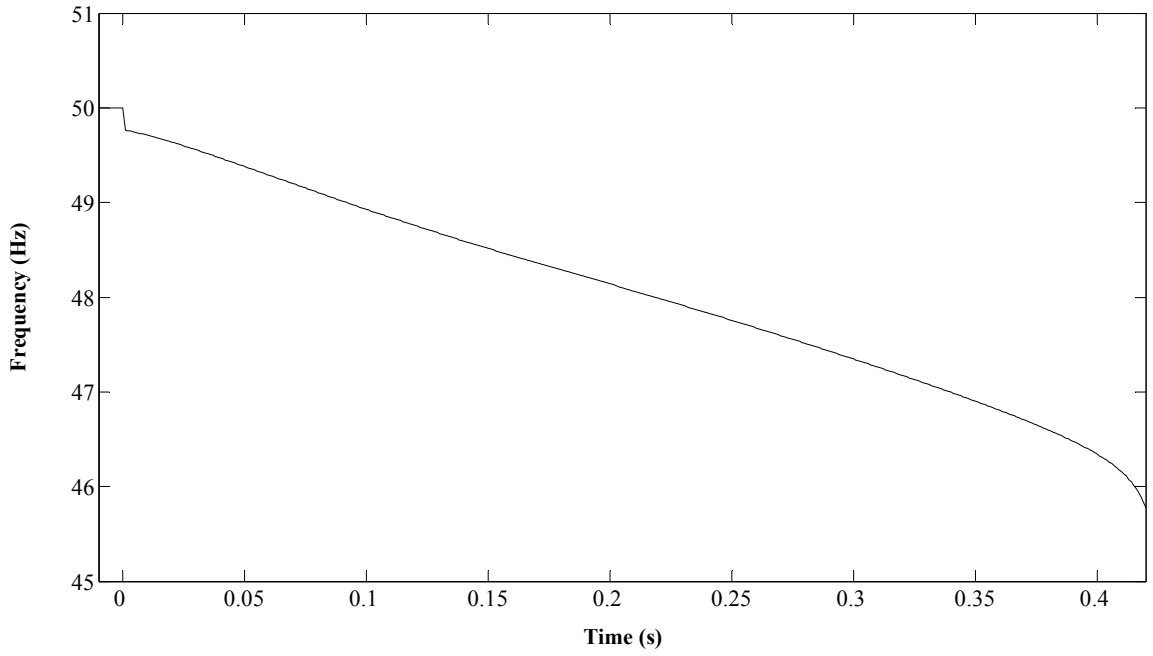

Fig. 5. 27. Frequency of the test distribution system when power reserve is less than deficiency after islanding

The load shedding strategy sheds the load when the frequency goes below a certain value. In case of the proposed methodology, it sheds the loads when frequency goes below 49 Hz. Hence, the frequency may stabilize above 49 Hz but below normal operating range of 49.9 Hz depending

on the power mismatch and loads' voltage and frequency dependency. However, as mentioned in the previous chapter, the frequency has to be minimum 49.8 Hz before the distribution system may be reconnected back to the transmission system. Even then, the distribution system may not be reconnected back if the transmission grid frequency is higher than 49.9 Hz. Hence, the possibility of reconnection to the grid can be increased by maintaining the frequency above 49.9 Hz. The distribution system can be kept running at a frequency below 49.9 Hz with the hope that a load decrease or load shedding, after fulfilment of the load shedding criteria, will bring the frequency above 49.9 Hz. On the other hand, some loads can be shed even when the frequency is just below 49.9 Hz for some time. Again, this is a choice to be made by the distribution system operator.

5.4 Conclusions

A strategy to shed an optimal number of loads in a distribution system, when it is islanded and does not have sufficient generation to supply all the loads, is presented to stabilize frequency. Frequency, rate of change of frequency, customers' willingness to pay and loads histories have been used to develop the load shedding strategy, which is implemented in relays responsible for shedding loads.

The conventional load shedding strategy that is being successfully used in large power systems cannot be implemented in the islanded distribution system because of the difference in characteristics of two systems. The load shedding strategy in the distribution system will not be based on the technical reason only but will depend on economic reasons as well. The proposed technique does not require communication between the components and real time system data. Rather, it uses load histories to shed the loads automatically with declining frequency. The proposed under-frequency load shedding can stabilize the frequency of the distribution system with DG units when it is islanded by shedding optimal number of loads. Two different scenarios, with different sets of load data and loads' voltage and frequency dependency, and six cases, with different WTP of loads, have been presented. Simulation results shows that the proposed load shedding techniques sheds an optimal number of loads under all conditions.

Chapter 6

Over-Current Protection of Distribution Systems

The fault current depends on available sources of short circuit power. The transmission grid generally has higher short circuit power compared to the small DG units connected to the distribution system. Hence, when the distribution system is islanded, the current seen by the protection relays, for a fault in the distribution system, is less compared to the case when the distribution system is connected to the transmission grid. Bolted three phase faults are simulated at the end of each line in the test distribution system shown in Fig. 6. 2. Maximum fault currents in the faulted line sections, for grid connected and island conditions, are presented in Fig. 6. 1.

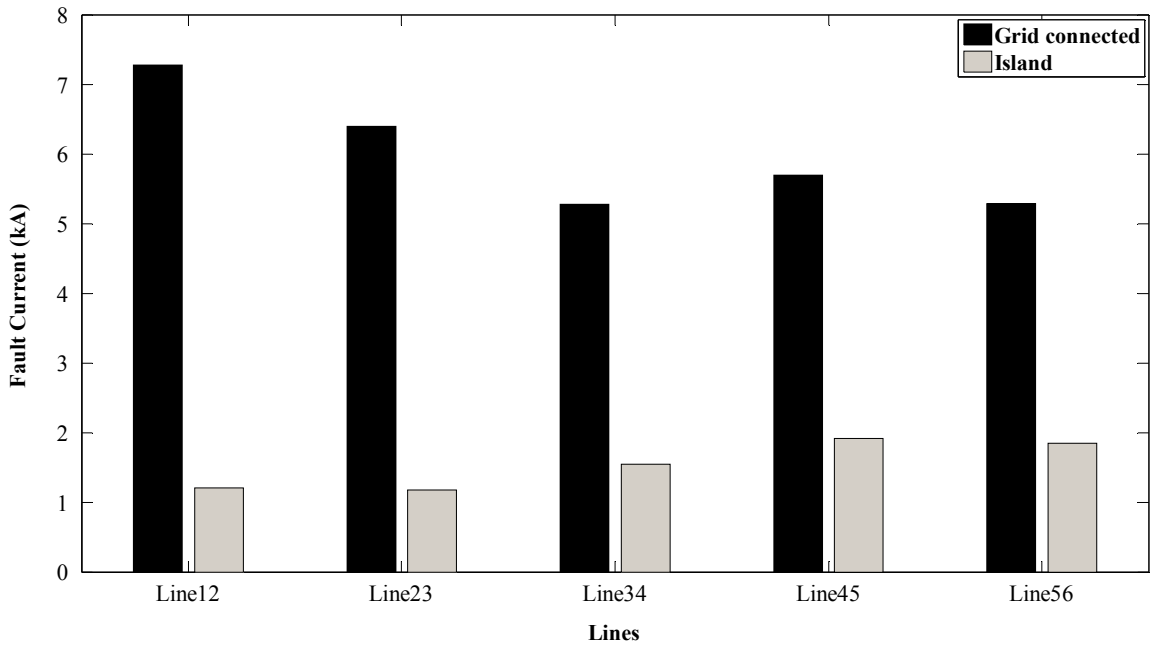

Fig. 6. 1. Fault current in the lines for a three phase fault at the end of the respective lines for grid connected and island conditions

Fig. 6. 1 shows that there is a significant difference in the fault currents during these two conditions. Therefore, an over-current protection system designed to operate in a grid connected mode may take longer time to clear faults when the distribution system is islanded. Electrical equipment (like motors connected at low voltage level) is equipped with protection systems that may disconnect them when the voltage goes below some value for a certain period of time. This may also apply to power sources like wind turbine generators, which are becoming common in many distribution systems. Thus, by not the clearing faults fast, not only the loads but also some generating units might also be lost, which is undesirable. On the other hand, if the over current

protection is designed for the islanded operation, then it might result in operation of breakers, even when it is unnecessary, due to excessive fault current from the transmission grid. This problem is discussed in more details in Section 6.4.

Few works have been done to solve this problem. In [95], a flywheel storage unit is used to increase the short-circuit power of a micro-grid to make the fault detection possible by the traditional relays. Another storage based method, for a high short circuit power is presented in [96]. Storage units require large investment and do not guarantee that the faults are cleared on time unless they can match the short circuit power of transmission grid. In [97], the over-current relays are designed for the islanded operation and the distribution system is islanded whenever there is a fault within a distribution system. Even though, the proposed methodology is simple, it frequently islands the distribution system and it is not desirable especially when the total amount of load is larger than the total amount of generation in the distribution system. In [98], a delay has been introduced to protect a micro-grid but it also runs into similar problems as described earlier. With the change in the state of a distribution system, the fault power changes. Therefore, the fault clearing time also changes. The problem of elongation of the fault clearing time or malfunction of relays due to change in fault power can be overcome by the use of communication. However, implementing such a communication system is considerable complex and requires high cost and it may not be economical for small distribution systems [30]. This research study proposes an adaptive directional over-current protection, which chooses the relay tripping characteristic based on the change in system conditions using only local information.

Adaptive protection is “an online activity that modifies the preferred protective response to a change in system conditions or requirements in a timely manner by means of externally generated signals or control action” [99]. Adaptive protection of a distribution system with distributed generation can be realized with the use of micro-processor based directional over-current relays (DOCR). DOCR have the possibility to choose different tripping characteristics. Modern digital over-current relays for low voltage applications have 2-4 settings groups [100]. Change in the system conditions is detected by identifying the operating states (grid connected or island condition).

The test distribution system is presented in Section 6.1. The design of the over current relays for the test distribution system is presented in Section 6.2. The protection of a variable speed wind turbine is discussed in Section 6.3. The issues with over current protection of a distribution system with some DG units and the solution are presented in Section 6.4 with some simulation results. An algorithm to detect a faulty Section is presented in Section 6.5. The adaptive relay configuration and some discussion on grounding are presented in Section 6.6 and Section 6.7, respectively. Section 6.8 draws some conclusions on the over current protection of distribution

systems.

6.1 Modelling of Distribution System

Fig. 6. 2 shows a model of the distribution system in which the proposed adaptive over-current protection is tested. The distribution system, shown in Fig. 6. 2, is modified from the original setup that is shown in Fig. 2. 6. This is done to demonstrate the effectiveness of the proposed methodology. The three fixed speed wind turbines from the original test distribution system are replaced by two GTGs and a variable speed wind turbine generator. The line data for the test system is given in Table AXVII. The variable speed wind turbine is modelled as in [101] and its data is presented in Table AXVIII. Currently, two-step definite-time over-current relays are used at the beginning of the feeder for over-current protection. Instead, digital directional over-current relays are proposed for the protection of the radial distribution system with distributed generation to facilitate its operation in island mode. The relays are represented by '**R**' in Fig. 6. 2 with numbers representing the buses that define the beginning and the end of a protection zone. The transmission grid is represented by GRID and its data is given in Table AV.

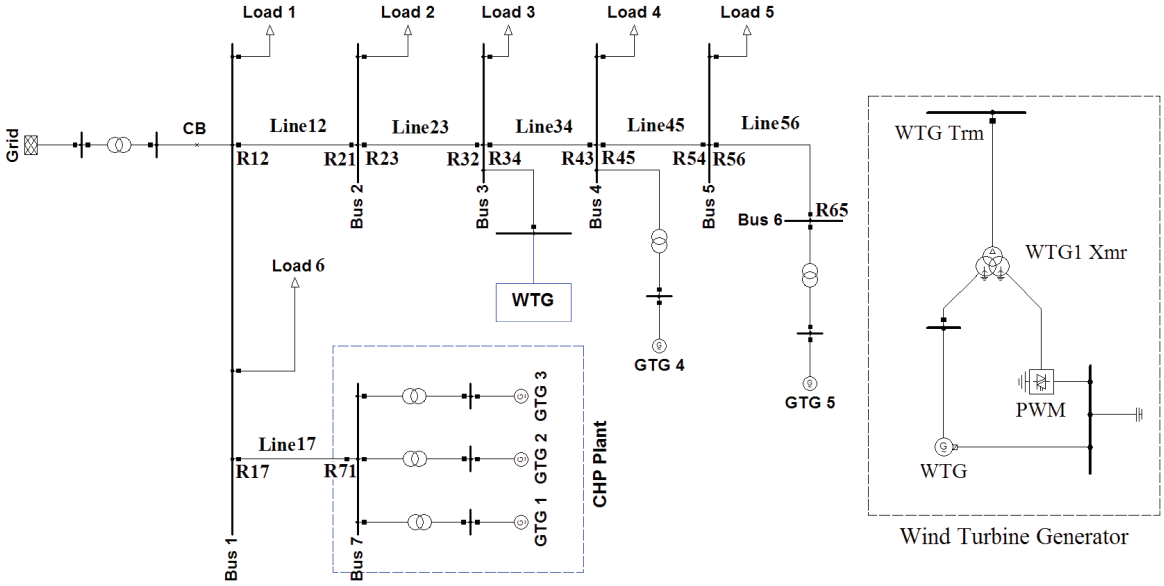

Fig. 6. 2. Modified test distribution system

6.2 Design of Over-Current Relays for the Test Distribution System

The adaptive protection is designed to choose from two trip characteristics based on the status of the distribution system. Two cases are simulated and they are:

- Case1 is the normal case when the distribution system is connected to the grid and
- Case2 is an island condition.

Relays R12, R23, R34 and R45 have two trip characteristics, one for Case1 and one for Case2. Both Relays R56 and R17 see forward current only when there is a fault in their protection zones and, hence, are designed to pickup for smaller currents and have just one trip characteristic. The only source of forward current for R71 is the CHP plant and, hence, it also has only one trip characteristic. The pickup currents (I_P) of all relays is set at 1.5 times maximum normal current. When Loads 1-5 are at peak and there are no WTG, GTG4 and GTG5, maximum normal currents will be seen in the relays R12, R23, R34 and R45. Similarly, when there are no loads, and WTG, GTG4 and GTG5 are operating at full load, maximum normal currents will be seen in R65, R54, R43, R32 and R21. As for R71, it sees maximum normal current when CHP power plant is operating at maximum. Instantaneous pick up times (T_{ins}) are set as *50ms* for a bolted three phase faults in the relays' protection zone. As mentioned earlier, R56 and R17 see forward current only when there is a fault in their protection zone and hence their instantaneous pickup is designed for *650 A* and *250 A*, respectively. The current values are chosen from design study of the test distribution system. The instantaneous pickup current of R56 is set at five times its minimum pickup current (*130 A*). As for R17, minimum pickup current is set at *100 A* and its instantaneous pickup is set at 2.5 times minimum pickup current (*250 A*). This current is guaranteed for a low resistance fault in Line17 even when only one fault power source is available. The sources of the fault current for a fault in Line17 can be GRID, GTG4, GTG5 and WTG. The relays' pickup is based on IEC 255-3 (nearly inverse) time over current characteristics, which is given by equation (6.1).

$$T = \frac{0.14 \times T_D}{\left(\frac{I}{I_P}\right)^{0.02} - 1} \qquad \textbf{(6.1)}$$

Where, T, I, and T_D are pickup time, current, and time dial setting of the relays, respectively. The time dial setting of each relay is designed in such way that the upstream relay will provide a backup function for the downstream relay. For example, let's assume that I^{34}_{max56} and I^{45}_{max56} are the currents seen by the relays R34 and R45, respectively, for a fault in Line56 near Bus 5. Now, R56 picks up after *50ms* (instantaneous pickup) to clear the fault. If it fails, then R45 picks up *500ms* after fault for I^{45}_{max56}. This makes sure that the fault is not cleared during the RPS while the distribution system is connected to the grid. Otherwise, clearing of fault would result in RoCoV and that may be confused with islanding. If both R56 and R45 fail to pickup, then R34 will pickup at *600ms* after fault for I^{34}_{max56}. It is assumed that clearing of fault takes around 7*0ms* after the picking up of the relay and upstream relays' reset time is well within *30ms*. This gives enough time for R45 to pickup and the corresponding circuit breaker to open to clear the fault before R34 picks up. Relays R23, R12 and R71 are designed similarly.

Table 6. 1

Time over-current characteristics of relays R71, R12, R23, R34, R45 and R56 for Case1

Relay	I_p (A)	T_D	Instantaneous pickup current (A)
R56	130	0.0117	650
R45	130	0.2731	5250
R34	260	0.2628	5300
R23	350	0.2892	6500
R12	350	0.3470	7000
R71	390	0.1146	940

The time dial settings, pickup currents and instantaneous pickup currents for the individual relays are listed in Table 6. 1. Fig. 6. 3 shows the time over-current plot of relays R71, R12, R23, R34, R45 and R56 for Case1.

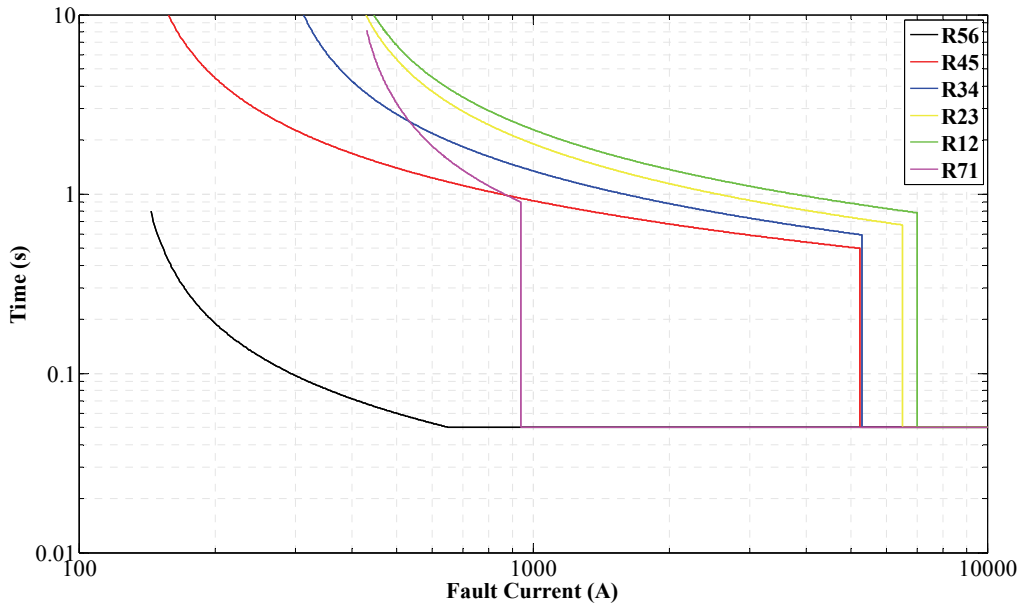

Fig. 6. 3. Time over-current characteristics plot of relays R71, R12, R23, R34, R45 and R56 for Case1

For relay R17, relays R21, R32, R43, R54 and R65 provide the backup function. The time dial settings, pickup currents and instantaneous pickup currents for the individual relays are listed in Table 6. 2.

Table 6. 2

Time over-current characteristics of relays R17, relays R21, R32, R43, R54 and R65 for Case1

Relay	I_p (A)	T_D	Instantaneous pickup current (A)
R17	100	0.0661	250
R21	350	0.0341	582
R32	350	0.0414	585
R43	260	0.0751	566
R54	130	0.0877	288
R65	130	0.0991	295

Fig. 6. 4 show the time over-current plot of relays R17, R21, R32, R43, R54 and R65 for Case1.

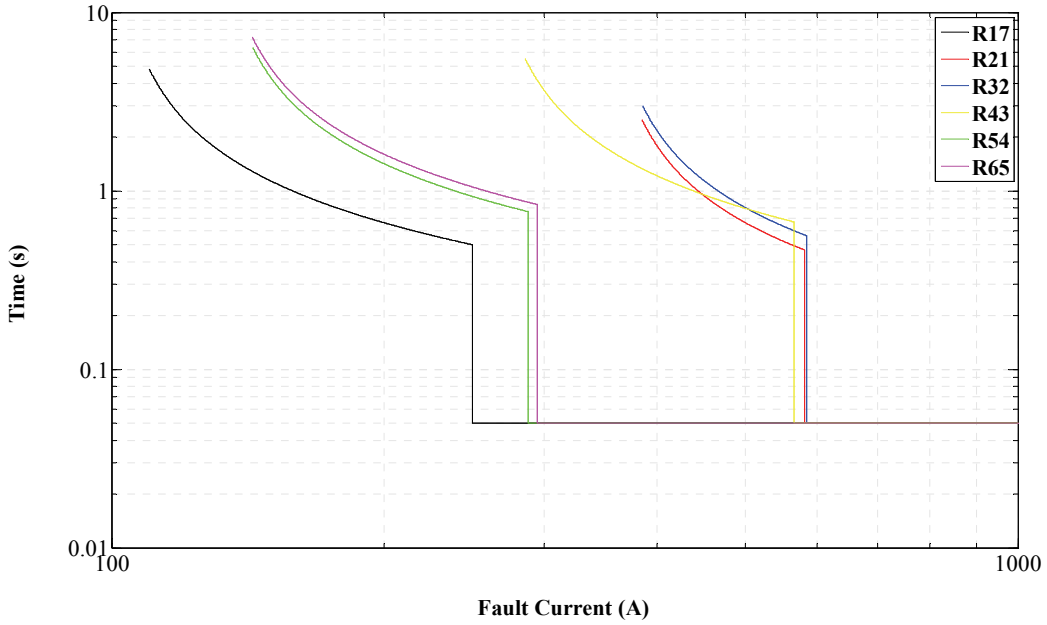

Fig. 6. 4. Time over-current characteristics plot of relays R17, R21, R32, R43, R54 and R65 for Case1

As mentioned earlier, there is a significant deference in fault current when the distribution system changes state from grid connected condition to island and vice versa. Hence, the trip characteristics of relays R12, R23, R34 and R45 are designed for the island condition as well. Their time dial settings, pickup currents and instantaneous pickup currents for Case2 are listed in Table 6. 3. The time over-current plots of the relays are shown in Fig. 6. 5. Note that the trip characteristics of R71 and R56 is not changed due to the reason mention earlier.

Table 6. 3

Time over-current characteristics of relays R71, R12, R23, R34, R45 and R56 for Case2

Relay	I_p (A)	T_d	Instantaneous pickup current (A)
R56	130	0.0117	650
R45	130	0.0460	1140
R34	260	0.0440	950
R23	350	0.0479	925
R12	350	0.0637	935
R71	390	0.1146	940

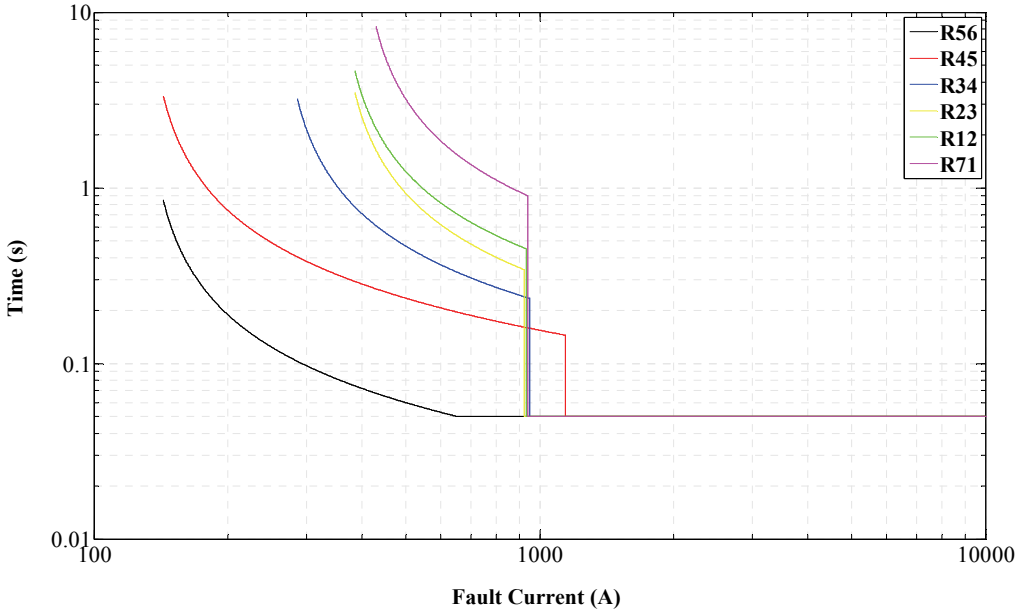

Fig. 6. 5. Time over-current characteristics plot of relays R71, R12, R23, R34, R45 and R56 for Case 2

Again, relays R45, R34, R23, R12 and R71 provide the backup for relay R56. When the distribution system is already islanded faults can be cleared anytime as the grid reconnection detection is not based on RoCoV. Now, if I^{34}_{max56i} and I^{45}_{max56i} are the currents seen by the relays R34 and R45, respectively, for a fault in Line56 near Bus 5 when the distribution system is islanded, R45 picks up at *150ms* after the fault for I^{45}_{max56i} and R34 picks up at *250ms* after the fault for I^{34}_{max56i}. All the time over current characteristic plots shows only the relay pickup time.

From a simple observation of Fig. 6. 3, it looks like the relays lack selectivity as the time over-current characteristics of R71 crosses the time over-current characteristics of other relays. However, this is not the case. As it can be seen from the Fig. 6. 2, R71 only sees the current from the CHP plant whereas other relays see current from both the CHP plant and the transmission grid for a fault beyond Bus 1. Moreover it can be seen, from Fig. 6. 5, that the relays have selectivity

when the distribution system is islanded. The source of fault current for R71, R12 and R23, now, is only the CHP plant. Furthermore, R45's time over-current characteristics crosses other relays time over-current characteristics because of the presence of a GTG at Bus 4. Similar explanation is true for the crossing of the time over-current characteristics curves of the relays in Fig. 6. 4.

6.3 Wind Turbine Generator Protection

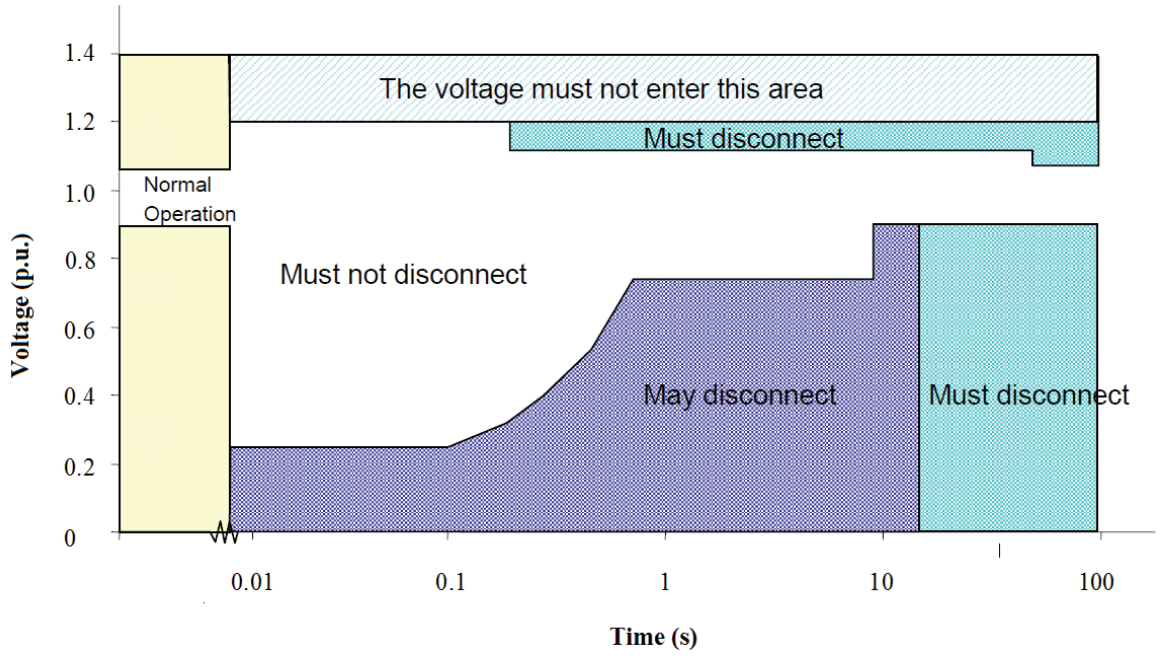

Fig. 6. 6. Danish grid code for fault ride through for wind turbines connected at below 100 kV

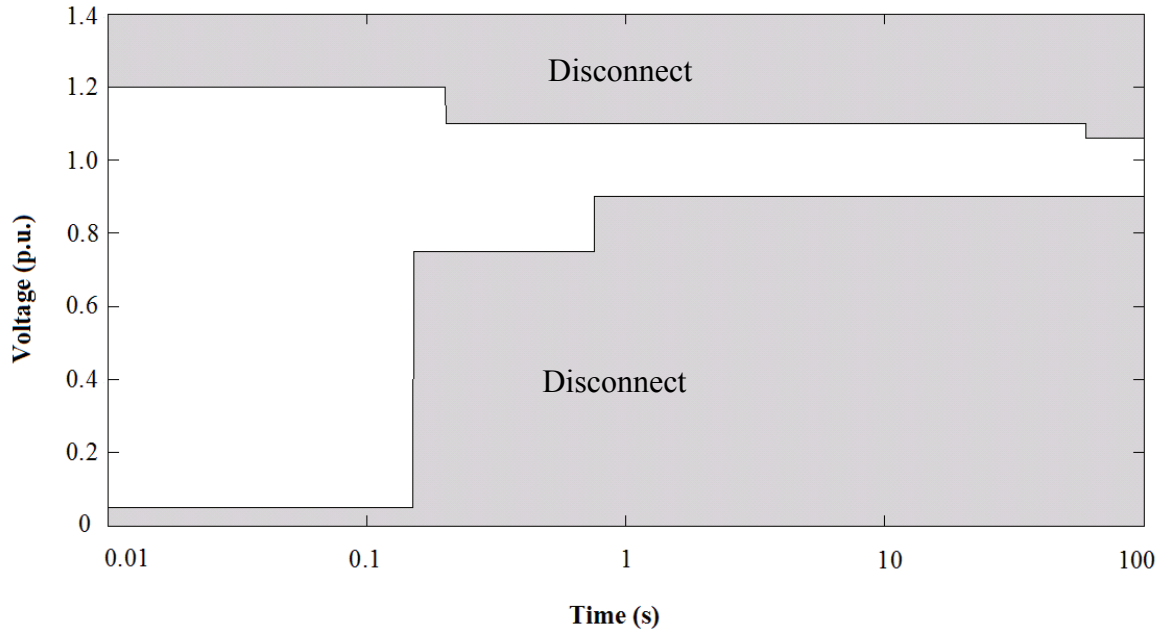

Fig. 6. 7. Protection of wind turbine for the simulaiton case

The wind turbines connected to the Danish power system should satisfy the Danish grid code. The fault ride through capability, according to the Danish grid code, is depicted in Fig. 6. 6 [94]. Based on the grid code, the protection of the wind turbine connected at Bus 4 is designed as depicted in Fig. 6. 7 for simplicity. In addition to the under/over voltage protection, a crowbar is inserted when the current is higher than 5 kA or more to protect the converters. Similarly, the WTG is tripped when the speed goes above 1.3 p.u. to protect the blades.

6.4 Simulation Results and Discussion

Islanding is simulated by opening the circuit breaker (CB). It is assumed that the relays take *10ms* to close their trip contacts and the circuit breakers takes *60ms* to clear the fault. All the faults are simulated at time *t=0s*.

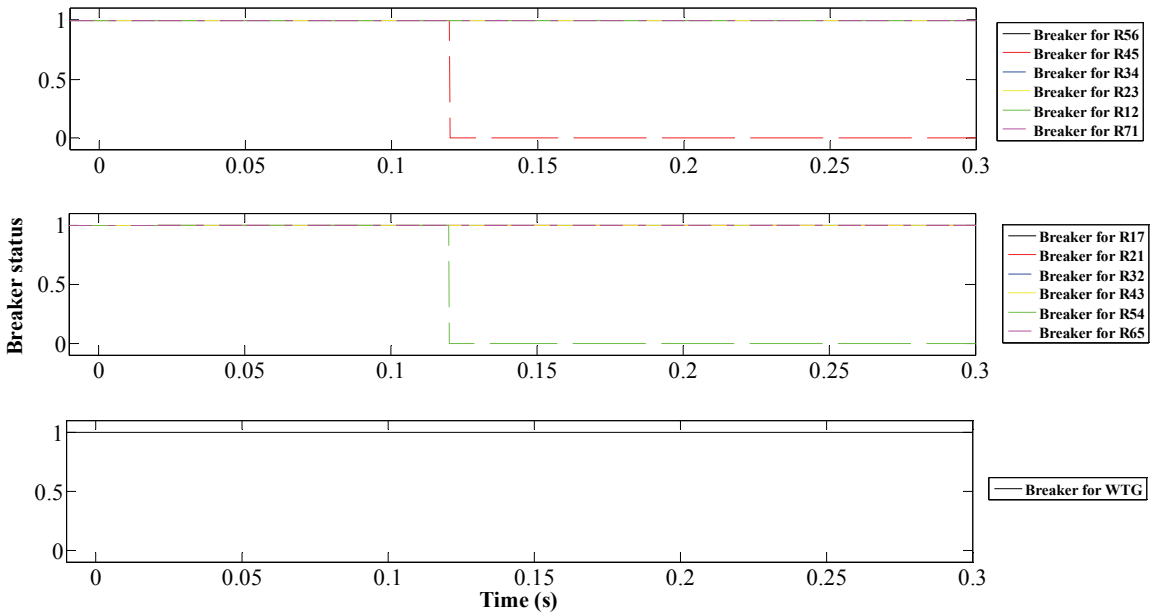

Fig. 6. 8. Status of circuit breakers for a three phase fault in Line45 for Case1 when relays are set according to Fig. 6. 3 and Fig. 6. 4

A three phase fault, with a fault resistance of *0.05 Ω*, is simulated at the middle of Line45 when the distribution system is connected to the transmission grid. The relays' time over current characteristics are as in Fig. 6. 3 and Fig. 6. 4. Fig. 6. 8 shows the breakers' status. 1 represents that the breaker is closed and 0 represents that it is open. It can be seen from the figure that the fault is cleared by opening the breakers at the two ends of Line45, *120ms* after the fault, due to the activation of instantaneous pickup.

Now the distribution system is islanded and the same fault is simulated again. Fig. 6. 9 shows the breakers' status. The breaker for R54 opens at *t=120ms* to clear the fault (same as in the

previous case). But, the breaker for R45 takes longer time to clear the fault, as there is a decrease in the fault current due to the islanding. Since the WTG's protection is designed to trip WTG if the voltage is below 5% for more than *150ms*, the longer fault clearing time trips the WTG.

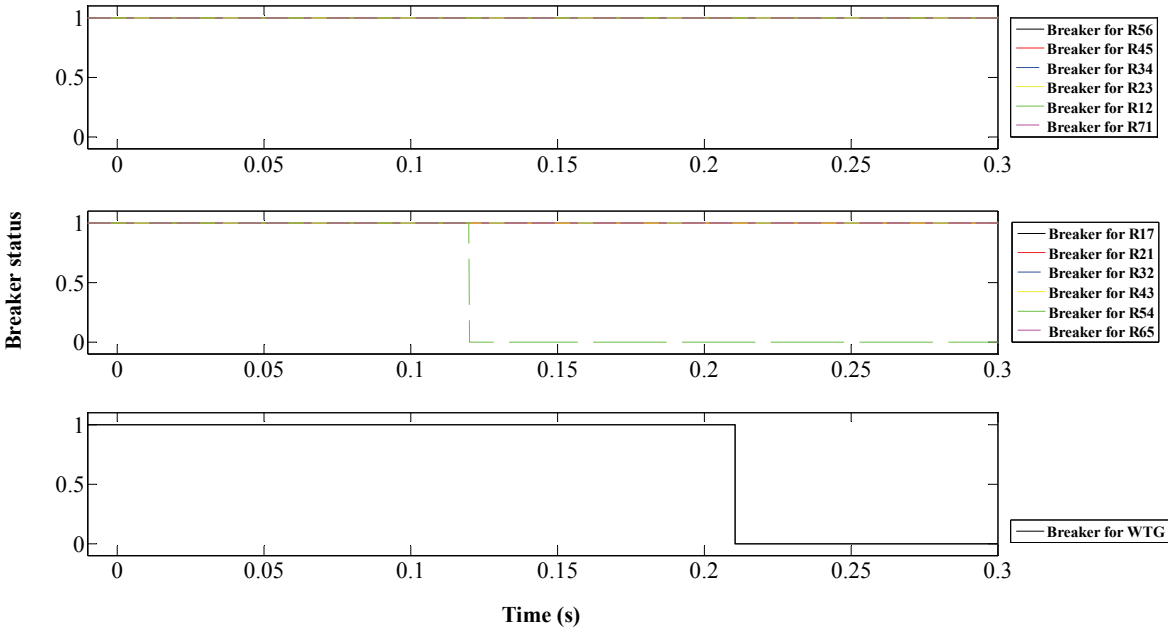

Fig. 6. 9. Status of circuits breaker for a three phase fault in Line45 for Case2 when relays are set according to Fig. 6. 3 and Fig. 6. 4

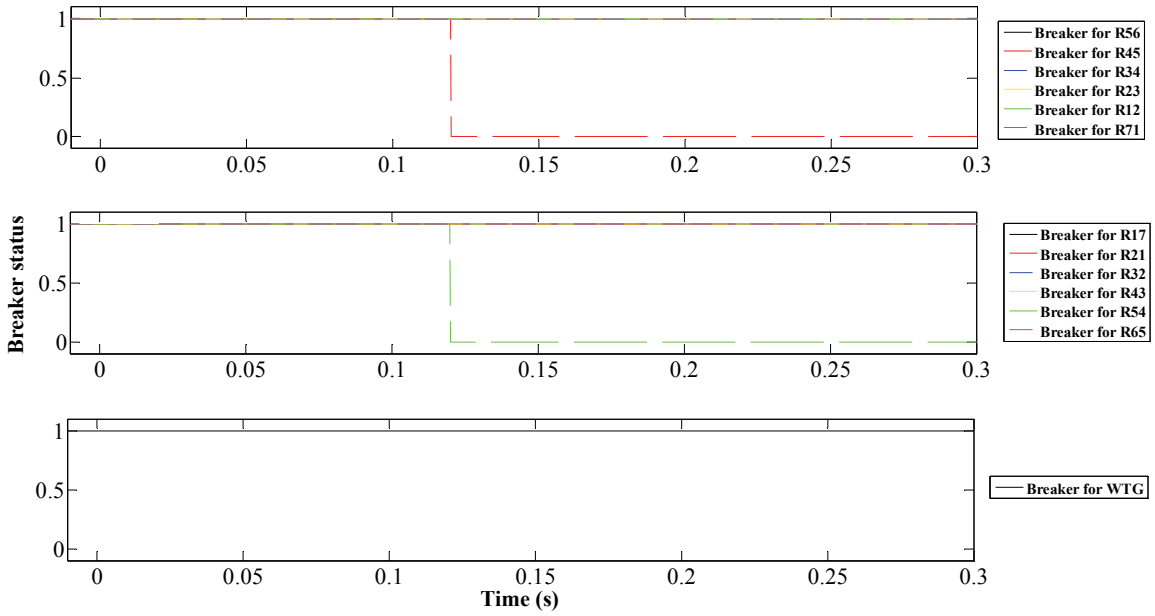

Fig. 6. 10. Status of circuit breakers for a three phase fault in Line45 for Case2 when relays are set according to Fig. 6. 4 and Fig. 6. 5

One might argue that making the WTG staying online for longer time, during voltage dip, may overcome this problem. But, there is always a possibility that unnecessary tripping of the WTG may occur no matter how the protection of the WTG is designed. This is because islanding decreases the short circuit power and that elongates the fault clearing time.

Now the relays' trip characteristics are set as in Fig. 6. 4 and Fig. 6. 5. The same fault is simulated again for Case2. Fig. 6. 10 shows the breakers' status. As expected, the fault is cleared by opening of breakers at the two ends of Line45 *120ms* after the fault and the WTG stays online.

Fig. 6. 10 verifies that the problem of longer fault clearing time due to lower short circuit power can be solved by changing the trip characteristics of the relays. Now, the distribution system is connected to the transmission system but the relays' trip characteristics are kept as in Fig. 6. 4 and Fig. 6. 5. The three phase fault with a fault resistance of *0.05 Ω* is simulated at the middle of Line45 again. Fig. 6. 11 shows the breakers' status.

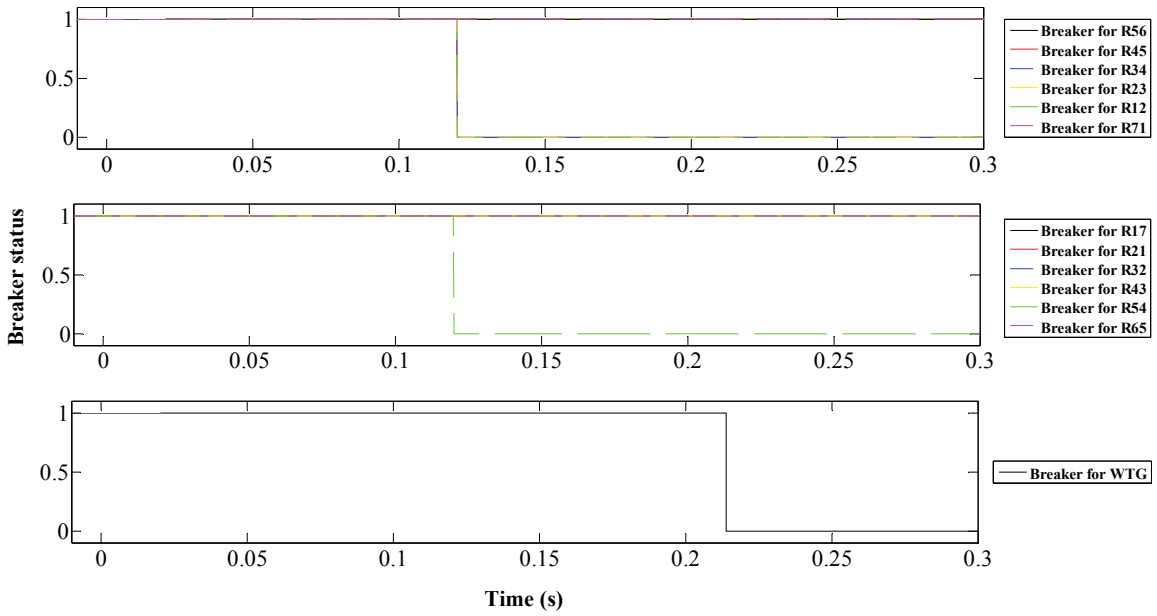

Fig. 6. 11. Status of circuit breakers for a three phase fault in Line45 for Case1 when relays are set according to Fig. 6. 4 and Fig. 6. 5

Some relays see the fault current that is higher than their instantaneous pickup setting because of the transmission grid. Hence relays R12, R23, R34 and R45 and R54 pickup as shown in Fig. 6. 11. The fault could have been cleared with the operation of just R45 and R54. Thus the operation of R12, R23 and R34 is unnecessary. Tripping of relays R23 and R34 leaves the WTG with only a small load to supply. This increases the WTG speed and the WTG over-speed protection trips it. The WTG control is designed to produce maximum power.

Fig. 6. 9 and Fig. 6. 11 show that setting only one trip characteristic for the relays doesn't work when the distribution system changes from grid connected mode to island mode and vice versa. On the other hand, Fig. 6. 8 and Fig. 6. 10 show that by changing the trip characteristics, the relays can clear faults quicker and thereby avoid the tripping of sensitive equipments like the WTG and also maintain protection co-ordination. Hence, by the use of the state detection algorithms, presented in chapters 2 and 4, the distribution system's state (connected to the transmission grid or islanded) can be identified. This information is used by the relays to choose the appropriate tripping characteristics.

When the fault at Line45 is cleared by opening the breakers at two ends of the line in (Case1), the part of the distribution system beyond Bus 4, including GTG5, is now disconnected from the test distribution system. A scenario is simulated by applying a new fault, a three phase fault with a fault resistance of 0.1 Ω, at the middle of Line23. The fault is assumed to occur at *t=0s* (Case3). Events like fault at Line45 and disconnection of GTG5 occurred before *t=0s*. Fig. 6. 12 shows the status of the circuit breakers. Since there is no GTG5, the fault current seen by R32 is less compared to Case1 when all DG units are present. Hence, it takes longer time to clear the fault and thus, as a result, the WTG is tripped.

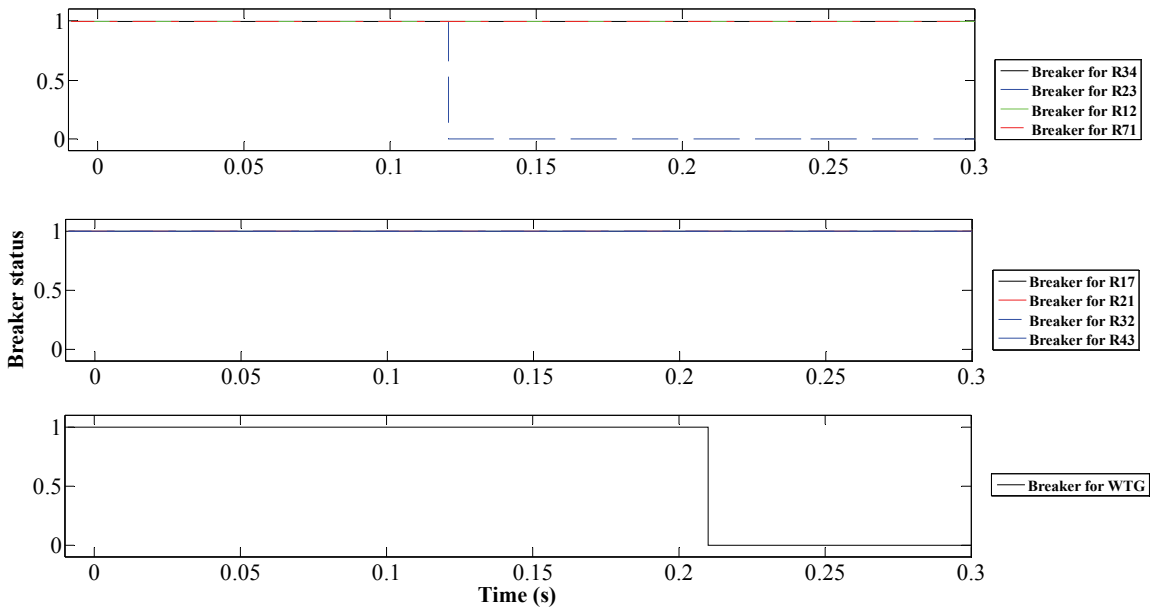

Fig. 6. 12. Status of circuit breakers for a three phase fault in Line23 for Case3 when relays are set according to Fig. 6. 3 and Fig. 6. 5

Bolted three phase faults are simulated at the beginning of the lines. Maximum currents in the faulted line sections, when all the DG units are present and when GTG5 is disconnected from

the test distribution system, are presented in Fig. 6. 13. It shows there is some difference in the fault currents during these two conditions.

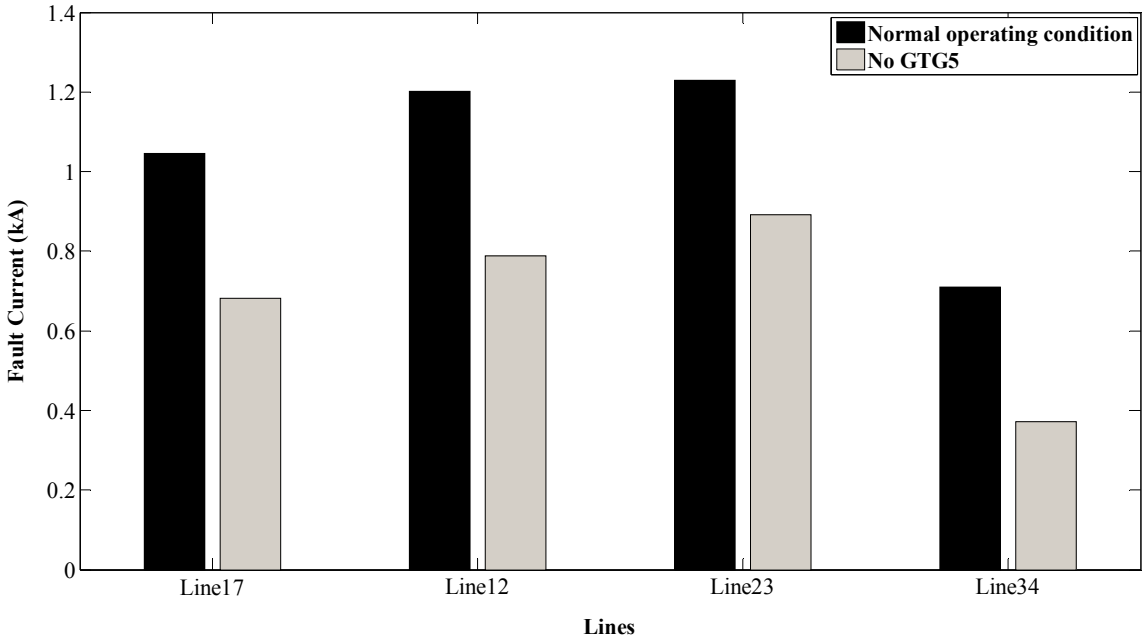

Fig. 6. 13. Fault current in the lines for a three phase fault at the end of the respective lines with all DG units and without GTG5

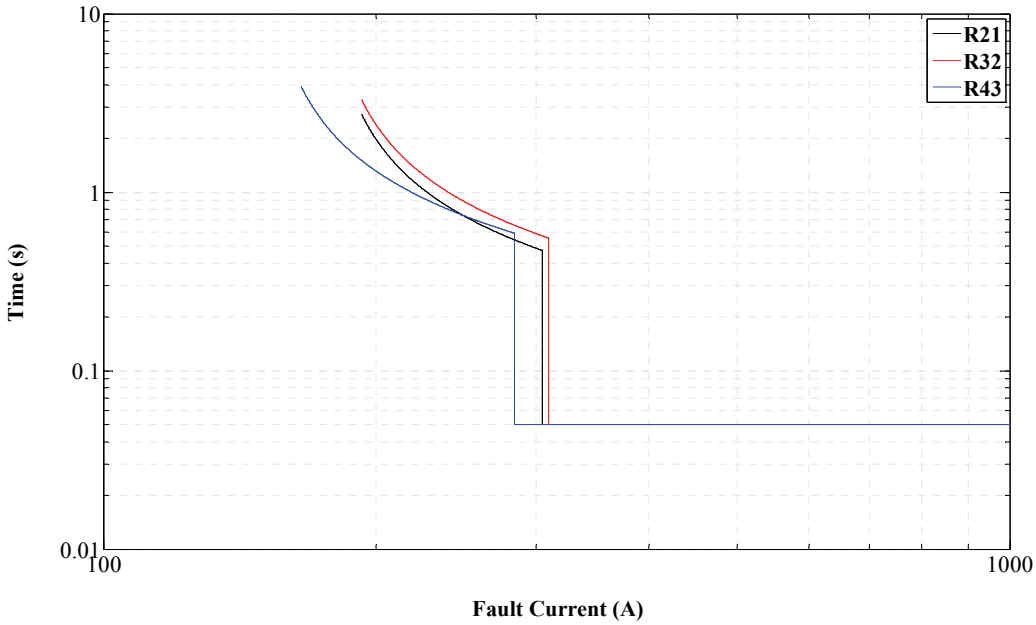

Fig. 6. 14. Time over-current characteristics plot of relays R43, R32 and R21 for Case3

Since there is some difference in fault current when the GTG5 is disconnected from the test distribution system compared to the case when all the DG units are present, the relays R42, R32 and R21 are also designed for Case3. The time dial settings, pickup currents and instantaneous

pickup currents for the individual relays are listed in Table 6. 4. Fig. 6. 14 show the time over-current plot of relays R42, R32 and R21 for Case3.

Table 6. 4

Time over-current characteristics of relays R21, R32 and R43 for Case3

Relay	I_p (A)	T_d	Instantaneous pickup current (A)
R21	175	0.0377	305
R32	175	0.0455	310
R43	150	0.0542	284

The three phase fault with a fault resistance of 0.1 Ω at the middle of Line23, is simulated again but now the trip characteristics for the relays R43, R32 and R21 are set as in Fig. 6. 14.

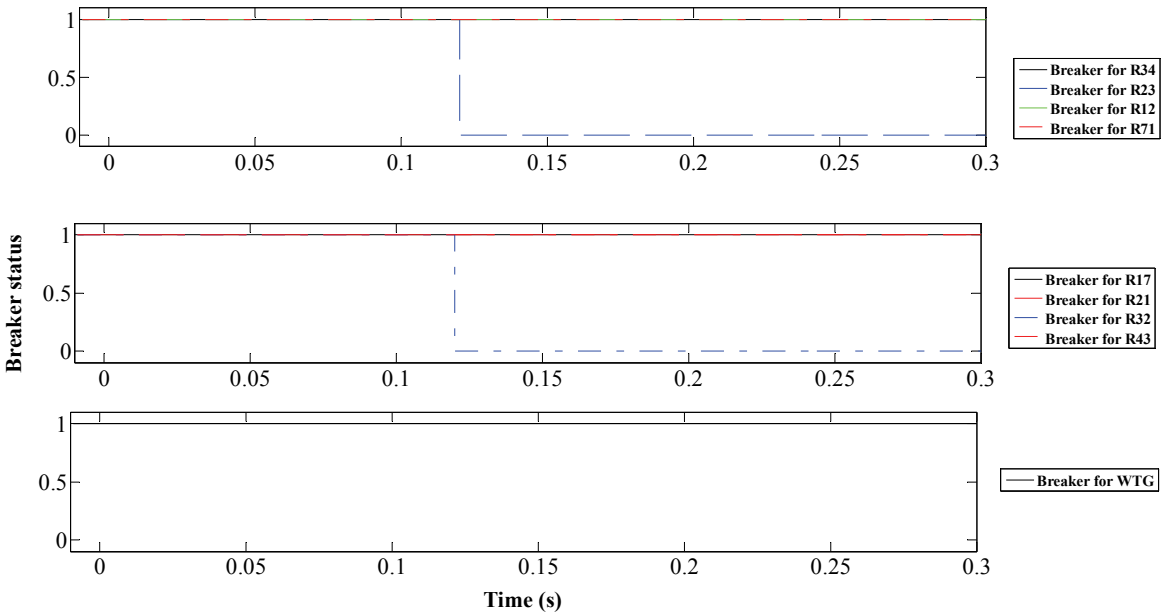

Fig. 6. 15. Status of circuit breakers for a three phase fault in Line23 for Case3 when relays are set according to Fig. 6. 3 and Fig. 6. 14

Fig. 6. 15 shows the circuit breaker status. As expected, the fault is cleared by opening of the breakers at the two ends of the line *120ms* after the fault (due to instantaneous pickup). The WTG stays online due to the quicker fault clearing. Fig. 6. 15 seems to suggest that designing the protection system for the case without GTG5 solves the problem. To test this, same fault is simulated again and the trip characteristics are set as in Fig. 6. 3 and Fig. 6. 14 but the GTG5 is connected to the test distribution system in this case. Fig. 6. 16 shows the status of the circuit breaker.

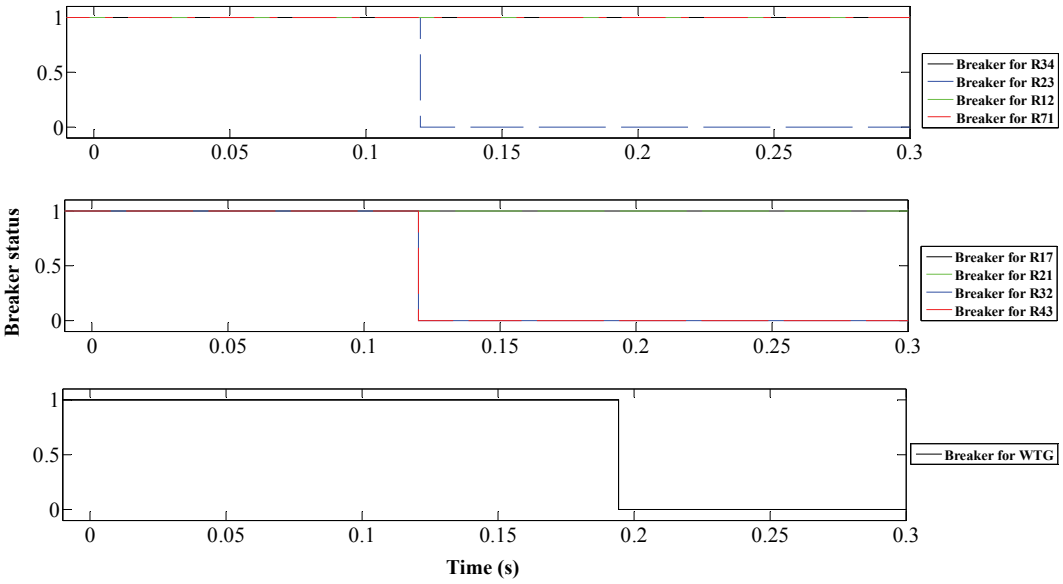

Fig. 6. 16. Status of circuit breaker for a three phase fault in Line23 for Case1 when relays are set according to Fig. 6. 3 and Fig. 6. 14

Due to the increase in fault current as a result of the GTG5, R43 also trips along with R23 and R32. This is unnecessary as the fault could have been cleared by opening of breakers corresponding to R23 and R32 only. Furthermore, the opening of R43 results in an increase in the Bus 3 voltage and tripping of the WTG. Fig. 6. 16 shows that using a single trip characteristic may result in unnecessary tripping of breakers and WTG. However, Fig. 6. 15 shows that changing the trip characteristics helps in avoiding those unnecessary trips. Change of distribution system status from grid connected mode to island mode or vice versa can be easily identified by the state detection techniques and that information can be used to update the trip characteristics of the relays. Furthermore, the trip characteristics should also be updated when some generators are lost. In the test distribution system, if R21 can know that a fault in Line45 is cleared by opening the breakers at the two ends of the line, it will know that GTG5 is disconnected from the test distribution system, and its settings should be changed. Hence, it is necessary to be able to detect the faulty area.

6.5 Detection of Faulty Section

The flow chart for the adaptive protection where the relays choose the appropriate trip characteristics based on the network condition is shown in Fig. 6. 17. To detect the faulted section, each relay stores the currents it sees when fault currents are large enough to initiate an instantaneous pickup of downstream relays. For an example, R34 stores minimum currents it sees when a fault in Line45 or Line56 initiates an instantaneous pickup of R45 or R56, respectively for grid connected and island condition. If R34 sees a fault current, for a fault, that is higher than the

instantaneous pickup current of R56 but lower than that of R45 and the fault is cleared in minimum time, then it is clear that the breaker corresponding to R56 has operated and that GTG5 is disconnected from the test distribution system. However, if the fault current is low, as a result of some fault resistance, then the fault can be cleared anytime based on the relays' time over-current characteristics.

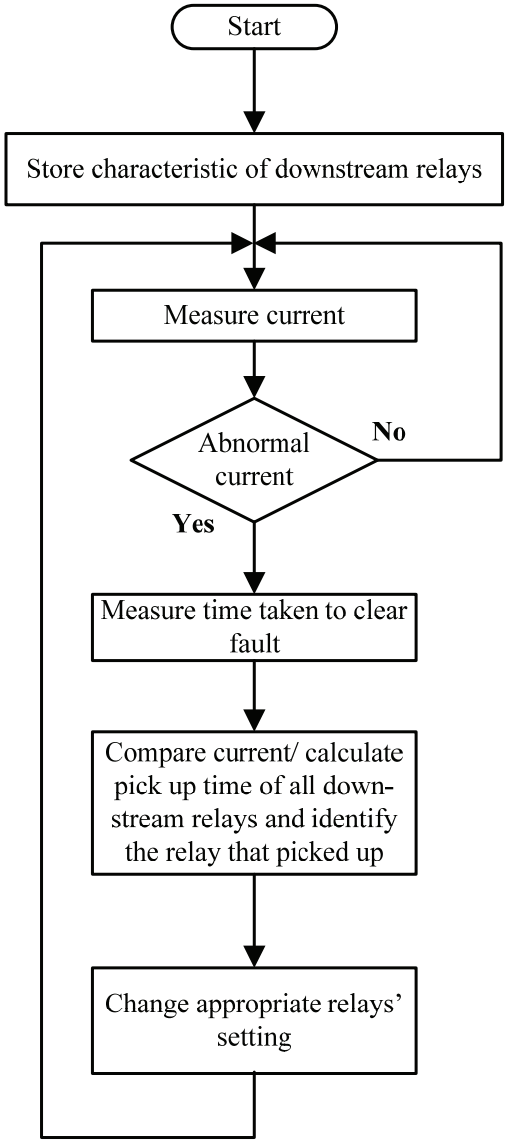

Fig. 6. 17. Flow chart for detecting faulty section

To identify the faulted section, during such a condition, the relays store the time over-current characteristics of all the downstream relays. When a relay sees current, which is higher than its pickup current, it assumes a fault and start counting time. Furthermore, when the current decreases by more than 10% in a successive measurement, the relay assumes the fault is cleared. It calculates the time taken to clear the fault and subtracts the total time taken for the relay contact to

close and the circuit breaker to open. The result is the time taken (T_m) by the relay, which initiated fault clearing, to pickup. Now, based on the current measurement during the fault and the time over-current characteristics of the downstream relays, the relays calculate the pickup time of all the downstream relays. It should be noted that the relay may not know the actual fault current and it is assuming that the current it measured is the actual fault current. The relay whose calculated pickup time is a little higher than T_m is identified to have picked-up and hence the faulty region is identified as the region protected by that relay. The actual fault current will be higher than the current seen by the upstream relays if some generators are present down the feeder. This is also the reason for choosing the relay that sees current in the forward direction to identify the faulty section and initiating an update of the tripping characteristics of the reverse relay. For an example, for a fault in Line56, R34 sees a current that is higher than what R32 sees, because of the presence of the WTG. However, it is still less than the actual fault current due to GTG4 at Bus 4. Let's assume that R34 measures the fault clearing time as *300ms*. Let's also assume that the normal time taken to clear the fault after the relay has picked up is *70ms*. Hence, which ever relay picked up, it picked up *230ms* after the fault. Now, based on the current R34 measured *230ms* after the fault it calculates the pickup time of the downstream relays (R45 and R56) and compares with *230ms*. The relay whose corresponding calculated pickup time is slightly higher than *230ms* is identified to have picked up. Now R34 may ask R32 to change its tripping characteristics based on its identification of the faulted area.

6.6 Simulation Results and Discussion for Detection of Faulty Section

Table 6. 5 shows minimum current the relays see for downstream faults, during grid connected condition, cleared by the instantaneous pickup of the relay protecting the faulted zone.

Table 6. 5

Minimum currents seen by the relays for faults that are cleared instantaneously by the corresponding relays and breakers for grid connected condition

Fault current seen by relays (A)	Fault at			
	Line23	**Line34**	**Line45**	**Line56**
R12	6486.6	5235	4921	548
R23	-	5235	4921	548
R34	-	-	4988	609
R45	-	-	-	650

For example, minimum amount of current that results in instantaneous pickup of relay R34 during grid connected condition is 5.4 kA. When this current flows through R34, R12 and R23 see 5.235 kA of current flowing through them. Relay R56 does not need to find the faulty section as

any fault downstream results in loss of GTG5. In fact, R45 also does not need to find the faulty section as any fault downstream results in loss of GTG5. However, it would have needed to find the faulty section if there were generator(s) at Bus 5. Similarly, relay R71 does not have any relays to update and, hence, it also does not need to find the faulty section.

A three phase fault with a fault resistance of 0.5 Ω is simulated at the middle of Line45 (Case1B) when the distribution system is connected to the grid and the relays' trip characteristics are set as in Fig. 6. 3 and Fig. 6. 4.

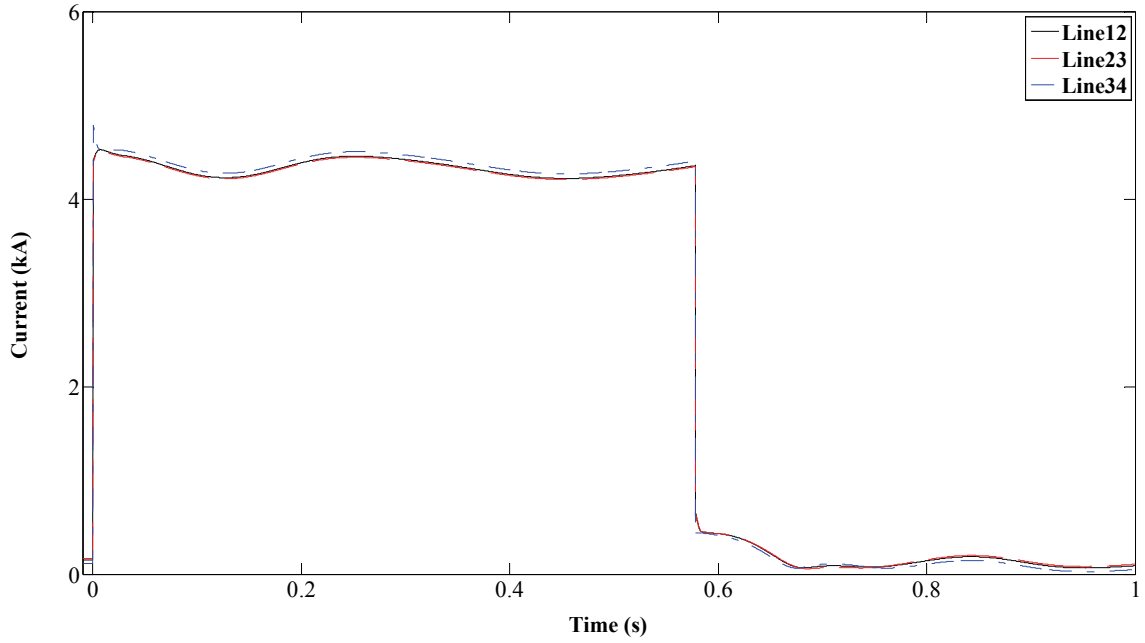

Fig. 6. 18. Current for a three phase fault in Line45 when the distribution system is connected to grid

It is assumed that the current is measured every half voltage period. The relays takes *10ms* to close their trip contacts and the circuit breaker takes *60ms* to clear the fault. Fig. 6. 18 shows the currents through the lines Line12, Line23 and Line34. The relays R12, R23 and R34 (forward relays) see that the current is higher than their pickup currents at *t=0s* and that it is reduced by more than 10 % in the successive measurement at *t=580ms*. Hence, the measured fault clearing time is *580ms*. This means whichever relay picked up to clear the fault, it picked up *510ms* after the fault, at the latest. All the relays now calculate the pickup times of the downstream relays based on the current they measured at *t=510ms* and the time over current characteristics of the downstream relays.

As an example, R23 sees a current of 4245.9 A for the above mentioned fault. Hence, if the fault was in Line56, R56 would have picked up at *0.05s* according to Table 6. 5. Now, R23 calculates the pickup time of R45 as seen by it $\left(T_{R23}^{R45}\right)$ as

$$T_{R23}^{R45} = \frac{0.14 \times 0.2731}{\left(\frac{4245.9}{130}\right)^{0.02} - 1} = 0.529\,s$$

Similarly, R23 also calculates the pickup time of R34 as seen by it $\left(T_{R23}^{R34}\right)$ as

$$T_{R23}^{R34} = \frac{0.14 \times 0.2627}{\left(\frac{4245.9}{260}\right)^{0.02} - 1} = 0.640\,s$$

Since the actual pickup time of *510ms* is slightly less than the calculated pickup time of R45, R23 identifies R45 to have picked up to clear the fault. R23, now, also knows that GTG5 is disconnected from the distribution system and asks R21 to change its trip characteristics according to Fig. 6. 14. The current each relay measures at the measured pickup time and the calculated pickup time for the downstream relays for Case1B are listed in Table 6. 6.

Table 6. 6

Summary of results for Case1B

Relay	Fault current measured by relays at *t=510ms* (A)	Calculated pickup times for relay (ms)			
		R23	R34	R45	R56
R12	4256.9	790	639	529	50
R23	4245.9	-	640	529	50
R34	4305.2	-	-	527	50

Table 6. 7 shows minimum current the relays see for downstream faults, during island condition, cleared by the instantaneous pickup of the relay protecting the faulted zone.

Table 6. 7

Minimum currents seen by the relays for faults that are cleared instantaneously by the corresponding relays and breakers for island condition

Fault current seen by relays (A)	Fault at			
	Line23	Line34	Line45	Line56
R12	932	914	905	402
R23	-	914	905	402
R34	-	-	928	467
R45	-	-	-	650

A three phase fault, with a fault resistance of 5 Ω, is simulated at the middle of Line45 when the system is islanded (Case2B) and the relay trip characteristics are set as in Fig. 6. 4 and Fig. 6. 5. Fig. 6. 19 shows the fault current through the lines.

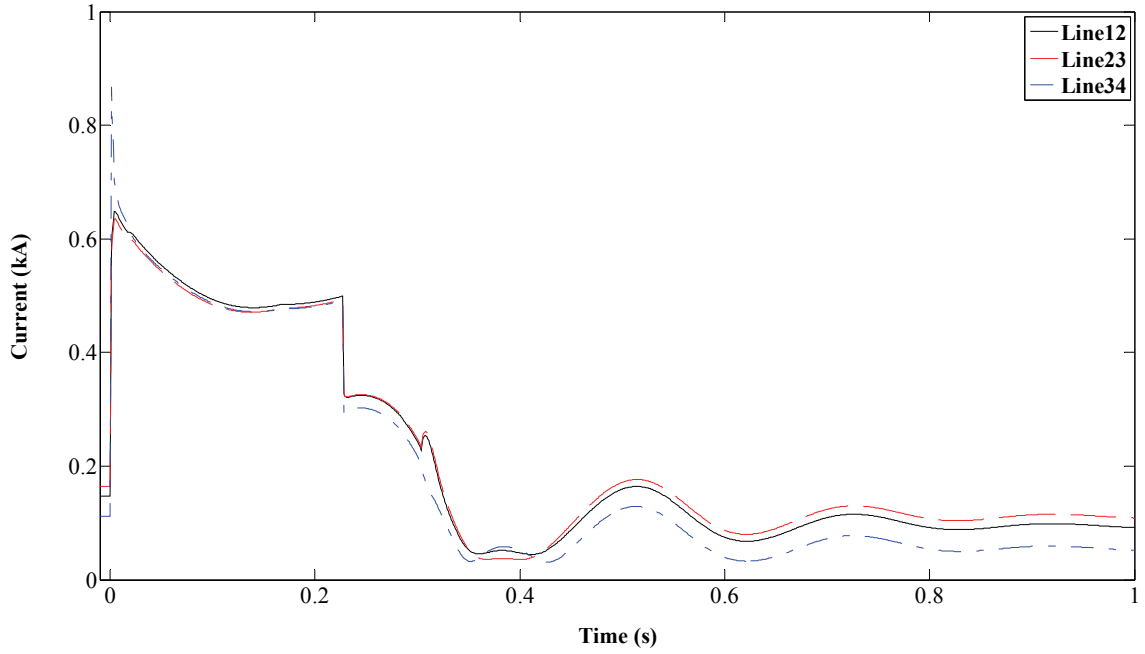

Fig. 6. 19. Current for a three phase fault in Line45 when the distribution system is islanded

The forward relays see that the current is higher than their pickup currents at *t=0s* and is reduced by more than 10 %, in successive measurements, at *t=230ms*. Therefore, the measured pickup time is *160ms*. Thus, whichever relay picked up to clear the fault, it picked up at *t=160ms*. The upstream relays calculate the pickup times of the downstream relays based on the current measurement and stored time over current characteristics. The current each relay measures at the measured pickup time and the pickup time it calculated for the downstream relays for Case2B is presented in Table 6. 8.

Table 6. 8

Summary of results for Case2B

Relay	Fault current measured by relays at *t=160ms* (A)	Calculated pickup times for relay (ms)			
		R23	R34	R45	R56
R12	485	1026	492	241	61
R23	478	-	503	244	62
R34	477	-	-	244	62

It can be seen from the table that the calculated pickup times for the relays R34 and R45 are higher than the measured pickup time. Relays R12, R23 and R34 identifies R45 to have picked up as its calculated pickup time is slightly higher than the measured pickup time compared to that of relay R34. GTG5 is disconnected from the test distribution system when the fault is cleared. Now, relays ask other appropriate relay(s) connected at the same bus to update their trip characteristics for the new operating condition.

Table 6. 7 and Table 6. 8 show that the relays identify the faulty section as Line45 in both cases. This is also the actual case. Even though the methodology is able to correctly identify the faulted section, the error between the calculated pickup time and the measured pickup time is much more in island condition than grid connected condition. This is because of the contributions from the DG units in total fault current in these two different situations. When the distribution system is connected to the grid, the difference in fault current with and without GTG4, for an example, is considerably less compared to the islanded case for a fault beyond Bus 4.

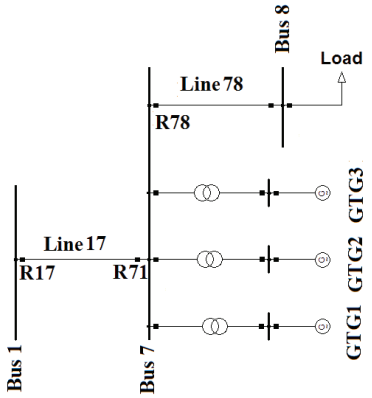

Fig. 6. 20. Expanded part of the test distribution system with a new line (Line 78) and a load

Now, let's assume that a part of the test distribution system is expanded as shown in Fig. 6. 20 with a new load and a new line. For a fault in the distribution system beyond Bus 1, when the test distribution system is connected to the transmission grid, the fault current can be few kilo amperes. However, relay R71 sees only few hundreds of ampere of fault current coming from the GTGs. In such a case, the methodology may fail to identify the fault location correctly and relay R78 may not be updated properly. Relay R78 can easily have 127 $\left(\sum_{r=1}^{7}\frac{n!}{r!(n-r)!}\right)$ adaptive settings with 6 DG units and the transmission grid. But, it is too complicated to implement 127 settings. Moreover, relay R78 sees a significant difference in fault current only when the distribution system changes its state from grid connected mode to island mode or vice versa. As mentioned before, this change in the state of the distribution system can easily be identified by the state detection algorithms. It is recommended that the adaptive settings are limited to a small

number; each for a significant difference in fault current. For a radial distribution system like the test distribution system, adaptive protection can have two settings. For forward relays, like R12 and R23, the two settings can be for the grid connected condition and the island condition. Similarly, for backward relays, like R43 and R32, one setting can be for normal operating condition and another setting for a loss of a significant generation.

Now, let us consider another case where Bus 6 and Bus 7 in the test distribution system, presented in Fig. 6. 2, are connected through a line as shown in Fig. 6. 21.

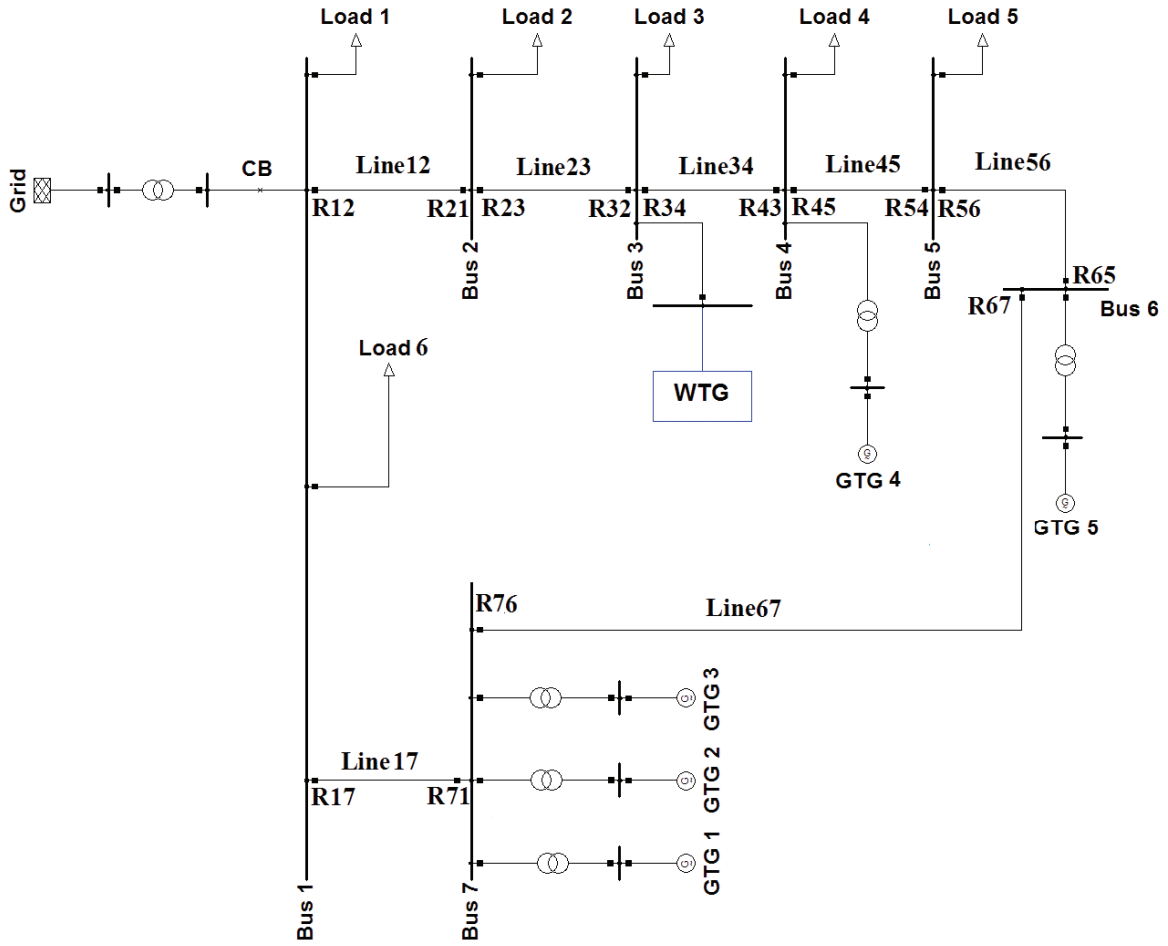

Fig. 6. 21. Meshed test distribution system

Now the distribution system becomes a meshed distribution system. The methodology to detect the faulty section still hold true. Now, if we assume a fault in Line67, the difference in fault current seen by relays R12, R23, R34, R45 and R56 will be small, as much of the fault current is supplied by the transmission grid. Similarly, difference in fault current seen by relays R17 and R76 will also be small. Hence, the methodology will be able to detect the faulty section correctly. However, the relay over current design has to be modified for the meshed distribution system.

When the breakers at the two ends of Line67 open to clear the fault, the loop is broken. Now a fault current seen by R43 for a new fault between Bus 1 and Bus 4, is considerably less. This also highlights the necessity of the adaptive protection.

6.7 Adaptive Relay Configuration

Based upon the above simulation results and discussions, each relay's trip characteristic have time over-current pickup characteristics and instantaneous pickup characteristics. Fig. 6. 22 shows the block diagram of a directional over-current relay and Fig. 6. 23 shows the block diagram of an adaptive relay. As shown in Fig. 6. 22, the current transformers (CTs) and voltage transformers (VTs) measure currents and voltages, respectively. If the current is higher than the instantaneous pickup current (I_{ins}) for T_{ins} seconds, then the instantaneous over-current setting gives trip signal. If the current is lower than I_{ins} but higher than the pickup current (I_P), a trip signal is produced according to the time over-current characteristics. Any of these trip signals can activate relay pickup (denoted by 'OR' operation in Fig. 6. 22). However, the trip signal is not activated until the direction detection detects that the current is in forward direction (denoted by 'AND' operation in Fig. 6. 22). As shown in Fig. 6. 23, the adaptive protection chooses trip characteristics based on the network condition detected by the states and the faulty section detection algorithms. The adaptive relay can have any number of settings and the relays need to have memory to store the trip characteristics of other relays. The choice of number of setting will be based on the network configuration.

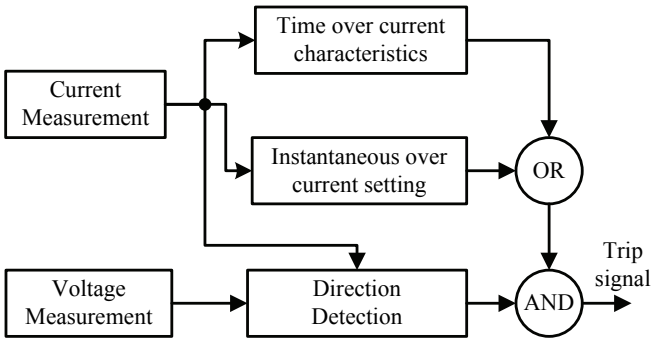

Fig. 6. 22. Block diagram of directional over current relay

Section 6.4 showed that by detecting the states of the distribution system, the relay trip characteristics can be changed from grid connected condition and island condition and vice versa. Similarly, Section 6.6 showed that the faulty section can be detected accurately and relay trip characteristics can be updated if some of the generators are disconnected from the test distribution system. Hence an adaptive relay chooses the trip characteristics based on the status of the

distribution system and clears the fault in timely manner. However, if the generations are connected to distribution system, the adaptive protection is not able to recognize it and update the trip characteristics.

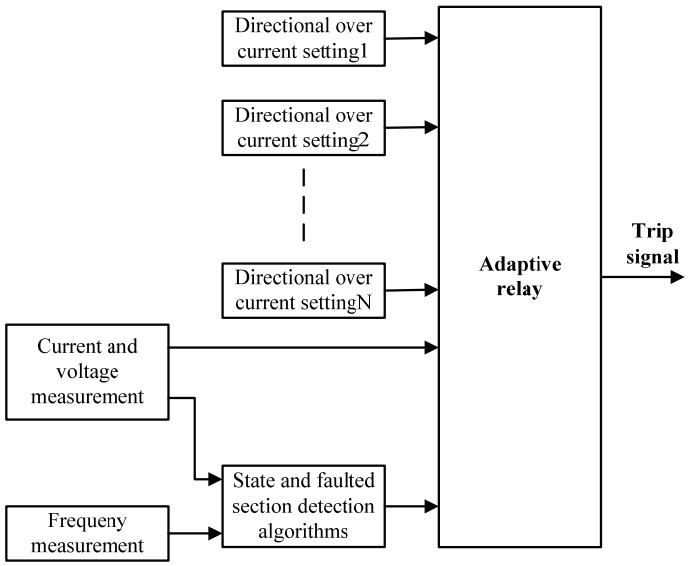

Fig. 6. 23. Block diagram of adaptive protection

6.8 Discussion on Grounding and Unsymmetrical Faults

The most common type of fault in power system is a single line to ground (SLG) fault. Unlike the three phase fault, the fault current during a SLG fault is mainly dependent on the grounding. The three main types of grounding are as follows:

Isolated ground

There is no direct connection to ground and the only connections are through the large zero sequence capacitance of the lines. Since the zero sequence, which is mostly capacitive, is much larger than the short circuit positive sequence impedance, single phase to ground fault currents are very small [102]. The healthy phases in this case see a rise in voltage during SLG

Resonant Grounding

The neutral is connected to the ground through an inductance in such a way that the capacitive fault current component is compensated to a small residual current. The inductor is often referred to as *Petersen-Coil*. Many countries in Europe, including Denmark, use this type of ground, which allows a sustained operation of the distribution system without opening of the feeder [103].

Low impedance grounding

Here the neutrals are connected to the ground directly or through small impedance. Even though the fault current is the largest, the voltage in the healthy phases rises the least in case of effective grounding (direct grounding) compared to other grounding for SLG fault.

Since the fault current is usually less for a SLG fault, it is difficult to detect SLG fault at times. Zero sequence relays and neutral voltage relays can be used [103] to detect SLG faults. The islanding of the distribution system may leave the DG source without any kind of grounding. The SLG fault in such a system could result in customers on the un-faulted phases supplied with voltage that can increase up to 173%, at worst case, of the pre-fault voltage level for an indefinite period [21]. Such a high voltage can result in damage of utility and customer equipment. For example, marginally rated lightning arresters may be destroyed if the voltage is 150% or more of the pre-fault condition [104]. Hence, it is necessary to ground the distribution system when it is islanded. Furthermore, effective grounding also ensures that faults are cleared with the use of only over current protection and need of other forms of protection for earth faults can be avoided. Moreover, during unsymmetrical faults, negative sequence currents are generated. The ability of machines to withstand these negative sequence current for short duration depends on the size. The smaller DG has less handling capacity compared to larger machines [105]. Hence, it is recommended that the distribution system is grounded for the island operation.

6.9 Conclusion

Significant DG penetration in the distribution system worldwide has presented an opportunity to operate distribution systems in an island mode during some disturbances in the grid upstream to improve the reliability of power supply. But, DG doesn't contribute as much fault current as the transmission grid. Hence an over-current protection system designed for the grid connected condition results in longer fault clearing time when the distribution system is islanded. This might result in loss of some generators and loads. Also, setting the protection system for islanded condition may result in unnecessary operation of some relays. Adaptive protection overcomes this by updating the trip characteristics of the relays when the distribution system condition changes (like grid connected, island and losing some generators). The adaptive protection uses only local information to update its setting. The state detection algorithms are used to change the setting from grid connected to island condition and vice versa. The faulty section is determined by using the time over-current characteristic, and the relay trip characteristic is updated, if necessary. Hence, by the use of state detection algorithms and detection of the faulty section, the network condition is known and based upon this, the relays trip characteristics are adapted to clear the fault fast and satisfy the protection philosophy.

Chapter 7

Conclusion

This dissertation has addressed various technical issues with islanded operation of the distribution system with distributed generation. The main objective of this research has been to develop efficient state detection algorithms, control and operation strategies for DG, over current protection of the distribution system and load control. These are the major issues that need to be resolved before islanding operation of a distribution system with DG becomes a technically viable option in the future.

7.1 Summary and Conclusion

Islanding is a situation in which a DG continues to supply loads connected locally even after it has been disconnected from the rest of the power system. Many utilities around the world practise automatic reclosing, which connects two parts of the power system after some time delay to cope up with the transient faults. In the past, the distribution systems did not have any active power generating sources in them. Hence, a reclosing action was similar to a load increase event. However, when a distribution system with DG is islanded, an automatic reclosing action may result in out of phase connection of two energised systems. As a result, utilities demand DG units to shut down in case of islanding and put strict requirement on islanding detection.

Many islanding detection techniques have been developed in the recent times and they can broadly be divided into remote and local techniques. Remote techniques use communication between utilities and DG units to detect islanding. Although, this technique has better reliability, it can be expensive to implement, especially for a small system. Hence, local techniques are widely used to detect islanding. Local techniques can further be divided into passive and active techniques. Passive methods set some kind of thresholds for system parameters such as voltage, frequency, etc. When islanding occurs, these system parameters exceed the thresholds and islanding is detected. However, when the load and generation in the islanded distribution system closely match, change in system parameters is small and hence it is difficult to detect islanding with passive techniques. Many common events in power system, like load changes, also result in small changes in the power system parameters. Thus, setting a lower threshold may result in false islanding detection. Active techniques overcome the disadvantage of the passive techniques and they can detect islanding, even under a perfect match of generation and demand in the islanded distribution system, by injecting perturbations. These perturbations drive the observed system parameter(s) outside the threshold when the distribution system is islanded. On the other hand, these perturbations have negligible

impact if the distribution system is still connected to grid. But perturbations degrade the power quality. To overcome the problem with the existing islanding detection techniques, a hybrid islanding detection, based on the average rate of voltage change and real power shift, is developed. It uses both passive (average rate of voltage change) and active (real power shift) techniques. The passive technique is first used to detect islanding and if it cannot clearly discriminate between island and grid connected conditions, then the active method is used. The active technique changes the real power set point of the DG units. Set points are defined and average rate of voltage change is used to decide if the distribution system is islanded or still connected to grid. The proposed hybrid islanding detection technique eliminates the necessity of injecting disturbances from time to time and can clearly distinguish islanding from other normal power system events like load changes, even when the mismatch between generation and demand in the islanded distribution system is very small.

Although the utilities require the DG units to disconnect in case of islanding, it will not be a practical and reliable solution in future with higher penetration of DG. Islanding can improve the reliability of power supply by supplying power to local loads during network outage. However, various technical issues have to be resolved before islanding operation of DG is realized. One of the major issues is maintaining voltage and frequency of an islanded distribution system within the power quality limits.

Synchronous generators can be operated at power factor/VAr control mode or voltage regulation mode. When a small generator is connected to a stronger transmission grid while operating in voltage regulation mode, it may cause either over or under excitation of the generator and may result in overload or loss of generator synchronism. Hence, the operation of small generators in power factor control mode, while connected to grid, is justifiable. Also, it makes economical sense to produce real power only. However, when a distribution system is islanded, responsibility to maintain the voltage in the islanded distribution system falls on these generators. Generators, with their governor, change their power with the change in frequency. One of the conventional ways to control the power of the generators and hence the frequency is speed droop control. When the droop controller is employed, the frequency might settle beyond the power quality limit when the distribution system is islanded depending on the power mismatch in the islanded distribution system. The frequency can be brought closer to the nominal value by changing the power set points of the generators through secondary control. However, implementing secondary control in distribution systems might be expensive. A possible solution is an isochronous controller. It is basically a PI controller, which can regulate the frequency to nominal value. However, with the isochronous control, the DG output power is driven to the extreme limits even with the slightest of changes in grid frequency when the DG is connected to grid. Isochronous controller with feedback for GTGs is developed in this research. It performs relatively well in both

islanded and grid connected conditions. Hence isochronous control with feedback can be used to control GTG's speed governor for both island and grid connected conditions. However, the droop controller performs the best during grid connected condition and the isochronous controller is the best during islanding among these three controllers. Hence, shifting the control strategy from droop control to isochronous control when the distribution system changes its state from grid connected to islanded condition results in the best performance. The output power of DG does not change much when it is connected to the grid and the frequency is maintained close to the nominal value when the distribution system is islanded. Unfortunately, the isochronous controller cannot be used with more than one generator connected to the same system since all the generators else would need to have the same speed set point; otherwise each generator tries to bring the frequency to its reference setting. During islanding, the isochronous controller with feedback performs better than the droop controller. Hence, if there is more than one DG unit in the distribution system, one DG unit employs isochronous control and the rest employ isochronous control with feedback during islanding.

Although, the island operation of the distribution system increases the reliability of the power supply, an islanded distribution system cannot equal the power grid in term of reliability. Hence, when the transmission grid is back to normal operating condition, it is desirable to reconnect the distribution system back to the transmission grid. Synchronous check relay should be installed at the place where the distribution system is islanded. It compares the frequency and the voltage magnitude of the two systems (distribution and transmission systems) and reconnects them when the differences in the frequency and the voltage are within the limits, and the two systems are in phase. It is based on the IEEE standard 1547 recommendations. Similar to the need of changing the control strategy from droop control and power factor control to isochronous control or isochronous control with feedback, and voltage control when the distribution system is islanded, it is necessary to change the control strategy back to droop control and power factor control when the distribution system is reconnected back to the grid. Based on the grid reconnection criteria, there will be a jump in the frequency when the distribution system and transmission system are reconnected as the two systems will be in phase from time to time only if they operate at different frequencies. Based on this, grid reconnection detection algorithms have been developed. One of the grid reconnection algorithms is for a simple distribution system with only one DG unit that is capable to supply the power to the local loads all the time. It is based on rate of change of speed over power. When the distribution system is reconnected to the transmission grid, change in the DG power hardly has any impact in the frequency of the system. Grid reconnection is detected when change in the DG power has none or opposite impact on the speed. Another grid reconnection detection technique has been developed for distribution systems with multiple DG units. It is based on frequency limits, average rate of frequency change and real power shift. The

frequency of a transmission system is usually maintained within a narrow range. Hence, when the distribution system is connected to the grid, the frequency does not go beyond this range even if DG changes its power. However, if the distribution system is still islanded, then a change in the real power of the DG drives the frequency outside this narrow range. Hence, by changing the real power of the DG, grid reconnection can be detected.

When the distribution system is islanded, its frequency either goes up or down depending on the power imbalance in the islanded distribution system. If the frequency goes up, due to excess generation, it can be brought into a reasonable limit by reducing the output power of the generators. On the other hand, if the frequency goes down, due to excess load, output of the generators has to be increased. Photovoltaic generators uses maximum power point tracking, variable speed wind turbine optimize the power co-efficient (Cp) to produce maximum power, central heat and power plants may operate at maximum power. Thus, if all the generators are operating at maximum power and the frequency goes down, some loads have to be shed to bring the frequency back within the power quality limit. The difficulty with load shedding in a distribution system is that often real time load and generation data are not available and load shedding may not be governed by technical reasons alone. Hence, in contrast to the load shedding in a larger power system where the objective is to shed the optimal amount of load, the load shedding in distribution system should try to shed the optimal number of loads based on some criteria. Moreover, small generators have small inertia and thus the frequency tends to decay more rapidly. If loads are shed one at a time, then enough loads may not be shed on time and the islanded distribution system may collapse. Hence, the first step of load shedding is crucial. An under-frequency load shedding for islanded distribution systems with DG units based on frequency information, rate of change of frequency (RoCoF), customers' willingness to pay (WTP) and loads' history is developed. It sheds the optimal number of loads if the islanded distribution system does not have enough generation. The strategy is able to maintain the frequency of islanded distribution system, by shedding some loads. The distribution system would have collapsed without load shedding.

Another major issue with the islanding is the protection. The magnitude of current during the fault depends on available sources. Transmission grids generally have higher fault power compared to small generators. Fault studies show that there is a signification difference in fault power when the distribution system is connected to the transmission grid and when it is islanded. A protection system designed to operate in the grid connected mode takes longer time to clear the faults when the distribution system is islanded. Equipments are designed to disconnect when the voltage goes low for a certain time period. This also applies to sources like wind turbines which are becoming common in many distribution systems. Thus, by not clearing the fault fast, not only the loads but also some generation might be lost, which is undesirable. Designing the protection for island operation also runs into problems when the distribution system is connected to grid. It may

trip the breakers even when it is unnecessary. Therefore, adaptive protection has been developed that changes its setting when the distribution system switches from grid connected to island mode and vice versa. Furthermore, when some generators are lost during a fault, the fault power of the distribution system changes again. An algorithm to detect a faulty section is developed. It is based on the relays' time over current characteristics. It determines the number of generators lost when a fault is cleared by identifying the faulty section. It, then, updates the time over current settings of appropriate relays so that the next fault is cleared on time.

As concluded above, this PhD dissertation addresses some of the major issues with island operation of distribution systems with distributed generation. Issues with islanding detection, voltage and frequency control, under frequency load shedding, grid reconnection detection and over current protection have been covered. Simulation results show that this research has been able to successfully address these issues by developing different strategies to operate DG units, techniques to detect states and algorithms to shed loads and detect faulty section.

7.2 Major Contributions

The major contributions of this dissertation are as follows:

- A hybrid islanding detection technique based on average rate of voltage change and real power shift that consists of a faster passive technique (average rate of voltage change) and an additional active technique (real power shift) to differentiate when the passive technique cannot give a discrimination between grid connected and island condition.

- A passive grid reconnection detection algorithm based on change of speed over power for simple distribution systems with a single DG unit whose capacity is higher than the maximum demand of the distribution system.

- An active grid reconnection detection algorithm for distribution system, with one or more DG units, based on frequency, average rate of frequency change, and real power shift.

- An isochronous controller with feedback for speed/power control of gas turbine generators that can maintain frequency within the power quality limits when the distribution system is islanded and does not change the GTGs' output power much with changing frequency when the GTGs are operating parallel to the grid.

- A DG control strategy to maintain frequency and voltage of islanded distribution system when islanded and to control power and power factor while it is connected to the grid.

- An under-frequency load shedding scheme, based on loads' history and customers' willingness to pay, frequency, and rate of change frequency, to maintain the frequency in a distribution system that has more demand than generations when it is islanded.

- A faulty section detection algorithm based on the time over current characterises of over current protection relays.

- An adaptive over current protection for distribution system with DG units and single infeed.

7.3 Future Work

Although many aspects of island operation of the distribution system with DG have been covered by this dissertation, several other issues are interesting for future investigation. Some of the issues that are deemed interesting are listed as follows:

- In future, a large number of power electronics interfaced DG units are expected to be integrated in the power system. Similarly, penetration of storage units is also expected to increase. This mix of conventional generators, power electronics interfaced generators and storage units may require new control techniques for stable island operation.

- The under frequency load shedding scheme could be improved to shed loads in the islanded distribution system when DG have some reserve margin.

- Over current protection may not work properly with significant penetration of power electronics interfaced DG units as they do not contribute as much short circuit current as conventional synchronous machine based DG. Protection of islanded distribution systems with large penetration of inverter based DG needs to be investigated.

- An adaptive protection that can update the trip characteristics of relays when generator(s) connect to the distribution system needs to be developed.

- Various algorithms have been developed during the course of this research project. The effectiveness of the proposed algorithms has been demonstrated through simulation results. Some of the algorithms may be validated through experiments.

- Economics related to island operation is not considered in this research project. However, the control strategy of DG units and/or the load shedding strategy can be modified to achieve economical operation of the islanded distribution system.

- The research shows that islanding is technically a viable option to improve the reliability of the power supply. However, economical feasibility of island operation needs to be investigated taking into account costs associated with outage, extra equipments and revenue generated from island operation.

Reference

[1] J. Casazza and F. Delea. *Understanding Electric Power Systems: An Overview of the Technology and the Marketplace*. New Jersey: IEEE Press, 2004.

[2] R. E. Brown, "Reliability assessment and design optimization in electric power distribution systems," Ph.D. Dissertation, University of Washington, USA, May 1996.

[3] L. Willis and W. G. Scott. *Distributed Power Generation*. New York: Marcel Dekker, 2000.

[4] Eurostat, "Electricity generated from renewable sources," [Online]. Available: http://epp.eurostat.ec.europa.eu/tgm/table.do?tab=table&init=1&language=en&pcode=tsien050&plugin=1, May 2009 [9 June 2010].

[5] U.S. Energy Information Administration, "Total capacity of dispersed and distributed generators by technology type," [Online]. Available: http://www.eia.doe.gov/cneaf/electricity/epa/epat1p6c.html, Jan. 2010. [9 June 2010].

[6] The Institute of Energy and Technology, "Distributed generation," [Online]. Available: http://www.theiet.org/factfiles/energy/dist-gen.cfm, July 2008 [14 June 2010].

[7] WADE, "World survey of decentralized energy 2006," [Online]. Available: http://www.localpower.org/documents/report_worldsurvey06.pdf, May 2006 [14 June 2010].

[8] Danish Energy Agency, "Danish power infrastructure in 1985," [Online]. Available: http://www.ens.dk/en-US/Info/FactsAndFigures/EnergyInfoMaps/DownloadPremadeMaps/Documents/Kort_1985_ac_dc.png, [14 June 2010].

[9] Danish Energy Agency, "Danish power infrastructure in 2009," [Online]. Available: http://www.ens.dk/en-US/Info/FactsAndFigures/EnergyInfoMaps/DownloadPremadeMaps/Documents/Kort_2009_ac_dc.png, [14 June 2010].

[10] Danish Energy Association, "Danish electricity supply 2008, statistical survey," [Online]. Available: http://www.danishenergyassociation.com/~/media/English_site/Statistics/DE_Statistik_08_UK_net.pdf.ashx, April 2009 [14 June 2010].

[11] European Commission, "The promotion of electricity from renewable energy sources". [Online]. Available: http://ec.europa.eu/energy/renewables/electricity/electricity_en.htm, [14 June 2010].

[12] Martin Clark, "Distributed generation markets in Europe expansion, investment and future opportunities," Business Insights Ltd, March 2010.

[13] International Energy Association, "Distributed Generation in Liberalized Electricity Market," [Online]. Available: http://iea.org/textbase/nppdf/free/2000/distributed2002.pdf, 2002 [14 June 2010].

[14] N. Acharya, P. Mahat, and N. Mithulananthan, "An Analytical Approach for DG Allocation in Primary Distribution Network," *Int. J. Elect. Power Energy Syst.*, vol. 28, no. 10, pp. 669-678, Dec. 2006.

[15] M. Begovic, A. Pregelj, A. Rohatgi, and D. Novosel, "Impact of Renewable Distributed Generation on Power System", in *Proc. 34th Hawaii Int. Conf. System Science*, 2001.

[16] D. C. Mayor, R. Picos, and E. G. Moreno, "State of the Art of the Virtual Utility: the Smart Distributed Generation Network," *Int. J. Energy Research*, vol. 28, pp. 65-80, 2004.

[17] F. Castro-Sayas and G. D. Clarke, "The costs and benefits of embedded generation islanding operation," [Online]. Available: http://webarchive.nationalarchives.gov.uk/tna/+/http://www.dti.gov.uk/renewables/publications/pdfs/kel00284.pdf/, 2002 [14 June 2010].

[18] *IEEE Standard for Interconnecting Distributed Resources into Electric Power Systems*, IEEE Standard 1547TM, June 2003.

[19] *Photovoltaic (PV) systems - Characteristics of the utility interface*, IEC 61727 Standard, December 2004.

[20] K. Christensen, et. al., "Technical Regulation for Thermal Power Station Units of 1.5 MW and higher," Energinet.dk, Fredericia, Denmark, Regulation for grid connection TF 3.2.3, 2008.

[21] P. P. Barker and R. W. de Mello, "Determining the Impact of Distributed Generation on Power Systems: Part 1 – Radial Distributed Systems," in *Proc. IEEE Power Eng. Soc. Summer Meeting*, 2000, vol. 3, pp. 1645-1656.

[22] S. P. Chowdhury, S. Chowdhury, P. A. Crossley, and C. T. Gaunt, "UK scenario of islanded operation of active distribution networks with renewable distributed generators," *Renewable Energy*, vol. 34, no. 12, pp. 2585-2591, Dec. 2009.

[23] R. A. Walling and N. W. Miller, "Distributed Generation Islanding-Implications on Power System Dynamic Performance," in *Proc. IEEE Power Eng. Soc. Summer Meeting*, 2002, vol.1, pp. 92-96.

[24] S. Abu-Sharkh, et. al., "Can microgrids make a major contribution to UK energy supply?," *Renewable and Sustainable Energy Reviews*, vol. 10, no. 2, pp. 78-127, April 2006.

[25] *Recommended Practice for Utility Interconnected Photovoltaic (PV) Systems*, IEEE Standard 929-2000, 2000.

[26] M. Ropp, K. Aaker, J. Haigh, and N. Sabhah, "Using Power Line Carrier Communications to Prevent Islanding," in *Proc. 28th IEEE Photovoltaic Specialist Conference*, 2000, pp. 1675-1678.

[27] W. Xu, G. Zhang, C. Li, W. Wang, G. Wang, and J. Kliber, "A power line signaling based technique for anti-islanding protection of distributed generators—part i: scheme and analysis," *IEEE Tran. Power Del.*, vol. 22, no. 3, pp. 1758-1766, July 2007.

[28] G. Wang, J. Kliber, G. Zhang, W. Xu, B. Howell, and T. Palladino, "A power line signaling based technique for anti-islanding protection of distributed generators—part ii: field test results," *IEEE Tran. Power Del.*, vol. 22, no. 3, pp. 1767-1772, July 2007.

[29] M. A. Refern, O. Usta, and G. Fielding, "Protection against loss of utility grid supply for a dispersed storage and generation unit," *IEEE Tran. Power Del.*, vol. 8, no. 3, pp. 948-954, July 1993.

[30] S. Barsali, M. Ceraolo, P. Pelacchi, and D. Poli, "Control techniques of dispersed generators to improve the continuity of electricity supply," in *Proc. IEEE Power Eng. Soc. Winter Meeting*, 2002, vol. 2, pp. 789-794.

[31] M. A. Redfern, J. I. Barren, and O. Usta, "A new microprocessor based islanding protection algorithm for dispersed storage and generation units," *IEEE Trans. Power Del.*, vol. 10, no. 3, pp. 1249-1254, July 1995.

[32] J. Warin and W. H. Allen, "Loss of mains protection," in *Proc. ERA Conf. on Circuit Protection for industrial and Commercial Installation*, London, UK, 1990, pp. 4.3.1-12.

[33] F. Pai and S. Huang, "A detection algorithm for islanding-prevention of dispersed consumer-owned storage and generating units," *IEEE Trans. Energy Convers.*, vol. 16, no. 4, pp. 346-351, 2001.

[34] S. I. Jang and K. H. Kim, "An islanding detection method for distributed generations using voltage unbalance and total harmonic distortion of current," *IEEE Tran. Power Del.*, vol. 19, no. 2, pp. 745-752, April 2004.

[35] S. I. Jang and K. H. Kim, "A new islanding detection algorithm for distributed generations interconnected with utility networks," in *Proc. IEE Int. Conf. Developments in Power System Protection*, April 2004, vol.2, pp. 571-574.

[36] S. Jang and K. Kim, "Development of a logical rule-based islanding detection method for distributed resources," in *Proc. IEEE Power Eng. Soc.Winter Meeting*, 2002, vol. 2, pp. 800-806.

[37] H. Kabayashi, K. Takigawa, and E. Hashimato, "Method for preventing islanding phenomenon on utility grid with a number of small scale PV systems," *2nd IEEE Photovoltaic Specialists Conf.*, 1991, vol.1, pp. 695-700.

[38] R. Belhomme, M. Plamondon, H. Nakra, G. Desrosiers, and C. Gagnon, "Case study on the integration of a non-utility induction generator to the Hydro-Quebec distribution network," *IEEE Tran. Power Del.*, vol. 10, no. 3, pp. 1677-1684, July 1995.

[39] K. El-Arroudi, G. Joos, I. Kamwa, and D. T. McGillis, "Intelligent-based approach to islanding detection in distributed generation," *IEEE Tran. Power Del.*, vol. 22, no. 2, pp. 828 – 835, April 2007.

[40] C. Hsieh, J. Lin, and S. Huang, "Enhancement of islanding-detection of distributed generation systems via wavelet transform-based approaches," *Int. J. Elect. Power Energy Syst.*, vol. 30, no. 10, pp. 575-580, Dec. 2008.

[41] N. W. A. Lidula, N. Perera, and A. D. Rajapakse, "Investigation of a fast islanding detection methodology using transient signals," in *Proc. IEEE Power Eng. Soc. General Meeting*, July 2009.

[42] P. O'Kane and B. Fox, "Loss of mains detection for embedded generation by system impedance monitoring," in *Proc. Sixth International Conference on Developments in Power System Protection*, March 1997, pp. 95-98.

[43] G. A. Smith, P. A. Onions, and D. G. Infield, "Predicting islanding operation of grid connected PV inverters," *IEE Proc. Electric Power Applications*, vol. 147, pp. 1-6, Jan. 2000.

[44] M. E. Ropp, M. Begovic, and A. Rohatgi, "Analysis and performance assessment of the active frequency drift method of islanding prevention," *IEEE Trans. Energy Convers*., vol. 14, no 3, pp. 810-816, Sep. 1999.

[45] G. Hung, C. Chang, and C. Chen. "Automatic phase shift method for islanding detection of grid connected photovoltaic inverter," *IEEE Trans. Energy Convers*., vol. 18, no. 1, pp. 169-173, Mar. 2003.

[46] J. Yin, L. Chang, and C. Diduch, "A new adaptive logic phase-shift algorithm for anti-islanding protections in inverter-based DG systems," *IEEE Power Electronics Specialists Conf.*, 2005, pp. 2482-2486.

[47] Program Operation Manual, Power Technologies, Inc. New York, USA, Power System Simulator - PSS/E.

[48] S. Santoso and H. T. Le, "Fundamental time-domain wind turbine models for wind power studies," *Renewable Energy*, vol. 32, no. 14. pp. 2436-2452, 2007.

[49] S. M. Muyeen, M. Hasan Ali, R. Takahashi, T. Murata, J. Tamura, Y. Tomaki, A. Sakahara, and E. Sasano, "Comparative study on transient stability analysis of wind turbine generator system using different drive train models," *IET Renewable Power Generation*, vol. 1, no. 2, pp. 131-141, 2007.

[50] P. Djapic, C. Ramsay, D. Pudjianto, G. Strbac, J. Mutale, N. Jenkins, and R. Allan, "Taking an active approach," *IEEE Power and Energy Magazine*, vol. 5, no. 4, pp. 68-77, Jul./Aug. 2007.

[51] Danish Energy Authority, "Energy Statistics 2006," 2007.

[52] K. Qiu, A.C.S. Hayden, and P. Sears, "Energy from waste/gas turbine hybrid combined cycles and their potential for GHG emissions reduction," in *Proc. IEEE EIC Climate Change Technology*, May 2006, pp. 1-9.

[53] A. D. Hansen, F. Iov, P. Sørensen, N. Cutululis, C. Jauch, and F. Blaabjerg, "Dynamic wind turbine models in power system simulation tool DIgSILENT," Risø DTU, Denmark, Risø-R-1400(EN), Aug. 2007.

[54] W. Qiao, R. G. Harley, and G. K. Venayagamoorthy, "Dynamic modelling of wind farms with fixed-speed wind turbine generators," in *Proc. IEEE Power Eng. Soc. General Meeting*, June 2007, pp. 1-8.

[55] L. Dusonchet, F. Massaro, and E. Telaretti, "Transient stability simulation of a fixed speed wind turbine by Matlab/Simulink," in *Proc. Int. Conf. Clean Electrical Power*, 2007, pp. 651-655.

[56] M. Martinsa, A. Perdanaa, P. Ledesmab, E. Agneholma, and O. Carlson, "Validation of fixed speed wind turbine dynamic models with measured data," *Renewable Energy*, vol. 32, no. 8, pp. 1301-1316, July 2007.

[57] G. L. Johnson. *Wind energy systems*. New Jersey: Prentice-Hall, 1985.

[58] V. Akhmatov, "Variable-speed wind turbines with doubly-fed induction generators. Part I: Modelling in dynamic simulation tools," *Wind Engineering*, vol. 26, no. 2, pp. 85 -108, 2002.

[59] Y. A. Cengel and M. A. Boles. *Thermodynamics: An Engineering Approach*. New York: McGraw-Hill, 1994.

[60] W. I. Rowen, "Simplified mathematical representations of heavy-duty gas turbines," *ASME J. Eng. Power*, vol. 105, pp. 865-869, 1983.

[61] W. I. Rowen, "Simplified mathematical representations of single shaft gas turbines in mechanical drive service," in *Proc. Int. Gas Turbine and Aeroengine Congress and Expo.*, Cologne, Germany, 1992.

[62] Working Group, on Prime Mover and Energy Supply Models, "Dynamic models for combined cycle plants in power system studies," *IEEE Trans. Power Sys.*, vol. 9, no. 3, pp. 1698-1708, Aug. 1994.

[63] CIGRE Task Force C4.02.25, Modeling of Gas Turbines and Steam Turbines in Combined Cycle Power Plants, 2003.

[64] S. K. Yee, J. V. Milanovic´, and F. M. Hughes, "Overview and comparative analysis of gas turbine models for system stability studies," *IEEE Trans. Power Sys.*, vol. 23, no. 1, pp. 108-118, Feb. 2008.

[65] M. Nagpal, A. Moshref, G. K. Morison, and P. Kundur, "Experience with testing and modelling of gas turbines," in *Proc. IEEE Power Eng. Soc. General Meeting*, 2001, vol. 2, pp. 652-656, 2001.

[66] T. W. Eberly and R. C. Schaefer, "Voltage versus var/power-factor regulation on synchronous generators," *IEEE Trans. Indus. Appl.*, vol. 38, no. 6, pp. 1682-1686, 2002.

[67] J. D. Hurley, L. N. Bize, and C. R. Mummert, "The adverse effects of excitation system var and power factor controllers," *IEEE Trans. Energy Convers.*, vol. 14, no. 4, pp. 1636-1641, 1999.

[68] IEEE, "IEEE recommended practice for excitation system models for power system stability studies," IEEE Press, 1992.

[69] H. Zeineldin, M. I. Marei, E. F. El-Saadany, and M. M. A. Salama, "Safe controlled islanding of inverter based distributed generation," in *Proc. 35th IEEE annual power electronics specialists conf.*, 2004, vol. 4, pp. 2515-2520.

[70] R. Caldon, F. Rossetto, and R. Turn, "Temporary islanded operation of dispersed generation on distribution networks," in *Proc 39th Int. Uni. Power Eng. Conf.*, 2004, vol. 3, pp. 987-991.

[71] S. Krishnamurthy, T. M. Jahns, and R. H. Lasseter, "The operation of diesel gensets in a CERTS microgrid," in *Proc. IEEE Power Eng. Soc. General Meeting*, July 2008.

[72] J. Björnstedt and O. Samuelsson, "Voltage and frequency control for island operated induction generators," in *Proc. IET CIRED Seminar: SmartGrids for Distribution*, June 2008.

[73] G. Lalor and M. O'Malley, "Frequency control on an island power system with increasing proportions of combined cycle gas turbines," in *Proc. IEEE Bologna PowerTech Conf.*, June 2003.

[74] S. P. Chowdhury, S. Chowdhury, C. F. Ten, and P. A. Crossley, "Operation and control of DG based power island in Smart Grid environment," in *Proc. IET CIRED Seminar: SmartGrids for Distribution*, June 2008.

[75] P. Kundur. *Power System Stability and Control*. New York: McGraw-Hill, 1994.

[76] M. Bollen, J. Zhong, O. Samuelsson, and J. Björnstedt, "Performance indicators for microgrids during grid-connected and island operation," in *Proc. IEEE Bucharest Power Tech Conf.*, 2009.

[77] B. Fox, D. Flynn, L. Bryans, N. Jenkins, and D. Milborrow. *Wind power integration: connection and system operational aspects*. UK: IET, 2007.

[78] P. G. Harrison, "Considerations when planning a load-shedding programme," *Brown Bovcri Rev*, no. 10, pp. 593-598, Sept. 1988.

[79] S. A. Nirenberg and D. A. McInnis, "Fast acting load shedding", *IEEE Trans. Power Systems*, vol. 7, no. 2, pp. 873-877, May 1992.

[80] M. Parniani and A. Nasri, "SCADA based under frequency load shedding integrated with rate of frequency decline," in *Proc. IEEE Power Eng. Soc. General Meeting*, June 2006.

[81] J. G. Thompson and B. Fox, "Adaptive load shedding for isolated power systems," *IEE Proc. Gen., Transm. Distrib.*, vol. 141, no.5, pp. 491-496, Sept. 1994.

[82] X. Xiong and W. Li, "A new under-frequency load shedding scheme considering load frequency characteristics," in *Proc. Int. Conf. Power System Technology*, pp. 1 - 4, Oct. 2006.

[83] V. N. Chuvychin, N. S. Gurov, S. S Venkata, and R. E. Brown, "An adaptive approach to load shedding and spinning reserve control during under-frequency conditions," *IEEE Trans. Power Sys.*, vol. 11, no. 4, pp. 1805-1810, Nov. 1996.

[84] L. Zhang and J. Zhong, "UFLS design by using f and integrating df/dt," in *Proc. IEEE Power Eng. Soc. Power Systems Conf. Expo.*, pp. 1840-1844, 2006.

[85] P. M. Anderson and M. Mirheydar, "An adaptive method for setting underfrequency load shedding relays," *IEEE Trans Power Sys.*, vol. 7, no. 2, pp. 647-655, May 1992.

[86] S. J. Huang and C. C. Huang, "An adaptive load shedding method with time-based design for isolated power systems," *Int. J. Elect. Power Energy Syst.*, vol. 22, pp. 51-58, Jan. 2000.

[87] D. Prasetijo, W. R. Lachs, and D. Sutanto, "A new load shedding scheme for limiting underfrequency," *IEEE Trans. Power Sys.*, vol. 9, no. 3, pp. 1371-1378, Aug. 1994.

[88] V. V. Terzija, "Adaptive under-frequency load shedding based on the magnitude of the disturbance estimation," *IEEE Trans. Power Sys.*, vol. 21, no. 3, pp. 1260-1266, Aug. 2006.

[89] M. H. Purnomo, C. A. Patria, and E. Purwanto, "Adaptive load shedding of the power system based on neural network", in *Proc. IEEE Region 10 Conf. Computers, Communications, Control Power Eng.*, Oct. 2002, vol. 3, pp. 1778–1781.

[90] F. Carlsson and P. Martinsson, "Willingness to pay among Swedish households to avoid power outages - a random parameter tobit model approach," Göteborg University, Department of Economics, Working Papers in Economics 154. [Online]. Available: http://hdl.handle.net/2077/19626, Dec. 2004, [15 June 2010].

[91] J. V. Milanovic and I. A. Hiskens, "Effects of load dynamics on power system damping," *IEEE Trans. Power Sys.*, vol. 10, no. 2, pp. 1022-1028, May 1995.

[92] O. Samuelsson, "Power system - damping structural aspects of controlling active power," Ph.D. Dissertation, Lund University, Sweden, 1997.

[93] E. Kyriakides and R. G. Farmer, "Modeling of Damping for Power System Stability Analysis," *Electric Power Components and System*, vol. 32, no. 8, pp. 827 – 837, August 2004.

[94] Transmission Lines Department, "Wind turbines connected to grids with voltages below 100 kV," Energinet.dk, Fredericia, Denmark, Technical regulations for the properties and the control of wind turbines TF 3.2.6, 2004.

[95] N. Jayawarna, N. Jenkins, M. Barnes, M. Lorentzou, S. Papthanassiou, and N. Hatziargyriou, "Safety Analysis of a Microgrid", in *Proc. Int. Conf. Future Power Sys.*, Nov. 2005.

[96] M. Pedrasa and T. Spooner, "A survey of techniques used to control microgrid generation and storage during island operation," in Proc. *Australian Uni. Power Eng. Conf. (AUPEC)*, Melbourne, Australia, Dec. 2006.

[97] H. Nikkhajoei and R. Lasseter, "Microgrid Protection," in *Proc. IEEE Power Eng. Soc. General Meeting*, Tampa, USA, June 24-28, 2007.

[98] T. Loix, T., Wijnhoven, and G.Deconinck, "Protection of microgrids with a high penetration of inverter-coupled energy sources," in *Proc. CIGRE/IEEE PES Joint Symposium Integration of Wide-Scale Renewable Resources into the Power Delivery System*, 2009.

[99] G. Rockefeller, et al., "Adaptive Transmission Relaying Concepts for Improved Performance," *IEEE Trans. Power Del.*, 1988.

[100] A. Oudalov and A. Fidigatti, "Adaptive network protection in microgrids," [Online]. Available: http://www.microgrids.eu/documents/519.pdf, [June 12, 2010].

[101] M. A. Poller, "Doubly-Fed Induction Machine Models for Stability Assessment of Wind Farms," *in Proc. IEEE Bologna Power Tech Conference*, 2003, vol. 3.

[102] P. Hansen, J. Østergaard, and J. S. Christiansen, "System grounding of wind farm medium voltage cable grids," in *Proc. Nordic Wind Power Conference*, Denmark, 2007.

[103] CIRED working group WG03, "Fault management in electrical distribution systems", Finland, December 1998.

[104] IEEE Std. C62.22-1997, "IEEE Guide for the Application of metal Oxide Surge Arresters for Alternating Current Systems," 1998.

[105] Dromey Design, "Synchronous Generation in Distribution Systems," [Online]. Available: http://www.dromeydesign.com/articles/SynchronousGeneration.pdf, 2007, [June 12, 2010].

Appendix A

Table AI

Line data for the test distribution system

From Bus	To Bus	Resistance (Ω)	Reactance (Ω)
5	6	0.1256	0.1404
5	7	0.1344	0.0632
7	8	0.1912	0.0897
8	9	0.4874	0.2284
9	10	0.1346	0.0906
10	11	1.4555	1.1130
11	12	0.6545	0.1634
12	13	0.0724	0.0181
13	14	0.7312	0.3114

Table AII

Gas turbine generator data

Parameters	Value
Rated power	3.3 MW
Rated voltage	6.3 kV
Stator resistance	0.0504 p.u.
Stator reactance	0.1 p.u.
Synchronous reactance d-axis	1.5 p.u.
Synchronous reactance q-axis	0.75 p.u.
Transient reactance d-axis	0.256 p.u.
Sub-transient reactance d-axis	0.168 p.u.
Sub-transient reactance q-axis	0.184 p.u.
Transient time constant d-axis	0.53 s
Sub-tran. Time constant d-axis	0.03 s
Sub-tran. Time constant q-axis	0.03 s
Inertia time constant	0.54 s

Table AIII

Wind turbine generator data

Parameters	WTG
Rated Power	630 kW
Rated Voltage	0.4 kV
Stator resistance	0.018 p.u
Stator reactance	0.015 p.u
Mag. Reactance	4.42 p.u.
Rotor Resistance	0.0108 p.u.
Rotor Reactance	0.128 p.u.
Inertia Time Constant	0.38 s

Table AIV

Transformer data

Parameters	Value		
	CHPXmr	WTGXmr	GridXmr
Rated Power	3.3 MVA	630 kVA	20 MVA
Rated Voltage HV Side	6.3 kV	0.4 kV	60 kV
Rated Voltage LV Side	20 kV	20 kV	20 kV
Copper losses	28 kW	8.1 kW	102.76 kW
No-load losses	4 kW	1.9 kW	10.96 kW

Table AV

Transmission system data

Parameters	Value
Maximum short circuit power	249 MVA
Minimum short circuit power	228 MVA
Maximum R/X ratio	0.1
Maximum Z2/Z1 ratio	1
Maximum X0/X1 ratio	1
Maximum R0/X0 ratio	0.1

Table AVI

GTG governor data

Parameters	Value
Speed droop (p.u.)	0.05
Controller time constant (s)	0.4
Fuel system time constant (s)	0.1
Load limiter time constant (s)	3.0
Ambient temperature load limit (p.u.)	1.0
Temperature control loop gain (p.u.)	2.0
Controller minimum output (p.u.)	0.0
Controller maximum output (p.u.)	1.0
Frictional losses factor (p.u.)	0.0

Table AVII

WTG system data

Parameters	Value
Rotor Inertia (kg mm)	$4*10^6$
Drive train Stiffness (Nm/rad)	$1*10^6$
Drive train Damping (Nm/rad)	10
Rotor radius (m)	20

Table AVIII

Load and generation data

Bus	**PG (MW)**	**QG (MVAr)**	**PL (MW)**	**QL (MVAr)**
05	0	0	7.6417	1.1607
06	8.9239	0	0.0	0.6446
07	0	0	0.4523	0.2003
08	0	0	0.7124	0.3115
09	0	2.5	0.1131	0.0501
10	0	0	0.1131	0.0501
11	0	0	0.1131	0.0501
12	0.31	0	0.0	0.0
13	0.31	0	0.0	0.0
14	0.31	0	0.0	0.0

Table AIX

Generator data

Parameters	DG	Grid
Type of generator	Synchronous	Synchronous
Number of Parallel Machines	1	20
Transformer	10.5/19 kV	
Individual generator's rating		
Rated Power	4.9 MW	255 MW
Rated Voltage	10.5 kV	19 kV
Stator resistance	0.0504 p.u.	0.0 p.u
Stator reactance	0.1 p.u.	0.014 p.u
Synchronous reactance d-axis	1.5 p.u.	2.01 p.u
Synchronous reactance q-axis	0.75 p.u.	1.89 p.u
Transient reactance d-axis	0.256 p.u.	0.21 p.u
Sub-transient reactance d-axis	0.168 p.u.	0.16 p.u
Sub-transient reactance q-axis	0.184 p.u.	0.17 p.u
Transient time constant d-axis	0.53 s	1.08 s
Sub-transient time constant d-axis	0.03 s	0.018 s
Sub-transient time constant q-axis	0.03 s	0.018 s
Inertia Time Constant	0.54 s	8 s

Table AX

Excitation system data

		DG	Grid
Excitation Model		IEEE Type AC5A	IEEE Type 1
Parameters		**Value**	
Tr	Measurement delay (s)	0	0
Ka	Controller gain (p.u.)	500	175
Ta	Controller time constant (s)	0.02	0.03
Ke	Exciter constant (p.u.)	1	1
Te	Exciter time constant (s)	0.9	0.266
Kf	Stabilization path gain (p.u.)	0.03	0.0025
Tf1	1st stabilization path time constant (s)	0.6	1.5
Tf2	2nd stabilization path time constant (s)	0.38	
Tf3	3rd stabilization path time constant (s)	0.058	
E1	Saturation factor 1 (p.u.)	5.6	4.5
Se1	Saturation factor 2 (p.u.)	0.86	1.5
E2	Saturation factor 3 (p.u.)	4.2	6.
Se2	Saturation factor 4 (p.u.)	0.5	2.46
Vmin	Controller minimum output (p.u.)	-7.3	-12.
Vmax	Controller maximum output (p.u.)	7.3	12.

Table AXI

Load and generation data for Section 3.6

Bus	PG (MW)	QG (MVAr)	PL (MW)	QL (MVAr)
05	0	0	6.31	1.48
06	8.1	0	0	0.54
07	0	0	0.45	0.20
08	0	0	0.71	0.312
09	0	0	0.113	0.05
10	0	0	0.113	0.05
11	0	0	0.113	0.05
12	0.31	0	0.0	0.0
13	0.31	0	0.0	0.0
14	0.31	0	0.0	0.0

Table AXII

GTG turbine generators governor system data

	Parameters	GTG1	GTG2	GTG3
R	Speed droop (p.u.)	0.05	0.05	0.045
K_i	Isochronous controller gain (p.u.)	10	20	20
T_i	Isochronous controller time constant (s)	6	5	5
K_{FB}	Feedback gain (p.u.)	-	0.01	0.01
T_1	Controller time constant (s)	1	1	1
T_2	Fuel system time constant (s)	0.1	0.1	0.1
T_3	Load limiter time constant (s)	3	3	3
A_T	Ambient temperature load limit (p.u.)	0.95	0.95	0.95
K_T	Temperature control loop gain (p.u.)	2	2	2
V_{Min}	Controller minimum output (p.u.)	0	0	0
V_{Max}	Controller maximum output (p.u.)	1	1	1
D_{Turb}	Frictional losses factor (p.u.)	0	0	0

Table AXIII

Power factor controller data

	Parameters	Value
K_{FB}	Controller gain (p.u.)	50
T_{FB}	Controller time constant (s)	20

Table AXIV

Line data for the test system in Fig. 4. 2

Line	Resistance (Ω)	Reactance (Ω)
1-2	0.1256	0.1404
1-3	0.1344	0.0632

Table AXV

Individual load's peak demand for different months in the test distribution system

Load	September 2006		October 2006	
	P (MW)	Q (MVAr)	P (MW)	Q (MVAr)
Load 07	0.509	0.308	0.503	0.243
Load 08	0.801	0.485	0.792	0.383
Load 09	0.127	0.077	0.126	0.061
Load 10	0.127	0.077	0.126	0.061
Load 11	0.127	0.077	0.126	0.061
Load FLØE	2.036	0.699	1.883	0.470
Load JUEL	0.919	0.195	0.882	0.187
Load MAST	1.588	0.454	3.173	1.030
Load STCE	2.489	0.420	1.759	0.24
Load STNO	1.878	0.278	2.143	0.168
Load STSY	2.992	0.926	2.907	0.963

Table AXVI

Test distribution system peak demand for different months

Load	October 2006		November 2006	
	P (MW)	Q (MVAr)	P (MW)	Q (MVAr)
Load 07	0.474	0.238	0.452	0.2
Load 08	0.747	0.374	0.712	0.316
Load 09	0.119	0.059	0.113	0.05
Load 10	0.119	0.059	0.113	0.05
Load 11	0.119	0.059	0.113	0.05
Load FLØE	1.6	0.532	1.787	0.465
Load JUEL	0.737	0.129	0.811	0.147
Load MAST	2.32	0.757	2.442	0.789
Load STCE	1.097	0.145	1.212	0.16
Load STNO	1.944	0.243	2.109	0.286
Load STSY	1.697	0.316	1.757	0.484

Table AXVII

Line data for the test distribution systems shown in Fig. 6. 2

From Bus	To Bus	Resistance (Ω)	Reactance (Ω)
1	7	0.1256	0.1404
1	2	0.1344	0.0632
2	3	0.1912	0.0897
3	4	0.4874	0.2284
4	5	0.1346	0.0906
5	6	0.1346	0.0906

Table AXVIII

Wind turbine generators data

Parameters	Value
Rated Power	2000.
Stator Rated Voltage	0.69 kV
Stator resistance	0.0108 p.u.
Stator reactance	0.0121 p.u.
Magnetic reactance	3.362 p.u.
Rotor resistance	0.004 p.u.
Rotor reactance	0.05 p.u.
Crowbar resistance	0.5 p.u.
Crowbar reactance	0.1 p.u.
Generator inertia	244.105 kgm^2
Rotor inertia	$61x10^5$ kgm^2
Drive train stiffness	$83x10^6$ Nm/rad
Drive train damping	$14x10^5$ Nm/rad
Nominal turbine speed	18 rpm
Rotor radius	50 m
Max. current for crowbar insertion	5 kA

Appendix B

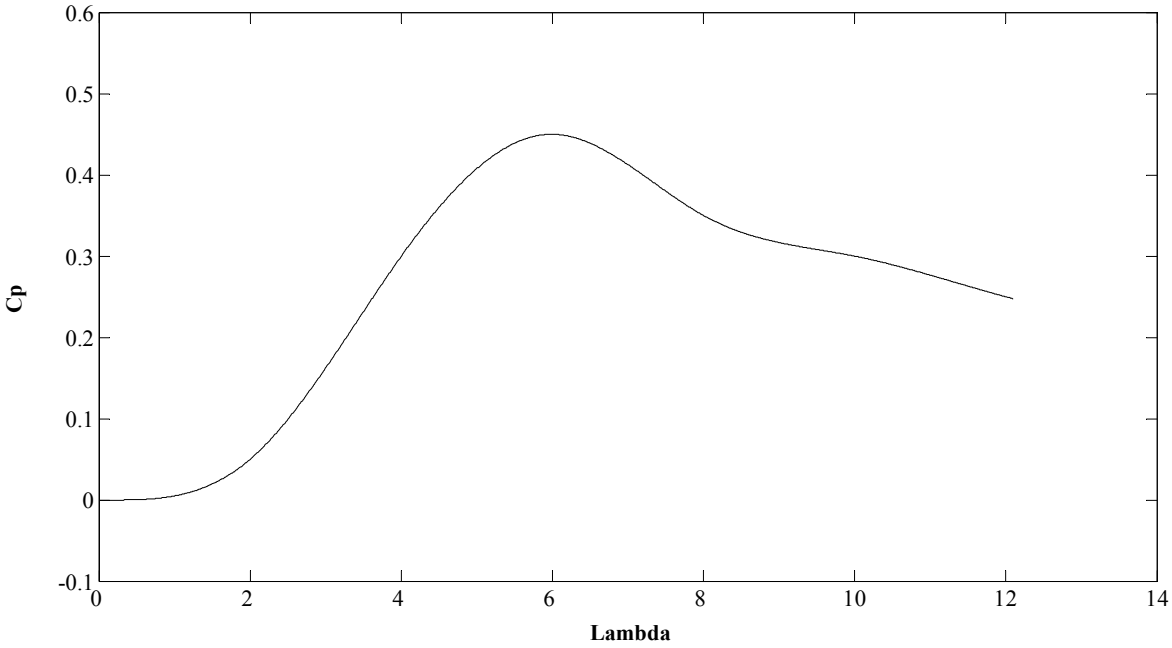

Fig. B. 1. Aerodynamic efficiency curve of WTG

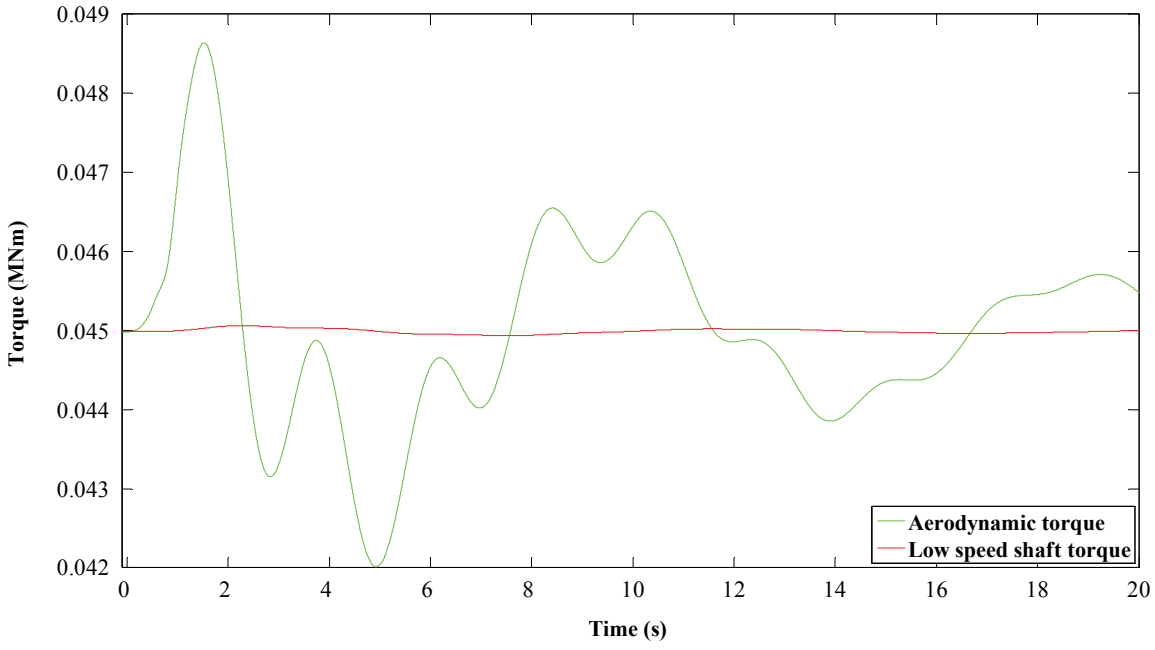

Fig. B. 2. Aerodynamic torque and low speed shaft torque of WTGs

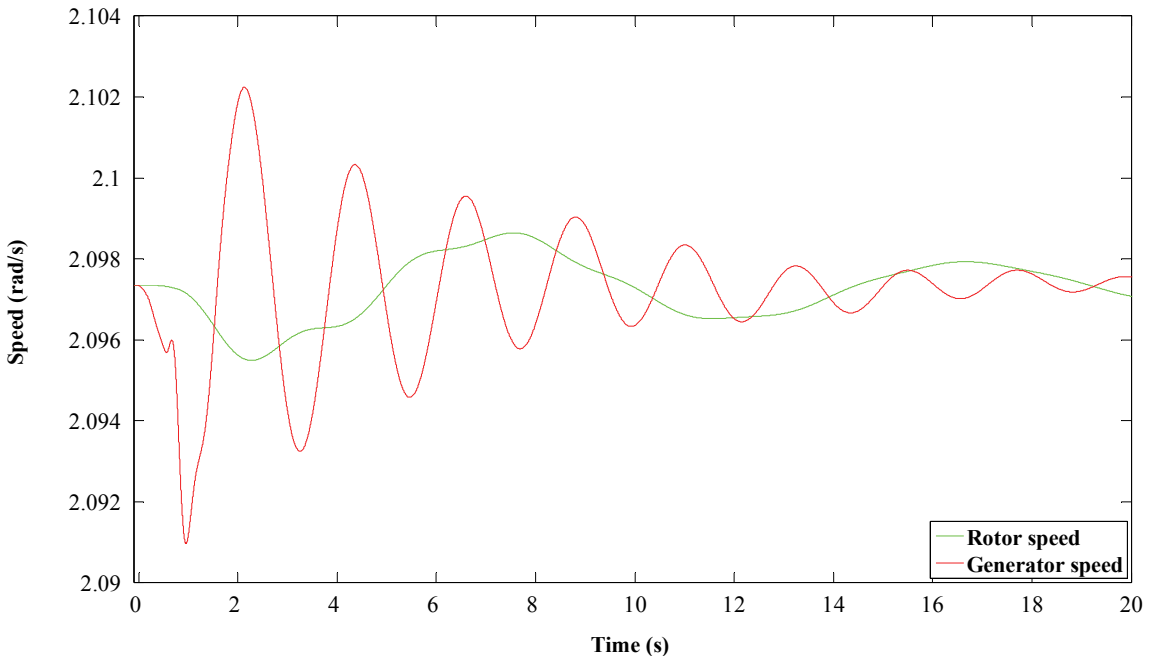

Fig. B. 3. WTGs rotor and generator speed

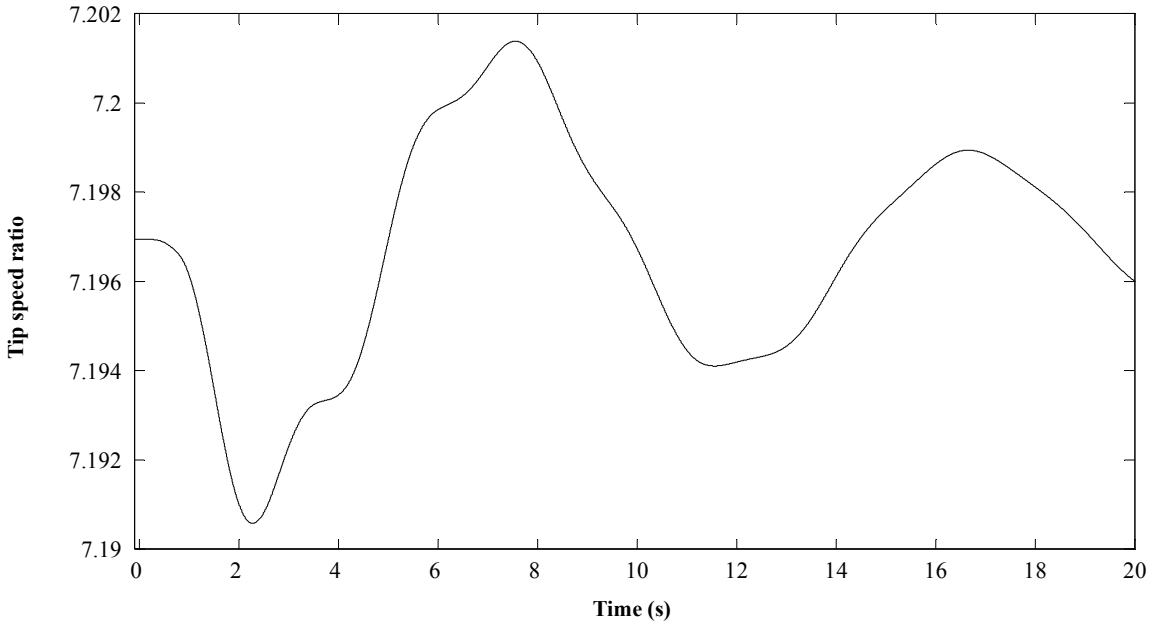

Fig. B. 4. WTGs tip speed ratio

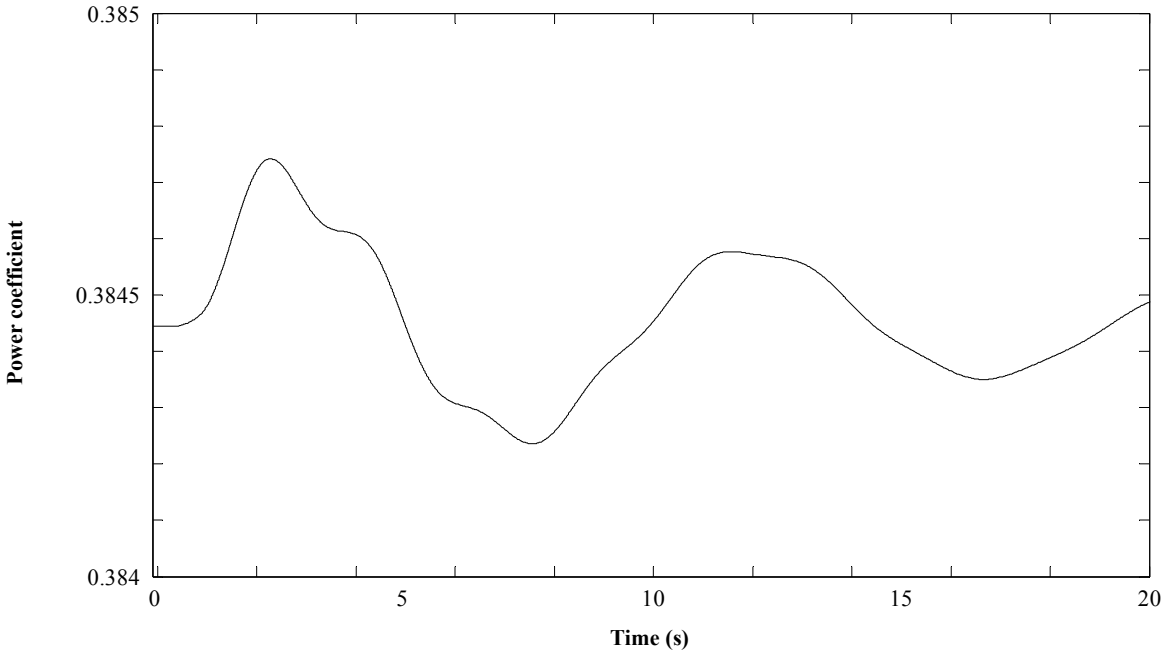

Fig. B. 5. WTGs power coefficient

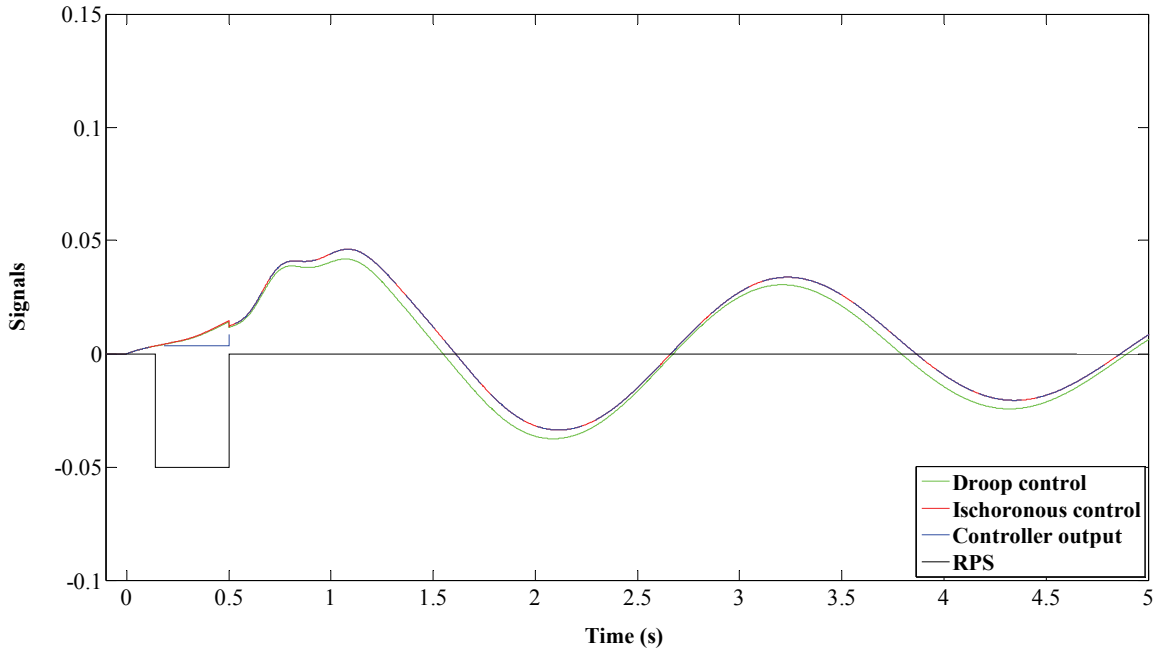

Fig. B. 6. Output signals of GTG2 and GTG3 turbine controller

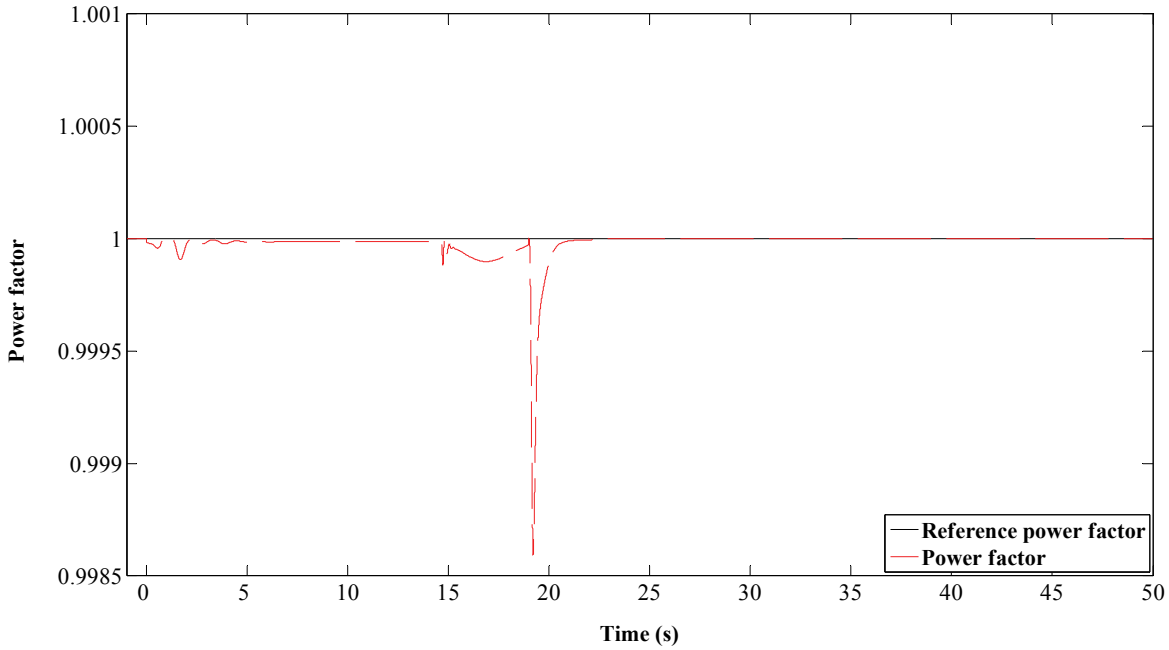

Fig. B. 7. Power factor and reference power factor of GTG

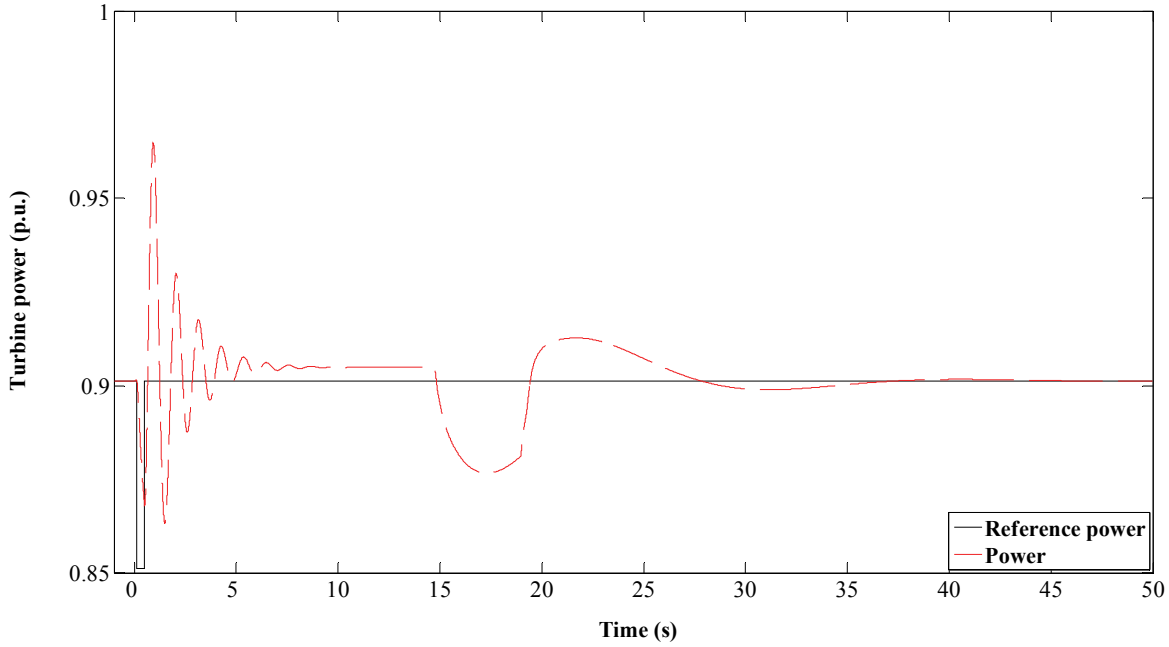

Fig. B. 8. Reference power and power of the GTG

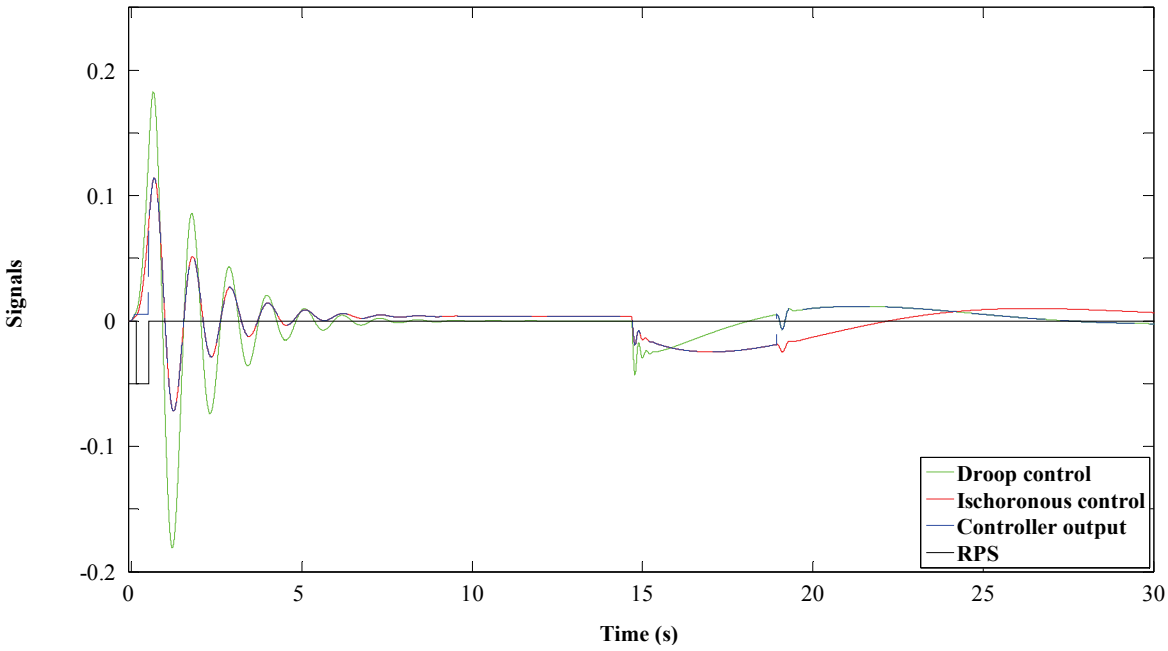

Fig. B. 9. Output signals of GTG turbine controller

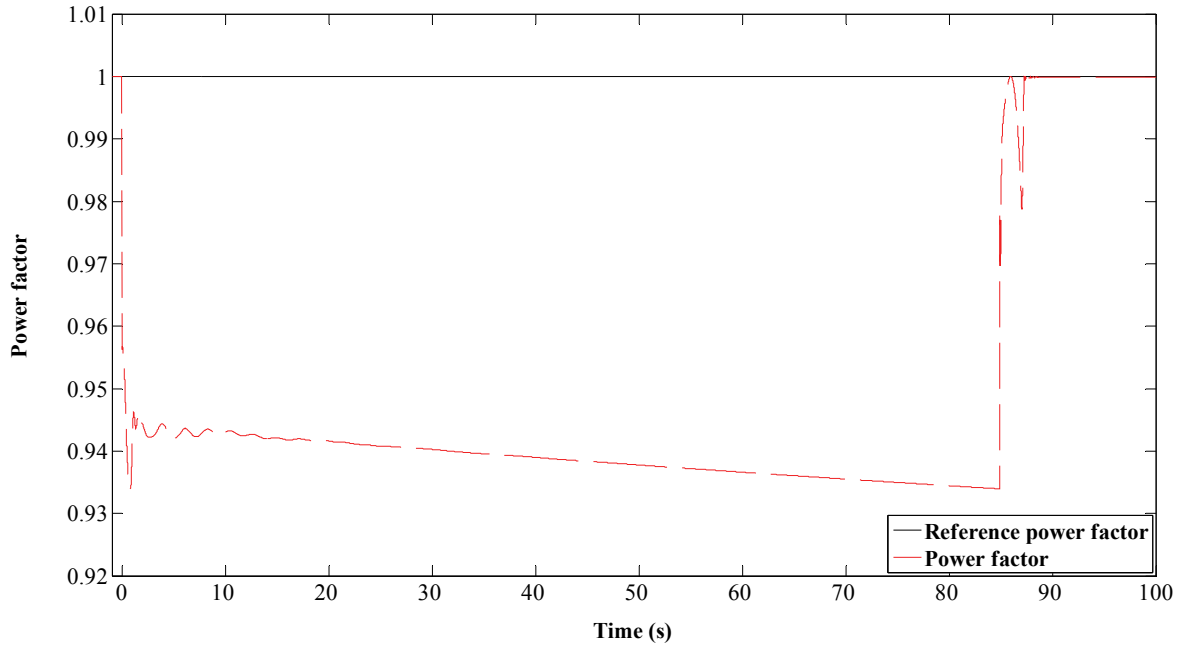

Fig. B. 10. Power factor and reference power factor of GTG1

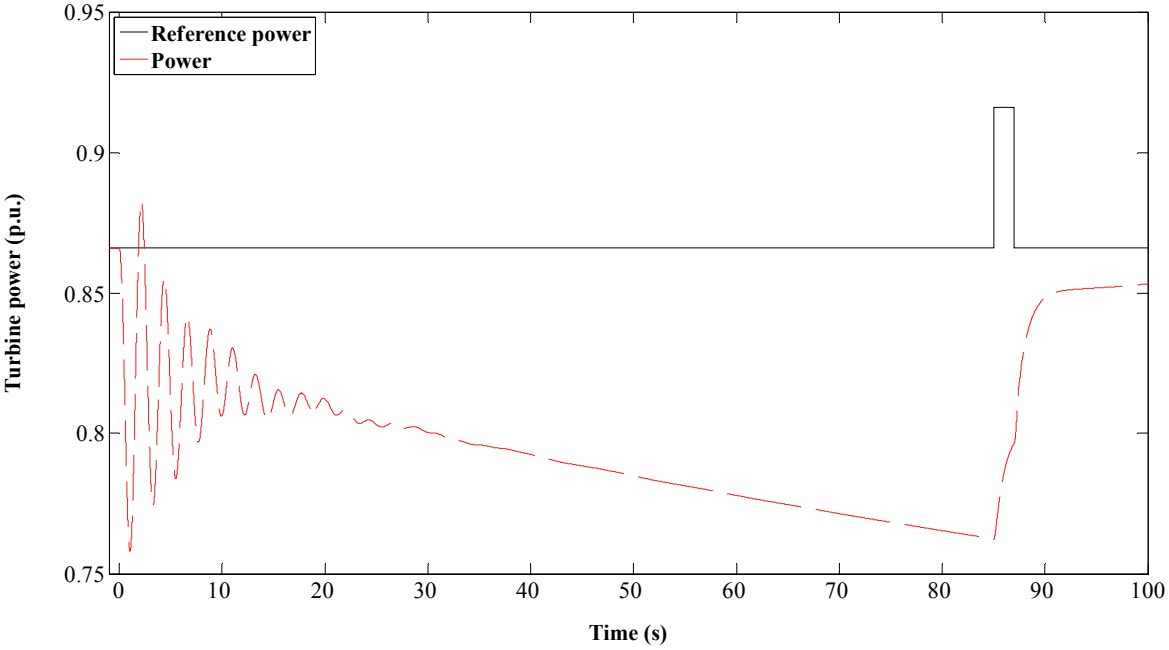

Fig. B. 11. Reference power and power of GTG1

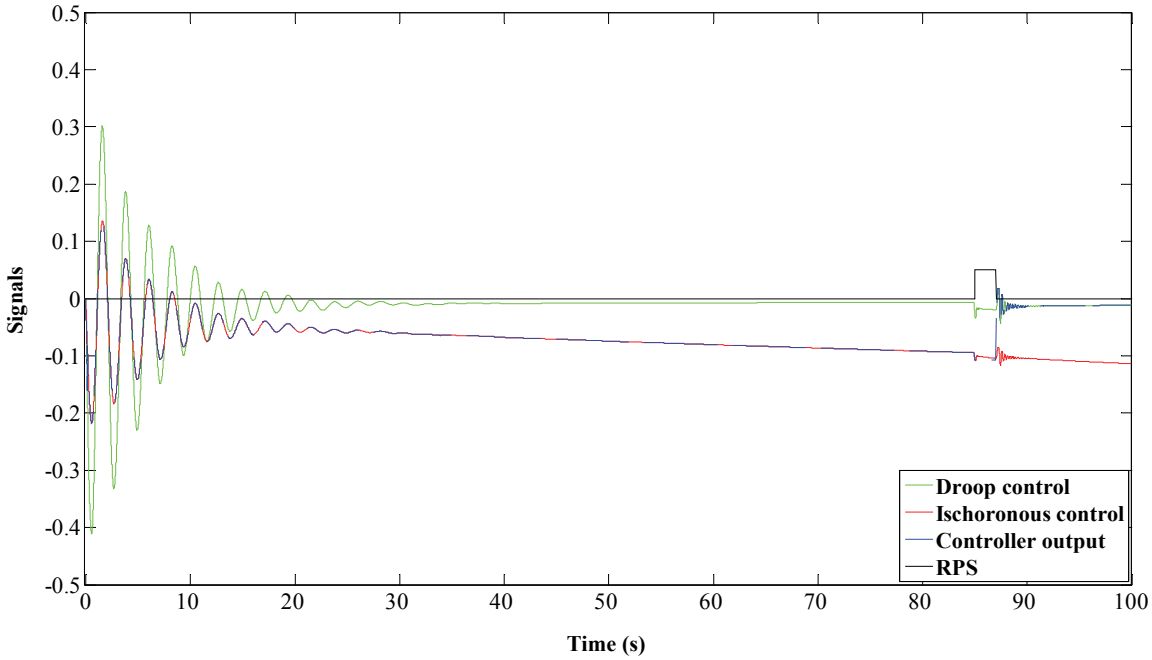

Fig. B. 12. Output signals of GTG1 turbine controller

Appendix C: Publications

This work has also been reported in following publications:

Journals

1. Pukar Mahat, Zhe Chen and Birgitte Bak-Jensen, "Control and Operation of Distributed Generation in Distribution Systems," *Electrical Power System Research,* 2010 (doi:10.1016/j.epsr.2010.10.015)
2. Pukar Mahat, Zhe Chen and Birgitte Bak-Jensen, "Under-Frequency Load Shedding for an Islanded Distribution System with Distributed Generators," *IEEE Transaction on Power Delivery*, Volume 25, Issue 2, Pages 911 -918, April 2010
3. Pukar Mahat, Zhe Chen and Birgitte Bak-Jensen, "A Hybrid Islanding Detection Technique Using Average Rate of Voltage Change and Real Power Shift," *IEEE Transaction on Power Delivery*, Volume 24, Issue 2, Pages 764 – 771, April 2009

Conferences

4. Pukar Mahat, Zhe Chen and Birgitte Bak-Jensen, "Control Strategies for Gas Turbine Generators for Grid Connected and Islanding Operations," *in Proc. 2010 IEEE PES Transmission and Distribution Conference and Exposition*, New Orleans, USA, 19-22 April 2010
5. Pukar Mahat, Zhe Chen and Birgitte Bak-Jensen, "Islanding Operation of Distribution System with Distributed Generations," *in Proc. 2010Danish PhD Seminar on detailed Modelling and Validation of Electrical Components and Systems*, Fredericia, Denmark, Feb. 2010
6. Pukar Mahat, Zhe Chen and Birgitte Bak-Jensen, "Gas Turbine Control for Islanding Operation of Distribution Systems ," *in Proc. 2009 IEEE PES General Meeting*, Calgary, Canada, 26-30 July 2009
7. Pukar Mahat, Zhe Chen, and Birgitte Bak-Jensen, "Review of islanding detection methods for distributed generation," *in Proc. International Conference on Electric Utility Deregulation and Restructuring and Power Technologies*, Nanjing, China, Pages 2743 – 2748, April 2008

Under Review

8. Pukar Mahat, Zhe Chen, Birgitte Bak-Jensen, and Claus Leth Bak "A Simple Adaptive Over-Current Protection of Distribution Systems with Distributed Generations," *IEEE Transaction on Smart Grid*